

*Control over Communication  
Networks:  
Modeling, Analysis, and Synthesis*

Marieke Posthumus-Cloosterman

This work has been carried out as part of the Boderc project under the responsibility of the Embedded Systems Institute. This project is partially supported by the Dutch Ministry of Economic Affairs under the Senter TS program.

A catalogue record is available from the Eindhoven University of Technology Library

ISBN: 978-90-386-1304-8

Typeset by the author with the  $\text{\LaTeX}$  2 $\epsilon$  documentation system

Cover Design: Gerda Cloosterman, Paul Verspaget

Printed by University Press Facilities, Eindhoven, the Netherlands

*Control over Communication  
Networks:  
Modeling, Analysis, and Synthesis*

PROEFSCHRIFT

ter verkrijging van de graad van doctor aan de  
Technische Universiteit Eindhoven,  
op gezag van de Rector Magnificus, prof.dr.ir. C.J. van Duijn,  
voor een commissie aangewezen door het College voor  
Promoties in het openbaar te verdedigen op  
woensdag 25 juni 2008 om 16.00 uur

door

Maria Bernardina Gertruda Posthumus-Cloosterman

geboren te Nijmegen

Dit proefschrift is goedgekeurd door de promotor:

prof.dr. H. Nijmeijer

Copromotoren:

dr.ir. N. van de Wouw

en

dr.ir. W.P.M.H. Heemels

# *Contents*

<b>List of abbreviations</b>	<b>ix</b>
<b>1 Introduction</b>	<b>1</b>
1.1 High-tech systems design . . . . .	1
1.2 Control, computation, and communication . . . . .	2
1.3 Networked Control Systems . . . . .	5
1.3.1 Modeling . . . . .	7
1.3.2 Stability analysis and controller synthesis . . . . .	9
1.3.3 Tracking . . . . .	12
1.3.4 Experiments . . . . .	12
1.4 Contribution of the thesis . . . . .	13
1.5 Structure of the thesis . . . . .	14
1.5.1 Reading suggestions . . . . .	16
<b>2 Preliminaries</b>	<b>17</b>
2.1 General mathematical notions . . . . .	17
2.2 Stability notions for continuous-time systems . . . . .	18
2.2.1 Input-to-state stability . . . . .	19
2.3 Stability of discrete-time systems . . . . .	20
2.3.1 Input-to-state stability . . . . .	22
2.3.2 Stability of switched linear systems . . . . .	23
2.4 Notation . . . . .	24
<b>3 Modeling of Networked Control Systems</b>	<b>25</b>
3.1 Small delays . . . . .	26
3.2 Large delays . . . . .	28
3.3 Large delays and packet dropouts . . . . .	32
3.4 Time-varying sampling intervals . . . . .	35
3.5 Discussion . . . . .	38
<b>4 Stability analysis</b>	<b>39</b>
4.1 Motivating examples . . . . .	40
4.2 NCS model formulation using the Jordan form . . . . .	42
4.3 Small delays . . . . .	44
4.3.1 A common quadratic Lyapunov function based on the extended state vector $\xi_k$ . . . . .	45
4.3.2 A Lyapunov-Krasovskii functional . . . . .	48
4.3.3 Comparison between the common quadratic Lyapunov approach and the Lyapunov-Krasovskii approach . . . . .	50
4.3.4 Intersample behavior . . . . .	51
4.4 Variable sampling intervals, large delays, and packet dropouts . . . . .	52

---

4.4.1	A common quadratic Lyapunov function based on the extended state vector $\xi_k$ . . . . .	54
4.4.2	A Lyapunov-Krasovskii functional . . . . .	58
4.5	Illustrative examples . . . . .	63
4.5.1	Time-varying delays . . . . .	63
4.5.2	Packet dropouts . . . . .	66
4.5.3	Time-varying sampling intervals . . . . .	67
4.6	Discussion . . . . .	69
<b>5</b>	<b>Controller synthesis</b>	<b>71</b>
5.1	Small delays . . . . .	72
5.1.1	A common quadratic Lyapunov function based on the extended state vector $\xi_k$ . . . . .	72
5.1.2	A Lyapunov-Krasovskii functional . . . . .	76
5.2	Variable sampling intervals, large delays, and packet dropouts . .	77
5.2.1	A common quadratic Lyapunov function based on the extended state vector $\xi_k$ . . . . .	78
5.3	Illustrative examples . . . . .	80
5.3.1	Motor-roller example . . . . .	81
5.3.2	Fourth-order motion control system . . . . .	89
5.4	Discussion . . . . .	91
<b>6</b>	<b>Tracking control</b>	<b>93</b>
6.1	Small delays . . . . .	94
6.1.1	Tracking problem . . . . .	94
6.1.2	Input-to-state stability . . . . .	96
6.2	Variable sampling intervals, large delays, and packet dropouts . .	100
6.2.1	Tracking problem . . . . .	101
6.2.2	Input-to-state stability . . . . .	102
6.3	Tracking control performance . . . . .	107
6.3.1	Feedforward error . . . . .	107
6.3.2	Solution to the approximate tracking problem . . . . .	109
6.4	Illustrative examples . . . . .	109
6.5	Discussion . . . . .	111
<b>7</b>	<b>Experimental validation of the stability of NCSs with delays</b>	<b>113</b>
7.1	NCS model . . . . .	113
7.2	Stability . . . . .	115
7.3	The experimental set-up . . . . .	117
7.4	Experimental results . . . . .	119
7.4.1	Constant delays . . . . .	119
7.4.2	Periodic Delays . . . . .	119
7.4.3	Randomly Time-Varying Delays . . . . .	120
7.5	Discussion . . . . .	126

<b>8</b>	<b>Conclusions and recommendations</b>	<b>127</b>
8.1	Conclusions . . . . .	127
8.1.1	Networked Control Systems . . . . .	127
8.1.2	High-tech systems design . . . . .	130
8.2	Recommendations . . . . .	131
<b>A</b>	<b>Proofs of theorems and lemmas</b>	<b>135</b>
A.1	Proof of Lemma 3.2.1 . . . . .	135
A.2	Proof of Lemma 3.3.1 . . . . .	136
A.3	Proof of Lemma 3.4.1 . . . . .	138
A.4	Proof of Theorem 4.3.2 . . . . .	139
A.5	Proof of Lemma 4.3.4 . . . . .	141
A.6	Proof of Lemma 4.3.5 . . . . .	142
A.7	Proof of Theorem 4.3.6 . . . . .	143
A.8	Proof of Lemma 4.4.2 . . . . .	146
A.9	Proof of Theorem 4.4.7 . . . . .	149
A.10	Proof of Theorem 5.1.1 . . . . .	152
A.11	Proof of Theorem 5.1.4 . . . . .	152
A.12	Proof of Lemma 6.1.1 . . . . .	155
A.13	Proof of Theorem 6.1.2 . . . . .	157
A.14	Proof of Lemma 6.2.2 . . . . .	160
	A.14.1 Determination of $c_0$ . . . . .	162
	A.14.2 Determination of $c_\rho$ . . . . .	164
A.15	Proof of Theorem 6.2.3 . . . . .	167
<b>B</b>	<b>Jordan form</b>	<b>171</b>
B.1	Jordan Canonical form and Real Jordan form . . . . .	171
B.2	Jordan forms of the NCS model . . . . .	174
B.3	Time-varying sampling intervals . . . . .	182
B.4	Output-feedback . . . . .	191
<b>C</b>	<b>Controller synthesis based on the Lyapunov-Krasovskii functional</b>	<b>193</b>
	<b>Summary</b>	<b>209</b>
	<b>Samenvatting</b>	<b>211</b>
	<b>Acknowledgments</b>	<b>213</b>
	<b>Curriculum vitae</b>	<b>215</b>





## *List of abbreviations*

BMI	bilinear matrix inequality
CAN	controller area network
ESF-CQLF	extended state-feedback controller, common quadratic Lyapunov function
GAS	globally asymptotically stable
GES	globally exponentially stable
ISS	input-to-state stability
LMI	linear matrix inequality
L-K	Lyapunov-Krasovskii
NCS	networked control system
SF-CQLF	state-feedback controller, common quadratic Lyapunov function
SF-CQLF*	state-feedback controller, common quadratic Lyapunov function (synthesis based on [19])
SF-LK	state-feedback controller, Lyapunov-Krasovskii functional
ZOH	zero-order-hold



# *Introduction*

---

1.1	High-tech systems design	1.3	Networked Control Systems
1.2	Control, computation, and communication	1.4	Contribution of the thesis
		1.5	Structure of the thesis

---

## *1.1 High-tech systems design*

The complexity of the design of mechatronic systems, such as wafersteppers, electron microscopes, and copiers, increased rapidly over the past decade. A major reason for this increase in complexity is the fact that more functionality and a higher performance is desired compared to preceding products, while the cost price should be kept as low as possible to have a competitive position in the market. To design such high-tech systems, different disciplines, such as mechanical, electrical, and software engineering, need to cooperate closely. During the design process, many choices have to be made that influence the later stages of the product design and the final product. If the consequences of these choices are not assessed correctly, especially the effects for the other disciplines, problems will occur later in the design process with various drawbacks such as longer development times, higher product costs, or non-optimal products. At present, these problems are difficult to prevent as it is hard to oversee the consequences of such design decisions. Several reasons why this is the case are described in [33]. Firstly, often there is a lack of a common background and language between the different engineering disciplines, cooperating in the design process, to properly make tradeoffs. Secondly, the project evolution is often out-of-phase for the different engineering disciplines. Thirdly, many choices are made in an implicit way, based on experience or intuition, which often hampers a well founded decision. Fourthly, dynamic, time depending aspects of a system are complex to understand, especially the relation with other disciplines. Of course, there are also many other reasons for making suboptimal design decisions in a multi-disciplinary design environment.

A way to reduce the number of non-optimal design decisions during high-tech systems design, is, based on the ‘Boderc philosophy’ [33], the use of models that capture the system behavior, and a reasoning method that indicates how and when to use these models. Two approaches can be followed to model system behavior. Firstly, multi-disciplinary models can be used, and secondly, mono-disciplinary models can be used that exploit information from or provide

knowledge to other mono-disciplinary models. For both approaches examples are given in [33]. An advantage of the first approach (multi-disciplinary model) is the combination of aspects from the different disciplines in one model, which allows for reasoning on the effects of a design decision on the different engineering disciplines. A disadvantage is the limited amount of information from each discipline that can be included in the model, to avoid that the model loses its transparency and therefore complicates the reasoning. An advantage of the second approach (the mono-disciplinary model) is that standard modeling and analysis tools from each discipline can be used, allowing for more details (and thus complexity) in the models. A disadvantage is that shared knowledge between models should contain information that is useful for the models of the other engineering disciplines. Due to the lack of a common background between the disciplines, reasoning on useful shared knowledge that defines the relation between the mono-disciplinary models, can be complicated.

This thesis presents a model (and related analysis and synthesis tools) that belongs to the second approach. The focus of the model, as well as the analysis, is on the relation between the disciplines control engineering and real-time software engineering, using a control engineering perspective. This work should facilitate the decisions made during the project stages where the controllers are designed and implemented in the software. This thesis is not the only work in the Boderc project that considers the coupling between real-time software engineering and control engineering. In [94], where also a control engineering perspective is used, an event-driven controller is proposed that results in a reduction of the processor load, therefore reducing the demands from control engineering on software engineering. In [21], where a software engineering perspective is used, a new software design method, including controller implementation, is proposed that has a deterministic and predictable timing behavior (which is favorable from a control engineering perspective). The next section will discuss the coupling between software and control engineering in more detail and discuss some domain specific properties and requirements.

## 1.2 *Control, computation, and communication*

The focus of the coupling between control engineering and software engineering is, in this thesis, on the information flows between the mechatronic system (in control engineering denoted as plant) and the processor, on which the controller is implemented. In particular, the timing aspects, related to delays, loss of information, and the sampling intervals in the control loop are considered. These effects are also discussed in literature related to control, communication, and computation, see e.g. [30; 66] and the references therein. Note that in this thesis the size of the data transmitted, which is related to quantization effects, is not considered.

Traditionally, the control scheme consists of a plant, that is via a direct, hard-wired connection, coupled to the controller, see Figure 1.1. In general, for the controller design, it is assumed that the delays in the control loop are

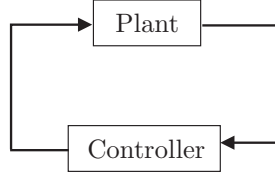


Figure 1.1: Traditional control scheme

negligible or constant. This assumption is (approximately) correct as long as the controller is implemented on a dedicated processor, i.e. it is only used for the control computations. However, in many high-tech systems, to decrease the cost price, the processor is used both for the control computation and for many other software tasks, such as interrupt and error handling, resulting in the fact that the control computation cannot start directly if the sensor data becomes available, e.g. due to the fact that another software task needs to be finished first. Even worse, the processor can be shared between different controllers for different plants or parts of the plant, which makes the use of a communication network, such as Ethernet or a CAN-bus [85], between the processor and the different plants necessary, see Figure 1.2. From a software point of view, in the first situation (without a communication network), latency and jitter, i.e. the combination of constant and time-varying delays that are caused by the computation time and the waiting times until the computation can start, occur. They cannot be avoided, and even worse, cannot be predicted accurately [8; 21; 115]. The size of the latency and jitter is affected by various aspects that are related to the software and its hardware, such as caches, pipelines, and the characteristics of the software architecture. In general, the combination of latency and jitter results in time-variations in the moment of actuation of the controlled system. In the second situation (with a communication network), besides the scheduling of the tasks, which induces latency and jitter because not all controllers can be computed at the same time, the communication network results in time-delays and also data packet loss may occur. The delays in the network are caused by the actual time that is needed to transmit data over the network, the encoding and decoding time of the data, and the waiting times until the network is empty, because for most networks only one data packet can be transmitted over the network at the same time [57; 71]. Data packet loss occurs if data packets collide, if the nodes loose contact with the network, which occurs for instance in wireless networks, or if wrong destination nodes are given to the data packet. These effects of the network may lead to time-variations in the sampling interval as well.

From a control point of view, time-delay, consisting of the combination of both the latency and jitter and the network delays is an undesired phenomenon that should be kept as small as possible, as it is well known [22] that these time-delays can degrade the performance of the controlled system and can even cause instability. For data packet loss similar observations can be made. In

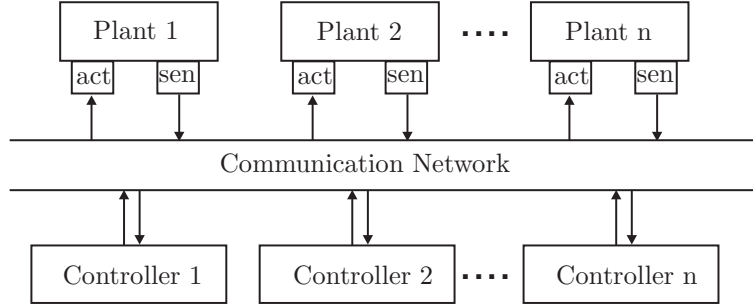


Figure 1.2: A typical NCS setup.

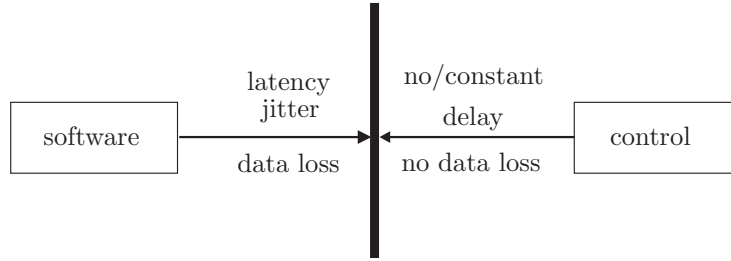


Figure 1.3: Schematic view of the traditional (absence of the) coupling between real-time software and control engineering.

practice, in many motion control applications it is assumed that, firstly, the time-delay is negligible compared to the chosen sampling frequency or it is at least constant, secondly, loss of data does not occur, and thirdly, the sampling interval is constant. Clearly, the occurrence of latency and jitter that are time-varying, and the possibility of data loss make that these general assumptions are often violated. Schematically, this lack of a common background between the two disciplines, resulting in the absence of a coupling, is depicted in Figure 1.3.

In this thesis, we describe a first step towards incorporating effects from the computation and implementation of the controller (which is in general part of the real-time software) and/or the communication network in the control design by developing analysis and design techniques that include time-varying delays, data loss, and time-varying sampling intervals. This is a major step compared to the traditional control techniques that are based on the general assumptions that the time-delay is constant or even zero, the sampling interval is constant, and data loss does not occur. Schematically, this improved situation is depicted in Figure 1.4. Now, in the coupling between control and real-time software engineering the demands on the maximum time-delay, the amount of data loss, and the variation in the sampling interval for which stability and a certain performance can be guaranteed, can be compared to the achievable latency, jitter,

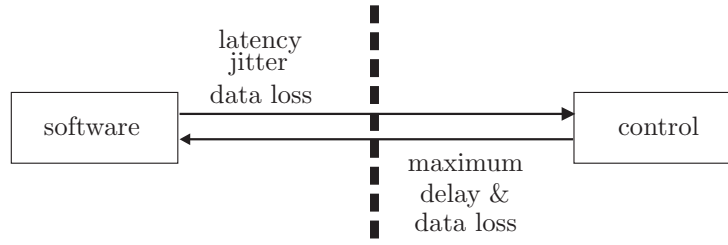


Figure 1.4: Schematic view of the proposed coupling between real-time software and control engineering with mutual consideration of requirements.

and the possibility of data loss in the software implementation. As depicted in Figure 1.4, the opposite direction is possible as well. This viewpoint allows for explicit tradeoffs by considering the consequences of the design choices in one domain on the performance or requirements in the other domain. This allows for a more integrated design process, thereby leading to products closer to optimality.

The presence of, firstly, latency and jitter that cannot be avoided in the software implementation of the controller, secondly, communication delays and/or, thirdly, packet dropouts in the communication network is, from a control engineering perspective, described in the part of literature that is involved with so-called Networked Control Systems (NCSs). In general, NCSs describe control systems with time-varying delays, time-varying sampling intervals, and packet dropouts, or a subset of these three. The next section introduces NCSs and gives an overview of the modeling approaches, analysis results, and design tools that are described in the NCS literature.

### 1.3 Networked Control Systems

Networked Control Systems (NCSs) are systems where the control loop, in general consisting of a continuous-time plant and a discrete-time controller, is closed over a communication channel. A schematic representation of a NCS is depicted in Figure 1.2. Here, different plants (or parts of plants) with sensors and actuators are connected over a communication network to their controllers that are all executed on one shared processor or on multiple processors.

Over the past decade, the interest in NCSs has increased rapidly [35; 107; 122; 133]. It is currently even considered to be one of the key research fields for control engineering, as advocated in [72]. The advantages of the use of a NCS are its flexible architecture [107], due to the use of distributed elements, and a reduction of installation and maintenance costs [35]. Typical applications are mobile sensor networks [54; 86], remote surgery [2; 65], automated highway systems, and unmanned aerial vehicles [93; 99; 100]. As already discussed before, the disadvantages of a NCS are caused by the unreliability and shared use of the network, resulting in time-varying delays, packet dropouts, the use

of multiple packets to transmit data, and variations in the sampling interval. The nature of the time-delays (both latency and jitter), the need for multiple packets, and the possibility of packet dropouts depend on the chosen network protocol, or more precisely the media access control protocol component, and the network [57; 71; 85; 113].

The CAN-protocol (e.g. used in DeviceNet) is a protocol that considers random access with collision arbitration. It ensures that ongoing transmissions are never corrupted and collisions are nondestructive (i.e. the data is not corrupted). Therefore, packet dropouts are not likely to happen. Moreover, time-delays are deterministic (meaning that a maximum response time can be guaranteed), but time-varying, although the variation is limited for the nodes with high priorities, see [57; 71; 85]. Disadvantages are the small size of data packets, the limited physical network length, and the slow data rate. The time-division multiplexing (TDM) protocol uses a round-robin fashion to allocate which node can send data. The allocation is either master-slave (e.g. used in Modbus) or token-passing (e.g. used in PROFIBUS and ControlNet). Master-slave means that data is only sent if the master asks, therefore collisions are avoided. For token passing, a network node, e.g. a sensor, can send data if it has the token, otherwise it has to wait until it receives the token. An advantage of TDM is that the behavior is deterministic, resulting in computable bounds on the variation of the delay. Moreover, packet dropouts are not likely to happen, because data collisions are avoided. A disadvantage of TDM, with token passing, is the inefficiency at low utilizations, due to the overhead of the token passing. Ethernet is a random access network, also denoted as carrier sense multiple access (CSMA). Standard Ethernet is not a complete protocol, it is nondeterministic and collisions are destructive, which means that the data is corrupted and the message must be retransmitted. To obtain more deterministic behavior, different Ethernet solutions are available, see e.g. [71] and the references therein. First, Hub-based Ethernet is available that considers a CSMA/CD protocol, where CD refers to collision detection. After a collision detection, the data is retransmitted. If this fails sixteen subsequent times, the data is discarded, resulting in a packet dropout. Based on different schemes of retransmission an upper bound for the delay of the successfully transmitted packets can be computed. Note that for control implementation, retransmission of data is often not useful, especially if newer data is already available. In that case, the try-once-discard (TOD) protocol can be used, where a packet is dropped if the transmission fails, see e.g. [113]. Second, Switched Ethernet can be used that is based on a CSMA/CA protocol, where CA refers to collision avoidance. Compared to Hub-based Ethernet, intelligence is used in forwarding packets, avoiding message collisions on the network. However, congestion at the switches may occur, which may lead to packet dropouts. The bounds on the variation of the delay can be computed, but the upper bound is, for a low network load, higher than the bound obtained for Hub-based Ethernet. Finally, Wireless Ethernet can be used that considers CSMA/CA as well. Here, packet dropouts are more likely to happen, due to link failures, and moreover, collisions that can still occur, [71]. The advantage of all Ethernet solutions compared to



CAN and TDM is the use of much larger data packet sizes and larger physical networks. In summary, all networks suffer from some variation in the delays, while packet dropouts mainly occur in Ethernet based networks.

The variation in the sampling interval may have different reasons. Different possible implementations, leading to time-varying sampling intervals, will be described shortly. Firstly, the controller requests, via the network, new measurement data from the sensor at certain (equidistantly spaced) time intervals. Due to the delay in the network, the sampling interval becomes time-varying. Secondly, the sensor obtains its measurement data at non-equidistantly spaced sampling intervals, which may happen if a sensor is programmed to wait a fixed amount of time *after* the data is sent to the controller, see [106]. Due to a network that may be occupied, the moment of sending the data is time-varying. Thirdly, the controller may be designed such that larger sampling intervals are used if the network load is high and smaller sampling intervals are used if the network load is low, see e.g. [89]. Fourthly, if event-driven controllers, as discussed in e.g. [10; 34; 94], are used, sensing and actuation is not performed at equidistantly spaced time-intervals. Fifthly, the timer that determines the sampling instants may show some deviation in its timing, leading to variation in the sampling intervals.

As already mentioned in the beginning of this section, for NCSs many papers are available in the literature. Below, the relevant literature is discussed, based on the differences in the modeling approach and the methods for stability analysis, controller synthesis, and tracking behavior. Finally, we also indicate what the available results for experimental validation are in the literature.

### 1.3.1 Modeling

An extensive literature is available on the modeling of NCSs, including the previously described effects of time-varying delays, time-varying sampling intervals, and packet dropouts, discussing both discrete-time and continuous-time NCS models.

One of the first discrete-time NCS models has been proposed in [31; 90]. Herein, a finite-dimensional time-varying discrete-time model for a NCS configuration is proposed with a continuous-time plant, a time-driven sensor and controller, that have the same sampling time, but a time skew between them is allowed, and an event-driven actuator. Moreover, the delays can be larger than the time skew between the sensor and controller, but need to be smaller than the sampling time of the sensor and controller, resulting in sequential arrivals of the measurements at the controller and the inputs at the actuator. The most common discrete-time NCS model is explained in e.g. [4; 85; 133]. Herein, a NCS configuration with a time-driven sensor and an event-driven controller and actuator is considered, where the time-varying delay is upper-bounded by the sampling interval. An extension for this standard discrete-time NCS model that incorporates delays larger than the sampling interval, although the variation of the delays is limited by the sampling interval, is presented in [55; 123]. A discrete-time model that considers arbitrary time-varying delays is described

in [124]. However, message rejection, being the effect that more recent control data becomes available before the older data is implemented resulting in the older data being discarded, is not considered. All the above mentioned models have in common that they consider a NCS with a continuous-time plant, with a constant sampling interval (of the sensor) and a network without packet dropouts.

In [39; 41; 42] packet dropouts, with a stochastic distribution, are modeled, while the delays are assumed to be equal to zero. A limitation is that in these approaches a discrete-time plant is used. A model that considers a discretization of the continuous-time plant is presented in [133], where deterministic packet dropouts, instead of dropouts originating from a stochastic distribution and no delays, are used. The number of papers that combine packet dropouts and time-varying delays is small. A first step is presented in [126], where packet dropouts and constant delays in combination with a discrete-time plant are included in the model. An improvement is presented in [28; 59], where packet dropouts and delays smaller than the sampling intervals are considered, in combination with a continuous-time plant. In [28], the packet dropouts are modeled as an increase of the sampling interval. In [59] time-delays are assumed to take values in a limited set of equidistantly spaced values smaller than the sampling interval and packet dropouts are modeled as a multiple of the delays. Note that this model is limited to delays between the sensor and the controller. A completely different model that can deal with packet dropouts, is presented in [36]. Here, instead of a model that describes the states of the system at the sampling instants, an event-based model is proposed, where the events are defined as the sampling and actuation actions. This representation allows to model, besides packet dropouts, delays that can be both smaller and larger than the sampling interval and time-varying sampling intervals. Note that, the modeling of the packet dropouts is implicit, because no actuation event occurs if a packet is dropped. This event-based model is not the only model that deals with time-varying sampling intervals; however, it is the only discrete-time model that combines time-varying sampling intervals, time-varying delays and packet dropouts. Other models that deal with time-varying sampling interval are proposed in [92; 95; 97; 98; 131], where in [92; 95] time-varying delays smaller than the sampling interval are included as well.

A continuous-time NCS modeling approach is given in [114] for a continuous-time plant and controller. Here, a variation in the transmission times is included, which refers for sampled-data systems to a variation in the sampling interval. A similar approach is considered in [69], where stochastic sampling intervals are allowed. An improvement for NCSs, where a discrete-time controller is considered, uses delay-differential equations, see [75; 125; 127; 128]. Here, a NCS with a constant sampling interval, packet dropouts, and delays that may be larger than the sampling interval is described. A main advantage of this delay-differential approach is the possibility to incorporate time-delays larger than the sampling interval without increasing model complexity, as is the case in the discrete-time modeling approach.

An impulsive differential modeling approach that considers plant dynam-

ics in combination with the network protocol is considered in e.g. [80]. Here NCSs with time-varying sampling intervals and packet dropouts are considered, however delays are neglected. An extension to this model is the impulsive *delay*-differential approach, as proposed in [73; 74; 76] that describes NCSs with variable sampling intervals, time-varying delays, and packet dropouts. Analogous to the delay-differential model, the main advantage of this modeling approach is the possibility to incorporate time-delays larger than the sampling interval without increasing model complexity.

Summarizing, for discrete-time NCS models, there are hardly any models that combine the effects of time-varying delays smaller and larger than the sampling interval, packet dropouts, and variations in the sampling interval. The development of a model that includes these effects gives the possibility to use the advantages of the existing analysis and design tools for discrete-time systems to analyze NCSs including all these effects. Note that recently in [36] such a model is proposed. However, the possibility of packet dropouts and message rejection is only included implicitly. Therefore, a discrete-time model that includes all these effects explicitly is still lacking. Alternative models, that deal with the effects of time-varying sampling intervals, time-varying delays, and packet dropouts, are based on (impulsive) delay-differential equations, see e.g. [76]. The next section will discuss the stability analysis and controller synthesis results that are available for both discrete-time and continuous-time models.

### 1.3.2 Stability analysis and controller synthesis

For the discrete-time NCS models, different approaches towards stability analysis and controller synthesis results are available in the literature. Most of them, see e.g. [36; 38; 55; 87; 88; 92; 119; 123; 126] consider a Lyapunov-based approach, although the method that is used to deal with the uncertainty (or time-variation) in the delays, sampling intervals, or packet dropouts is different. In [38; 119] a NCS with time-varying delays smaller than the constant sampling time and no packet dropouts is considered. In [38], the analysis is based on a Taylor series approximation of the NCS model, which leads to an uncertain system with polytopic uncertainties. For this approximated system, linear matrix inequalities (LMIs) are proposed for both the stability analysis and the controller synthesis problem. The procedure is iterative in the sense that the order of the Taylor series approximation is increased until -if ever- a feasible controller is found for the approximated system. An additional LMI test is used to evaluate whether the constructed controller is also stabilizing for the original plant, i.e. including the approximation error. In [119], another Lyapunov-based controller synthesis approach is proposed, where the time-delays are considered as time-varying parametric uncertainties. The set of discrete-time system matrices is overestimated based on the maximum singular value of the continuous-time system matrix, resulting in a single set of LMIs. Therefore, the iterative procedure and additional LMI test of [38] are avoided, however, leading to more conservative results compared to [38].

NCSs with delays larger than the sampling interval are considered in [55; 60;

87; 88; 123; 124]. A stability analysis and controller synthesis approach based on discrete-time Lyapunov-Krasovskii functionals for deterministic variations in the delay are proposed in [55; 87; 88]. The uncertainties in the system, due to the delays, are written as a multiplication of constant matrices and a time-varying matrix that is Lebesgue measurable. Then, standard robust stability techniques for uncertain systems are applied. For delays that vary based on a stochastic distribution, in [123], a stochastic Lyapunov approach is considered and in [60; 124] an optimal controller is proposed.

Stability analysis and controller synthesis techniques for NCSs with packet dropouts are discussed in [28; 41; 120; 126]. An approach based on a common quadratic Lyapunov function and a convex overapproximation of the uncertain discrete-time system matrices, which depend on the variation in the delays smaller than the sampling interval, is given in [28]. In [126], a common quadratic Lyapunov function is considered for a NCS with a discrete-time plant, packet dropouts, and constant delays. In [120], a similar configuration is studied based on a packet dropout dependent Lyapunov function. An optimal control approach is presented in [41], based on a stochastic approach. A necessary and sufficient condition for stability analysis of NCSs with packet dropouts and delays that take values from a finite set of delays is proposed in [59]. In general, the analysis conditions are difficult, or even impossible, to check, due to the number of different solutions for the switched system that need to be considered separately. Only for a small number of different delays or packet dropouts a solution can be obtained.

For time-varying sampling intervals, the literature is limited. In [92], a common quadratic Lyapunov approach is considered in combination with a finite gridding approach, which exists of a previously defined finite set of delays. The proposed LMI conditions for control design are, in general, not sufficient for arbitrary (bounded) time-variations in the delay. In [97] an optimal controller is proposed that deals with a system with two different sampling intervals. In [36], a Lyapunov approach is considered for an event-based model that includes time-varying sampling intervals, time-varying delays, and packet dropouts. The analysis and synthesis conditions are based on a similar Taylor overapproximation as in [38]. A disadvantage compared to the other Lyapunov approaches for discrete-time models is that, due to the use of the events, the Lyapunov function needs to be decreasing at smaller time instants, because the time between the events, which are determined by the sampling and the actuation instants, is typically smaller than the time between two sequential sampling instants. This may induce some conservatism compared to the models that are consider the sampling instants only.

A completely different stability analysis approach is described in [45], where frequency-domain stability conditions for single-input-single-output systems, based on the small gain theorem are proposed. The related analysis is applicable to systems with both small and large delays, because the discretization of the continuous-time plant is based on the non-delayed system. A disadvantage of this approach is the fact that it is limited to systems with a strictly proper and stable plant and a constant sampling interval. This restriction is

avoided in the approach presented in [46].

For the continuous-time NCS models, the analysis and synthesis conditions are mainly based on Lyapunov or Lyapunov-like functions. First, for the continuous-time NCS model, in [113], a maximum allowable transfer interval (MATI) is computed, based on a common quadratic Lyapunov function, which gives the maximum amount of time between two consecutive sensor messages for which stability can be guaranteed. An improvement is presented in [49], based on a Lyapunov-Krasovskii functional that is more suitable for systems with time-delays. Second, for delay-differential models, stability conditions based on Lyapunov-Razumikhin functionals [127] and based on Lyapunov-Krasovskii functionals [27; 75; 125; 128] are available. It is shown that, in general, the Lyapunov-Krasovskii functionals are less conservative. Unfortunately in all these papers, the use of the candidate Lyapunov-Krasovskii functionals results in conservative results, because the complete quadratic Lyapunov-Krasovskii functional that gives exact stability bounds is not solvable in practice, see [51; 52]. The stability analysis conditions presented in [27] and [75] consider both the minimum value and the maximum value of the delays and packet dropouts, while the other papers consider only the maximum value. Typical for these approaches is that the uncertain and time-varying delays are included in the Lyapunov function itself and are not part of the system matrices, as is the case for the discretized NCS models, see e.g. [38; 87; 119]. Therefore the need of uncertainty matrices and the corresponding overapproximation is avoided. Third, for the impulsive differential equations, without delays, input-to-state (and input-output) stability properties have been studied in [18; 80; 81; 104]. In these works, specific attention is given to the role of the network protocol in guaranteeing stability. Finally, for the impulsive delay-differential model, sufficient LMI conditions for the exponential stability of NCSs are proposed in [76], using a Lyapunov-Krasovskii approach.

Summarizing, for stability analysis and controller synthesis, many results are available for discrete-time NCS models, but most of the results are, due to the models used, limited to NCSs with, firstly, time-varying delays or, secondly, packet dropouts and delays smaller than the constant sampling interval, or, thirdly, time-varying sampling intervals. The combination of time-varying delays (smaller and larger than the sampling interval), time-varying sampling intervals, and packet dropouts is only handled in [36] based on an event-driven model. The amount of literature for continuous-time NCS models is smaller. For the (impulsive) delay-differential models, see e.g. [76], that include time-varying sampling intervals, time-varying delays, and packet dropouts, results are available for stability analysis and controller synthesis. A disadvantage of these approaches is that in general, for standard and basic Lyapunov-Krasovskii functionals, the results are rather conservative. To obtain less conservative conditions, Lyapunov-Krasovskii functionals consisting of many different terms are used to obtain a candidate Lyapunov-Krasovskii functional that describes the exact Lyapunov-Krasovskii functional as close as possible. However, this results in rather complex LMI conditions that need to be solved for stability analysis or controller synthesis.

### 1.3.3 Tracking

In the NCS literature, the tracking problem has received very little attention. Recent works related to the tracking control of systems over networks are [25; 129]. In [25], an  $H_\infty$ -approach towards the tracking control problem of NCSs with network delays (and constant sampling intervals) is presented. However, the fact that the feedforward generally experiences delays is not taken into account. In [129], the optimal tracking control problem is studied with a focus on the effects of quantization in the feedforward.

In this thesis, the tracking problem is investigated based on input-to-state stability conditions of the tracking error dynamics with respect to network-induced perturbations on the ‘ideal’ feedforward. Note that input-to-state conditions are proposed in [18; 80; 81; 104] for a NCS model based on impulsive differential equations, including packet dropouts and time-varying sampling intervals (no delays), as discussed above.

### 1.3.4 Experiments

The experimental validation of the obtained stability analysis and controller synthesis results has received very little attention to this date. A first attempt towards validation is co-simulation [32; 133] for NCSs, where two computers are connected over a communication network. Herein, one computer is used as a controller, while the other is used for simulation of the plant model.

Experimental validation in the field of NCSs is described in [29; 50; 62; 89; 92]. In [89], validation of an optimal controller, designed for the zero-delay situation, in combination with a sampling-rate adaptation algorithm is described. It is shown that the system is stabilized for constant delays that are either zero or equal to one sampling interval. It is worth noting that, in [89], periodic time-delays are not considered, while this periodicity, according to the examples in [16; 118], can lead to instability. In [92], experimental results are presented that consider variations in the sampling interval, with, however, negligible time-delays. In [50] experiments for a NCS with sporadic packet dropouts and no delays are performed. Other examples of experimentally validated networked control approaches deal with model predictive controllers, see e.g. [29; 62], where a NCS with time-varying delays is considered, and [105], where besides the delays, packet dropouts are allowed.

Other experimental work deals with measurements of the time-delays of different networks under different network loads, see e.g. [57; 71; 85]. In [89], similar measurements are performed to determine the occurrence of packet dropouts.

Summarizing, the literature on validation of stability analysis results is limited to some specific examples. Especially, validation for NCSs with time-varying delays is lacking, except for the model predictive controller designs.

## 1.4 Contribution of the thesis

In this thesis, a discrete-time NCS model, for a system with a continuous-time plant and a discrete-time controller, is derived. The model includes time-varying delays larger than the sampling interval, packet dropouts, and time-varying sampling intervals. It is an extension to the existing discrete-time approaches that are limited to, firstly, delays smaller than the constant sampling interval, with or without packet dropouts or, secondly, time-varying delays larger than the constant sampling interval without packet dropouts, or, thirdly, time-varying sampling intervals with delays that are always smaller than the sampling interval. Compared to [59], where it is assumed that the variation in the delays is limited to  $\tau_k \in \{0, 0.1h, 0.2h, \dots, h\}$ , the model proposed in this thesis assumes that the delays take values from a bounded set, containing an infinite number of values (i.e.  $\tau_k \in [\tau_{\min}, \tau_{\max}]$ ). Compared to [124], the effect of message rejection will be included in the NCS model proposed in this thesis. Message rejection means that data is dropped if it occurs out of order at its destination. In practice, this drop of data is desired to avoid implementation of old data on the system, while more recent data is already available, and it is achieved by means of time-stamping [85]. The model proposed in this thesis is an alternative to the event-based model in [36]. A difference is that in our model the time-instants on which a control input is implemented are defined explicitly and that message rejection and packet dropouts are included explicitly as well. The model proposed in this thesis is an alternative to the (impulsive) delay-differential models proposed in [74; 76; 125; 127; 128]. A difference between the approaches in [74; 76; 125; 127; 128] and the discrete-time NCS model in this thesis, is that here message rejection is included explicitly, while in the (impulsive) delay-differential models it is included implicitly, by demanding a sequential sequence of the samples.

Based on the NCS model, sufficient conditions for stability analysis and controller synthesis of a state feedback controller and an extended state feedback controller [38] are proposed. These conditions are given in terms of linear matrix inequalities (LMIs) and are derived based on either a common quadratic Lyapunov approach or a Lyapunov-Krasovskii approach for discrete-time systems. To deal with the variation in the delays, sampling intervals, and packet dropouts, the discrete-time NCS model is rewritten using a (real) Jordan form of the continuous-time system matrices. This leads to a combination of uncertainty functions that capture the variations in the sampling interval, delays, and packet dropouts. For analysis purposes, based on these uncertainty functions, an overapproximation of the discrete-time model is used that contains the bounds of the sampling intervals, delays, and packet dropouts explicitly (which is not the case in [55; 87; 88]). Compared to [38], the iterative procedure and the large number of LMIs that are needed for an accurate Taylor approximation are avoided. Compared to [119], a different approach is used, because the results are based on the Jordan form and in [119] a singular value decomposition is used. The singular value decomposition yields comparable or more conservative results than the use of the Jordan form, due to the difference between



the singular values and the eigenvalues. Compared to the large delay results of [124], a reduction of the number of uncertain parameters in the stability analysis and controller synthesis is achieved, which is beneficial for reduction of conservatism. Additionally, in this thesis, the controller synthesis results are used to obtain a performance bound on the transient behavior of the NCS.

To this date, the work on NCSs has largely focussed on modeling, stability, and stabilization problems. Tracking control, however, poses additional challenges, some of which are specifically due to the communication network. In tracking control, typical high-performance designs include feedforward control thereby inducing the desired solution in the controlled system, whereas feedback assures convergence to the desired solution and favorable robustness and disturbance attenuation properties. Due to the delays, packet dropouts, and variation in sampling intervals, the feedforward control signal generally does not arrive at the actuator at the intended time, leading to a (network-induced) feedforward error and reduced tracking performance. Consequently, only approximate tracking can be achieved. Therefore, the input-to-state stability (ISS) of NCSs with respect to the feedforward error is investigated. Based on the ISS property, an asymptotic upper bound for the tracking error depending on the properties of the plant, the controller, and the network is studied.

Theoretical studies of stability of NCSs with constant and time-varying delays smaller and larger than the sampling interval have received much attention in the NCS literature. However, the number of studies on experimental validation is limited to certain specific controllers or measurements on the variation and the size of the delays and the number of subsequent packet dropouts. In this thesis, we present experimental results for a continuous-time plant and a discrete-time controller, with time-delays in the control loop. These delays are either constant or time-varying. For constant delays, the existing NCS stability results provide a stability region in the controller space (i.e. the region describing all stabilizing controllers for given constant delays, see e.g. [133]). However, validation of such a region is lacking. Therefore, such a stability region is validated on a typical motion-control set-up, i.e. a single inertia system. Moreover, the effect of periodic delays is experimentally studied on the same set-up. The obtained stabilizing controllers, based on the proposed stability analysis conditions for arbitrary time-varying delays, are validated on this single inertia system and also on a motor-load system, which is another, slightly more complicated, motion control example. These experimental results illustrate the value of the theoretical results in practice.

## 1.5 Structure of the thesis

The outline of the thesis is as follows. Chapter 2 gives some basic preliminaries on stability and input-to-state stability of continuous-time and (switched) discrete-time systems that will be used in Chapters 4, 5 and 6.

Chapter 3 discusses the modeling of NCSs. For the sake of simplicity, first, the NCS model for time-varying delays smaller than the constant sampling in-



terval, without packet dropouts, as available in the NCS literature, is given. Both a continuous-time model and a discrete-time model, based on an exact discretization of the continuous-time model, are discussed. Next, the extensions needed for time-varying delays larger than the sampling interval, packet dropouts, and time-varying sampling intervals are presented. Additionally, a discussion on the differences and the commonalities between the presented NCS models is given.

In Chapter 4, the stability analysis techniques for the NCS models derived in Chapter 3 are discussed. Stability analysis conditions for the discrete-time NCS model are proposed, based on two different controllers, i.e. a state feedback and an extended state feedback controller that includes, next to the state variable, also part of the control input history. The conditions depend on two different candidate Lyapunov functions, i.e. a common quadratic Lyapunov function and a Lyapunov-Krasovskii functional. Based on the obtained stability conditions for the discrete-time NCS model, the stability of the continuous-time plant of the NCS is analyzed. Illustrative examples are presented that give a comparison between the different stability conditions in terms of the candidate Lyapunov functions and the control law.

In Chapter 5, constructive LMI conditions for the controller synthesis for the NCS models are proposed based on the different control laws and candidate Lyapunov functions. Moreover, a performance measure in terms of the transient decay rate is derived in each case. Illustrative examples are given that show the differences between the three Lyapunov-based approaches and the different control laws.

In Chapter 6, a solution to the approximate tracking problem for NCSs is proposed. The effects of the time-varying delays, sampling intervals, and packet dropouts on the feedforward signal are investigated in detail, resulting in a definition of the feedforward error, which can be seen as a perturbation on the tracking error dynamics. Sufficient conditions for input-to-state stability of the tracking error dynamics with respect to the feedforward error are proposed, resulting in bounds on the steady-state tracking error. An illustrative example is given that shows the applicability of the presented approach, compared to the results that are obtained with a delay impulsive differential model (see [74; 111]).

In Chapter 7, experimental results performed on two typical motion control set-ups are presented. A single inertia set-up, which is a second-order system, and a motor-load set-up, which is a fourth-order system, are considered. The measurements on both set-ups are used to validate the stability conditions for NCSs with constant, periodic, and arbitrary, though bounded, time-varying delays smaller and larger than the sampling interval. Compared to Chapter 4, the stability conditions are adapted such that an output-feedback controller in combination with a velocity-estimator is considered, instead of a state-feedback controller.

Chapter 8 states the conclusions and recommendations for future research.

The appendices give the proofs of the proposed theorems and lemmas, which are not included in the main text for readability, and an explanation of the use of the Jordan form for Networked Control Systems.

### 1.5.1 Reading suggestions

For the readers less familiar with NCSs, we suggest to focus on the modeling and control aspects of NCSs with constant sampling intervals, time-delays smaller than this sampling interval, and no packet dropouts. In this way, the reader will encounter the basic modeling formalism used and the strategies towards stability analysis and control design, while avoiding the additional complexity involved when studying large delays, packet dropouts, and time-varying sampling intervals.

Therefore, we suggest to focus on the following sections at first reading. The NCS model for small delays is presented in Section 3.1. Then, Section 4.1 motivates the importance of the investigation of systems with time-varying delays smaller than the sampling interval and Section 4.2 explains the use of the Jordan form to rewrite the NCS model in a form that is applicable for stability analysis. Section 4.3 presents the stability analysis conditions. Illustrative examples are given in Section 4.5 (note that in this section also examples involving delays larger than the sampling interval, packet dropouts, and time-varying sampling intervals are treated). The controller synthesis conditions for a NCS with delays smaller than the sampling interval are discussed in Section 5.1. Illustrative examples are presented in Section 5.3, however again partly merged with examples on the case with delays larger than the sampling interval. The tracking control problem is discussed in Sections 6.1 and 6.3. An illustrative example is presented in Section 6.4. Finally, Chapter 7 can be read to get an idea on the applicability of the proposed stability analysis conditions. However, if one is only interested in the measurement results, Sections 7.1 and 7.2 can be skipped, especially because these sections discuss the generic model, including large delays. Note that Chapter 2 gives a general overview on stability properties that are exploited in Chapters 4, 5, and 6.

## 2

### *Preliminaries*

---

2.1	General mathematical notions	2.3	Stability of discrete-time
2.2	Stability notions for		systems
	continuous-time systems	2.4	Notation

---

This thesis deals with networked control systems that consist of a continuous-time linear plant and a discrete-time controller. Due to the connection of the plant and controller over a network, time-varying delays, time-varying sampling intervals, and packet dropouts occur that need to be considered in the model. To determine whether or not the complete controlled system behaves properly, continuous-time notions of Lyapunov stability are needed. Section 2.2 presents these basic stability notions, including the notion of input-to-state stability, which is a valuable stability notion for systems with inputs and will be exploited in Chapter 6 in the scope of the tracking problem. As the NCS model, proposed in Chapter 3, is based on a discretization of the continuous-time plant also discrete-time notions of Lyapunov stability and input-to-state stability are of importance. These concepts will be introduced in Section 2.3. The discrete-time NCS model that we will use in this thesis belongs, due to the variation of the delays, to the class of switched discrete-time systems. Therefore, the stability of switched discrete-time systems is discussed in Section 2.3.2. Before the different stability notions are presented for the different model structures, Section 2.1 provides basic definitions that are needed in the sequel.

#### **2.1**    *General mathematical notions*

Before the stability and input-to-state stability (ISS) conditions are presented, some typical function classes are introduced.

**Definition 2.1.1** [48] A continuous function  $\alpha : [0, a) \rightarrow [0, +\infty)$  is said to belong to class  $\mathcal{K}$  if it is strictly increasing and  $\alpha(0) = 0$ . It is said to belong to class  $\mathcal{K}_\infty$  if  $a = +\infty$  and  $\alpha(r) \rightarrow +\infty$  as  $r \rightarrow +\infty$ .

**Definition 2.1.2** [48] A continuous function  $\beta : [0, a) \times [0, +\infty) \rightarrow [0, +\infty)$  is said to belong to class  $\mathcal{KL}$  if, for each fixed  $s$ , the mapping  $\beta(r, s)$  belongs to class  $\mathcal{K}$  with respect to  $r$  and, for each fixed  $r$ , the mapping  $\beta(r, s)$  is decreasing with respect to  $s$  and  $\beta(r, s) \rightarrow 0$  as  $s \rightarrow +\infty$ .

In this thesis, the set of all non-negative integers is given by  $\mathbb{N}$  and the set of all non-negative real values is given by  $\mathbb{R}_+$ .

## 2.2 Stability notions for continuous-time systems

This section discusses the stability of continuous-time dynamic systems. Consider the non-autonomous continuous-time system

$$\dot{x} = f(x, t), \quad (2.1)$$

with  $x \in \mathbb{R}^n$  the state,  $t \in \mathbb{R}$  and  $f(x, t)$  is locally Lipschitz in  $x$  and piecewise continuous in  $t$ . Suppose that  $x = 0$  is an equilibrium point of (2.1), i.e.  $f(0, t) = 0$  for all  $t \in \mathbb{R}$ .

**Definition 2.2.1** [48] The equilibrium point  $x = 0$  of (2.1) is

- stable if, for each  $\varepsilon > 0$  and all  $t_0 \in \mathbb{R}_+$ , there is a  $\delta = \delta(\varepsilon, t_0) > 0$  such that

$$|x(t_0)| < \delta \Rightarrow |x(t)| < \varepsilon, \quad \forall t \geq t_0. \quad (2.2)$$

- uniformly stable if, for each  $\varepsilon > 0$ , there is  $\delta = \delta(\varepsilon) > 0$  independent of  $t_0$ , such that for all  $t_0 \in \mathbb{R}_+$  (2.2) is satisfied.
- unstable if it is not stable.
- asymptotically stable if it is stable, for all  $t_0 \in \mathbb{R}_+$  and there is a positive constant  $c = c(t_0)$  such that  $x(t) \rightarrow 0$  as  $t \rightarrow \infty$ , for all  $|x(t_0)| < c$ .
- uniformly asymptotically stable if it is uniformly stable and there is a positive constant  $c$ , independent of  $t_0$ , such that for all  $t_0 \in \mathbb{R}_+$  and for all  $|x(t_0)| < c$ ,  $x(t) \rightarrow 0$  as  $t \rightarrow \infty$ , uniformly in  $t_0$ ; that is, for each  $\eta > 0$ , there is a  $T = T(\eta) > 0$  such that for all  $t_0 \in \mathbb{R}_+$

$$|x(t)| < \eta, \quad \forall t \geq t_0 + T(\eta), \quad \forall |x(t_0)| < c.$$

- globally uniformly asymptotically stable if it is uniformly stable,  $\delta(\varepsilon)$  can be chosen to satisfy  $\lim_{\varepsilon \rightarrow \infty} \delta(\varepsilon) = \infty$ , and, for each pair of positive numbers  $\eta$  and  $c$ , there is a  $T = T(\eta, c) > 0$  such that

$$|x(t)| < \eta, \quad \forall t \geq t_0 + T(\eta, c), \quad \forall |x(t_0)| < c.$$

Note that these definitions describe stability in the sense of Lyapunov. The following lemma give some equivalent definitions, based on comparison functions (class  $\mathcal{K}$  and class  $\mathcal{KL}$  functions).

**Lemma 2.2.2** [48] *The equilibrium point  $x = 0$  of (2.1) is*

- *uniformly stable if and only if there exist a class  $\mathcal{K}$  function  $\alpha$  and a positive constant  $c$ , independent of  $t_0$ , such that for all  $x(t_0)$ , with  $|x(t_0)| < c$  and for all  $t_0 \in \mathbb{R}_+$*

$$|x(t)| \leq \alpha(|x(t_0)|), \forall t \geq t_0.$$

- *uniformly asymptotically stable if and only if there exist a class  $\mathcal{KL}$  function  $\beta$  and a positive constant  $c$  independent of  $t_0$ , such that for all  $x(t_0)$ , with  $|x(t_0)| < c$  and for all  $t_0 \in \mathbb{R}_+$*

$$|x(t)| \leq \beta(|x(t_0)|, t - t_0), \forall t \geq t_0, \forall |x(t_0)| < c. \quad (2.3)$$

- *globally uniformly asymptotically stable if and only if (2.3) is satisfied for any initial state  $x(t_0)$ .*

**Definition 2.2.3** The equilibrium point  $x = 0$  of (2.1) is exponentially stable if there exist positive constants  $c$ ,  $d$ , and  $\lambda$  such that for all  $x(t_0)$ , with  $|x(t_0)| < c$

$$|x(t)| \leq d|x(t_0)|e^{-\lambda(t-t_0)}, \quad (2.4)$$

and globally exponentially stable if (2.4) is satisfied for any initial state  $x(t_0)$ .

### 2.2.1 Input-to-state stability

Consider the system

$$\dot{x} = f(x, t, u), \quad (2.5)$$

where  $f : \mathbb{R}^n \times [0, \infty) \times \mathbb{R}^m \rightarrow \mathbb{R}^n$  is piecewise continuous in  $t$  and locally Lipschitz in  $x$  and  $u$ . The input  $u(t)$  is a piecewise continuous, bounded function of  $t$  for all  $t \geq 0$ .

The definitions for ISS are obtained from [48] and the work presented in [103].

**Definition 2.2.4** [48] The system (2.5) is said to be input-to-state stable if there exist a class  $\mathcal{KL}$  function  $\beta$  and a class  $\mathcal{K}$  functions  $\gamma$  such that for any initial state  $x(t_0)$  and any bounded input  $u(t)$ , the solution  $x(t)$  exists for all  $t \geq t_0$  and satisfies:

$$|x(t)| \leq \beta(|x(t_0)|, t - t_0) + \gamma \left( \sup_{t_0 \leq s \leq t} |u(s)| \right). \quad (2.6)$$

This guarantees that for bounded inputs  $u(t)$  the state  $x(t)$  is bounded. The following Lyapunov-like theorem gives a sufficient condition for ISS.

**Definition 2.2.5** [48] Let  $V : \mathbb{R}^n \times [0, \infty) \rightarrow \mathbb{R}^n$  be a continuously differentiable function such that

$$\alpha_1(|x|) \leq V(x, t) \leq \alpha_2(|x|), \quad (2.7)$$

$$\frac{\partial V}{\partial t} + \frac{\partial V}{\partial x} f(x, t, u) \leq -W_3(x), \quad \forall |x| \geq \rho(|u|) > 0, \quad (2.8)$$

for all  $(x, t, u) \in \mathbb{R}^n \times [0, \infty) \times \mathbb{R}^m$ , where  $\alpha_1, \alpha_2$  are class  $\mathcal{K}_\infty$  functions,  $\rho$  is a class  $\mathcal{K}$  function, and  $W_3$  is a continuous positive definite function on  $\mathbb{R}^n$ . Then, the system (2.5) is input-to-state stable with  $\gamma = \alpha^{-1} \circ \alpha_2 \circ \rho$ .

## 2.3 Stability of discrete-time systems

Consider the nonlinear discrete-time system

$$x_{k+1} = f(x_k, k), \quad (2.9)$$

with  $x_k \in \mathbb{R}^n$  the state,  $k \in \mathbb{N}$  the sampling instant and  $f : \mathbb{R}^n \times \mathbb{N} \rightarrow \mathbb{R}^n$  a possibly discontinuous function. Suppose that  $x = 0$  is a fixed point of (2.9), i.e.  $f(0, k) = 0, \forall k \in \mathbb{N}$ . Analogous to the continuous-time case, stability in the sense of Lyapunov can be considered. The definitions are based on [23; 44] and [70].

**Definition 2.3.1** The fixed point  $x = 0$  of (2.9) is

- stable if, for each  $\varepsilon > 0$  and all  $k_0 \in \mathbb{N}$ , there is a  $\delta = \delta(\varepsilon, k_0) > 0$  such that

$$|x_{k_0}| < \delta \Rightarrow |x_k| < \varepsilon, \quad \forall k \geq k_0. \quad (2.10)$$

- uniformly stable if, for any  $\varepsilon > 0$ , there is a  $\delta = \delta(\varepsilon) > 0$ , independent of  $k_0$ , such that for all  $k_0 \in \mathbb{N}$  (2.10) is satisfied.
- unstable if it is not stable.
- asymptotically stable if it is stable for all  $k_0 \in \mathbb{N}$  and there is a positive constant  $c = c(k_0)$  such that  $x_k \rightarrow 0$  as  $k \rightarrow \infty$ , for all  $|x_{k_0}| < c(k_0)$ .
- uniformly asymptotically stable if it is uniformly stable and there is a positive constant  $c$ , independent of  $k_0$ , such that for each  $\eta > 0$ , there is a  $T = T(\eta) > 0$  such that for all  $k_0 \in \mathbb{N}$

$$|x_k| < \eta, \quad \forall k \geq k_0 + T(\eta), \quad \forall |x_{k_0}| < c. \quad (2.11)$$

- globally uniformly asymptotically stable if it is uniformly stable,  $\delta(\varepsilon)$  can be chosen to satisfy  $\lim_{\varepsilon \rightarrow \infty} \delta(\varepsilon) = \infty$ , and, for each pair of positive numbers  $\eta$  and  $c$ , there is a  $T = T(\eta, c) > 0$  such that

$$|x_k| < \eta, \quad \forall k \geq k_0 + T(\eta, c), \quad \forall |x_{k_0}| < c.$$

**Definition 2.3.2** The fixed point  $x = 0$  of (2.9) is exponentially stable if there exist positive constants  $\theta > 0$ ,  $m \in [0, 1)$ , and  $c > 0$ , such that for all  $x(k_0)$  with  $|x(k_0)| < c$

$$|x_k| \leq \theta |x(k_0)| m^{k-k_0}, \quad \forall k \geq k_0, \quad k_0 \in \mathbb{N}, \quad (2.12)$$

and globally exponentially stable if (2.12) holds for any  $x(k_0)$  and  $k_0 \in \mathbb{N}$ .

To prove stability in the sense of Lyapunov of a fixed point of (2.9), a difference function based on the Lyapunov function  $V$  is used, defined as:

$$\Delta V(x, k) = V(x_{k+1}, k+1) - V(x_k, k).$$

The following stability conditions, based on Lyapunov functions are derived from [23; 44]. Let us start with some definitions on the function  $V(x, k)$  and its forward difference  $\Delta V(x, k)$ .

**Definition 2.3.3** If there exists a function  $V : \mathbb{R}^n \times \mathbb{N} \rightarrow [0, \infty)$  that is continuous and satisfies  $V(0, k) = 0$  for all  $k$  and

- (i) there exists a scalar function  $w_1 \in \mathcal{K}$ , such that for all  $k$  and all  $x \neq 0$ :  

$$V(x, k) \geq w_1(|x|);$$
- (ii) the forward difference  $\Delta V(x, k)$  satisfies for all  $k \in \mathbb{N}$  and all  $x \neq 0$   

$$\Delta V(x, k) = V(f(x, k), k+1) - V(x_k, k) \leq 0;$$
- (iii) there exists a scalar function  $w_3 \in \mathcal{K}$ , such that the forward difference  $\Delta V(x, k)$  satisfies for all  $k \in \mathbb{N}$  and for all  $x \neq 0$   

$$\Delta V(x, k) = V(f(x, k), k+1) - V(x_k, k) \leq -w_3(|x|) < 0;$$
- (iv) there exists a function  $w_2 \in \mathcal{K}$ , such that for all  $k \in \mathbb{N}$  and all  $x \neq 0$ ,  

$$V(x, k) \leq w_2(|x|);$$
- (v)  $w_1(|x|) \rightarrow \infty$  when  $|x| \rightarrow \infty$ , i.e. the function  $w_1(|x|)$  in (i) is of class  $\mathcal{K}_\infty$ , instead of  $w_1(|x|) \in \mathcal{K}$ .

Based on these definitions, the following stability conditions hold [44]. The origin of system (2.9) is

1. stable, if (i) and (ii) are satisfied;
2. uniformly stable, if (i), (ii), and (iv) are satisfied;
3. asymptotically stable, if (i) and (iii) are satisfied;
4. asymptotically stable, if (i) and (iii) are satisfied;
5. uniformly asymptotically stable, if (i), (iii), and (iv) are satisfied;
6. globally asymptotically stable, if (i), (iii), and (v) are satisfied;
7. globally uniformly asymptotically stable, if (i), (iii), (iv), and (v) are satisfied.

For global exponential stability of the origin of system (2.9), consider  $V(0, k) = 0$ , condition (i), (iv), and (v) in Definition 2.3.3, and

$$\Delta V(x_k, k) = V(x_{k+1}, k+1) - V(x_k, k) < -\gamma V(x_k, k), \quad (2.13)$$

with  $0 < \gamma < 1$ . In [53] and [70] it is proven that this relation for  $\Delta V$  provides global exponential stability. To obtain the ‘exponential’ decay rate, analogous to  $m^{k-k_0}$  in Definition 2.3.2, (2.13) can be rewritten as:

$$V(x_{k+1}, k) \leq (1 - \gamma)V(x_k, k) \Rightarrow V(x_k, k) \leq (1 - \gamma)^{k-k_0} V(x_0, k). \quad (2.14)$$

In [70], based on (2.14), it is shown that an exponential decay rate of the form  $de^{-\lambda(k-k_0)}|x(k_0)|$ , analogous to the continuous-time case in Definition 2.2.3, can be retrieved if the Lyapunov condition (2.13) is satisfied. In this thesis, we consider the decay rate  $(1 - \gamma)^{k-k_0}$  from (2.14), if (2.13) is satisfied, as a measure of the rate of convergence of the exponential stability.

### 2.3.1 Input-to-state stability

To derive the discrete-time equivalent for input-to-state stability, consider the discrete-time autonomous system:

$$x(k+1) = f(x_k, k, u_k), \quad (2.15)$$

with the state  $x_k \in \mathbb{R}^n$  and the input  $u_k \in \mathbb{R}^m$ , and for each time instant  $k \in \mathbb{N}$ . The function  $f : \mathbb{R}^n \times \mathbb{R}^m \times \mathbb{N} \rightarrow \mathbb{R}^n$  is assumed to be continuous and satisfies  $f(0, k_0, 0) = 0$ . For the sake of brevity, in what follows it is assumed that  $k_0 = 0$ . Moreover, the inputs  $u$  are functions  $u : \mathbb{N} \rightarrow \mathbb{R}^m$ . The set of all these functions with the supremum norm satisfying  $\|u\| = \sup\{|u(k)| : k \in \mathbb{N}\} < \infty$  is denoted by  $l_\infty^m$ , where  $|\cdot|$  denotes the Euclidean norm. For each  $x_0 \in \mathbb{R}^n$  and each input  $u$ , the trajectory of the system (2.15) is denoted by  $x(x_0, k, u)$ , with  $x_0$  the initial state and  $u$  the input. Clearly, this trajectory is uniquely defined on  $\mathbb{N}$ , and for each input  $u$  and  $k \in \mathbb{N}$ ,  $x_k(x_0, u, k) = x(x_0, u, k)$  continuously depends on  $x_0$ .

**Definition 2.3.4** [43] System (2.15) is input-to-state stable (ISS) if there exists a class  $\mathcal{KL}$ -function  $\beta : [0, \infty) \times [0, +\infty) \rightarrow [0, +\infty)$  and a class  $\mathcal{K}$ -function  $\gamma$  such that, for each input  $u \in l_\infty^m$  and each  $x_0 \in \mathbb{R}^n$ , it holds that for each  $k \geq k_0 := 0$ :

$$|x(x_0, k, u)| \leq \beta(|x_0|, k) + \gamma(\|u_{[k-1]}\|), \quad (2.16)$$

where  $k \geq 1$  and, for each  $l \geq 0$ ,  $u_{[l]}$  denotes the truncation of  $u$  at  $l$ ; i.e.  $u_{[l]}(j) = u(j)$  if  $j \leq l$ , and  $u_{[l]}(j) = 0$  if  $j > l$ .

**Definition 2.3.5** [43] A continuous function  $V : \mathbb{R}^n \times \mathbb{N} \rightarrow \mathbb{R}^n$  is called an ISS-Lyapunov function for system (2.15) if for all  $x \in \mathbb{R}^n$

$$\gamma_1(|x|) \leq V(x) \leq \gamma_2(|x|), \quad (2.17)$$



holds for some  $\gamma_1, \gamma_2 \in \mathcal{K}_\infty$ , and for all  $x \in \mathbb{R}^n$  and for all  $u \in \mathbb{R}^m$

$$V(f(x, k, u)) - V(x) \leq -\gamma_3(|x|) + \sigma(|u|), \quad (2.18)$$

for some  $\gamma_3 \in \mathcal{K}_\infty$ , and  $\sigma \in \mathcal{K}$ .

The extension for non-autonomous discrete-time systems does not change the proof for ISS of discrete-time systems that was used in [43].

**Proposition 2.3.6** [43] *If system (2.15) admits an ISS-Lyapunov function, then it is ISS.*

### 2.3.2 Stability of switched linear systems

As obtained in the previous paragraph, stability can be proven based on Lyapunov functions. Conditions that guarantee global asymptotic stability based on common quadratic Lyapunov functions will be discussed below. Consider the linear time-invariant discrete-time system:

$$x_{k+1} = Ax_k. \quad (2.19)$$

Stability can be proven based on the candidate Lyapunov function  $V = x_k^T P x_k$ . If there exists a matrix  $P$  that satisfies the following LMI conditions:

$$P = P^T > 0, \quad A^T P A - P < 0,$$

then (2.19) is globally asymptotically stable, see e.g. [6]. Note that  $\Delta V(x_k) = x_{k+1}^T P x_{k+1} - x_k^T P x_k = x_k^T (A^T P A - P) x_k < 0$  is a necessary and sufficient condition for asymptotic stability for (2.19). Moreover, due to the fact that (2.19) is time-invariant, uniform stability is obviously guaranteed. Due to the linearity of the system, global stability is also guaranteed automatically.

To study the stability of time-varying discrete-time systems, we first present results for one of the simplest examples. Consider the following system that consists of a finite set of linear time-invariant systems:

$$x_{k+1} = A_i x_k. \quad (2.20)$$

with  $A_i \in \mathbb{R}^{n \times n}$  and  $i \in \{1, 2, \dots, q\}$ . Note that there exists a finite number of matrices  $A_i$  between which system (2.20) switches, resulting in a switched linear discrete-time system. A sufficient condition for asymptotic stability of  $x = 0$ , based on a common quadratic Lyapunov function candidate  $V = x_k^T P x_k$  is given by:

$$\begin{aligned} P &= P^T > 0, \\ A_i^T P A_i - P &< 0, \quad i \in \{1, 2, \dots, q\}, \end{aligned} \quad (2.21)$$

see [20; 47; 82]. Once this system is asymptotically stable, it is also globally asymptotically stable.

In this thesis, we are also interested in systems of the form:

$$x_{k+1} = A_{i(k)}x_k, \quad x \in \mathbb{R}^n, \quad (2.22)$$

in which for all  $k \in \mathbb{N}$   $A_{i(k)} \in \mathcal{A}$ , which is some infinite set of matrices. In particular, we are interested in the case where  $\mathcal{A}$  is the convex hull of a finite number of matrices  $A_1, \dots, A_q$ :

$$\mathcal{A} := \text{co} \{A_1, \dots, A_q\} = \left\{ \sum_{i=1}^q \alpha_i A_i : \alpha_i \geq 0, \sum_{i=1}^q \alpha_i = 1 \right\},$$

with  $A_1, \dots, A_q$  known and constant matrices. The system (2.22) is globally asymptotically stable if the conditions in (2.21) are satisfied for each matrix  $A_1, \dots, A_q$ , see e.g. [47; 82].

## 2.4 Notation

As mentioned above, the set  $\mathbb{N}$  contains all non-negative integers and the set  $\mathbb{R}$  all real values. The function  $\lfloor f \rfloor$  denotes the floor function of  $f$ , i.e. the largest integer smaller than or equal to  $f$ . The function  $\lceil f \rceil$  denotes the ceil function of  $f$ , i.e. the smallest integer larger than or equal to  $f$ .  $\dim(A)$  denotes the dimension of the matrix  $A$  and  $\text{diag}(1, 2)$  denotes the diagonal matrix  $\begin{pmatrix} 1 & 0 \\ 0 & 2 \end{pmatrix}$ .

$\star$  is used to denote the symmetric part of a matrix, i.e.  $\begin{pmatrix} A & B \\ B^T & C \end{pmatrix} = \begin{pmatrix} A & B \\ \star & C \end{pmatrix}$ .

Unless denoted else,  $\|B\|$  denotes the induced matrix norm of the matrix  $B$  and  $|x|$  denotes the norm of the vector  $x$ .

# 3

## *Modeling of Networked Control Systems<sup>1</sup>*

---

3.1	Small delays	3.4	Time-varying sampling intervals
3.2	Large delays		
3.3	Large delays and packet dropouts	3.5	Discussion

---

This chapter introduces a discrete-time model for Networked Control Systems, based on an exact discretization of the underlying continuous-time model of the controlled plant. The communication network can induce effects such as network delays, time-varying sampling intervals, and information loss (packet dropout). Different modeling cases, considering delays smaller or larger than the sampling interval, time-varying sampling intervals, and packet dropouts are distinguished. The time-variation in the delays is due to the network effects, such as waiting time until the network is empty, transmission time, which is the time that the network needs to transmit the data, and pre- and postprocessing times, which are the times that are needed to encode and decode the data, see e.g. [57; 71]. Packet dropouts can occur due to different reasons, see e.g. [35; 71]. Firstly, failures in the network links may occur, which is more likely to happen in wireless networks than in wired networks. Secondly, buffer overflows due to congestion happen for switched Ethernet, resulting in loss of data. Thirdly, if for a packet too many retransmissions are needed, because of packet collisions during the transmission, the packet may be discarded. This might happen for standard Ethernet-based networks if the network load is high. In CAN-based networks, packet dropouts are not likely to happen. Time-variation in the sampling interval occurs if, e.g. instead of a clock on the measurement system, the controller requests for sensor information at several previously determined, fixed moments in time. This request is sent over the network to the sensor, which measures the data at the moment that the request is received.

This chapter describes a NCS model that incorporates all these network effects, including variation in the sampling interval. This model will be built up in steps. To develop this model, it is assumed that the NCS contains a single sensor and a single actuator. First, in Section 3.1, a constant sampling interval is assumed to describe a standard discrete-time NCS model, as used in e.g. [133], that includes time-varying delays smaller than this constant sampling interval.

---

<sup>1</sup>This chapter is partially based on [14] and [110].

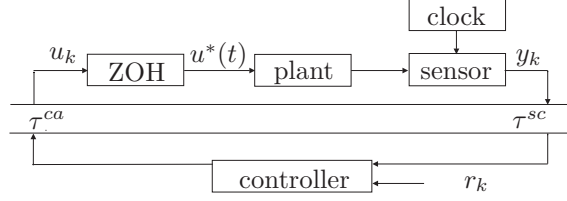


Figure 3.1: Schematic overview of the networked control system.

This restricted case is considered to explain the effects of time-varying delays and the use of a continuous-time plant and a discrete-time controller. Second, in Section 3.2, the discrete-time model for small delays is extended such that it includes time-varying delays that can be larger than the constant sampling interval. In this model it is assumed that always the most recent data is used in the control computation and that the most recent data is used for actuation of the system. This assumption is preferable and useful for most systems, because implementing older data results in a decreased performance in general. Based on this assumption, message rejection is included in the model, which means that if data does not arrive in the correct order, the older data is rejected. Third, in Section 3.3, the model is extended such that packet dropouts, resulting in loss of data are included. Finally, the discrete-time NCS model is extended in Section 3.4 to incorporate the case of time-varying sampling intervals. This chapter ends with a discussion on the similarities between the presented models in Section 3.5.

### 3.1 Small delays

In this section, the discrete-time description of a NCS, as presented in [85] and [133], is adopted. The NCS is schematically depicted in Figure 3.1. It consists of a continuous-time plant (modeled according to  $\dot{x}(t) = Ax(t) + Bu(t)$ ) and a discrete-time controller that are connected over a communication network that induces network delays ( $\tau^{sc}$  and  $\tau^{ca}$ ). The output measurements ( $y(t)$ ) are sampled with a constant sampling interval  $h > 0$ , based on a clock, resulting in the sampling time instants  $s_{k+1} := s_k + h$ , for all  $k \in \mathbb{N}$  and  $s_0 = 0$ . The zero-order-hold (ZOH) function is applied to transform the discrete-time control input  $u_k := u(s_k)$  to a continuous-time control input  $u^*(t)$  that reflects the actuation of the plant. The reference signal  $r_k := r(s_k)$  is known and obtained based on the same time instant  $s_k$  as the measurement data  $y_k := y(s_k)$ , by means of time-stamping of the measurement data. For stability analysis, it is assumed that the reference signal  $r_k$  is equal to zero.

In the model, both the computation time ( $\tau^c$ ), needed to evaluate the controller, and the network-induced delays, i.e. the sensor-to-controller delay ( $\tau^{sc}$ ) and the controller-to-actuator delay ( $\tau^{ca}$ ), are taken into account. Under the assumption that the sensor acts in a time-driven fashion (i.e. sampling occurs

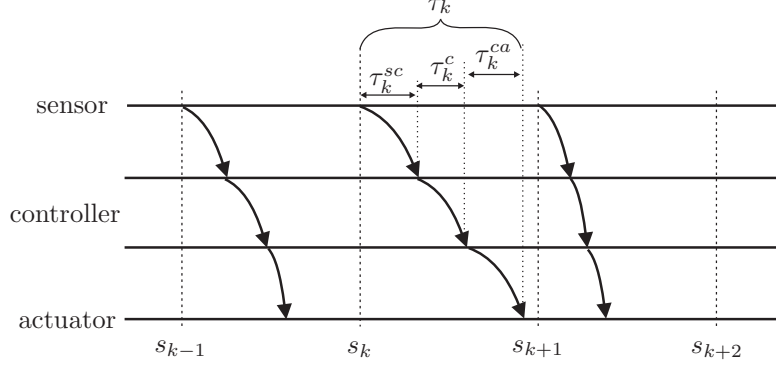


Figure 3.2: Timing diagram of a NCS with a time-driven sensor and an event-driven controller and actuator and  $\tau_k \in [0, h)$ .

at the times  $s_k = kh$ ), that the controller and actuator act in an event-driven fashion (i.e. responding instantaneously to newly arrived data), and that the controller is static and time-invariant, all three delays can be captured by a single delay  $\tau_k := \tau_k^{sc} + \tau_k^c + \tau_k^{ca}$ , see [85], [133]. A timing diagram of a NCS with time-delays  $\tau_k$  smaller than the constant sampling interval, satisfying these assumptions, is given in Figure 3.2. Based on these assumptions, the continuous-time model of the plant of the NCS is given by:

$$\begin{aligned} \dot{x}(t) &= Ax(t) + Bu^*(t), \\ y(t) &= Cx(t) \\ u^*(t) &= u_k, \quad \text{for } t \in [s_k + \tau_k, s_{k+1} + \tau_{k+1}) \end{aligned} \quad (3.1)$$

with  $A \in \mathbb{R}^{n \times n}$ ,  $B \in \mathbb{R}^{n \times m}$ , and  $C \in \mathbb{R}^{r \times n}$ , the system matrices,  $u^*(t) \in \mathbb{R}^m$  the continuous-time control input,  $x(t) \in \mathbb{R}^n$  the state at time  $t \in \mathbb{R}$ ,  $y(t) \in \mathbb{R}^r$  the output,  $s_k$  the sampling instants with  $s_k := kh$ ,  $k \in \mathbb{N}$ ,  $u_k := u(s_k) \in \mathbb{R}^m$  the discrete-time control input based on the measurement data at (sensor) sampling instant  $s_k$ , and  $\tau_k$  the time-varying delay. For the initial time  $t_0 = 0$ , the initial condition of (3.1) is given by  $x_0 = x(0)$ ,  $u^*(t)$  for  $t \in [0, \tau_0)$ , and possibly additional initial states used in the discrete-time controller. The use of such additional states will become clear in Chapters 4 and 5.

To model the variation in the delay two approaches can be considered. Firstly, a stochastic approach, as e.g. used in [85; 124; 130], and secondly, an approach based on bounded delays, as e.g. used in [38; 76; 87] can be considered. Based on measurements that are performed on several communication networks, such as Ethernet, CAN, and Profibus as presented in [57; 71] and [85] both delay modeling approaches are relevant. Based on the chosen network, its network protocol (e.g. CAN or Ethernet), and the network load, different stochastic distributions of the delay are possible, which can be determined (approximately) by performing suitable measurements. Alternatively, based on these measurements it is often possible to determine a minimum and maximum bound on the

delays, which can be used to model time-varying delays, but without considering a specific distribution of the variations in the delay. Here, we consider the latter approach and assume bounded time-varying delays  $\tau_k \in [\tau_{\min}, \tau_{\max}]$ . In this section, we limit ourselves to  $0 \leq \tau_{\min} \leq \tau_{\max} < h$ , representing the small delay case. In the following sections, the upper bound  $\tau_{\max}$  can be larger than  $h$  to study delays larger than the sampling interval.

The NCS model (3.1) including the assumptions on the sampling interval and the delays can be captured in a discrete-time NCS representation, based on an exact discretization of (3.1) at the sampling instant  $s_k$  [4]:

$$\begin{aligned} x_{k+1} &= e^{Ah}x_k + \int_0^{h-\tau_k} e^{As}dsBu_k + \int_{h-\tau_k}^h e^{As}dsBu_{k-1} \\ y_k &= Cx_k, \end{aligned} \quad (3.2)$$

with  $x_k := x(s_k)$  the discrete-time state at the  $k^{th}$  sampling instant. The corresponding discrete-time state-space notation of the NCS model (3.2) for small delays is given by:

$$\begin{aligned} \xi_{k+1} &= \tilde{A}(\tau_k)\xi_k + \tilde{B}(\tau_k)u_k \\ y_k &= \tilde{C}\xi_k, \end{aligned} \quad (3.3)$$

with  $\tilde{A}(\tau_k) = \begin{pmatrix} e^{Ah} & \int_{h-\tau_k}^h e^{As}dsB \\ 0_{m,n} & 0_{m,m} \end{pmatrix}$ ,  $\tilde{B}(\tau_k) = \begin{pmatrix} \int_0^{h-\tau_k} e^{As}dsB \\ I_m \end{pmatrix}$ ,  $\tilde{C} = (C \ 0_{r \times m})$ ,  $\xi_k = (x_k^T \ u_{k-1}^T)^T$ , and  $\tau_k \in [\tau_{\min}, \tau_{\max}] \ \forall k \in \mathbb{N}$ , with  $\tau_{\max} < h$ . Note that  $0_{i,j}$  denotes a matrix with zeros of dimension  $i \times j$  and  $I_m$  is the identity matrix of dimension  $m \times m$ .

### 3.2 Large delays

In this section, the NCS model for small delays (3.3) will be extended to incorporate the case of large delays, i.e. delays larger than the sampling interval. To be relevant in practical situations, this model must include the effects of, firstly, a varying number of active control inputs during one sampling interval and, secondly, message rejection, as will be shown in this section. As a first step, we consider the exact discretization of (3.1) for a time-varying delay  $\tau_k \in [\tau_{\min}, \tau_{\max}] \ \forall k$ , with  $[\tau_{\min}, \tau_{\max}] \subseteq [(\bar{d}-1)h, \bar{d}h)$ , for some *constant integer*  $\bar{d}$  that is obtained from  $\lceil \frac{\tau_{\max}}{h} \rceil$ , i.e. the smallest integer larger than or equal to  $\frac{\tau_{\max}}{h}$ . Note that, for delays larger than the sampling interval,  $\tau_{\min} > h$  and  $\bar{d} > 1$  hold. This results in the following discrete-time NCS model [55; 123]:

$$\begin{aligned} x_{k+1} &= e^{Ah}x_k + \int_0^{h-\tau_k^*-\bar{d}+1} e^{As}dsBu_{k-\bar{d}+1} + \int_{h-\tau_k^*-\bar{d}+1}^h e^{As}dsBu_{k-\bar{d}} \\ y_k &= Cx_k, \end{aligned} \quad (3.4)$$

with  $\tau_{k-\bar{d}+1}^* = \tau_k + (1-\bar{d})h$ . Note that (3.2) and (3.4) result in the same NCS model for  $\tau_k < h \ \forall k$ . If  $\tau_k = \tau \ \forall k$  is used, (3.4) corresponds to the NCS model

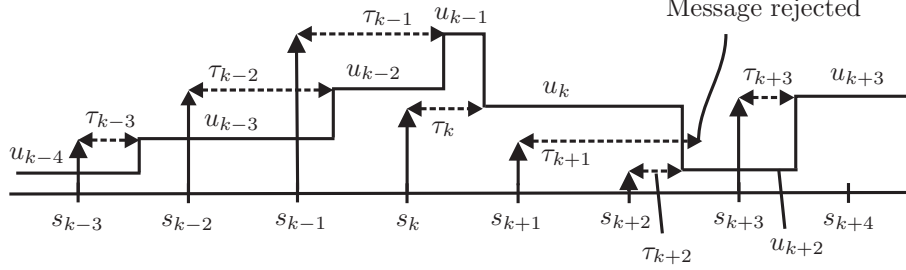


Figure 3.3: Influence of time-delays that can be smaller and larger than the sampling interval (with  $s_{k+1} := (k+1)h$  and  $\tau_k \in [0, 2h]$ ,  $k \in \mathbb{N}$ ).

for constant time-delays, as is presented in e.g. [4; 133]. The presented case, with variations of  $\tau_k$  within an interval of at most length  $h$ , in particular as  $\tau_k \in [\tau_{\min}, \tau_{\max}] \subseteq [(\bar{d}-1)h, \bar{d}h)$ , is rather simple as in each interval  $[s_k, s_{k+1})$  two control values are active (analogous to the small delay case described in (3.2)) and phenomena such as message rejection cannot occur. If the variation in the delay becomes larger than one sampling interval, i.e.  $\tau_k \in [(\bar{d}-1)h, \bar{d}h)$  does not hold, the discrete-time model becomes more complex. This will be illustrated for the case  $\tau_k \in [0, 2h]$ , as depicted in Figure 3.3. Here, the vertical arrows denote the control input that belongs to the sampling instant, the horizontal arrows denote the corresponding time-delays, and the solid line denotes the control input  $u(t)$  that is obtained by the zero-order hold function in combination with the discrete-time control inputs. This figure shows that *message rejection*, i.e. the effect that more recent control data becomes available before the older data is implemented and therefore the older data is neglected, occurs in the interval  $[s_{k+2}, s_{k+3})$  causing  $u_{k+1}$  to be never implemented. In general, from Figure 3.3 it can be concluded that the number of active control inputs in one sampling interval is variable and dependent on the previous and current time-delays. All described effects are not included in (3.4).

To derive the NCS model for time-delays larger than the sampling interval, first, consider  $\tau_k \in [0, 2h]$ ,  $\forall k$ , as in Figure 3.3. The corresponding model consists of the following subsystems:

$$x_{k+1} = \begin{cases} e^{Ah}x_k + \int_0^{h-\tau_k} e^{As}dsBu_k + \int_{h-\tau_k}^h e^{As}dsBu_{k-1}, & \text{if } \tau_k \leq h \wedge \tau_{k-1} \leq h \\ e^{Ah}x_k + \int_0^{h-\tau_{k-1}^*} e^{As}dsBu_{k-1} + \int_{h-\tau_{k-1}^*}^h e^{As}dsBu_{k-2}, & \\ & \text{if } h \leq \tau_k \leq 2h \wedge h \leq \tau_{k-1} \leq 2h \\ e^{Ah}x_k + \int_0^h e^{As}dsBu_{k-1}, & \text{if } h \leq \tau_k \leq 2h \wedge \tau_{k-1} \leq h \\ e^{Ah}x_k + \int_0^{h-\tau_k} e^{As}dsBu_k + \int_{h-\tau_k}^{h-\tau_{k-1}^*} e^{As}dsBu_{k-1} + \int_{h-\tau_{k-1}^*}^h e^{As}dsBu_{k-2}, & \\ & \text{if } \tau_k \leq h \wedge h \leq \tau_{k-1} \leq 2h \wedge \tau_{k-1} - h < \tau_k \\ e^{Ah}x_k + \int_0^{h-\tau_k} e^{As}dsBu_k + \int_{h-\tau_k}^h e^{As}dsBu_{k-2}, & \text{if } \tau_{k-1} - h \geq \tau_k, \end{cases} \quad (3.5)$$

with  $\tau_{k-1}^* = \tau_{k-1} - h$  and  $\wedge$  the logical ‘and’ symbol. The last subsystem describes the case where message rejection occurs, which results in omission of some control data ( $u_{k-1}$  in this case). The second subsystem corresponds to (3.4) (with  $\bar{d} = 2$ ) and the first subsystem corresponds to the model for the small delay case, see (3.2).

Now, we will consider the general case, with  $0 \leq \tau_{\min} \leq \tau_{\max} \leq \bar{d}h$ , with  $\bar{d} \in \mathbb{N}$ . A NCS modeling approach that considers the different subsystems (see e.g. (3.5)) that can occur, except message rejection, is described in [124]. Note that this is not the first paper that includes the possibility of a different number of control inputs during one sampling interval. In [31; 61; 90], for a NCS model with a sensor and a controller that behave in a time-driven fashion and a time-varying time skew between the sensor and the controller, the effect of different control inputs during one sampling interval was already taken into account. However in [31; 61; 90], it is assumed that the control inputs arrive at the actuator in a sequential order, thereby excluding the possibility of message rejection for variations in the delay larger than the sampling interval. The model of [124], as well as the identical model of [101] describe an adaptation on the model in [31; 61; 90], such that a NCS with a controller that operates in an event-driven fashion is described. In this thesis, we will use the model description of [124], which is based on (3.4), to develop a NCS model, *including message rejection*, which is an essential feature for NCS modeling with large delays, because it ensures the implementation of the most recent available actuation data on the plant. This requires a modification of the continuous-time model in (3.1). Therefore, define  $k^*(t) := \max\{k \in \mathbb{N} | s_k + \tau_k \leq t\}$ , which denotes the index of the most recent control input that is available at time  $t$ . Using this definition, the NCS of (3.1) becomes:

$$\begin{aligned} \dot{x}(t) &= Ax(t) + Bu^*(t) \\ y(t) &= Cx(t) \\ u^*(t) &= u_{k^*(t)}, \end{aligned} \tag{3.6}$$

where  $u^*(t)$  remains to be a piecewise constant signal. This is a description of the ZOH-based control signal in the NCS. Due to the definition of  $k^*(t)$ , the possibility of message rejection is included explicitly, while it was only included implicitly in [76], via the assumption that the values of  $k$  form a strictly increasing sequence.

In Lemma 3.2.1, the general description of the control input  $u^*(t)$  in (3.6) is reformulated to indicate explicitly which control inputs are active in the sampling interval  $[s_k, s_{k+1})$ . Such a formulation is needed to derive the discrete-time NCS model for large delays (incorporating all possibilities as done in (3.5) for  $\tau_k \in [0, 2h]$ ), which will ultimately be employed in the stability analysis and controller synthesis results in Chapters 4 and 5. Moreover, the time interval in which the control input is active will be determined explicitly.

**Lemma 3.2.1** *Consider the continuous-time NCS as defined in (3.6). Define  $\underline{d} := \lfloor \frac{\tau_{\min}}{h} \rfloor$ , the largest integer smaller than or equal to  $\frac{\tau_{\min}}{h}$  and  $\bar{d} := \lceil \frac{\tau_{\max}}{h} \rceil$ ,*



the smallest integer larger than or equal to  $\frac{\tau_{\max}}{h}$ . Then, the control action  $u^*(t)$  in the sampling interval  $[s_k, s_{k+1})$  is completely described by

$$u^*(t) = u_j \text{ for } t \in [s_k + t_j^k, s_k + t_{j+1}^k),$$

where  $t_j^k$  is defined as:

$$t_j^k = \min \left\{ \max\{0, \tau_j - (k-j)h\}, \max\{0, \tau_{j+1} - (k-j-1)h\}, \dots, \max\{0, \tau_{k-\underline{d}} - \underline{d}h\}, h \right\}, \quad (3.7)$$

with  $t_j^k \leq t_{j+1}^k$  and  $j \in [k - \bar{d}, k - \bar{d} + 1, \dots, k - \underline{d}]$ . Moreover,  $0 =: t_{k-\bar{d}}^k \leq t_{k-\bar{d}+1}^k \leq \dots \leq t_{k-\underline{d}}^k \leq t_{k-\underline{d}+1}^k := h$ .

**Proof** The proof is given in Appendix A.1.  $\square$

Based on this lemma, we can define the NCS model for large delays as:

$$\begin{aligned} x_{k+1} &= e^{Ah}x_k + \sum_{j=k-\bar{d}}^{k-\underline{d}} \int_{h-t_{j+1}^k}^{h-t_j^k} e^{As} ds B u_j \\ y_k &= Cx_k, \end{aligned} \quad (3.8)$$

with  $t_{k-\underline{d}+1}^k := h$  and  $t_j^k$  as defined in (3.7). According to Lemma 3.2.1, this model contains all possible control inputs that can be active during the sampling interval  $[s_k, s_{k+1})$ . Note that  $t_j^k = t_{j+1}^k$  corresponds to the situation that the integral related to  $u_j$  in (3.8) is zero and results in an inactive control input  $u_j$  during the sampling interval  $[s_k, s_{k+1})$ . Therefore, this equality allows to include message rejection. Moreover, as guaranteed by the lemma, (3.8) captures all the different situations that are given in (3.5) for  $\tau_k \in [0, 2h]$ , because each subsystem can be obtained by the proper selection of  $t_j^k$ , as defined in (3.7).

In the lemma, no distinction is made between the position in the network where message rejection occurs (i.e. from sensor to controller or from controller to actuator), because in both cases one control input is not implemented, caused by rejection of either the control input or the measurement data. To allow this simplification, some assumptions on the controller or its computation are needed. The simplest assumption is that it should hold that the control input does not depend on the past control inputs. Otherwise, problems in the control computation may arise if the measurement data is not received sequentially. However, if the control input depends on past control inputs, still the difference between the positions of message rejection may be neglected, if the control computation only starts if all previous measurement data are available. Obviously, this adaptation in the control implementation leads to larger computational delays than for the case where all measurements arrive in a sequential order. In Chapter 4, we will discuss the relation between the controller and message rejection in more detail.

**Remark 3.2.2** Equation (3.8) was also stated in [124]. However, the explicit definition of  $t_j^k$  as we presented here in Lemma 3.2.1 was not mentioned. Moreover, in [124] it is implicitly assumed that message rejection does not occur, as  $t_j^k < t_{j+1}^k$  is supposed to hold for all  $k - \bar{d} \leq j \leq k - \underline{d}$ . Finally, the model proposed here exhibits less uncertain parameters than the model in [124], because we consider only  $t_j^k$  as uncertain, time-varying parameters, while in [124] additional boolean parameters are introduced that describe whether a control input is active or inactive in the sampling interval  $[s_k, s_{k+1})$ .

To make the model of (3.8) suitable for the stability analysis and controller synthesis, we rewrite it in a discrete-time state-space notation, using the augmented state vector  $\xi_k = (x_k^T \ u_{k-1}^T \ u_{k-2}^T \ \dots \ u_{k-\bar{d}}^T)^T$ . Then, the state-space representation of the discrete-time NCS model is given by:

$$\begin{aligned} \xi_{k+1} &= \tilde{A}(\mathbf{t}^k) \xi_k + \tilde{B}(\mathbf{t}^k) u_k \\ y_k &= \tilde{C} \xi_k, \end{aligned} \quad (3.9)$$

$$\text{with } \tilde{A}(\mathbf{t}^k) = \begin{pmatrix} e^{Ah} & \tilde{M}_1 & \tilde{M}_2 & \dots & \tilde{M}_{\bar{d}} \\ 0 & 0 & 0 & \dots & 0 \\ 0 & I & 0 & \dots & 0 \\ \vdots & & \ddots & \ddots & \\ 0 & \dots & 0 & I & 0 \end{pmatrix}, \tilde{B}(\mathbf{t}^k) = \begin{pmatrix} \tilde{M}_0 \\ I \\ 0 \\ \vdots \\ 0 \end{pmatrix},$$

$$\tilde{C} = (C \ 0 \ \dots \ 0), \text{ and}$$

$$\tilde{M}_\rho = \begin{cases} \int_{h-t_{k-\rho+1}^k}^{h-t_{k-\rho}^k} e^{As} ds B & \text{if } \rho \geq \underline{d}, \\ 0 & \text{if } \rho < \underline{d}, \end{cases} \quad (3.10)$$

for  $\rho \in \{0, 1, \dots, \bar{d}\}$  and  $t_{k-\rho}^k$  defined in (3.7), with  $j = k - \rho$ . Finally,  $\mathbf{t}^k$  denotes the combination of the time-varying parameters used, i.e.  $\mathbf{t}^k = (t_{k-\bar{d}+1}^k, \dots, t_{k-\underline{d}}^k)$ .

For the initial time  $t_0 = 0$ , the initial condition of (3.6) and its discrete-time equivalent (3.9) is given by  $x_0 = x(0)$  and the past control inputs  $u_{-1}, \dots, u_{-\bar{d}}$ .

### 3.3 Large delays and packet dropouts

In this section, we consider a NCS, where the controller and plant are connected through a network, in which packets may be dropped, as depicted in Figure 3.4 by the parameter  $m_k$ . This parameter denotes whether or not a packet is dropped:

$$m_k = \begin{cases} 0, & \text{if } y_k \text{ and } u_k \text{ are received} \\ 1, & \text{if } y_k \text{ and/or } u_k \text{ is lost.} \end{cases} \quad (3.11)$$

In (3.11), we make no distinction between packet dropouts that occur in the sensor-to-controller connection in the network and packet dropouts that occur

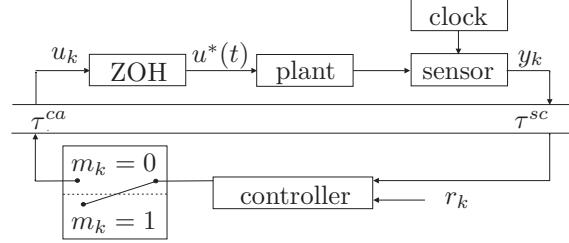


Figure 3.4: Schematic overview of the NCS with packet dropouts and network delays.

in the controller-to-actuator connection. This can be justified by evaluating the effect of the packet dropouts on the control updates implemented on the plant. For packet dropouts between the sensor and the controller no new control update is computed and thus no new control input is sent to the actuator. For packet dropouts between the controller and the actuator no new control update is received by the actuator. These observations indicate that the effect in both cases is the same, being that no new control update  $u_k$  is implemented on the plant, which confirms that the differences in packet dropout locations can be neglected. However, in this reasoning it is assumed that the control input depends on the current state only. If the new control value depends on past control values, this new value cannot be updated in case these old inputs are not computed. Hence, in this case, there is a difference between the situation of a dropout between the sensor and controller and a dropout between the controller and actuator. In the latter case the control value is still computed and available, while this is not true in the former case, which may lead to a halt in the controller updates. We return to this issue in Chapter 4.

Similar to message rejection not all data is used in the case of packet dropouts, but the reason of not implementing that data is now also dependent on the parameter  $m_k$ . Therefore the continuous-time model of (3.6) needs to be adapted, such that packet dropout is included as well. Let us redefine the parameter  $k^*(t)$  that denotes the index of the most recent control input that is available at time  $t$  as  $k^+(t) := \max\{k \in \mathbb{N} | s_k + \tau_k \leq t \wedge m_k = 0\}$ . The continuous-time model of the plant of the NCS is then given by:

$$\begin{aligned} \dot{x}(t) &= Ax(t) + Bu^*(t) \\ y(t) &= Cx(t) \\ u^*(t) &= u_{k^+(t)}. \end{aligned} \tag{3.12}$$

Here, we assume that the most recent control input remains active in the plant if a packet is dropped.

To derive the discrete-time NCS model for this situation, we assume that at maximum  $\bar{\delta} \in \mathbb{N}$  subsequent packet dropouts occur. Also for packet dropouts, two approaches can be distinguished in the literature, i.e. deterministic packet dropouts, where the number of subsequent packet dropouts is bounded and

known beforehand, see e.g. [75; 127; 128], or stochastic dropouts, where e.g. a Bernoulli process or Markov chain is used for the probability of the packet dropout see e.g. [39; 99]. Here, we consider deterministic packet dropouts. The bound on the number of subsequent packet dropouts is modeled by:

$$\sum_{v=k-\bar{\delta}}^k m_v \leq \bar{\delta}, \quad (3.13)$$

where  $\bar{\delta}$  is thus the maximum number of successive dropouts. This guarantees that from the control inputs  $u_{k-\bar{\delta}}, u_{k-\bar{\delta}+1}, \dots, u_k$  at least one control input is implemented. Let us now introduce the class  $\mathcal{M}$  of admissible sequences  $\{(\tau_k, m_k)\}_{k \in \mathbb{N}}$  as follows:

$$\mathcal{M} := \left\{ \{(\tau_k, m_k)\}_{k \in \mathbb{N}} : \tau_{\min} \leq \tau_k \leq \tau_{\max}, \sum_{v=k-\bar{\delta}}^k m_v \leq \bar{\delta}, \forall k \in \mathbb{N} \right\}, \quad (3.14)$$

that allows for both the occurrence of large delays and packet dropout. For the sake of brevity, we will use the notation  $\mu := \{(\tau_k, m_k)\}_{k \in \mathbb{N}} \in \mathcal{M}$ .

Similar to Lemma 3.2.1, in Lemma 3.3.1 (see below) the control input  $u^*(t)$  of (3.12) is reformulated to describe explicitly which control inputs are active in the sampling interval  $[s_k, s_{k+1})$ . Such a formulation is needed to derive the discrete-time NCS model for large delays (incorporating message rejection) and packet dropouts that will be used for stability analysis and controller synthesis. Moreover, the duration of the control input will be defined explicitly.

**Lemma 3.3.1** *Consider the continuous-time NCS as defined in (3.12) and the admissible sequences of delays and packet dropouts in  $\mathcal{M}$ . Define  $\underline{d} := \lfloor \frac{\tau_{\min}}{h} \rfloor$ , the largest integer smaller than or equal to  $\frac{\tau_{\min}}{h}$  and  $\bar{d} := \lceil \frac{\tau_{\max}}{h} \rceil$ , the smallest integer larger than or equal to  $\frac{\tau_{\max}}{h}$ . Then, the control action  $u^*(t)$  in the sampling interval  $[s_k, s_{k+1})$  is described by*

$$u^*(t) = u_j \text{ for } t \in [s_k + t_j^k, s_k + t_{j+1}^k),$$

with  $t_j^k$  defined as:

$$\begin{aligned} t_j^k = \min \Big\{ & \max\{0, \tau_j - (k-j)h\} + m_j h, \\ & \max\{0, \tau_{j+1} - (k-j-1)h\} + m_{j+1} h, \dots, \\ & \max\{0, \tau_{k-\underline{d}} - \underline{d}h\} + m_{k-\underline{d}} h, h \Big\}, \end{aligned} \quad (3.15)$$

with  $t_j^k \leq t_{j+1}^k$  and  $j \in [k - \bar{d} - \bar{\delta}, k - \bar{d} - \bar{\delta} + 1, \dots, k - \underline{d}]$ . Moreover,  $0 = t_{k-\bar{d}-\bar{\delta}}^k \leq t_{k-\bar{d}-\bar{\delta}+1}^k \leq \dots \leq t_{k-\underline{d}}^k \leq t_{k-\underline{d}+1}^k := h$ .

**Proof** The proof is given in Appendix A.2.  $\square$

For  $\mu \in \mathcal{M}$ , we can exploit Lemma 3.3.1 to define the discrete-time NCS model as follows:

$$\begin{aligned} x_{k+1} &= e^{Ah}x_k + \sum_{j=k-\bar{d}-\bar{\delta}}^{k-\bar{d}} \int_{h-t_{j+1}^k}^{h-t_j^k} e^{As}dsBu_j \\ y_k &= Cx_k, \end{aligned} \quad (3.16)$$

with  $t_j^k$  as defined in (3.15). According to Lemma 3.3.1, this model contains all possible control inputs that can be active during the sampling interval  $[s_k, s_{k+1})$ . Note that  $t_j^k = t_{j+1}^k$  corresponds to the situation that the integral related to  $u_j$  in (3.16) is zero, which corresponds to an inactive control input  $u_j$  during the sampling interval  $[s_k, s_{k+1})$ .

To make the model (3.16) suitable for the stability analysis and controller synthesis, the state-space notation of (3.9) holds, if the augmented state vector is redefined by

$$\xi_k = \begin{pmatrix} x_k^T & u_{k-1}^T & u_{k-2}^T & \dots & u_{k-\bar{d}-\bar{\delta}}^T \end{pmatrix}^T, \quad (3.17)$$

and the matrices are redefined as

$$\tilde{A}(\mathbf{t}^k) = \begin{pmatrix} e^{Ah} & \tilde{M}_1 & \tilde{M}_2 & \dots & \tilde{M}_{\bar{d}+\bar{\delta}} \\ 0 & 0 & 0 & \dots & 0 \\ 0 & I & 0 & \dots & 0 \\ \vdots & & \ddots & & \dots \\ 0 & \dots & 0 & I & 0 \end{pmatrix}, \quad \tilde{B}(\mathbf{t}^k) = \begin{pmatrix} \tilde{M}_0 \\ I \\ 0 \\ \vdots \\ 0 \end{pmatrix}, \quad (3.18)$$

$\tilde{C} = (C \ 0 \ \dots \ 0)$ , and  $\tilde{M}_\rho$  defined in (3.10) for  $\rho \in \{0, 1, \dots, \bar{d} + \bar{\delta}\}$ ,  $t_{k-\rho}^k$  defined in (3.15), with  $j = k - \rho$ . Finally,  $\mathbf{t}^k$  denotes the combination of the time-varying parameters used, i.e.  $\mathbf{t}^k = (t_{k-\bar{d}-\bar{\delta}+1}^k, \dots, t_{k-\bar{d}}^k)$ .

For the initial time  $t_0 = 0$ , the initial condition of (3.6) and its discrete-time equivalent (3.9), (3.18) is given by  $x_0 = x(0)$ , and the past control inputs  $u_{-1}, \dots, u_{-\bar{d}-\bar{\delta}}$ .

### 3.4 Time-varying sampling intervals

The previous NCS models did not allow for varying sampling intervals. To include this effect, we consider a NCS as depicted in Figure 3.5. The variable  $h_k$  describes the variation in the sampling intervals, which is related to the sampling instants through  $h_k = s_{k+1} - s_k$ . Similar to the previous sections, the sensor is assumed to behave in a time-driven fashion, although variable in time, and the controller and actuator are assumed to behave in an event-driven fashion. The sensor data ( $y_k$ ) is obtained only at the sampling instants:

$$s_k = \sum_{i=0}^{k-1} h_i \quad \forall k \geq 1, \quad s_0 = 0, \quad (3.19)$$

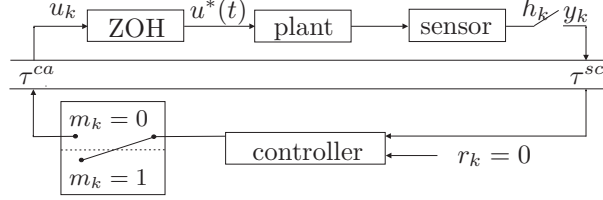


Figure 3.5: Schematic overview of the NCS with variable sampling intervals, network delays and packet dropouts

which are non-equidistantly spaced in time, due to the time-varying values  $h_k$ . Note that the sequence of sampling instants  $s_0, s_1, s_2, \dots$  is strictly increasing in the sense that  $s_{k+1} > s_k$ , for all  $k \in \mathbb{N}$ . Any sequence of sampling instants is assumed to be either bounded or in case it is infinite, it is unbounded (i.e.  $\lim_{k \rightarrow \infty} s_k = \infty$ ).

Similar to Section 3.3, we include packet dropouts and time-delays larger than the sampling interval in the NCS model. The continuous-time model including packet dropouts and large delays (3.12) is also valid for the case with time-varying sampling intervals if  $s_k$  is derived according to (3.19). The class  $\mathcal{M}$  in (3.14) needs to be redefined, such that the variation in the sampling interval is included as well. Therefore, we introduce the class  $\mathcal{S}$ :

$$\mathcal{S} := \left\{ \{(s_k, \tau_k, m_k)\}_{k \in \mathbb{N}} : h_{\min} \leq s_{k+1} - s_k \leq h_{\max}, \tau_{\min} \leq \tau_k \leq \tau_{\max}, \sum_{v=k-\bar{\delta}}^k m_v \leq \bar{\delta}, \forall k \in \mathbb{N} \right\}, \quad (3.20)$$

which describes variable sampling intervals, large delays, and packet dropouts. For the sake of brevity, we will sometimes use  $\sigma := \{(s_k, \tau_k, m_k)\}_{k \in \mathbb{N}} \in \mathcal{S}$ . Here, a minimum and maximum sampling interval are assumed, given by  $h_{\min}$  and  $h_{\max}$ , respectively. This is indeed natural, because a sampling interval (nearly) equal to zero is not realistic in practical applications and a sampling interval of infinite size results in hardly any control feedback and is avoided as well. Moreover, it describes a typical situation in practice, where a nominal sampling interval, with some variations around it, occurs. Other literature assumes similar bounds on the sampling interval, see e.g. [76] (where only an upper bound on the sampling interval is considered and the lower bound is assumed to be equal to zero) and [92], where a finite gridding of possible sizes of the sampling interval is considered. Note that  $\mathcal{S}$  is equal to  $\mathcal{M}$  if in  $\mathcal{S}$  it is used that the sampling interval is constant, i.e.  $h_{\min} = h_{\max} = h$ .

Lemma 3.3.1 has to be adapted to include the variation of the sampling intervals. This results in the following lemma that describes the active control inputs in the sampling interval  $[s_k, s_{k+1})$  and the duration of these control inputs.

**Lemma 3.4.1** Consider the continuous-time NCS as defined in (3.12) and the admissible sequences of sampling instants, delays, and packet dropouts as defined in  $\mathcal{S}$ . Define  $\underline{d} := \lfloor \frac{\tau_{\min}}{h_{\max}} \rfloor$ , the largest integer smaller than or equal to  $\frac{\tau_{\min}}{h_{\max}}$  and  $\bar{d} := \lceil \frac{\tau_{\max}}{h_{\min}} \rceil$ , the smallest integer larger than or equal to  $\frac{\tau_{\max}}{h_{\min}}$ . Then, the control action  $u^*(t)$  in the sampling interval  $[s_k, s_{k+1})$  is described by:

$$u^*(t) = u_j \text{ for } t \in [s_k + t_j^k, s_k + t_{j+1}^k), \quad (3.21)$$

where  $t_j^k$  is defined as:

$$\begin{aligned} t_j^k = \min \bigg\{ & \max\{0, \tau_j - \sum_{l=j}^{k-1} h_l\} + m_j h_{\max}, \\ & \max\{0, \tau_{j+1} - \sum_{l=j+1}^{k-1} h_l\} + m_{j+1} h_{\max}, \dots, \\ & \max\{0, \tau_{k-\underline{d}} - \sum_{l=k-\underline{d}}^{k-1} h_l\} + m_{k-\underline{d}} h_{\max}, h_k \bigg\}, \end{aligned} \quad (3.22)$$

with  $t_j^k \leq t_{j+1}^k$  and  $j \in [k - \bar{d} - \bar{\delta}, k - \bar{d} - \bar{\delta} + 1, \dots, k - \underline{d}]$ . Moreover,  $0 = t_{k-\bar{d}-\bar{\delta}}^k \leq t_{k-\bar{d}-\bar{\delta}+1}^k \leq \dots \leq t_{k-\underline{d}}^k \leq t_{k-\underline{d}+1}^k := h_k$ .

**Proof** The proof is given in Appendix A.3.  $\square$

Based on Lemma 3.4.1 and  $\sigma \in \mathcal{S}$ , we can rewrite the discrete-time NCS model as:

$$\begin{aligned} x_{k+1} &= e^{Ah_k} x_k + \sum_{j=k-\bar{d}-\bar{\delta}}^{k-\underline{d}} \int_{h_k - t_{j+1}^k}^{h_k - t_j^k} e^{As} ds B u_j \\ y_k &= C x_k, \end{aligned} \quad (3.23)$$

with  $t_j^k$  as defined in Lemma 3.4.1. Similar to (3.8) and (3.16) and according to Lemma 3.4.1, this model contains all possible control inputs that can be active during the sampling interval  $[s_k, s_{k+1})$ .

To render the model (3.23) suitable for the stability analysis and controller synthesis later, we rewrite it in a discrete-time state-space notation:

$$\begin{aligned} \xi_{k+1} &= \tilde{A}(\mathbf{t}^k, h_k) \xi_k + \tilde{B}(\mathbf{t}^k, h_k) u_k \\ y_k &= \tilde{C} \xi_k, \end{aligned} \quad (3.24)$$

$$\text{with } \tilde{A}(\mathbf{t}^k, h_k) = \begin{pmatrix} e^{Ah_k} & \tilde{M}_1 & \tilde{M}_2 & \dots & \tilde{M}_{\bar{d}+\bar{\delta}} \\ 0 & 0 & 0 & \dots & 0 \\ 0 & I & 0 & \dots & 0 \\ \vdots & & \ddots & & \vdots \\ 0 & \dots & 0 & I & 0 \end{pmatrix}, \tilde{B}(\mathbf{t}^k, h_k) = \begin{pmatrix} \tilde{M}_0 \\ I \\ 0 \\ \vdots \\ 0 \end{pmatrix}, \tilde{C} =$$

$(C \ 0 \ \dots \ 0)$ ,  $\xi_k$  defined in (3.17),  $\bar{d}$  and  $\bar{\delta}$  defined in Lemma 3.4.1, and

$$\tilde{M}_\rho(\mathbf{t}^k, h^k) = \begin{cases} \int_{h_k - t_{k-\rho+1}^k}^{h_k - t_{k-\rho}^k} e^{As} ds B & \text{if } \rho \geq \underline{d}, \\ 0 & \text{if } \rho < \underline{d}, \end{cases} \quad (3.25)$$

for  $\rho \in \{0, 1, \dots, \bar{d} + \bar{\delta}\}$  and  $t_{k-\rho}^k$  defined in (3.22), with  $j = k - \rho$ . Finally,  $\mathbf{t}^k$  denotes the combination of all time-varying parameters, i.e.  $\mathbf{t}^k = (t_{k-\bar{d}-\bar{\delta}+1}^k, \dots, t_{k-\underline{d}}^k)$ .

For the initial time  $t_0 = 0$ , the initial condition of (3.6) and its discrete-time equivalent (3.24) is given by  $x_0 = x(0)$  and the past control inputs  $u_{-1}, \dots, u_{-\bar{d}-\bar{\delta}}$ .

### 3.5 Discussion

In this chapter several discrete-time NCS models have been derived, based on an exact discretization of the continuous-time NCS model at the sampling instants. It is assumed that the sensor behaves in a time-driven fashion with constant or uncertain, time-varying sampling intervals, and that the controller and actuator behave in an event-driven fashion. Different cases have been considered, namely a distinction was made between small delays, large delays, and large delays including packet dropouts and a distinction was made between constant and time-varying sampling intervals. The number of time-varying parameters is different for each case. For the small delay case, only the delay  $\tau_k$  is uncertain. For the large delay case, the uncertain parameters are given by the delays  $\tau_{k-\underline{d}}, \tau_{k-\underline{d}-1}, \dots, \tau_{k-\bar{d}+1}$ , with  $\underline{d}$  dependent on  $\tau_{\min}$  and  $h$ , and  $\bar{d}$  dependent on  $\tau_{\max}$  and  $h$ . Similarly, for the case with large delays and packet dropouts the uncertain parameters are given by the delays  $\tau_{k-\underline{d}}, \tau_{k-\underline{d}-1}, \dots, \tau_{k-\bar{d}-\bar{\delta}+1}$ , with  $\bar{\delta}$  the maximum number of subsequent packet dropouts. For the case with time-varying sampling intervals, including time-varying delays larger than the sampling interval and packet dropouts, the uncertain parameters are the delays  $\tau_{k-\underline{d}}, \tau_{k-\underline{d}-1}, \dots, \tau_{k-\bar{d}-\bar{\delta}+1}$  and the sampling interval  $h_k$ , with  $\underline{d}$  dependent on  $\tau_{\min}$  and  $h_{\max}$  and  $\bar{d}$  dependent on  $\tau_{\max}$  and  $h_{\min}$ . Note that each of the presented models can be obtained from the NCS model that includes time-varying delays larger than the sampling interval, packet dropouts, and time-varying sampling intervals, by adapting the assumptions on the sampling interval  $h_k$  and the time-delay  $\tau_k$ .

In the models with packet dropouts it is assumed that the controller depends on the current state and not on past control inputs. This assumption allows to neglect the distinction between packet dropouts between the sensor and the controller and packet dropouts between the controller and the actuator.

In the next chapters, the obtained NCS models will be used for stability analysis (Chapter 4), controller synthesis for both stabilization and performance (Chapter 5), and tracking (Chapter 6).



## 4

### *Stability analysis*<sup>1</sup>

---

4.1	Motivating examples	4.4	Variable sampling
4.2	NCS model formulation		intervals, large delays, and
	using the Jordan form		packet dropouts
4.3	Small delays	4.5	Illustrative examples
		4.6	Discussion

---

This chapter deals with the stability analysis of the NCS model described in Chapter 3. Before the stability conditions are presented, two examples illustrating that network effects can lead to instability of the NCS are given in Section 4.1. The first example considers periodic delays and will demonstrate the destabilizing effect of time-varying delays, even if the delays are smaller than the sampling interval and the system is stable for any corresponding constant delay. Second, an example of the destabilizing effect of time-varying sampling intervals is given, based on [132].

After these motivating examples, sufficient conditions for the global asymptotic stability of a NCS for bounded time-varying delays, a bounded number of subsequent packet dropouts, and bounded variations in the sampling interval are presented. These conditions will be obtained using a Lyapunov approach, and will be written in the form of Linear Matrix Inequalities (LMIs). To derive the stability conditions, the NCS models, obtained in Chapter 3, are rewritten based on the Jordan form representation of the continuous-time system matrix  $A$ . The conditions are derived, firstly, for the simplest situation, being the small delay case (delays smaller than the sampling interval) with a constant sampling interval (Section 4.3). These conditions are derived for different types of controllers and are based on different types of Lyapunov functions. Additionally, conditions that guarantee the stability of the intersample behavior are provided, as the stability of the discretized NCS model does not directly guarantee stability of the original continuous-time NCS model. After tackling the small delay case, the stability conditions are extended such that they can be applied to time-varying sampling intervals, time-varying delays larger than the sampling interval, and packet dropouts in Section 4.4. The proposed stability conditions are applied to a motion control example in Section 4.5. Finally, in Section 4.6, a discussion on the obtained stability criteria is given.

---

<sup>1</sup>This chapter is partially based on [14], [15], and [16].

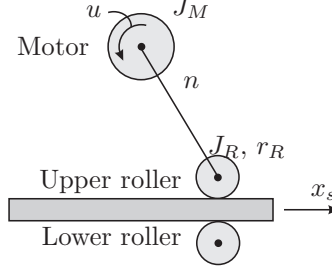


Figure 4.1: Schematic overview of the motor-roller example.

## 4.1 Motivating examples

To motivate the study of the stability of NCSs with time-varying delays and time-varying sampling intervals, we present examples that illustrate the destabilizing effects that these network-induced uncertainties can have on systems that are globally asymptotically stable without uncertainties being present. Firstly, we consider an example with time-varying delays and a constant sampling interval and, secondly, an example without delays, but with variation in the sampling intervals.

The example for time-varying delays is based on a dynamic model obtained from the document printing domain [7]. In general, a paper path, consisting of rollers, driven by motors, is used to move a sheet of paper through the printer. Here, all the motor controllers share the CPU-time of one processor, which is connected to the motors and sensors via a network that causes unpredictable time-varying delays in the control loop.

We limit ourselves to one single motor driving one roller, as depicted in Figure 4.1. Still, the controller is connected to the motor via the shared network. In the motor-roller model, the motor is assumed to behave ideally and slip between the paper and the roller is neglected, which gives rise to the following equation of motion:

$$\ddot{x}_s(t) = \frac{nr_R}{J_M + n^2 J_R} u^*(t), \quad (4.1)$$

with  $J_M = 1.95 \cdot 10^{-5} \text{kgm}^2$  the inertia of the motor,  $J_R = 6.5 \cdot 10^{-5} \text{kgm}^2$  the inertia of the roller,  $r_R = 14 \text{mm}$  the radius of the roller,  $n = 0.2$  the transmission ratio between motor and roller,  $x_s$  [m] the position of the sheet of paper, and  $u$  [Nm] the motor torque. Recall, from (3.1), that it holds that  $u^*(t) = u_k$ , for  $t \in [s_k + \tau_k, s_{k+1} + \tau_{k+1})$ , with  $\tau$  the time-delay smaller than the sampling interval. For the sake of simplicity, the reference signal in the control computation is assumed to be equal to zero. This allows for stability analysis, as is studied in this chapter. However, in practice, a reference signal unequal to zero is used, to allow for transportation of the sheet of paper in the printer. The use of a reference signal, unequal to zero, is studied in Chapter 6, where the tracking problem of NCSs is investigated.

If we assume that the delays  $\tau_k$  are time-varying, but at all times smaller

than the sampling interval  $h$ , the continuous-time state-space representation of (4.1), where the delays are accounted for in the discrete-time input  $u_k$  is given by (3.1), with  $A = \begin{pmatrix} 0 & 1 \\ 0 & 0 \end{pmatrix}$ ,  $B = \begin{pmatrix} 0 \\ \frac{nr_R}{J_M + n^2 J_R} \end{pmatrix}$ ,  $C = \begin{pmatrix} 1 & 0 \\ 0 & 1 \end{pmatrix}$ , and  $x(t) = (x_s^T(t) \quad \dot{x}_s^T(t))^T$ . Adopting a state-feedback controller of the form  $u_k = -\bar{K}y_k$ , with  $y_k = x_k$  and  $\bar{K} = (K_a \quad K_b)$ , allows to rewrite (3.3) as:

$$\xi_{k+1} = \tilde{A}(\tau_k)\xi_k, \quad (4.2)$$

with  $\tilde{A}(\tau_k) = \begin{pmatrix} 1 - \frac{1}{2}\hat{\alpha}^2 K_a b & h - \frac{1}{2}\hat{\alpha}^2 K_b b & -\tau_k \hat{\beta} b \\ -\hat{\alpha} K_a b & 1 - \hat{\alpha} K_b b & \tau_k b \\ -K_a & -K_b & 0 \end{pmatrix}$ ,  $b = \frac{nr_R}{J_M + n^2 J_R}$ ,  $\hat{\alpha} = h - \tau_k$ , and  $\hat{\beta} = \frac{1}{2}\tau_k - h$ .

If the delay is constant ( $\tau_k = \tau, \forall k$ ), the stability of (4.2) can be determined by checking that the eigenvalues of  $\tilde{A}(\tau)$  are within the unit circle for all relevant constant  $\tau$ . This system is assumed to have a constant sample-time  $h = 1\text{ms}$ , and two possible constant delays,  $\tau^a = 0.2\text{ms}$  if the network load is low, and  $\tau^b = 0.6\text{ms}$  if the network load is high. A linear feedback gain  $\bar{K} = (50 \quad 11.8)$ , results in an asymptotically stable system (4.2) for any constant delay  $\tau$  in the interval  $[0, \tau_{\max}]$ , with  $\tau_{\max} = 0.66h$ , as is illustrated for  $\tau = \tau^a$  and  $\tau = \tau^b$  and the initial condition  $\xi_0 = (0 \quad 1 \quad 0)^T$  in the upper plot of Figure 4.2. The eigenvalues of the matrix  $\tilde{A}(\tau^a)$  are  $\lambda_1 = 0.996$ ,  $\lambda_{2,3} = -0.097 \pm 0.539i$ . The eigenvalues of  $\tilde{A}(\tau^b)$  are  $\lambda_1 = 0.996$ ,  $\lambda_{2,3} = 0.203 \pm 0.927i$ . The fact that both matrices are Schur confirms stability. However, the system becomes unstable, if the delays occur in an alternating sequence  $(\tau^a, \tau^b, \tau^a, \tau^b, \dots)$ , as is shown in the lower plot in Figure 4.2 for the initial condition  $\xi_0 = (0 \quad 1 \quad 0)^T$ . The instability of this periodic system can be shown by computing the eigenvalues of the matrix  $\tilde{A}(\tau^b)\tilde{A}(\tau^a)$  [31], which are  $\lambda_1 = 0.992$ ,  $\lambda_2 = -1.012$ , and  $\lambda_3 = -0.267$ , and observing that one eigenvalue is outside the unit disk.

In many practical situations this periodic stability test is intractable (as there are infinitely many periodic sequences possible) and still it will not cover all possible sequences. Namely, the use of the network results in variations in the time-delay, which are in general not periodic (see e.g. [85]) and these would not be included in such a test. Therefore, an alternative route has to be considered. This thesis will do so by proposing stability conditions for uncertain time-varying, though bounded, delays.

An example of the destabilizing effect of variations in the sampling interval is presented in [132]. Briefly, we recall this example in which it is assumed that time-delays are zero. Consider system (3.1), where  $A = \begin{pmatrix} 1 & 3 \\ 2 & 1 \end{pmatrix}$ ,  $B = \begin{pmatrix} 1 \\ 0.6 \end{pmatrix}$ , and the control law  $u_k = -Kx_k$ , with  $K = (1 \quad 6)$ . The discrete-time NCS representation, including the control law, is, according to (3.2), given by:

$$x_{k+1} = \bar{A}(h_k)x_k, \quad (4.3)$$

with  $\bar{A}(h_k) = e^{Ah_k} - \int_0^{h_k} e^{As} ds BK$ . Two sampling intervals  $h_k$  are considered:

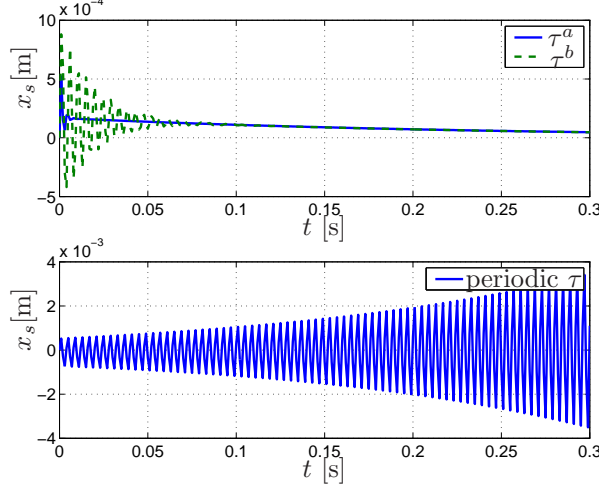


Figure 4.2: Time behavior of system (4.2) for constant  $\tau^a = 0.2\text{ms}$  and constant  $\tau^b = 0.6\text{ms}$  (upper figure), and the alternating sequence  $\tau^a, \tau^b, \tau^a, \tau^b, \dots$ , with  $h = 1\text{ms}$  (lower figure).

$h^a = 0.18$  and  $h^b = 0.54$  time units. For both constant sampling intervals, the NCS model is asymptotically stable, because the eigenvalues of  $\bar{A}(h^a)$  are  $\lambda_{1,2} = 0.718 \pm 0.294i$  and of  $\bar{A}(h^b)$  are  $\lambda_{1,2} = -0.49 \pm 0.512i$ . Note that the system is even stable for constant sampling intervals  $h$  taken from the set  $[0.01, 0.59]$ . The stable time-responses for  $h^a$  and  $h^b$  of  $x^1$  (i.e. the first state of the vector  $x$ ) are given in the upper plot of Figure 4.3. For periodic sampling intervals, e.g.  $h^a, h^b, h^a, h^b, \dots$ , the NCS is unstable, because the eigenvalues of  $\bar{A}(h^b)\bar{A}(h^a)$  are  $\lambda_1 = 0.3007$  and  $\lambda_2 = 1.0049$ . The corresponding unstable time-response is given in the lower plot of Figure 4.3. Similar to the periodic delay example, this shows the need for stability conditions for NCSs with time-varying sampling intervals. Clearly, checking the eigenvalues for the minimum and maximum sampling interval only does not suffice. In this thesis, we will present stability conditions that can deal with bounded time-variations in the sampling interval.

## 4.2 NCS model formulation using the Jordan form

For the purpose of stability analysis (and controller synthesis), we will exploit the Jordan form of the continuous-time system matrix of the NCS model to rewrite the integrals in the matrices  $\bar{A}(\tau_k)$  and  $\bar{B}(\tau_k)$  in (3.3) for the small delay case, (or equivalently  $\bar{A}(\mathbf{t}^k)$  and  $\bar{B}(\mathbf{t}^k)$  in (3.24) for time-varying sampling intervals, large delays, and packet dropouts). The Jordan form of the

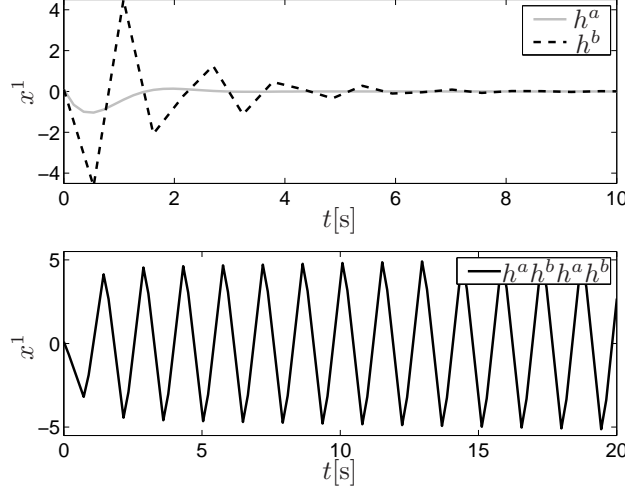


Figure 4.3: Time response of system (4.3) for: (upper figure) constant  $h^a = 0.18\text{s}$ ,  $h^b = 0.54\text{s}$ , and (lower figure) the alternating sequence  $h^a$ ,  $h^b$ .

continuous-time system matrix  $A$  is given by  $A = QJQ^{-1}$  [67], [108] and is applied to find generic solutions for the integrals and the exponential matrices. Details on the use of the Jordan form, both for real and complex eigenvalues, are given in Appendix B. The generic solutions of the integrals and matrix exponentials are used to rewrite the NCS model of (3.3) that is valid for small delays (or equivalently (3.24) for time-varying sampling intervals, large delays, and packet dropouts) in terms of constant matrices and time-varying parameters that depend on  $\tau_k$  (or on  $\mathbf{t}^k$  and  $h_k$  for the case with time-varying sampling intervals, large delays, and packet dropouts). Before we introduce this generic notation, we study the matrix  $A$  and its Jordan form in more detail. Recall that a Jordan block belonging to the  $\tilde{i}^{th}$  distinct eigenvalue may exist of different Jordan blocks  $J_{\tilde{i},1}, J_{\tilde{i},2}, \dots, J_{\tilde{i},g_{\tilde{i}}}$ , with  $g_{\tilde{i}}$  the geometric multiplicity of the  $\tilde{i}^{th}$  distinct real eigenvalue or of the  $\tilde{i}^{th}$  distinct complex eigenvalue with a positive imaginary part. Firstly, we define the parameter  $q_{\tilde{i}}$  that denotes the maximum size of the Jordan blocks that represent the  $\tilde{i}^{th}$  distinct real eigenvalue or the  $\tilde{i}^{th}$  distinct pair of complex eigenvalues:

$$q_{\tilde{i}} = \max_{\tilde{j} \in \{1,2,\dots,g_{\tilde{i}}\}} (\dim J_{\tilde{i},\tilde{j}}),$$

where  $\dim J$  denotes the dimension of the matrix  $J$ . Note that for a pair of complex eigenvalues  $\lambda = a \pm bj$ , based on the real Jordan form it holds that  $J = \begin{pmatrix} a & -b \\ b & a \end{pmatrix}$ . Secondly, we define the number of different uncertain time-varying parameters that occur if the integral  $\int_{s_1}^{s_2} e^{As} ds$  is solved, with either  $s_1$

or  $s_2$  an uncertain and time-varying scalar parameter, as  $\nu$

$$\nu = \sum_{\tilde{i}=1}^p q_{\tilde{i}}, \quad (4.4)$$

with  $p$  the number of distinct eigenvalues of  $A$  that are either real or pairs of complex eigenvalues. Note that  $\nu$  is always smaller than or equal to  $n$ . Then, the NCS description for the small delay case, which is valid for all possible combinations of eigenvalues, is given by:

$$\xi_{k+1} = \left( F_0 + \sum_{i=1}^{\nu} \alpha_i(\tau_k) F_i \right) \xi_k + \left( G_0 + \sum_{i=1}^{\nu} \alpha_i(\tau_k) G_i \right) u_k, \quad (4.5)$$

with  $\alpha_i(\tau_k)$  functions dependent on the time-varying delay  $\tau_k$ , the constant sampling interval  $h$ , and one of the (known and constant) eigenvalues of  $A$ . The constant matrices  $F_0$ ,  $G_0$ ,  $F_i$ , and  $G_i$ , for  $i = 1, 2, \dots, \nu$ , and the time-varying parameters  $\alpha_i$ ,  $i = 1, 2, \dots, \nu$ , are derived in Appendix B.2. For the large delay case with or without packet dropouts, the NCS description is given by

$$\xi_{k+1} = \left( F_0 + \sum_{i=1}^{\beta} \alpha_i(t_j^k) F_i \right) \xi_k + \left( G_0 + \sum_{i=1}^{\beta} \alpha_i(t_j^k) G_i \right) u_k, \quad (4.6)$$

with  $\beta = (\bar{d} + \bar{\delta} - \underline{d})\nu$  and  $t_j^k$  defined in (3.7) or (3.15) for the cases without or with packet dropouts, respectively. The constant matrices  $F_0$ ,  $G_0$ ,  $F_i$ , and  $G_i$  in (4.6), for  $i = 1, 2, \dots, \beta$ , and the time-varying parameters  $\alpha_i$ ,  $i = 1, 2, \dots, \beta$ , are given in Appendix B.3. For the case with time-varying sampling intervals, including time-varying delays and packet dropouts, the NCS description is given by

$$\xi_{k+1} = \left( F_0 + \sum_{i=1}^{\zeta} \alpha_i(t_j^k, h_k) F_i \right) \xi_k + \left( G_0 + \sum_{i=1}^{\zeta} \alpha_i(t_j^k, h_k) G_i \right) u_k, \quad (4.7)$$

with  $\zeta = (\bar{d} + \bar{\delta} - \underline{d} + 1)\nu$ ,  $t_j^k$  defined in (3.22), and  $h_k$  the time-varying sampling interval. The constant matrices  $F_0$ ,  $G_0$ ,  $F_i$ , and  $G_i$  in (4.7), for  $i = 1, 2, \dots, \zeta$ , and the time-varying parameters  $\alpha_i$ ,  $i = 1, 2, \dots, \zeta$ , are given in Appendix B.3. For each of these general model descriptions, the stability conditions are derived in the next sections.

### 4.3 Small delays

First, we consider the stability analysis for time-delays that are upper bounded by the sampling interval. For the purpose of stability analysis as well as controller synthesis (see Chapter 5) we consider two types of controllers. First, we consider a controller that depends on the state  $x_k$  and the previous control input  $u_{k-1}$ , similar to the one proposed in [38]

$$u_k = -K\xi_k = -\bar{K}x_k - K_1u_{k-1}, \quad (4.8)$$

with  $K = (\overline{K} \quad K_1) \in \mathbb{R}^{m \times (m+n)}$ . Second, we consider a state-feedback controller that depends only on the state  $x_k$

$$u_k = -\overline{K}x_k, \quad (4.9)$$

with  $\overline{K} \in \mathbb{R}^{m \times n}$ . This control law is a special case of (4.8) with  $K = (\overline{K} \quad 0_{m,m})$ . Therefore, in this section, if we consider (4.8), the same derivations hold for (4.9) as well. The reason to apply these two types of controllers is to compare their advantages and disadvantages. A main advantage to apply a controller of form of (4.8) will be explained in detail in Section 5.1.1, where it is shown that for such a controller the standard controller synthesis problem is easier to solve than for (4.9). The reason is that for (4.8) the structured control synthesis problem is avoided, which is not the case for (4.9).

Based on a given control law (4.8), the NCS model of (4.5) can be subjected to stability analysis. Different candidate Lyapunov functions can be considered, to determine whether a given controller gain  $K$  in (4.8) stabilizes (4.5). Here, we consider two different candidate Lyapunov functions. A common quadratic Lyapunov function approach and an approach based on a specific Lyapunov-Krasovskii (L-K) functional. A common quadratic Lyapunov approach gives LMI conditions, which are rather easy to verify, but is known to be somewhat more conservative in general. For L-K functionals, a general expectation is that they are less conservative than a common quadratic Lyapunov function approach (see, for instance, [63] for an approach for switched systems that studies this difference in conservatism). This expectation is, firstly, based on the results that are obtained for continuous-time systems with time-delays [24] for which the applicability of L-K functionals is known to be advantageous, because L-K functionals can deal with the infinite dimension of the delayed system and, secondly, it is based on the wealth of research performed on L-K functionals for stability analysis of discrete-time delayed systems (see e.g. [12; 26; 40; 68; 127]). However, it is not certain whether the L-K functional gives indeed less conservative stability conditions than the common quadratic Lyapunov function for discrete-time NCS models. For example, in [37] it is shown that a delay dependent L-K functional is equivalent to a switched Lyapunov function that is based on the augmented state vector  $\chi_k = (x_k^T \quad x_{k-1}^T)$ , resulting in the same amount of conservatism for both approaches. To get insight in the possible advantages of the use of L-K functionals, a candidate L-K functional is compared to the common quadratic candidate Lyapunov function in terms of conservatism and complexity.

#### 4.3.1 A common quadratic Lyapunov function based on the extended state vector $\xi_k$

Here, we consider a common quadratic candidate Lyapunov function that depends on the extended state vector  $\xi_k$ , defined in (3.3). System (4.5) contains the uncertain time-varying parameters  $\alpha_i$ , which typically depend nonlinearly on  $\tau_k$ . These parameters, together with the constant matrices  $F_0$ ,  $G_0$ ,  $F_i$ , and

$G_i$ ,  $i = \{1, 2, \dots, \nu\}$ , as defined in Appendix B.2, lead to the uncertain linear system  $\xi_{k+1} = (F(\tau_k) - G(\tau_k)K)\xi_k$ , with  $F(\tau) := F_0 + \sum_{i=1}^{\nu} \alpha_i(\tau)F_i$  and  $G(\tau) := G_0 + \sum_{i=1}^{\nu} \alpha_i(\tau)G_i$ . This gives rise to the set of matrices

$$\mathcal{FG} = \left\{ \left( F(\tau), G(\tau) \right) \in \left( \mathbb{R}^{(n+m) \times (n+m)} \times \mathbb{R}^{(n+m) \times m} \right) : \tau \in [\tau_{\min}, \tau_{\max}] \right\}, \quad (4.10)$$

that contains all uncertainties. The set  $\mathcal{FG}$  shows that the matrices  $F(\tau)$  and  $G(\tau)$  always depend on the same value of  $\tau$  and also on the same value of  $\alpha_i(\tau)$ . This property will be exploited in the derivation of the stability properties. To guarantee the stability of the fixed point  $\xi = 0$  of the closed loop system (4.5), (4.8), it is sufficient to prove that there exists a common quadratic Lyapunov function  $V(\xi_k) = \xi_k^T P \xi_k$  for the uncertain linear system  $\xi_{k+1} = (F(\tau_k) - G(\tau_k)K)\xi_k$ , for all  $(F(\tau), G(\tau)) \in \mathcal{FG}$ , as defined in (4.10). Note in this respect that  $\xi_{k+1} = (F(\tau_k) - G(\tau_k)K)\xi_k$  represents a switching, linear discrete-time system. Therefore, stability is guaranteed if the following LMIs [6] are feasible

$$\begin{aligned} P = P^T &> 0 \\ (F(\tau_k) - G(\tau_k)K)^T P (F(\tau_k) - G(\tau_k)K) - P &< -\gamma P, \forall \tau \in [\tau_{\min}, \tau_{\max}], \end{aligned} \quad (4.11)$$

with  $0 \leq \gamma < 1$ . Due to the definition of  $F(\tau_k)$  and  $G(\tau_k)$ , (4.11) consists of an infinite number of LMIs. In Theorem 4.3.1, we propose a stability condition for  $\tau_k \in [\tau_{\min}, \tau_{\max}]$ ,  $\forall k$ , with  $\tau_{\max} \in [0, h]$ , based on a finite number of LMIs guaranteeing the satisfaction of (4.11).

**Theorem 4.3.1** *Consider the discrete-time representation of the networked control system given in (3.3), (4.8) for a given control gain matrix  $K$ . Moreover, consider the equivalent Jordan form based representation (4.5) of (3.3). Let the sampling interval  $h > 0$  and a minimum and maximum time-delay  $0 \leq \tau_{\min} \leq \tau_{\max} < h$  be given. Define the set of matrices  $\mathcal{H}_{FG}$ <sup>2</sup>*

$$\mathcal{H}_{FG} = \left\{ \left( (\bar{F}_0 + \sum_{i=1}^{\nu} \delta_i \bar{F}_i), (\bar{G}_0 + \sum_{i=1}^{\nu} \delta_i \bar{G}_i) \right) : \delta_i \in \{0, 1\}, i = 1, 2, \dots, \nu \right\}, \quad (4.12)$$

with  $\bar{F}_0 = F_0 + \sum_{i=1}^{\nu} \underline{\alpha}_i F_i$ ,  $\bar{F}_i = (\bar{\alpha}_i - \underline{\alpha}_i) F_i$ ,  $\bar{G}_0 = G_0 + \sum_{i=1}^{\nu} \underline{\alpha}_i G_i$ ,  $\bar{G}_i = (\bar{\alpha}_i - \underline{\alpha}_i) G_i$ ,  $\bar{\alpha}_i = \max_{\tau \in [\tau_{\min}, \tau_{\max}]} \alpha_i(\tau)$ ,  $\underline{\alpha}_i = \min_{\tau \in [\tau_{\min}, \tau_{\max}]} \alpha_i(\tau)$ , and  $F_0, G_0, F_i, G_i$  defined for  $i = 1, 2, \dots, \nu$  in Appendix B.2. If there exist a matrix  $P \in \mathbb{R}^{(n+m) \times (n+m)}$  and a scalar  $0 \leq \gamma < 1$  such that the following LMI conditions are satisfied

$$\begin{aligned} P = P^T &> 0 \\ (H_{F,j} - H_{G,j}K)^T P (H_{F,j} - H_{G,j}K) - P &< -\gamma P, \end{aligned} \quad (4.13)$$

for all  $(H_{F,j}, H_{G,j}) \in \mathcal{H}_{FG}$ , with  $j = 1, 2, \dots, 2^{\nu}$ , then (3.3), (4.8) is globally exponentially stable (GES).

<sup>2</sup>This set consists of a finite number of matrices and contains the generators of a set that describes a convex overapproximation of the infinite set of matrices  $\mathcal{FG}$  (see (4.10)).



To refer to the controller and Lyapunov combination used in this theorem we will use one of the following acronyms, SF-CQLF or ESF-CQLF (state-feedback controller or extended state-feedback controller, with a common quadratic Lyapunov function).

**Proof** <sup>3</sup> The proof of Theorem 4.3.1 consists of two parts. First, we exploit a convex overapproximation of the set  $\mathcal{FG}$ , defined in (4.10). Second, we prove the stability of the discrete-time closed-loop NCS model (4.5), (4.8), and its equivalent (3.3), (4.8), based on a common quadratic candidate Lyapunov function for the discrete-time dynamics.

With  $\bar{\alpha}_i$  and  $\underline{\alpha}_i$ , as defined in the theorem, we can write any  $\alpha_i \in [\underline{\alpha}_i, \bar{\alpha}_i]$  as  $\alpha_i = \underline{\alpha}_i + \delta_i(\bar{\alpha}_i - \underline{\alpha}_i)$ , for some  $\delta_i \in [0, 1]$  and  $i = 1, 2, \dots, \nu$ . Hence, the set  $\overline{\mathcal{FG}}$ , defined as

$$\overline{\mathcal{FG}} = \left\{ \left( (\bar{F}_0 + \sum_{i=1}^{\nu} \delta_i \bar{F}_i), (\bar{G}_0 + \sum_{i=1}^{\nu} \delta_i \bar{G}_i) \right) : \delta_i \in [0, 1], i = 1, 2, \dots, \nu \right\},$$

with  $\bar{F}_0$ ,  $\bar{G}_0$ ,  $\bar{F}_i$ , and  $\bar{G}_i$  as defined in the theorem, is an overapproximation of the set  $\mathcal{FG}$  in the sense that  $\mathcal{FG} \subseteq \overline{\mathcal{FG}}$ . Due to the fact that the new uncertainty parameters  $\delta_i$  can take values in the set  $[0, 1]$ , the set  $\overline{\mathcal{FG}}$  is still an infinite set of matrices. However, each matrix in this set can be written as a convex combination of the generators of the corresponding set. The set of generators of  $\overline{\mathcal{FG}}$  is given by  $\mathcal{H}_{FG}$  in (4.12). Note that  $\mathcal{H}_{FG}$  consist of  $2^\nu$  combinations of matrices, which we denote individually by  $H_{F,j}$ ,  $H_{G,j}$ ,  $j = 1, 2, \dots, 2^\nu$ . Based on these generators,  $\overline{\mathcal{FG}}$  can be written as the convex hull of its generators:

$$\begin{aligned} \overline{\mathcal{FG}} &= \text{co}(\mathcal{H}_{FG}) := \\ &\left\{ \left( \sum_{j=1}^{2^\nu} (\phi_j H_{F,j}), \sum_{j=1}^{2^\nu} (\phi_j H_{G,j}) \right) : \sum_{j=1}^{2^\nu} \phi_j = 1, \phi_j \in [0, 1], j = 1, 2, \dots, 2^\nu \right\}, \end{aligned}$$

in the sense that

$$\mathcal{FG} \subseteq \overline{\mathcal{FG}} = \text{co}(\mathcal{H}_{FG}). \quad (4.14)$$

Next, we show that indeed (4.13) is sufficient to guarantee the satisfaction of (4.11). Since (4.13) holds for all  $(H_{F,j}, H_{G,j}) \in \mathcal{H}_{FG}$ , with  $j = 1, 2, \dots, 2^\nu$ , we have that, by using the Schur complement

$$\begin{pmatrix} (1-\gamma)P & (H_{F,j} - H_{G,j}K)^T P \\ P(H_{F,j} - H_{G,j}K) & P \end{pmatrix} > 0, \quad (4.15)$$

with  $0 \leq \gamma < 1$ . Since  $\phi_j \geq 0 \forall j \in \{1, 2, \dots, 2^\nu\}$  and  $\sum_{j=1}^{2^\nu} \phi_j = 1$ , (4.15) implies

$$\begin{aligned} 0 &< \sum_{j=1}^{2^\nu} \phi_j \begin{pmatrix} (1-\gamma)P & (H_{F,j} - H_{G,j}K)^T P \\ P(H_{F,j} - H_{G,j}K) & P \end{pmatrix} \\ &= \begin{pmatrix} (1-\gamma)P & \sum_{j=1}^{2^\nu} \phi_j (H_{F,j} - H_{G,j}K)^T P \\ \sum_{j=1}^{2^\nu} \phi_j P(H_{F,j} - H_{G,j}K) & P \end{pmatrix}. \end{aligned}$$

---

<sup>3</sup>This proof is presented here to give insight in the reasoning behind Theorem 4.3.1.

Consequently, it holds that

$$\begin{pmatrix} (1-\gamma)P & (\overline{H}_F - \overline{H}_G K)^T P \\ P(\overline{H}_F - \overline{H}_G K) & P \end{pmatrix} > 0, \forall (\overline{H}_F, \overline{H}_G) \in \text{co}(\mathcal{H}_{\mathcal{FG}}). \quad (4.16)$$

Based on (4.14), we have that (4.16) implies that

$$\begin{pmatrix} (1-\gamma)P & (F(\tau_k) - G(\tau_k)K)^T P \\ P(F(\tau_k) - G(\tau_k)K) & P \end{pmatrix} > 0, \forall \tau_k \in [\tau_{\min}, \tau_{\max}].$$

Applying the Schur complement again gives (4.11), which shows that  $V(\xi_k) = \xi_k^T P \xi_k$  is a common quadratic Lyapunov function for (4.5), (4.8) which proves the global exponential stability of the origin  $\xi = 0$  of (3.3), (4.8).  $\square$

### 4.3.2 A Lyapunov-Krasovskii functional

To overcome the possible conservatism of the common quadratic Lyapunov function as considered in Theorem 4.3.1, a Lyapunov-Krasovskii (L-K) functional that indicates the difference between the current and the previous state (i.e.  $x_k - x_{k-1}$ ) is considered. The proposed candidate L-K functional is given by

$$V(x_k, x_{k-1}) = x_k^T \tilde{P} x_k + x_{k-1}^T R x_{k-1} + (x_k - x_{k-1})^T T (x_k - x_{k-1}). \quad (4.17)$$

To use this candidate L-K functional, the NCS model of (3.3), with the state  $\xi_k = (x_k^T \ u_{k-1}^T)^T$  is rewritten based on a state  $\chi_k = (x_k^T \ x_{k-1}^T)^T$ . The disadvantage of this approach is that the number of states increases, which results in larger LMIs. An advantage of this reformulation is that the system is written in a form that allows for the application of other candidate L-K functionals, that are discussed in the literature, see e.g. [55; 87]. For the small delay case, the applicability of other L-K functionals does not lead to an extension of the solution space, due to the fact that they can be reformulated as (4.17). However, for the large delays case including packet dropouts, differences between (4.17) and the available L-K functionals in the literature can be distinguished, see also [37].

To redefine the state-space NCS model of (3.3), including the controller (4.9), system (3.2) is rewritten as

$$\begin{aligned} x_{k+1} &= e^{Ah} x_k - \int_0^{h-\tau_k} e^{As} ds B \overline{K} x_k - \int_{h-\tau_k}^h e^{As} ds B \overline{K} x_{k-1} \\ y_k &= C x_k, \end{aligned} \quad (4.18)$$

such that  $u_{k-1}$  is ‘replaced’ by  $x_{k-1}$ . For the sake of brevity, only the state-feedback controller (4.9) is considered. Note that the extended state-feedback controller (4.8) can be considered as well if the state vector is adapted to  $\chi_k$  instead of  $\xi_k$  and the controller gain  $K_1$  is adapted accordingly, but it will result in more complicated LMI conditions. The state-space representation of (4.18) is given by

$$\chi_{k+1} = \begin{pmatrix} e^{Ah} x_k - \int_0^{h-\tau_k} e^{As} ds B \overline{K} & - \int_{h-\tau_k}^h e^{As} ds B \overline{K} \\ I & 0 \end{pmatrix} \chi_k, \quad (4.19)$$

where

$$\chi_k = \begin{pmatrix} x_k^T & x_{k-1}^T \end{pmatrix}^T. \quad (4.20)$$

To derive LMI conditions for stability analysis, based on the L-K function  $V(\chi_k) = \chi_k^T \begin{pmatrix} \tilde{P} + T & -T \\ -T & R + T \end{pmatrix} \chi_k$ , the Jordan form representation is considered, similar to the use of (4.5) instead of (3.3) in Section 4.3.1. To obtain the Jordan form representation for (4.19), the matrices  $F_0, G_0, F_i, G_i, i = 1, 2, \dots, \nu$  as used in (4.5), are partitioned. Then, we write, based on the definitions in Appendix B.2,

$$\begin{aligned} e^{Ah} &= Q\Theta_0Q^{-1} =: \hat{\Theta}_0, \\ \int_{h-\tau_k}^h e^{As}dsB &= Q \left( \Theta_1 + \sum_{i=1}^{\nu} \alpha_i(\tau_k)\Gamma_{1,i} \right) Q^{-1}B, \\ \int_0^{h-\tau_k} e^{As}dsB &= Q \left( \Xi_0 + \sum_{i=1}^{\nu} \alpha_i(\tau_k)\Xi_i \right) Q^{-1}B, \end{aligned}$$

with  $\Theta_0, \Theta_1, \Xi_0, \Gamma_{1,i}$ , and  $\Xi_i, i = 1, 2, \dots, \nu$ , defined in Appendix B.2, and  $Q$  a matrix with generalized eigenvectors that occurs due to the use of the Jordan form of  $A$ . For the sake of brevity, we define

$$F_0^x = Q\Theta_1Q^{-1}B, \quad G_0^x = Q\Xi_0Q^{-1}B,$$

$$F_i^x = Q\Gamma_{1,i}Q^{-1}B, \quad G_i^x = Q\Xi_iQ^{-1}B, \quad \forall i \in \{1, 2, \dots, \nu\}.$$

Similar to the set  $\mathcal{FG}$  in (4.10), the set  $\mathcal{FG}^x$  describes all possible system matrices that depend on the time-varying delay  $\tau_k$ :

$$\mathcal{FG}^x = \left\{ \begin{pmatrix} F^x(\tau), G^x(\tau) \end{pmatrix} : \tau \in [\tau_{\min}, \tau_{\max}] \right\}, \quad (4.21)$$

with  $F^x(\tau) = F_0^x + \sum_{i=1}^{\nu} \alpha_i(\tau)F_i^x$ ,  $G^x(\tau) = G_0^x + \sum_{i=1}^{\nu} \alpha_i(\tau)G_i^x$  for  $0 \leq \tau_{\min} \leq \tau_{\max} < h$ . Then, system (3.3) or its equivalent (4.5) that is based on the Jordan form, is written as

$$\chi_{k+1} = \begin{pmatrix} \hat{\Theta}_0 - G^x(\tau_k)\overline{K} & -F^x(\tau_k)\overline{K} \\ I & 0 \end{pmatrix} \chi_k, \quad (4.22)$$

for all  $(F^x, G^x) \in \mathcal{FG}^x$ . Stability conditions of this system with a known controller (4.9) and for  $\tau_k \in [\tau_{\min}, \tau_{\max}]$ , with  $0 \leq \tau_{\min} \leq \tau_{\max} < h$ , can be derived analogously to the proof of Theorem 4.3.1.

**Theorem 4.3.2 (SF-LK<sup>4</sup>)** *Consider the discrete-time representation of the NCS, denoted by (4.19) that considers the control law (4.9), with time-varying delays  $\tau_k, k \in \mathbb{N}$  taken from a bounded set  $[\tau_{\min}, \tau_{\max}]$ , with  $0 \leq \tau_{\min} \leq \tau_{\max} <$*

---

<sup>4</sup>To refer to the combination of the controller and the Lyapunov functional used in this theorem we will use the acronym SF-LK (state-feedback controller, with a Lyapunov-Krasovskii functional).

h. Moreover, consider the equivalent discrete-time representation (4.22) that is based on the Jordan form of  $A$ . Consider the set of matrices  $\mathcal{H}_{FG}^x$

$$\mathcal{H}_{FG}^x = \left\{ \left( \bar{F}_0^x + \sum_{i=1}^{\nu} \delta_i \bar{F}_i^x, \bar{G}_0^x + \sum_{i=1}^{\nu} \delta_i \bar{G}_i^x \right) : \delta_i \in \{0, 1\}, i = 1, 2, \dots, \nu \right\}, \quad (4.23)$$

with  $\bar{F}_0^x = F_0^x + \sum_{i=1}^{\nu} \underline{\alpha}_i F_i^x$ ,  $\bar{F}_i^x = (\bar{\alpha}_i - \underline{\alpha}_i) F_i^x$ ,  $\bar{G}_0^x = G_0^x + \sum_{i=1}^{\nu} \underline{\alpha}_i G_i^x$ ,  $\bar{G}_i^x = (\bar{\alpha}_i - \underline{\alpha}_i) G_i^x$ ,  $i = 1, 2, \dots, \nu$ ,  $\bar{\alpha}_i = \max_{\tau \in [\tau_{\min}, \tau_{\max}]} \alpha_i(\tau)$ , and  $\underline{\alpha}_i = \min_{\tau \in [\tau_{\min}, \tau_{\max}]} \alpha_i(\tau)$ .

If there exist matrices  $\tilde{P} \in \mathbb{R}^{n \times n}$ ,  $R \in \mathbb{R}^{n \times n}$ ,  $T \in \mathbb{R}^{n \times n}$ , and a scalar  $0 \leq \gamma < 1$  that satisfy

$$\begin{aligned} \tilde{P} = \tilde{P}^T &> 0 \\ R = R^T &> 0 \\ T = T^T &> 0 \\ \begin{pmatrix} \mathbf{H}_{1,j} + R - (1 - \gamma)(\tilde{P} + T) & \mathbf{H}_{2,j} + (1 - \gamma)T \\ \star & \mathbf{H}_{3,j} - (1 - \gamma)(R + T) \end{pmatrix} &< 0, \end{aligned} \quad (4.24)$$

with

$$\begin{aligned} \mathbf{H}_{1,j} &= \left( \hat{\Theta}_0 - H_{G,j}^x \bar{K} \right)^T \tilde{P} \left( \hat{\Theta}_0 - H_{G,j}^x \bar{K} \right) \\ &\quad + \left( \hat{\Theta}_0 - H_{G,j}^x \bar{K} - I \right)^T T \left( \hat{\Theta}_0 - H_{G,j}^x \bar{K} - I \right), \\ \mathbf{H}_{2,j} &= - \left( \left( \hat{\Theta}_0 - H_{G,j}^x \bar{K} \right)^T \tilde{P} + \left( \hat{\Theta}_0 - H_{G,j}^x \bar{K} - I \right)^T T \right) H_{F,j}^x \bar{K}, \\ \mathbf{H}_{3,j} &= \left( H_{F,j}^x \bar{K} \right)^T (\tilde{P} + T) H_{F,j}^x \bar{K}, \end{aligned}$$

for all  $(H_{F,j}^x, H_{G,j}^x) \in \mathcal{H}_{FG}^x$  and  $j = 1, 2, \dots, 2^\nu$ , then (4.19), (4.9) is GES for any time-varying delay  $\tau_k$  satisfying  $\tau_k \in [\tau_{\min}, \tau_{\max}] \forall k \in \mathbb{N}$ .

**Proof** The proof is given in Appendix A.4.  $\square$

### 4.3.3 Comparison between the common quadratic Lyapunov approach and the Lyapunov-Krasovskii approach

The use of the L-K functional results in more complex LMI conditions than the use of a common quadratic Lyapunov function (compare e.g. (4.24) with (4.13)). Moreover, it is interesting to compare the conservatism of both approaches. To do so, we observe that a similar characterization of the stability as that presented in Theorem 4.3.1 can be formulated based on a common quadratic Lyapunov function in terms of the extended state  $\chi_k$ . Such a characterization guarantees stability for the NCS described by (4.19) and is presented in Corollary 4.3.3.

**Corollary 4.3.3 (SF-CQLF)** Consider the discrete-time representation of the NCS given in (4.19) and its equivalent Jordan form based representation (4.22).

Let the sampling interval  $h > 0$  and a minimum and maximum time-delay  $0 \leq \tau_{\min} \leq \tau_{\max} < h$  be given. Moreover, consider the set of matrices  $\mathcal{H}\mathcal{G}_{FG}^x$ , as defined in (4.23). If there exist a matrix  $\bar{P} \in \mathbb{R}^{2n \times 2n}$  and a scalar  $0 \leq \gamma < 1$  such that the following LMI conditions are satisfied

$$\begin{pmatrix} (1-\gamma)\bar{P} & \begin{pmatrix} \hat{\Theta}_0 - H_{G,j}^x \bar{K} & -H_{F,j}^x \bar{K} \end{pmatrix}^T \bar{P} \\ \star & \bar{P} \end{pmatrix} > 0, \forall (H_{F,j}^x, H_{G,j}^x) \in \mathcal{H}_{FG}^x, \quad (4.25)$$

with  $j = 1, 2, \dots, 2^\nu$ , then (4.19) is GES.

Based on this observation, in Lemma 4.3.4 the difference in conservatism between the use of a common quadratic Lyapunov function and the use of a L-K functional to prove stability is discussed.

**Lemma 4.3.4** *If there exists a L-K functional ( $V_{LK}$ ) of the form (4.17), such that  $\Delta V_{LK}(\chi_k) \leq \gamma V_{LK}(\chi_k)$ , with  $0 \leq \gamma < 1$ , then there exists a common quadratic Lyapunov function of the form  $\chi_k^T \bar{P} \chi_k$  that satisfies the LMIs (4.25) in Corollary 4.3.3.*

**Proof** The proof is given in Appendix A.5 □

This lemma states the the characterization of the stability of the closed-loop NCS model (3.1), (4.9) based on the L-K functional as presented in (4.24) is never less conservative than the characterization based on the common quadratic Lyapunov function, as given in (4.25).

For other L-K functionals a similar reasoning holds, because they consist, especially for the small delay case, of combinations of current and past states or of combinations of current states and past control inputs, see e.g. [55; 87]. For both groups of L-K functionals, it is possible to rewrite the L-K functional dependent on either  $\chi_k$  or  $\xi_k$ , showing that the L-K functional can be rewritten as a common quadratic Lyapunov function.

In Section 4.5, the differences in conservatism between the different proposed theorems will be studied numerically for the motor-roller example.

#### 4.3.4 Intersample behavior

In Theorems 4.3.1 and 4.3.2, sufficient conditions for the asymptotic stability of the discrete-time NCS model (describing the behavior at the sampling instants  $s_k$ ,  $k \in \mathbb{N}$ ) are provided. However, the behavior of the continuous-time system (3.1) between the sampling instants remains unknown. In this section, it will be shown that the intersample behavior is asymptotically stable as well under the conditions of these theorems. As an example, we study the intersample behavior under the conditions of Theorem 4.3.1.

Consider the continuous-time system (3.1). To study the intersample behavior an additional variable  $\tilde{t} = t - s_k$ ,  $t \in [s_k, s_{k+1})$ , is introduced for which

it holds that  $\tilde{t} \in [0, h)$ . To determine the time-evolution of the state of the continuous-time system for  $t \in [s_k, s_{k+1})$ , the well-known convolution integral has to be solved. Two different cases can be distinguished, due to the uncertainty of the value of the delay  $\tau_k \in [0, h)$ , namely  $\tau_k > \tilde{t}$  and  $\tau_k \leq \tilde{t}$ . It holds that

$$x(s_k + \tilde{t}) = e^{A\tilde{t}}x_k + \int_0^{\tilde{t}} e^{As}dsBu_{k-1}, \text{ for } \tilde{t} < \tau_k, \quad (4.26)$$

and

$$x(s_k + \tilde{t}) = e^{A\tilde{t}}x_k + \int_0^{\tilde{t}-\tau_k} e^{As}dsBu_k + \int_{\tilde{t}-\tau_k}^{\tilde{t}} e^{As}dsBu_{k-1}, \text{ for } \tilde{t} \geq \tau_k. \quad (4.27)$$

Recall that it holds that  $u_k = u(s_k)$ ,  $u_{k-1} = u(s_{k-1})$ , and  $x_k = x(s_k)$ . For both cases, (4.26) and (4.27), an upper bound for  $|x(s_k + \tilde{t})|$  can be derived, as is stated in the following lemma.

**Lemma 4.3.5** *Consider the continuous-time system (3.1) and the continuous-time state evolutions (4.26) and (4.27), and the discrete-time system (3.3). Then, the state evolution of the continuous-time system (3.1) can be upper bounded as follows*

$$|x(s_k + \tilde{t})| \leq c_0|x_k| + c_1|u_k| + c_2|u_{k-1}|, \quad (4.28)$$

for the positive constants  $c_0$ ,  $c_1$ , and  $c_2$ , defined in (A.24), (A.22), (A.21), (A.18), (A.17), and (A.16) in Appendix A.6, and for all  $\tilde{t} \in [0, h)$ .

**Proof** The proof of this lemma is given in Appendix A.6.  $\square$

Next, Theorem 4.3.6 shows that the conditions in Theorem 4.3.1 or 4.3.2 under which the discrete-time system is globally asymptotically stable also imply global asymptotic stability of the intersample behavior.

**Theorem 4.3.6** *If system (3.3) satisfies the LMI conditions in either (4.13) or (4.24), then the continuous-time system (3.1) is asymptotically stable as well.*

**Proof** The proof is given in Appendix A.7.  $\square$

#### 4.4 Variable sampling intervals, large delays, and packet dropouts

With the case of small delays as a stepping stone, we consider the case with variable sampling intervals, variable delays that may be larger than the sampling interval, and a bounded number of subsequent packet dropouts. Recall that the continuous-time NCS representation is given by (3.12), the discrete-time NCS representation is given by (3.24), or equivalently, by (4.7) which describes the discrete-time NCS model based on the Jordan form of the continuous-time

system matrix  $A$ . The situations with constant sampling intervals with or without packet dropouts can be derived easily from the stability conditions that are presented in this section. We consider the same controllers as in Section 4.3. However, for the extended state-feedback controller we propose an adaptation to include past control input information based on  $\xi_k$ :

$$u_k = -K\xi_k = -\overline{K}x_k - K_1u_{k-1} - K_2u_{k-2} \dots - K_{\overline{d}+\overline{\delta}}u_{k-\overline{d}-\overline{\delta}}, \quad (4.29)$$

with  $K \in \mathbb{R}^{m \times (\overline{d}+\overline{\delta})m+n}$ . The standard state-feedback controller is given by (4.9). Still, (4.9) is a special case of (4.29) if  $K = \begin{pmatrix} \overline{K} & 0_{m,(\overline{d}+\overline{\delta})m} \end{pmatrix}$  is considered. In contrast to the previous section, there are some limitations on the use of (4.29) in combination with the proposed model (3.24), which is only valid for a static and time-invariant controller. In the case of a packet dropout related to  $u_k$ , i.e.  $m_k = 1$ , two situations are possible:

1.  $y_k = x_k$  does not arrive at the controller and thus  $u_k$  cannot be computed,
2.  $y_k = x_k$  arrives at the controller, and  $u_k$  is computed, but  $u_k$  does not arrive at the actuator.

In the second case, in principle,  $u_k$  is available in the implementation of the controller and the update  $u_{k+1}$ , using (4.29), can be made. In the first case, however, the controller (4.29) cannot be updated anymore, due to the unknown  $u_k$  and a deadlock in the controller will occur for  $u_{k+1}$ . A remedy might be to use  $u_k := u_{k-1}$  if  $m_k = 1$ , but this results in a controller that depends explicitly on the time-varying parameter  $m_k$ . Consequently, we obtain a switching controller, where the switching depends on time. This contradicts the assumption that the controller has to be time-invariant in NCS model of Chapter 3. The occurrence of a deadlock means that controller (4.29), as proposed in [38] for the delays smaller than the sampling interval, does not function properly in the case of packet dropouts between the sensor and the controller (first case). The state-feedback controller (4.9) does not suffer from this problem as it only depends on the state  $x_k$  (and not on the previous control inputs). A similar reasoning holds for message rejection between the sensor and the controller. For the computation of  $u_k$ , based on (4.29), both  $y_k = x_k$  and the previous control inputs  $u_{k-1}, \dots, u_{k-\overline{d}-\overline{\delta}}$  need to be known. In the case of message rejection of e.g.  $y_{k-1}$  (because  $y_k$  is available in the controller before  $y_{k-1}$  is received at the controller), the control input  $u_{k-1}$  is not known to the controller, which makes it impossible to compute  $u_k$ . Clearly, similar to the case with packet dropouts, a deadlock occurs. A remedy might be to wait with the computation of  $u_k$  until  $y_{k-1}$  is available. Then, first  $u_{k-1}$  can be computed and then  $u_k$  can be computed. A disadvantage of this proposal is the increase of the computation time, due to the waiting time until the past measurement data arrives, and therefore an increase of the delay in the control input  $u_k$ . Moreover, the control implementation needs to include a check whether all past control inputs are available; consequently, an additional increase in the computation time can be expected. In the remaining part of the thesis, we limit ourselves to the less

complicated controller implementation, in which the waiting on previous data is not possible. Therefore, in the case of controller (4.29), we adopt the following assumption:

**Assumption 4.4.1** There is no packet dropout between the sensor and the controller and  $y_k$  always arrives at the controller after the moment that  $u_{k-1}$  is sent to the actuator, i.e.  $s_k + \tau_k^{sc} > s_{k-1} + \tau_{k-1}^{sc} + \tau_{k-1}^c$ , therefore it should hold that  $\tau_{\min}^{sc} > \tau_{\max}^{sc} - h_{\min} + \tau_{\max}^c$ .

Note that in this assumption  $\tau_{\max}^c$  is considered, to avoid that a computation of a control action is stopped, when new measurement data arrives at the controller during a computation. Without this assumption, the worst case scenario would result in sending no control action at all to the actuator.

#### 4.4.1 A common quadratic Lyapunov function based on the extended state vector $\xi_k$

Theorem 4.3.1 can be extended to the NCS model with time-varying sampling intervals, large delays, and packet dropout. Recall that in Theorem 4.3.1 an overapproximation based on the minimum and maximum values of  $\alpha_i(\tau_k)$ ,  $i = 1, 2, \dots, \nu$ , was exploited. Because for the large delay case (including variable sampling intervals)  $\alpha_i$ ,  $i = 1, 2, \dots, \zeta$ , depends on  $t_j^k$  and  $h_k$  instead of only on  $\tau_k$ , the corresponding minimum and maximum values of the functions  $\alpha_i(t_j^k, h_k)$  have to be redefined. To determine the minimum and maximum values of the uncertain parameters  $\alpha_i(t_j^k, h_k)$  in (4.7) (or equivalently (4.6) for constant sampling intervals), the minimum and maximum values of  $t_j^k$  and  $h_k$ , that depend on the size of the time-delays, the number of subsequent packet dropouts, and the size of the sampling interval, need to be defined. Recall that it holds that  $h_k \in [h_{\min}, h_{\max}]$ . In Lemma 4.4.2, the minimum and maximum values of  $t_j^k$ ,  $j \in \{k - \bar{d} - \bar{\delta}, \dots, k - \underline{d} + 1\}$ , are described.

**Lemma 4.4.2** Consider the time instants  $t_j^k$  as defined in (3.22), where  $s_j$  (with  $h_j = s_{j+1} - s_j$ ),  $\tau_j$ , and  $m_j$  are taken from the class  $\mathcal{S}$  defined in (3.20). The minimum value of  $t_j^k$ ,  $j \in \{k - \bar{d} - \bar{\delta} + 1, \dots, k - \underline{d}\}$ , is given by

$$t_{j,\min}^k = \begin{cases} \min\{\tau_{\min} - \underline{d}h_{\max}, h_{\min}\} & \text{if } j = k - \underline{d} \\ 0 & \text{if } j < k - \underline{d}, \end{cases} \quad (4.30)$$

and the maximum value of  $t_j^k$ ,  $j \in \{k - \bar{d} - \bar{\delta} + 1, \dots, k - \underline{d}\}$ , is given by

$$t_{j,\max}^k = \begin{cases} \min\{\tau_{\max} - (k - j - \bar{\delta})h_{\min}, h_{\max}\} & \text{if } j \in \{k - \bar{d} - \bar{\delta} + 1, \dots, k - \bar{\delta} - \underline{d}\}, \\ h_{\max} & \text{if } j \in \{k - \bar{\delta} - \underline{d} + 1, \dots, k - \underline{d}\}. \end{cases} \quad (4.31)$$

Note that  $t_{k-\bar{d}-\bar{\delta}}^k := 0$  and  $t_{k-\underline{d}+1}^k := h_k$ , which gives for the minimum and maximum bound  $t_{k-\underline{d}+1} \in [h_{\min}, h_{\max}]$ . Moreover,  $\tau_{\max} - (\bar{d} - 1)h_{\min}$  is by



definition smaller than (or equal to)  $h_{\max}$ , which guarantees that at least one value of  $t_j^k$  depends on the maximum delay  $\tau_{\max}$ .

**Proof** The proof is given in Appendix A.8.  $\square$

**Remark 4.4.3** If the sampling interval is constant (i.e.  $h_{\min} = h_{\max} = h$ ), the minimum and maximum values of  $t_j^k$  are slightly simpler. The minimum bound, defined in (4.30) can be replaced by

$$t_{j,\min}^k = \begin{cases} \tau_{\min} - \underline{d}h & \text{if } j = k - \underline{d} \\ 0 & \text{if } j < k - \underline{d}, \end{cases} \quad (4.32)$$

for  $j \in \{k - \bar{d} - \bar{\delta} + 1, \dots, k - \underline{d}\}$ , as  $\tau_{\min} - \underline{d}h \leq h$ , due to the definition of  $\underline{d}$  in Lemma 3.3.1. This proves the correctness of (4.32). The maximum value of  $t_j^k$  for  $j \in \{k - \bar{d} - \bar{\delta} + 1, k - \bar{d} - \bar{\delta} + 2, \dots, k - \underline{d}\}$  for constant sampling intervals  $h$  is obtained from (4.33):

$$t_{j,\max}^k = \begin{cases} h & \text{if } j > k - \bar{d} - \bar{\delta} + 1 \\ \tau_{\max} - (\bar{d} - 1)h & \text{if } j = k - \bar{d} - \bar{\delta} + 1. \end{cases} \quad (4.33)$$

To explain these bounds, note that based on the definition of  $\bar{d}$  in Lemma 3.3.1, it holds for  $j = k - \bar{d} - \bar{\delta} + 1$  that  $\tau_{\max} - (k - j - \bar{\delta})h = \tau_{\max} - (\bar{d} - 1)h \leq h$ . For larger values of  $j$ , it holds that  $\tau_{\max} - (k - j - \bar{\delta})h > h$ , which simplifies the computation of the upper bound of  $t_j^k$ . Finally, recall from Lemma 3.3.1 that  $t_{k-\bar{d}-\bar{\delta}}^k := 0$  and  $t_{k-\underline{d}+1}^k := h$ , which shows that both parameters are constant and do not need to be included in (4.32) and (4.33).

To derive the stability conditions, similar to Theorem 4.3.1, the set of matrices  $\mathcal{FG}$  is redefined, such that the variation of the sampling interval, the variation of the delay, and packet dropouts are included:

$$\mathcal{FG} = \left\{ \left( F(\mathbf{t}^k, h_k), G(\mathbf{t}^k, h_k) \right) : \mathbf{t}^k = (t_{k-\bar{d}-\bar{\delta}+1}^k, \dots, t_{k-\underline{d}}^k), \right. \\ \left. t_j^k \in [t_{j,\min}^k, t_{j,\max}^k], k - \bar{d} - \bar{\delta} < j \leq k - \underline{d}, h_k \in [h_{\min}, h_{\max}] \right\}, \quad (4.34)$$

with  $F(\mathbf{t}^k, h_k) = F_0 + \sum_{i=1}^{\zeta} \alpha_i(t_j^k, h_k) F_i$ ,  $G(\mathbf{t}^k, h_k) = G_0 + \sum_{i=1}^{\zeta} \alpha_i(t_j^k, h_k) G_i$ ,  $\alpha_i(t_j^k, h_k)$ ,  $i = 1, 2, \dots, \zeta$ , defined in Appendix B.3 by (B.38), (B.39), (B.40), and (B.41). The constant matrices  $F_0$ ,  $G_0$ ,  $F_i$ , and  $G_i$ ,  $i = 1, 2, \dots, \zeta$ , are also defined in Appendix B.3. Note that in (4.34) the parameter  $j$  takes values from  $j \in \{k - \bar{d} - \bar{\delta} + 1, k - \bar{d} - \bar{\delta} + 2, \dots, k - \underline{d} + 1\}$ , because  $t_{k-\bar{d}-\bar{\delta}}^k := 0$  and  $t_{k-\underline{d}+1}^k := h_k$ , as defined in Lemma 3.4.1. Moreover,  $\alpha_i(t_j^k, h_k)$  depends either on only one uncertain time-varying parameter  $t_j^k$ ,  $j \in \{k - \bar{d} - \bar{\delta} + 1, k - \bar{d} - \bar{\delta} + 2, \dots, k - \underline{d} + 1\}$  in combination with  $h_k$  or only on  $h_k$ . Based on Lemma 3.4.1, this definition of  $j$  gives all possible time-varying terms in (3.24). For the case with a constant

sampling interval the number of uncertain parameters is reduced from  $\zeta$  to  $\beta = \zeta - \nu$ , with  $\nu$  as in (4.4). Moreover, the definitions of the matrices  $F_0$ ,  $G_0$ ,  $F_i$ , and  $G_i$  are then slightly adapted, as is described in Appendix B.3. To prove stability of the discrete-time representation of the NCS (3.24), which includes time-varying sampling intervals, packet dropouts, and time-varying delays, Theorem 4.3.1 is adapted. Additionally, the stability of the continuous-time NCS (3.12) can be evaluated based on the study of the intersample behavior as proposed in Theorem 4.3.6 for the small delay case. Therefore, Theorem 4.4.4 proposes conditions that guarantee the stability of the continuous-time and discrete-time NCS model. Note that these conditions are also valid for the large delay case with constant sampling intervals and without packet dropouts, if the assumptions on the parameter  $h_k$  and  $\bar{\delta}$  are adapted, correspondingly.

**Theorem 4.4.4 ((E)SF-CQLF)** *Consider the continuous-time NCS model (3.12), (3.21), (3.22) with sequences of sampling instants, time-delays, and packet dropouts  $\sigma = \{(s_k, \tau_k, m_k)\}_{k \in \mathbb{N}} \in \mathcal{S}$ , with  $\mathcal{S}$  defined in (3.20) and consider the corresponding discrete-time representation (3.24), (3.25) and its equivalent representation (4.7) that is based on the Jordan form of the continuous-time system matrix  $A$  of (3.12). Moreover, consider a known extended state-feedback controller (4.29), with  $\bar{d}$  defined in Lemma 3.4.1, including Assumption 4.4.1, or consider the known state-feedback controller (4.9) which is of the form of (4.29), with  $K = \begin{pmatrix} \bar{K} & 0_{m, (\bar{d}+\bar{\delta})m} \end{pmatrix}$ . Define the set of matrices  $\mathcal{H}_{FG}$ :*

$$\mathcal{H}_{FG} = \left\{ \left( (\bar{F}_0 + \sum_{i=1}^{\zeta} \delta_i \bar{F}_i), (\bar{G}_0 + \sum_{i=1}^{\zeta} \delta_i \bar{G}_i) \right) : \delta_i \in \{0, 1\}, i = 1, 2, \dots, \zeta \right\}, \quad (4.35)$$

with  $\bar{F}_0 = F_0 + \sum_{i=1}^{\zeta} \underline{\alpha}_i F_i$ ,  $\bar{F}_i = (\bar{\alpha}_i - \underline{\alpha}_i) F_i$ ,  $\bar{G}_0 = G_0 + \sum_{i=1}^{\zeta} \underline{\alpha}_i G_i$ ,  $\bar{G}_i = (\bar{\alpha}_i - \underline{\alpha}_i) G_i$ , and

$$\begin{aligned} \bar{\alpha}_i &= \max_{t_j^k \in [t_{j,\min}^k, t_{j,\max}^k], h_k \in [h_{\min}, h_{\max}]} \alpha_i(t_j^k, h_k), \\ \underline{\alpha}_i &= \min_{t_j^k \in [t_{j,\min}^k, t_{j,\max}^k], h_k \in [h_{\min}, h_{\max}]} \alpha_i(t_j^k, h_k), \end{aligned} \quad (4.36)$$

the maximum and minimum value of  $\alpha_i(t_j^k, h_k)$ , respectively, with  $t_{j,\min}^k$  and  $t_{j,\max}^k$  defined in (4.30) and (4.31), respectively.

If there exist a matrix  $P \in \mathbb{R}^{(n+(\bar{d}+\bar{\delta})m) \times (n+(\bar{d}+\bar{\delta})m)}$  and a scalar  $0 \leq \gamma < 1$ , such that the following LMI conditions are satisfied:

$$\begin{pmatrix} (1-\gamma)P & (H_{F,j} - H_{G,j}K)^T P \\ P(H_{F,j} - H_{G,j}K) & P \end{pmatrix} > 0, \quad (4.37)$$

for all  $(H_{F,j}, H_{G,j}) \in \mathcal{H}_{FG}$ , with  $j = 1, 2, \dots, 2^\zeta$ , then (3.12), (3.21), (3.22), with the controller defined in (4.29) or (4.9), is globally asymptotically stable (GAS) for any sequence of sampling instants, time-varying delays, and packet dropouts  $\sigma \in \mathcal{S}$ .

**Proof** The proof is completely analogous to the proof of Theorem 4.3.1 and Theorem 4.3.6.  $\square$

**Remark 4.4.5** Note that for time-varying delays and packet dropouts with a constant sampling interval, the set  $\mathcal{S}$  in Theorem 4.4.4 can be replaced by the set  $\mathcal{M}$  in (3.14) that defines the sequences of delays and packet dropouts. Then, the parameter  $\zeta$  is replaced by  $\beta$ , as defined in Lemma 3.3.1. Moreover, it holds that

$$\mathcal{FG} = \left\{ \left( F(\mathbf{t}^k), G(\mathbf{t}^k) \right) : \mathbf{t}^k = (t_{k-\bar{d}-\bar{\delta}+1}^k, \dots, t_{k-\underline{d}}^k), t_j^k \in [t_{j,\min}^k, t_{j,\max}^k], \right. \\ \left. k - \bar{d} - \bar{\delta} < j \leq k - \underline{d} \right\},$$

with  $F(\mathbf{t}^k) = F_0 + \sum_{i=1}^{\beta} \alpha_i(t_j^k) F_i$ ,  $G(\mathbf{t}^k) = G_0 + \sum_{i=1}^{\beta} \alpha_i(t_j^k) G_i$ ,  $\alpha_i$  defined in Appendix B.3 for  $i \in \{1, 2, \dots, \beta\}$ , and  $F_0$ ,  $G_0$ ,  $F_i$ , and  $G_i$ ,  $i = 1, 2, \dots, \beta$ , defined in the same appendix, based on the remarks that hold for the case with constant sampling intervals.

**Remark 4.4.6** The use of Theorem 4.4.4 removes the clear difference between packet dropouts and time-varying delays, due to the overapproximation of  $\alpha_i$ ,  $i = 1, 2, \dots, \zeta$ , and therefore of  $t_j^k$ . Studying this difference shows that the maximum number of subsequent packet dropouts and the maximum time-delay are interchangeable (at least on the level of the derived stability conditions). For constant sampling intervals, the minimum and maximum values of  $t_j^k$  are defined in (4.32) and (4.33), respectively. Then, the values of  $\tau_{\max}$  and  $\bar{\delta}$  are interchangeable as long as their summation remains constant. For time-varying sampling intervals, the value of  $\tau_{\max} + \bar{\delta}$  remains constant if  $\bar{d} + \bar{\delta}$  remains constant as well (i.e.  $h_{\min}$  should keep the same value).

The validity of this remark can be shown by considering the minimum and maximum values of  $t_j^k$  in (4.30), (4.31), (4.32), and (4.33). Clearly, for different values of  $\tau_{\max} + \bar{\delta} = \text{constant}$  (and all other parameters unchanged) the minimum and maximum values of  $t_j^k$  do not change. This effect is caused by the chosen analysis approach. To explain that the observed similarity is not true for a real NCS, consider the following example for constant sampling intervals. The difference between the situation with small delays and without packet dropouts, i.e.  $\tau_{\max} = h$ ,  $\tau_{\min} = 0$ ,  $\bar{\delta} = 0$  is compared to the situation without delays and with maximally one subsequent packet dropout:  $\tau_{\max} = \tau_{\min} = 0$ ,  $\bar{\delta} = 1$ . The discrete-time NCS model for  $\tau_k \in [0, h]$  is given by (3.2):

$$x_{k+1} = e^{Ah} x_k + \int_0^{h-\tau_k} e^{As} ds B u_k + \int_{h-\tau_k}^h e^{As} ds B u_{k-1}. \quad (4.38)$$

The discrete-time NCS model for the case without delays and with  $\bar{\delta} = 1$  is given by:

$$x_{k+1} = \begin{cases} e^{Ah} x_k + \int_0^h e^{As} ds B u_k & \text{if } m_k = 0 \\ e^{Ah} x_k + \int_0^h e^{As} ds B u_{k-1} & \text{if } m_k = 1. \end{cases} \quad (4.39)$$

Clearly, the obtained NCS models differ. If the NCS model is derived according to (3.16) and Lemma 3.3.1 the following model is obtained ( $\underline{d} = 0, \bar{d} + \bar{\delta} = 1$ ):

$$\begin{aligned} x_{k+1} &= e^{Ah} x_k + \int_{h-t_{k+1}^k}^{h-t_k^k} e^{As} ds Bu_k + \int_{h-t_k^k}^{h-t_{k-1}^k} e^{As} ds Bu_{k-1} \\ &= e^{Ah} x_k + \int_0^{h-t_k^k} e^{As} ds Bu_k + \int_{h-t_k^k}^h e^{As} ds Bu_{k-1}. \end{aligned}$$

Implementing  $t_k^k$  gives indeed (4.38) if  $\tau_k \in [0, h)$  and  $m_k = 0$  for the small delay case and (4.39) if  $\tau = 0$  and  $m_k \in \{0, 1\}$ . For analysis, as shown in Theorem 4.4.4,  $t_k^k$  is replaced by its upper and lower bound. For both cases, the lower bound is equal to zero (from (4.32)) and the upper bound is equal to  $h$  (from (4.33)), resulting in the same LMIs for stability analysis. Therefore, in the stability analysis the difference between packet dropouts and time-varying delays is partly lost.

The next section describes the adaptation of the stability analysis conditions, based on the L-K functional, presented in Theorem 4.3.2, such that it is applicable for the large delay case including packet dropouts and time-varying sampling intervals. Note that Remark 4.4.6 holds for the next section as well.

#### 4.4.2 A Lyapunov-Krasovskii functional

To apply the stability analysis approach based on the Lyapunov-Krasovskii (L-K) functional, the extended state vector, consisting of the current and past states, is given by  $\chi_k = \begin{pmatrix} x_k^T & x_{k-1}^T & \dots & x_{k-\bar{d}-\bar{\delta}}^T \end{pmatrix}^T$ . The proposed candidate L-K functional is given by:

$$V(\chi_k) = x_k^T P x_k + \sum_{i=1}^{\bar{d}+\bar{\delta}} x_{k-i}^T R_i x_{k-i} + \sum_{i=1}^{\bar{d}+\bar{\delta}} (x_{k-i+1} - x_{k-i})^T T_i (x_{k-i+1} - x_{k-i}). \quad (4.40)$$

Note that for the sake of simplicity, (4.40) considers only the difference between the sequential states, instead of the differences between all states in the extended state vector. Therefore, additional difference equations, such as  $\sum_{i=2}^{\bar{d}+\bar{\delta}} (x_{k-i+2} - x_{k-i})^T T_i (x_{k-i+2} - x_{k-i})$  can be considered as well, but result in more complex, however less conservative, stability conditions.

Here, we only consider the state-feedback controller (4.9), because no additional assumptions (as given in Assumption 4.4.1) on the size of the delays are needed and the complexity of the LMIs remains acceptable. Before the stability conditions are derived, we first define the NCS model, based on the state vector  $\chi_k$ , as

$$\chi_{k+1} = \begin{pmatrix} e^{Ah_k} - \tilde{M}_0 \bar{K} & -\tilde{M}_1 \bar{K} & \dots & -\tilde{M}_{\bar{d}+\bar{\delta}-1} \bar{K} & -\tilde{M}_{\bar{d}+\bar{\delta}} \bar{K} \\ I & 0 & \dots & 0 & 0 \\ 0 & I & \dots & 0 & 0 \\ \vdots & & \ddots & & \vdots \\ 0 & \dots & 0 & I & 0 \end{pmatrix} \chi_k, \quad (4.41)$$

$$\text{with } \tilde{M}_\rho(t_{k-\rho+1}^k, t_{k-\rho}^k, h^k) = \begin{cases} \int_{h_k - t_{k-\rho+1}^k}^{h_k - t_{k-\rho}^k} e^{As} ds B & \text{if } \rho \geq \underline{d}, \\ 0 & \text{if } \rho < \underline{d}, \end{cases}$$

for  $\rho \in \{0, 1, \dots, \bar{d} + \bar{\delta}\}$  and  $t_{k-\rho}^k$  defined in (3.22), with  $j = k - \rho$ .

To determine the stability conditions, the matrices in (4.41) need to be rewritten, based on the Jordan form of the continuous-time system matrix  $A$ . Therefore, we adopt the following notation

$$\begin{aligned} e^{Ah_k} &= Q \left( \Theta_0 + \sum_{i=1}^{\zeta} \alpha_i(t_j^k, h_k) \Gamma_{0,i} \right) Q^{-1}, \\ \tilde{M}_0 &= Q \left( \Xi_0 + \sum_{i=1}^{\zeta} \alpha_i(t_j^k, h_k) \Xi_i \right) Q^{-1} B, \\ \tilde{M}_1 &= Q \left( \Theta_1 + \sum_{i=1}^{\zeta} \alpha_i(t_j^k, h_k) \Gamma_{1,i} \right) Q^{-1} B, \\ &\vdots \\ \tilde{M}_{\bar{d}+\bar{\delta}} &= Q \left( \Theta_{\bar{d}+\bar{\delta}} + \sum_{i=1}^{\zeta} \alpha_i(t_j^k, h_k) \Gamma_{\bar{d}+\bar{\delta},i} \right) Q^{-1} B, \end{aligned}$$

with  $Q$  a matrix with generalized eigenvectors that appears due to the use of the Jordan form of  $A$  and the matrices  $\Theta_0, \Xi_0, \Gamma_{0,i}, \Xi_i, \Theta_i, \Gamma_{i,i}, \hat{i} = 1, 2, \dots, \bar{d} + \bar{\delta}$ , and the parameters  $\alpha_i(t_j^k, h_k)$ ,  $i = 1, 2, \dots, \zeta$ , defined in Appendix B.3. For brevity of the notation, we define

$$\begin{aligned} F_{0,0}^x &= Q\Theta_0Q^{-1}, & F_{0,i}^x &= Q\Gamma_{0,i}Q^{-1}, \\ G_0^x &= Q\Xi_0Q^{-1}B, & G_i^x &= Q\Xi_iQ^{-1}B, \\ F_{i,0}^x &= Q\Theta_iQ^{-1}B, & F_{i,i}^x &= Q\Gamma_{i,i}Q^{-1}B, \end{aligned}$$

with  $\hat{i} = 1, 2, \dots, \bar{d} + \bar{\delta}$  an index that denotes the position in the matrix  $\tilde{A}$ , similar to the matrices  $\tilde{M}_{\hat{i}}$  and  $i = 0, 1, \dots, \zeta$ , the index that corresponds to the time-varying parameter  $\alpha_i$ . Then, define the sets of matrices:

$$\begin{aligned} \mathcal{FG}^x &= \left\{ \left( F_0^x(\mathbf{t}^k, h_k), F_1^x(\mathbf{t}^k, h_k), \dots, F_{\bar{d}+\bar{\delta}}^x(\mathbf{t}^k, h_k), G^x(\mathbf{t}^k, h_k) \right) : \right. \\ &\quad \mathbf{t}^k = (t_{k-\bar{d}-\bar{\delta}+1}^k, \dots, t_{k-\underline{d}}^k), \quad t_j^k \in [t_{j,\min}^k, t_{j,\max}^k], \quad h_k \in [h_{\min}, h_{\max}], \\ &\quad \left. k - \bar{d} - \bar{\delta} < j \leq k - \underline{d} \right\}, \end{aligned} \tag{4.42}$$

$$\begin{aligned} \text{with } F_0^x(\mathbf{t}^k, h_k) &:= F_{0,0}^x + \sum_{i=1}^{\zeta} \alpha_i(t_j^k, h_k) F_{0,i}^x, \\ G^x(\mathbf{t}^k, h_k) &:= G_0^x + \sum_{i=1}^{\zeta} \alpha_i(t_j^k, h_k) G_i^x, \quad F_i^x(\mathbf{t}^k, h_k) := F_{i,0}^x + \sum_{i=1}^{\zeta} \alpha_i(t_j^k, h_k) F_{i,i}^x, \end{aligned}$$

for  $\hat{i} = 1, 2, \dots, \bar{d} + \bar{\delta}$ . Then, the discrete-time NCS description, based on the state-vector  $\chi_k$  and the Jordan form representation of the continuous-time system matrix  $A$ , is given by:

$$\chi_{k+1} = \begin{pmatrix} \mathbf{F} & -F_1^x(\mathbf{t}^k, h_k)\bar{K} & -F_2^x(\mathbf{t}^k, h_k)\bar{K} & \dots & -F_{\bar{d}+\bar{\delta}}^x(\mathbf{t}^k, h_k)\bar{K} \\ I & 0 & 0 & \dots & 0 \\ 0 & I & 0 & \dots & 0 \\ \vdots & \vdots & \ddots & \ddots & \vdots \\ 0 & \dots & 0 & I & 0 \end{pmatrix} \chi_k, \quad (4.43)$$

with  $\mathbf{F} = F_0^x(\mathbf{t}^k, h_k) - G^x(\mathbf{t}^k, h_k)\bar{K}$ , for all  $\left( F_0^x(\mathbf{t}^k, h_k), F_1^x(\mathbf{t}^k, h_k), \dots, F_{\bar{d}+\bar{\delta}}^x(\mathbf{t}^k, h_k), G^x(\mathbf{t}^k, h_k) \right) \in \mathcal{FG}^x$ . The stability conditions for the case with time-varying sampling intervals, packet dropouts, and delays larger than the sampling interval are given in Theorem 4.4.7.

**Theorem 4.4.7 (SF-LK)** Consider the continuous-time NCS model (3.12), (3.21), (3.22), with sequences of sampling instants, time-delays, and packet dropouts  $\sigma \in \mathcal{S}$ , and the state-feedback controller (4.9). Moreover, consider the discrete-time representation (4.41) and its equivalent, based on the Jordan form of the continuous-time system matrix  $A$ , (4.43) and the set of matrices  $\mathcal{H}_{FG}^x$

$$\mathcal{H}_{FG}^x = \left\{ \left( \bar{F}_{0,0}^x + \sum_{i=1}^{\zeta} \delta_i \bar{F}_{0,i}^x, \bar{F}_{1,0}^x + \sum_{i=1}^{\zeta} \delta_i \bar{F}_{1,i}^x, \dots, \bar{F}_{\bar{d}+\bar{\delta},0}^x + \sum_{i=1}^{\zeta} \delta_i \bar{F}_{\bar{d}+\bar{\delta},i}^x, \bar{G}_0^x + \sum_{i=1}^{\zeta} \delta_i \bar{G}_i^x \right) : \delta_i \in \{0, 1\}, i = 1, 2, \dots, \zeta \right\}, \quad (4.44)$$

with  $\bar{F}_{0,0}^x = F_{0,0}^x + \sum_{i=1}^{\zeta} \underline{\alpha}_i F_{0,i}^x$ ,  $\bar{F}_{0,i}^x = (\bar{\alpha}_i - \underline{\alpha}_i) F_{0,i}^x$ ,  $\bar{F}_{i,0}^x = F_{i,0}^x + \sum_{i=1}^{\zeta} \underline{\alpha}_i F_{i,i}^x$ ,  $\bar{F}_{i,i}^x = (\bar{\alpha}_i - \underline{\alpha}_i) F_{i,i}^x$ ,  $\bar{G}_0^x = G_0^x + \sum_{i=1}^{\zeta} \underline{\alpha}_i G_i^x$ ,  $\bar{G}_i^x = (\bar{\alpha}_i - \underline{\alpha}_i) G_i^x$ , for  $i = 1, 2, \dots, \zeta$ ,  $\hat{i} = 1, 2, \dots, \bar{d} + \bar{\delta}$ , and

$$\begin{aligned} \bar{\alpha}_i &= \max_{t_j^k \in [t_{j,\min}^k, t_{j,\max}^k], h_k \in [h_{\min}, h_{\max}]} \alpha_i(t_j^k, h_k), \\ \underline{\alpha}_i &= \min_{t_j^k \in [t_{j,\min}^k, t_{j,\max}^k], h_k \in [h_{\min}, h_{\max}]} \alpha_i(t_j^k, h_k), \end{aligned}$$

If there exist matrices  $\tilde{P} \in \mathbb{R}^{n \times n}$ ,  $R_{\hat{i}} \in \mathbb{R}^{n \times n}$ ,  $T_{\hat{i}} \in \mathbb{R}^{n \times n}$ , and a scalar  $0 \leq \gamma < 1$  that satisfy

$$\begin{aligned} \tilde{P} = \tilde{P}^T &> 0 \\ R_{\hat{i}} = R_{\hat{i}}^T &> 0 \\ T_{\hat{i}} = T_{\hat{i}}^T &> 0 \end{aligned} \quad (4.45)$$

for  $\hat{i} = 1, 2, \dots, \bar{d} + \bar{\delta}$ , and satisfy

$$\left( \begin{array}{ccc} \mathbf{M}_{0,j} & \mathbf{L}_{0,j} & -(\mathbf{G}_{0,j}^T \tilde{P} + \mathbf{H}_{0,j}^T T_1) \mathbf{F}_{2,j} & -(\mathbf{G}_{0,j}^T \tilde{P} + \mathbf{H}_{0,j}^T T_1) \mathbf{F}_{3,j} \\ * & \mathbf{M}_{1,j} & \mathbf{L}_{1,j} & \mathbf{F}_{1,j}^T (\tilde{P} + T_1) \mathbf{F}_{3,j} \\ * & * & \mathbf{M}_{2,j} & \mathbf{L}_{2,j} \\ * & * & * & \mathbf{M}_{3,j} \\ * & * & * & * \\ * & * & * & * \\ * & * & * & * \\ * & * & * & * \\ \dots & & -(\mathbf{G}_{0,j}^T \tilde{P} + \mathbf{H}_{0,j}^T T_1) \mathbf{F}_{\bar{d}+\bar{\delta}-1,j} & -(\mathbf{G}_{0,j}^T \tilde{P} + \mathbf{H}_{0,j}^T T_1) \mathbf{F}_{\bar{d}+\bar{\delta},j} \\ \dots & & \mathbf{F}_{1,j}^T (\tilde{P} + T_1) \mathbf{F}_{\bar{d}+\bar{\delta}-1,j} & \mathbf{F}_{1,j}^T (\tilde{P} + T_1) \mathbf{F}_{\bar{d}+\bar{\delta},j} \\ \dots & & \mathbf{F}_{2,j}^T (\tilde{P} + T_1) \mathbf{F}_{\bar{d}+\bar{\delta}-1,j} & \mathbf{F}_{2,j}^T (\tilde{P} + T_1) \mathbf{F}_{\bar{d}+\bar{\delta},j} \\ \dots & & \mathbf{F}_{3,j}^T (\tilde{P} + T_1) \mathbf{F}_{\bar{d}+\bar{\delta}-1,j} & \mathbf{F}_{3,j}^T (\tilde{P} + T_1) \mathbf{F}_{\bar{d}+\bar{\delta},j} \\ & & \vdots & \vdots \\ \mathbf{M}_{\bar{d}+\bar{\delta}-2,j} & \mathbf{L}_{\bar{d}+\bar{\delta}-2,j} & & \mathbf{F}_{\bar{d}+\bar{\delta}-2,j}^T (\tilde{P} + T_1) \mathbf{F}_{\bar{d}+\bar{\delta},j} \\ * & \mathbf{M}_{\bar{d}+\bar{\delta}-1,j} & & \mathbf{L}_{\bar{d}+\bar{\delta}-1,j} \\ * & * & & \mathbf{M}_{\bar{d}+\bar{\delta},j} \end{array} \right) < 0, \quad (4.46)$$

with

$$\begin{aligned} \mathbf{M}_{0,j} &= \mathbf{G}_{0,j}^T \tilde{P} \mathbf{G}_{0,j} + \mathbf{H}_{0,j}^T T_1 \mathbf{H}_{0,j} + R_1 - (1 - \gamma) \tilde{P} + T_2 - (1 - \gamma) T_1, \\ \mathbf{M}_{1,j} &= \mathbf{F}_{1,j}^T (\tilde{P} + T_1) \mathbf{F}_{1,j} + R_2 - (1 - \gamma) R_1 + \gamma T_2 - (1 - \gamma) T_1 + T_3, \\ \mathbf{M}_{2,j} &= \mathbf{F}_{2,j}^T (\tilde{P} + T_1) \mathbf{F}_{2,j} + R_3 - (1 - \gamma) R_2 + \gamma T_3 - (1 - \gamma) T_2 + T_4, \\ \mathbf{M}_{3,j} &= \mathbf{F}_{3,j}^T (\tilde{P} + T_1) \mathbf{F}_{3,j} + R_4 - (1 - \gamma) R_3 + \gamma T_4 - (1 - \gamma) T_3 + T_5, \\ \mathbf{M}_{\bar{d}+\bar{\delta}-2,j} &= \mathbf{F}_{\bar{d}+\bar{\delta}-2,j}^T (\tilde{P} + T_1) \mathbf{F}_{\bar{d}+\bar{\delta}-2,j} + R_{\bar{d}+\bar{\delta}-1} - (1 - \gamma) (R_{\bar{d}+\bar{\delta}-2} + T_{\bar{d}+\bar{\delta}-2}) \\ &\quad + \gamma T_{\bar{d}+\bar{\delta}-1} + T_{\bar{d}+\bar{\delta}}, \\ \mathbf{M}_{\bar{d}+\bar{\delta}-1,j} &= \mathbf{F}_{\bar{d}+\bar{\delta}-1,j}^T (\tilde{P} + T_1) \mathbf{F}_{\bar{d}+\bar{\delta}-1,j} + R_{\bar{d}+\bar{\delta}} - (1 - \gamma) (R_{\bar{d}+\bar{\delta}-1} + T_{\bar{d}+\bar{\delta}-1}) + \gamma T_{\bar{d}+\bar{\delta}}, \\ \mathbf{M}_{\bar{d}+\bar{\delta},j} &= \mathbf{F}_{\bar{d}+\bar{\delta},j}^T (\tilde{P} + T_1) \mathbf{F}_{\bar{d}+\bar{\delta},j} - (1 - \gamma) (R_{\bar{d}+\bar{\delta}} + T_{\bar{d}+\bar{\delta}}), \\ \mathbf{L}_{0,j} &= -\mathbf{G}_{0,j}^T \tilde{P} \mathbf{F}_{1,j} - \mathbf{H}_{0,j}^T T_1 \mathbf{F}_{1,j} + (1 - \gamma) T_1 - T_2, \\ \mathbf{L}_{1,j} &= \mathbf{F}_{1,j}^T (\tilde{P} + T_1) \mathbf{F}_{2,j} + (1 - \gamma) T_2 - T_3, \\ \mathbf{L}_{2,j} &= \mathbf{F}_{2,j}^T (\tilde{P} + T_1) \mathbf{F}_{3,j} + (1 - \gamma) T_3 - T_4, \\ \mathbf{L}_{\bar{d}+\bar{\delta}-2,j} &= \mathbf{F}_{\bar{d}+\bar{\delta}-2,j}^T (\tilde{P} + T_1) \mathbf{F}_{\bar{d}+\bar{\delta}-1,j} + (1 - \gamma) T_{\bar{d}+\bar{\delta}-1} - T_{\bar{d}+\bar{\delta}}, \\ \mathbf{L}_{\bar{d}+\bar{\delta}-1,j} &= \mathbf{F}_{\bar{d}+\bar{\delta}-1,j}^T (\tilde{P} + T_1) \mathbf{F}_{\bar{d}+\bar{\delta},j} + (1 - \gamma) T_{\bar{d}+\bar{\delta}}, \end{aligned}$$

$\mathbf{G}_{0,j} = H_{F,0,j}^x - H_{G,j}^x \bar{K}$ ,  $\mathbf{H}_{0,j} = H_{F,0,j}^x - H_{G,j}^x \bar{K} - I$ ,  $\mathbf{F}_{\hat{i},j} = -H_{F,\hat{i},j}^x \bar{K}$ , for all  $(H_{F,0,j}^x, H_{F,1,j}^x, \dots, H_{F,\bar{d}+\bar{\delta},j}^x, H_{G,j}^x) \in \mathcal{H}_{FG}^x$  and for  $j = 1, 2, \dots, 2^\zeta$ , then the continuous-time NCS (3.12), (3.21), (3.22), with the controller (4.9) is GAS for any  $\sigma \in \mathcal{S}$ .

**Proof** The proof is given in Appendix A.9  $\square$

**Remark 4.4.8** For constant sampling intervals  $\sigma \in \mathcal{S}$  is replaced by  $\mu \in \mathcal{M}$  and the parameter  $\zeta$  is replaced by  $\beta$ . Moreover, the matrix  $F_0^x(\mathbf{t}^k, h_k)$  is a constant matrix and given by  $Q\Theta_0Q^{-1}$  defined in Appendix B.3 and  $\Gamma_{0,i}$  is

equal to zero. The matrices  $\Gamma_{\hat{i},0}$ ,  $\Gamma_{\hat{i},i}$ ,  $\Xi_0$ ,  $\Xi_i$  are defined according to the remarks in Appendix B.3. Then, for Theorem 4.4.7, it holds that

$$\mathbf{G}_0 = \Theta_0 - H_{G,j}^x \bar{K}, \mathbf{H}_0 = \Theta_0 - H_{G,j}^x \bar{K} - I, \mathbf{F}_{\hat{i}} = -H_{F,\hat{i},j}^x \bar{K},$$

for all  $(H_{F,1,j}^x, \dots, H_{F,\bar{d}+\bar{\delta},j}^x, H_{G,j}^x) \in \mathcal{H}_{FG}^x$  and  $j = 1, 2, \dots, 2^\beta$ .

**Remark 4.4.9** Note that adaptations based on other L-K functionals can be derived in a straightforward manner, by replacing the L-K functional used for Theorem 4.4.7. In the literature, many other L-K functionals are available, see e.g. [24], [87], and [127].

Clearly, the use of the candidate L-K functional results in more complex LMIs than the use of the candidate common quadratic Lyapunov function. Moreover, analogous to Lemma 4.3.4, it holds that the L-K functional is not less conservative than the common quadratic Lyapunov approach. To explain this, we use, analogously to Corollary 4.3.3, an equivalent of Theorem 4.4.4 that is based on the state vector  $\chi_k$ . The LMI conditions of (4.37), however with  $\bar{P} \in \mathbb{R}^{(\bar{d}+\bar{\delta}+1)n \times (\bar{d}+\bar{\delta}+1)n}$  need to be considered and  $H_{F,j}$ ,  $H_{G,j}$ , and  $K$  need to be adapted such that the states  $x_{k-1}, x_{k-2}, \dots$  are included instead of  $u_{k-1}, u_{k-2}, \dots$

$$H_{F,j} = \begin{pmatrix} H_{F,0,j}^x & -H_{F,1,j}^x \bar{K} & \dots & -H_{F,\bar{d}+\bar{\delta},j}^x \bar{K} \\ I & 0 & \dots & 0 \\ & \ddots & & \vdots \\ 0 & & I & 0 \end{pmatrix}, H_{G,j} = \begin{pmatrix} H_{G,j}^x \\ 0 \\ \vdots \\ 0 \end{pmatrix}, \quad (4.47)$$

$$K = \begin{pmatrix} \bar{K} & 0_{m \times (\bar{d}+\bar{\delta})n} \end{pmatrix}.$$

Note that (4.37), based on this adapted version of the common quadratic Lyapunov function, will give similar results or less conservative results than the stability conditions based on the common quadratic Lyapunov function  $\xi_k^T P \xi_k$ . For the comparison of the stability results based on this adapted common quadratic Lyapunov function and based on the L-K functional, as an example the case  $\bar{d} + \bar{\delta} = 2$  is considered. The state-vector is given by  $\chi_k = (x_k^T \ x_{k-1}^T \ x_{k-2}^T)^T$ . Then,  $V = \chi_k^T P \chi_k$ , with  $P \in \mathbb{R}^{(\bar{d}+\bar{\delta}+1)n \times (\bar{d}+\bar{\delta}+1)n}$  can be compared with  $V = \chi_k^T \begin{pmatrix} \tilde{P} + T_1 & -T_1 & 0 \\ -T_1 & R_1 + T_1 + T_2 & -T_2 \\ 0 & -T_2 & R_2 + T_2 \end{pmatrix} \chi_k$ . This shows that the L-K functional is a subset of the common quadratic Lyapunov function for  $\chi_k$ , and therefore the results of the L-K functional will be more conservative than the results obtained with the common quadratic Lyapunov function based on  $\chi_k$ . In Section 4.5, the conservatism of the different theorems will be studied based on an illustrative motion control example.



## 4.5 Illustrative examples

In this section, we will apply the proposed stability results to several examples, by using LMITOOL in Matlab. First, we consider the second-order motion control system, as used in Section 4.1. The effects of delays smaller and larger than the sampling interval and packet dropouts on the closed-loop stability are analyzed. Stability regions, that describe the combination of controllers that stabilize the system for a bounded variation in the delays (with or without packet dropouts) are determined. Such a region is useful to determine the maximum allowable delay variation that is allowed in the network (or in the network in combination with a processor if the processor is used for other computations as well) for which the system is still stabilized. Moreover, the effect of different constant sampling intervals on the maximum allowable delays for which a previously defined controller can still stabilize the system is investigated. Such a study is useful in choosing the sampling interval in such a way that the system can still be stabilized on one hand, and the amount of data that needs to be sent over the communication network is limited on the other hand. A reduction of the data that needs to be transmitted may be desirable if the network load is relatively high. More details on the effect of the sampling interval on the occupancy of the network and, therefore, the size of the communication delays can be found in [56; 71; 85]. Second, we consider the example of Section 4.1 that showed the destabilizing effect that time-varying sampling intervals can have. For this example, Theorem 4.4.4 is applied to determine a stabilizing controller in combination with a bound on the variation in the sampling interval. We would like to stress that the stability conditions proposed in the previous sections only provide sufficient conditions. Consequently, the infeasibility of the stability LMIs does necessarily not imply instability.

### 4.5.1 Time-varying delays

To show the applicability of the presented stability conditions, the stability for the motor-roller example, as presented in Section 4.1 is studied, for the case of a constant sampling interval and known bounds for the time-varying delays. We assume that the sampling interval is given by  $h = 1\text{ms}$  and that the state-feedback controller (4.9) is given by  $\bar{K} = (K_a \ K_b)$  with a constant position controller gain  $K_a = 50\text{N}$ . In first instance, we focus on the applicability of Theorem 4.3.1 (SF-CQLF) and 4.4.4 (SF-CQLF), without packet dropouts and for constant sampling intervals; i.e. we will consider both the case of small and large delays. All controller gains  $K_b$  that stabilize the system with time-varying delays  $\tau_k \in [0, \tau_{\max}]$ , with  $\tau_{\max} \leq 2h$ , according to Theorem 4.4.4, with  $\bar{\delta} = 0$ ,  $\gamma = 0$ , and  $h_{\max} = h_{\min} = h$  are determined. Recall that, for  $\tau_{\max} \in [0, h)$ , Theorem 4.4.4 provides the same results as Theorem 4.3.1. The maximum and minimum controller gains  $K_b$  that stabilize system (4.1) for a given variation in the delay  $\tau_k \in [0, \tau_{\max}]$  are given by the solid lines in Figure 4.4<sup>5</sup>. The region between these two lines is denoted as the stability region, which characterizes the

<sup>5</sup>In this figure the x- and y-axis are chosen similar as in e.g. [90] and [133].

stabilizing controllers for (4.1), with  $\tau \in [0, \tau_{\max}]$ . For comparison, the stability region for constant time-delays equal to  $\tau_{\max}$  is depicted by the dash-dotted line in Figure 4.4. As expected, the upper bound for time-varying delays is smaller than the upper bound for constant time-delays. For time-delays equal to zero, the upper bounds for  $K_b$  are equal, which shows that for these delays the stability conditions are not conservative. For larger delays, the upper bound for time-varying delays cannot become larger, because  $\tau_k = 0, \forall k$  is a possible delay sequence (since we used  $\tau_{\min} = 0$ ). Therefore, the conservatism for the small delay case remains limited. For the large delay case, the distance between the bounds for constant and time-varying delays remains similar to the small delay case. The dashed line in Figure 4.4 gives the values of two delays, i.e.  $\tau^a = 0.2\text{ms}$  and  $\tau^b = 0.6\text{ms}$  (for  $K = (50 \ 11.8)$ ), for which the example (4.2) is stable for either the constant delay  $\tau^a$  or the constant delay  $\tau^b$ . Moreover, the NCS is stable for all *constant* delays taken from the interval  $[\tau^a, \tau^b]$ . If these delays occur in an alternating sequence  $(\tau^a, \tau^b, \tau^a, \tau^b, \dots)$  the system becomes unstable, as was shown in Section 4.1. As expected, for fixed  $K_b$ , this delay combination is outside the obtained stabilizing region of Theorem 4.3.1 (SF-CQLF). This observation, in combination with the comparison between the stability regions for time-varying and constant delays, reveals the fact that the stability bound is hardly conservative both for the small and large-delay case. Additionally, the dotted line in Figure 4.4 gives the stability region of our earlier stability conditions as presented in [16]. These stability conditions used an overapproximation of the matrix entries that depend on the uncertain time-varying delays, considering the use of interval matrices, instead of an overapproximation that is based on the Jordan form of the continuous-time system matrix  $A$  as proposed in this chapter. Clearly, the results obtained by Theorem 4.4.4 (SF-CQLF) (and for  $\tau \in [0, h)$  also the results obtained by Theorem 4.3.1) are less conservative than the results obtained in [16]. This difference is caused by a much tighter overapproximation of the discrete-time NCS model by using the Jordan form. Moreover, the number of LMIs is decreased for the small delay case from  $2^{n \times (n+m)}$  in [16] to  $2^\nu$ , with  $\nu$  defined in (B.29), where it holds that  $\nu \leq n$ .

To obtain an improved understanding of the differences in conservatism between the stability analysis results using the candidate Lyapunov function and the candidate Lyapunov-Krasovskii (L-K) functional, the stability regions for the motor-roller system (4.1), obtained from Corollary 4.3.3 (SF-CQLF) and Theorem 4.3.2 (SF-LK) for the small delay case and from Theorems 4.4.4 (SF-CQLF) (with  $\chi_k^T \bar{P} \chi_k$  and (4.47)) and 4.4.7 (SF-LK) for the large delay case (with  $\bar{\delta} = 0$ ,  $h_{\min} = h_{\max} = h$ ), are depicted in Figure 4.5. We note that there is no difference between the results obtained using Theorem 4.3.1 or Corollary 4.3.3 for the small delay case. The same observation holds for the equivalent conditions for the large delay case. This means that, for this example, no difference is found between the use of  $V(\xi_k)^T P \xi_k$  or  $V(\chi_k)^T \bar{P} \chi_k$ . Figure 4.5 shows that Theorem 4.4.7 (SF-LK) gives comparable results as Theorem 4.4.4 (SF-CQLF), except for delays  $\tau_{\max} \in [0, 0.5]\text{ms}$  and  $\tau_{\max} > h = 1\text{ms}$ , where a small difference between both approaches is observed. This comparison

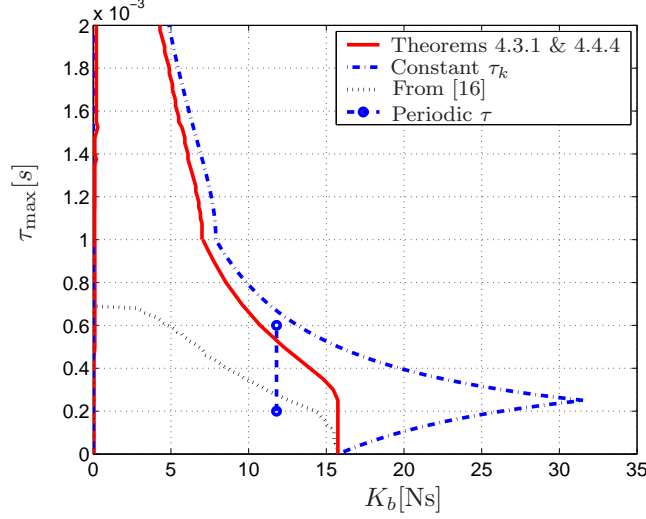


Figure 4.4: Minimum and maximum allowable controller gains  $K_b$  for system (4.1), (3.21), (3.22), (4.9), with  $h = 1\text{ms}$ ,  $\bar{K} = (K_a K_b)$ ,  $K_a = 50\text{N}$  and time-varying delays in the interval  $[0, \tau_{\max}]$  for Theorem 4.3.1, Theorem 4.4.4, and based on [16], as well as for constant time-delays equal to  $\tau_{\max}$ .

shows that using L-K functionals (as in Theorem 4.4.7) for discrete-time NCSs does not necessarily result in less conservative results, compared to a standard common quadratic Lyapunov function.

The previously obtained results consider a constant sampling interval  $h = 1\text{ms}$ . To determine the dependence of the stability region on the magnitude of the constant sampling interval  $h$ , the stability conditions of Theorem 4.3.1 (SF-CQLF) and 4.4.4 (SF-CQLF) are analyzed for different values of  $h$ . The obtained stability conditions are depicted in Figure 4.6 by the black lines, including the corresponding stability regions for constant delays that are depicted by the gray lines. For increasing sampling intervals, both the stability region for constant and for time-varying delays decrease. The fact that the distance between the lines for the time-varying delays and the corresponding constant delays does not change dramatically for increasing values of the sampling interval  $h$  shows that Theorem 4.3.1 and 4.4.4 are not overly conservative (at least for this example), as was already concluded for the case with  $h = 1\text{ms}$  from Figure 4.4. The maximum stabilizing value of the controller gain  $K_b$  decreases slightly, if the same maximum delay ( $\tau_{\max} = 2\text{ms}$ ) is compared for different values of the sampling interval  $h$  (based on the delay fractions  $\tau_{\max}/h = 2$  for  $h = 1\text{ms}$ ,  $\tau_{\max}/h = 1$  for  $h = 2\text{ms}$ , and  $\tau_{\max}/h = 0.2$  for  $h = 5\text{ms}$ ). The maximum stabilizing values of  $K_b$  are  $4.3\text{N}$ ,  $3.45\text{N}$ , and  $3.09\text{N}$ , respectively, which shows that the stability region becomes smaller for larger sampling intervals. Another way to determine the effect of the sampling interval on the stability region is to compare the largest maximum delay for which a stabilizing controller can be

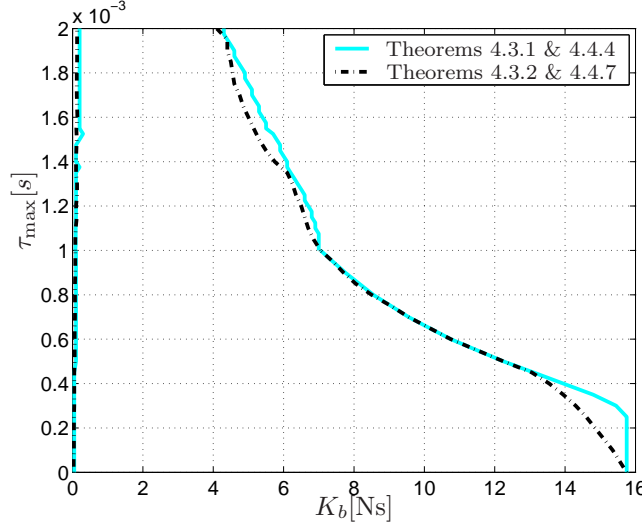


Figure 4.5: Stability region for (4.1), (3.21), (3.22), (4.9) with  $h = 1\text{ms}$ ,  $\bar{K} = (50 K_b)$ ,  $\tau \in [0, \tau_{\max}]$ , and  $\bar{\delta} = 0$ , based on Theorems 4.4.4 and 4.4.7.

found. Based on Figure 4.7, it is concluded that the largest allowable maximum delay decreases slightly for increasing sampling intervals. For  $h = 4\text{ms}$ , it holds that  $\tau_{\max} = 6.56\text{ms}$  is the largest delay for which a stabilizing controller gain  $K_b$  can be found, while for  $h = 5\text{ms}$ ,  $\tau_{\max} = 6\text{ms}$  is the largest delay. The decrease of the maximum allowable delay and the decrease of the maximum allowable controller gain for increasing sampling intervals do not mean that the smallest sampling interval is the best possible choice, because smaller sampling intervals result in more data that needs to be transmitted over the network, resulting in a larger network load (and possible larger delays). Therefore, dependent on the network load, it may be advantageous to choose a larger sampling interval, such that less data needs to be transmitted, possibly resulting in a lower network load and therefore smaller time-delays. More details on the relation between the sampling interval, the network load, and the size of the delays can be found in [56; 71; 85] that deal with a communication network and in [112], where a comparison between different modeling tools for the software that include the (net)work load to predict the delays in terms of latency and jitter is made.

In the analysis presented in this section, the performance of the NCS, e.g. in terms of settling time is not considered, while in practice the performance is influenced both by the time-delay and by the chosen sampling interval.

#### 4.5.2 Packet dropouts

To determine the effect of packet dropouts on the stability region, the stability analysis results of Theorem 4.4.4 (SF-CQLF) are used for a different number

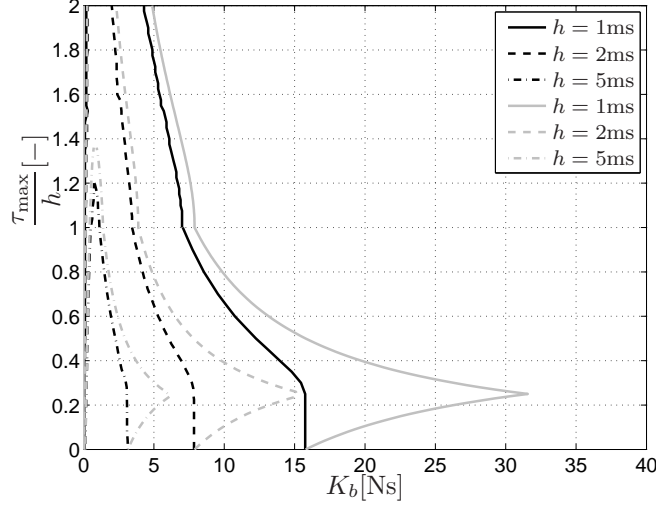


Figure 4.6: Stability region for (4.1), (3.21), (3.22), (4.9) for different values of the constant sampling interval  $h$ , based on Theorem 4.4.4 (black lines) and for constant delays (gray lines), with  $\bar{K} = (50 \ K_b)$ .

of subsequent packet dropouts, in combination with a time-varying delay that is upper bounded by the sampling interval ( $h = 1$  ms,  $\tau_{\min} = 0, \tau_{\max} \leq h$ ). Similar to the previous paragraph, a state-feedback controller as in (4.9), with  $\bar{K} = (50 \ K_b)$  is used. Based on the LMIs of Theorem 4.4.4, the stability region, given by an upper and lower bound for  $K_b$ , for  $\bar{\delta} = 0$ , i.e. no packet dropouts,  $\bar{\delta} = 1$  and  $\bar{\delta} = 2$ , in combination with  $\tau \in [0, \tau_{\max}]$  is depicted in Figure 4.8. Clearly, packet dropouts decrease the allowable controller gains that stabilize the NCS. Note that the allowable controller gain  $K_b$  for a time-varying delay upper bounded by the sampling interval without packet dropouts is the same as the allowable controller gain  $K_b$  for one subsequent packet dropout, without delays (as denoted by the arrow in the figure). The same holds for one packet dropout in combination with a time-varying delay upper-bounded by the sampling interval and two packet dropouts without time-varying delays, as already discussed in Remark 4.4.6. This similarity is evident from the analysis as presented in Theorem 4.4.4 (SF-CQLF), as well as for the analysis presented in Theorem 4.4.7 (SF-LK). Note that this is a consequence of the analysis techniques, while it might not reflect the real stability bounds, as was explained in Section 4.4.

### 4.5.3 Time-varying sampling intervals

For time-varying sampling intervals, system (4.3), obtained from [132], is considered. Here, we consider the case without time-delays and packet dropouts. Based on Theorem 4.4.4 (SF-CQLF), variations in the sampling interval are

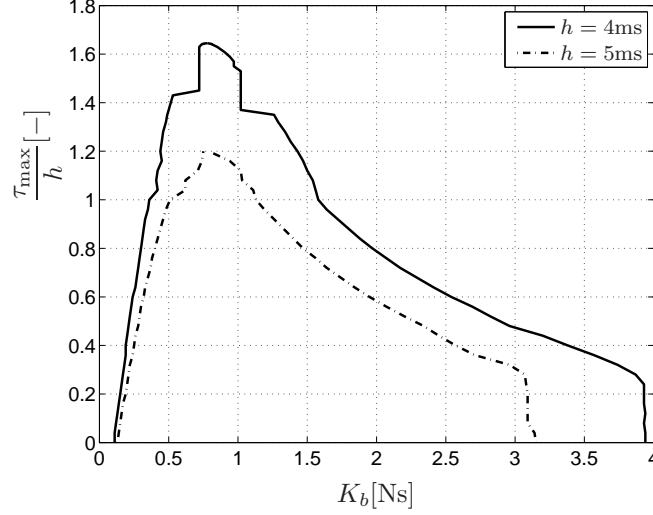


Figure 4.7: Stability region for (4.1), (3.21), (3.22), (4.9) for different values of the constant sampling interval  $h$ , based on Theorem 4.4.4 (black lines), with  $\bar{K} = (50 K_b)$ .

determined, for which a given controller can still stabilize the system (4.3). Investigating these bounds provides insight in when the destabilizing effect as shown in Section 4.1 can occur. For the purpose of stability analysis, we consider the state-feedback controller  $u_k = -Kx_k$ . Here, the controllers obtained from (4.9) and (4.8) are exactly equal, due to the absence of delays (therefore only the current state is used in the discrete-time NCS model). Based on the LMIs in Theorem 4.4.4 (SF-CQLF), the controller  $K = \begin{pmatrix} 1 & 6 \end{pmatrix}$  stabilizes (4.3) for  $h \in [0.46, 0.54]$  or  $h \in [0.5, 0.56]$ . For the presented destabilizing variation in the sampling interval  $h \in [0.18, 0.54]$  (see Section 4.1), indeed, the LMIs of Theorem 4.4.4 are not feasible. These examples show that Theorem 4.4.4 can be used to derive bounds on the variation of the sampling interval, guaranteeing closed-loop stability.

The fact that Theorem 4.4.4 can be used to prove stability for bounded variations in the sampling interval shows an advantage of the proposed method. Other criteria, such as [75; 76; 132] use  $h_{\min} := 0$  and are not able to find a stabilizing controller for system (4.3), while Theorem 4.4.4 gives a minimum and maximum value of the variation in the sampling interval, i.e.  $h_{\min}$  and  $h_{\max}$  respectively. This allows for less conservative results compared to the criteria that consider  $h_{\min} := 0$ .

The derivation of upper and lower bounds for the sampling interval is interesting for a NCS that has to deal with variable sampling intervals. This is the case if the controller requests for new sensor data on previously determined (equidistantly spaced) time-instants, which results in variations in the sampling interval, because the request is transmitted over the communication network.

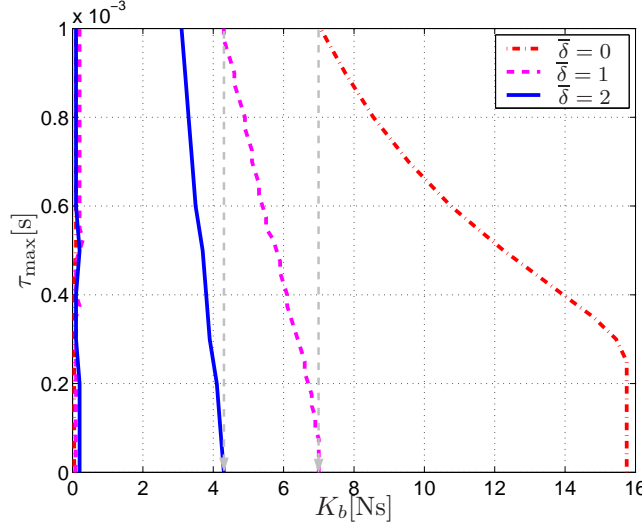


Figure 4.8: Upper and lower bounds of the stability region for (4.1), (3.21), (3.22), (4.9) with  $\bar{K} = (50 K_b)$  for  $\bar{\delta} = 0, 1, 2$ ,  $\tau \in [0, \tau_{\max}]$  and  $h = 1\text{ms}$ .

Another reason to apply this kind of analysis is to design a system with a variation in the sampling interval, such that the network load (or processor load) can be decreased, e.g. resulting in a decrease of packet dropouts in wireless networks as discussed in [89] or a decrease of the time-delays as discussed in the previous paragraph. Another example to apply variation in the sampling interval deals with different performance demands in time. In an industrial printer, the motors are running on an average velocity if no sheet of paper has to be transported by the motor, but speed up if a sheet of paper needs to be transported by the motor. In the first case, the performance measure, in terms of accuracy of the velocity is less strict than in the second case, where the position of the sheet of paper needs to be controlled. This difference on the performance demands allows for a larger sampling interval in the first case than in the second case. For both cases, as well as in the switching situation between different sampling intervals, the system needs to be stable, and therefore analysis in terms of the variation in the sampling interval may be useful, because the switching between the slow and fast sampling intervals is included in the analysis LMIs presented in Section 4.4.

## 4.6 Discussion

In this chapter, different stability conditions for discrete-time models of NCSs with time-varying delays, packet dropouts, and time-varying sampling intervals are proposed. These stability conditions differ in terms of the type of candidate Lyapunov function (a common quadratic Lyapunov function or a Lyapunov-

Krasovskii functional) and the control laws (state-feedback or extended state-feedback) that are considered. The extended state-feedback controller, which contains a state-feedback term and terms related to past control input information, is only applicable if all previous control inputs are known to the controller. Therefore, if delays larger than the sampling interval and packet dropouts may occur, additional assumptions are necessary to be able to apply such a controller. For the standard state-feedback controller these assumptions are not needed, because it does not depend on the control history.

For a specific example, it is shown that the use of the common quadratic Lyapunov function based on the extended state did not result in overly conservative stability results, as was concluded based on the comparison with the periodic destabilizing delay sequence and the difference between the case with constant and time-varying delays. Both in general and based on the example, it is shown that the common quadratic Lyapunov function gives less conservative stability results than the Lyapunov-Krasovskii (L-K) functional, if the state-feedback controller is considered. This difference in conservatism is caused by the fact that the L-K functional can be rewritten, such that it is a subset of the common quadratic Lyapunov function (based on the same state vector). Besides the larger conservatism, the use of the L-K functional results in more complex LMI conditions, due to the larger number of matrices that need to be solved for. However, the number of LMIs that are used to describe the time-varying behavior of the NCS is equal for the Lyapunov approach and the L-K approach, because it depends on the number of time-varying parameters in the NCS model.

In studying the stability of a NCS with packet dropouts and time-varying delays a similarity is found in terms of the effect of packet dropouts and delays on the stability. Namely, the stability region remains the same if  $\tau_{\max} + \bar{\delta} = c$ , with  $c \in \mathbb{R}^+$  an arbitrary constant value larger than or equal to zero. This might not be the case for the actual stability boundaries.

Finally, an advantage of the presented stability conditions is that the analysis depends explicitly on the bounds on the sampling interval  $h_{\min}$ ,  $h_{\max}$  and the bounds on the delay  $\tau_{\min}$  and  $\tau_{\max}$ . Therefore, bounds on the sampling interval and the time-variation of the delays can be found for which the system can be stabilized. The use of a lower bound on the sampling interval  $h_{\min}$  is advantageous for systems that are destabilized if large variations in the sampling interval occur. Our approach gives a bound for which stability is guaranteed, while other approaches are not able to find a stabilizing controller, due to the fact that  $h_{\min}$  is always taken equal to zero, (see e.g. [74–76; 132]). The use of the lower bound on the delay  $\tau_{\min}$  is advantageous if the lower bound on the delay is known and the system is unstable for the case without time-delays, but can be stabilized by adding some time-delay or has a smaller stability region for delays equal to zero.



# 5

## *Controller synthesis*

---

5.1	Small delays	5.3	Illustrative examples
5.2	Variable sampling intervals, large delays, and packet dropouts	5.4	Discussion

---

This chapter deals with extending the stability results for NCSs of Chapter 4 such that they are applicable for controller synthesis. The synthesis conditions that will be proposed in the current chapter provide constructive conditions to design a controller that ensures stability. Similar to the stability conditions, the controller synthesis conditions are given in terms of LMIs, as these are efficient to solve. Note that the conditions in Chapter 4 are currently not in a LMI form if they are solved for both the Lyapunov function (or L-K functional) and the controller. Again, the different situations based on the size of the time-varying delays, packet dropouts, and time-variations in the sampling interval are considered. Similar to Chapter 4, for the sake of brevity only two cases, i.e. time-varying delays smaller than the constant sampling interval and time-varying sampling intervals, with delays that may be larger than this sampling interval and packet dropouts are considered. The case with time-delays smaller than the sampling interval is described to explain the conditions for controller synthesis, without all the complexity that arises in the case with time-varying sampling intervals, packet dropouts, and large delays. Similar to Chapter 4, the different controllers and the different Lyapunov-based approaches are considered and for each of them controller synthesis conditions are derived. Based on the obtained LMIs, conditions that guarantee a lower bound on the transient decay rate are described. This results in a performance measure in terms of the transient response of the system, which is a performance criterium that is of interest for many practical control problems.

This chapter is organized as follows. Section 5.1 describes the controller synthesis conditions and a performance bound in terms of the transient decay rate for the small delay case. Section 5.2 considers the case with time-varying sampling intervals, large delays, and packet dropouts. Note that this case includes the scenarios with time-varying delays larger than the constant sampling interval with and without packet dropouts as defined in Chapter 3, as well. Illustrative examples for the controller synthesis conditions and the transient performance bound are presented in Section 5.3. A discussion on the obtained controller synthesis conditions for the different controllers and the different Lyapunov functions is given in Section 5.4.

## 5.1 Small delays

In this section, the stability conditions for NCSs with delays smaller than the sampling interval presented in Chapter 4 will be extended towards controller synthesis conditions in terms of LMIs. Both the extended state-feedback controller, defined in (4.8) as

$$u_k = -K\xi_k = -\bar{K}x_k - K_1u_{k-1}, \quad (5.1)$$

with  $K = (\bar{K} \quad K_1) \in \mathbb{R}^{m \times (m+n)}$ , and the state-feedback controller, defined in (4.9) as

$$u_k = -\bar{K}x_k, \quad (5.2)$$

with  $\bar{K} \in \mathbb{R}^{m \times n}$ , will be considered. Recall that the NCS for delays smaller than the sampling interval is described by (3.1):

$$\begin{aligned} \dot{x}(t) &= Ax(t) + Bu^*(t), \\ y(t) &= Cx(t) \\ u^*(t) &= u_k, \quad \text{for } t \in [s_k + \tau_k, s_{k+1} + \tau_{k+1}). \end{aligned} \quad (5.3)$$

### 5.1.1 A common quadratic Lyapunov function based on the extended state vector $\xi_k$

Analogous to the stability analysis conditions presented in Chapter 4, the discrete-time representation of (5.3) is considered to derive controller synthesis conditions. Recall, from Chapter 3 that this discrete-time model is given by (3.3):

$$\begin{aligned} \xi_{k+1} &= \tilde{A}(\tau_k)\xi_k + \tilde{B}(\tau_k)u_k \\ y_k &= \tilde{C}\xi_k, \end{aligned} \quad (5.4)$$

with  $\xi_k = (x_k^T \quad u_{k-1}^T)^T$  and  $\tau_k \in [\tau_{\min}, \tau_{\max}] \forall k \in \mathbb{N}$ , with  $\tau_{\max} < h$ . In this section, we present controller synthesis results using a common quadratic Lyapunov function. In first instance, we focus on synthesis conditions for the extended state-feedback controller (5.1) and not on synthesis conditions for the state-feedback controller (5.2). The reasoning behind this choice becomes clear after presenting the synthesis conditions. Based on the same overapproximation procedure as exploited in Theorem 4.3.1 (ESF-CQLF), sufficient conditions for the existence of controllers globally asymptotically stabilizing system (5.3), (5.1) for  $\tau \in [\tau_{\min}, \tau_{\max}]$ ,  $0 \leq \tau_{\min} \leq \tau_{\max} < h$  are given in Theorem 5.1.1.

**Theorem 5.1.1 (ESF-CQLF)** *Consider the NCS model (5.3), (5.1) and its discrete-time NCS description (5.4), (5.1), both parameterized by the time-varying delays  $\tau_k \in [\tau_{\min}, \tau_{\max}]$ , with  $0 \leq \tau_{\min} \leq \tau_{\max} < h$ . Moreover, consider the equivalent representation of (5.4) that is based on the Jordan form of the continuous-time system matrix  $A$ , given by (4.5). Consider the set of matrices  $\mathcal{H}_{FG}$  as defined in (4.12).*

If there exist a symmetric matrix  $Y \in \mathbb{R}^{(n+m) \times (n+m)}$ , a matrix  $Z \in \mathbb{R}^{m \times (n+m)}$ , and a scalar  $0 \leq \gamma < 1$  such that the following LMIs are satisfied:

$$\begin{pmatrix} (1-\gamma)Y & YH_{F,j}^T - Z^TH_{G,j}^T \\ H_{F,j}Y - H_{G,j}Z & Y \end{pmatrix} > 0, \forall (H_{F,j}, H_{G,j}) \in \mathcal{H}_{FG}, \quad (5.5)$$

and  $j = 1, 2, \dots, 2^\nu$ , then  $K = ZY^{-1}$  gives a control gain that renders system (5.3), (5.1) GAS and  $V(\xi_k) = \xi_k^T P \xi_k$ , with  $P = Y^{-1}$  is a Lyapunov function for (5.4).

**Proof** The proof is given in Appendix A.10.  $\square$

Note that the use of the extended state-feedback controller, including past control inputs avoids the so-called structured control synthesis problem, because all entries in  $K$  can be freely assigned [102]. This structured control synthesis problem, which is in general known to be notoriously difficult [6; 102], is found if the state-feedback controller  $u_k = -\bar{K}x_k$ , as in (5.2), is considered. This can be explained by rewriting  $u_k = -\bar{K}x_k$  as  $u_k = -K\xi_k$ , with  $K = (\bar{K} \ 0_{m \times m})$ . Then, both  $Z$  and  $Y$  in (5.5) need to be structured to guarantee a controller of the form  $(\bar{K} \ 0_{m \times m})$ . A possible choice is to use  $Z = (\bar{Z} \ 0_{m \times m})$  and  $Y = \begin{pmatrix} \bar{Y}_1 & 0 \\ 0 & \bar{Y}_2 \end{pmatrix}$ , then  $K$  is obtained from  $K = ZY^{-1}$  or  $\bar{K}$  from  $\bar{K} = \bar{Z}\bar{Y}_1^{-1}$ .

The use of these structured matrices  $Y$  and  $Z$ , in combination with a similar partitioning as in Section 4.3.2, leading to the system description

$$\xi_{k+1} = \begin{pmatrix} \hat{\Theta}_0 & F^x(\tau_k) \\ 0 & 0 \end{pmatrix} \xi_k + \begin{pmatrix} G^x(\tau_k) \\ I \end{pmatrix} u_k, \quad (5.6)$$

for all  $(F^x, G^x) \in \mathcal{FG}^x$ , with  $\mathcal{FG}^x$  defined in (4.21), results in the following corollary:

**Corollary 5.1.2 (SF-CQLF)** Consider the NCS model (5.3), (5.2) and its discrete-time representation (5.4), (5.2), both parameterized by  $\tau_k \in [\tau_{\min}, \tau_{\max}]$ ,  $0 \leq \tau_{\min} \leq \tau_{\max} < h$ . Moreover, consider the equivalent representation that is based on the Jordan form of the continuous-time system matrix  $A$  (5.6), (5.2) and the set of matrices  $\mathcal{H}_{FG}^x$  as defined in (4.23). If there exist symmetric matrices  $\bar{Y}_1 \in \mathbb{R}^{n \times n}$ ,  $\bar{Y}_2 \in \mathbb{R}^{m \times m}$ , a matrix  $Z \in \mathbb{R}^{m \times n}$ , and a scalar  $0 \leq \gamma < 1$  that satisfy

$$\begin{pmatrix} (1-\gamma)\bar{Y}_1 & 0 & \bar{Y}_1\Theta_1^T - Z^T(H_{G,j}^x)^T & Z^T \\ 0 & (1-\gamma)\bar{Y}_2 & \bar{Y}_2(H_{F,j}^x)^T & 0 \\ \Theta_1\bar{Y}_1 - H_{G,j}^xZ & H_{F,j}^x\bar{Y}_2 & \bar{Y}_1 & 0 \\ Z & 0 & 0 & \bar{Y}_2 \end{pmatrix} > 0, \quad (5.7)$$

for all  $(H_{F,j}^x, H_{G,j}^x) \in \mathcal{H}_{FG}^x$ ,  $j = 1, 2, \dots, 2^\nu$ , then the controller  $\bar{K} = Z\bar{Y}_1^{-1}$  renders system (5.3), (5.2) GAS. Moreover,  $\xi_k^T \begin{pmatrix} P_1 & 0 \\ 0 & P_2 \end{pmatrix} \xi_k$ , with  $P_1 = \bar{Y}_1^{-1}$  and  $P_2 = \bar{Y}_2^{-1}$ , is a Lyapunov function for (5.4).

The use of this state-feedback controller results in a rather conservative approach, due to the imposed structure in  $Y$  and  $Z$ . This will be illustrated in the examples discussed in Section 5.3. However, in [17; 19], an approach is presented that avoids the use of the structure in the matrix  $Y$  (or equivalently  $P$ ). The obtained synthesis conditions, that consider the results presented in [17; 19], are given in the following theorem.

**Theorem 5.1.3 (SF-CQLF\*)** *Consider the NCS model (5.3), (5.2) and its discrete-time NCS description (5.4), (5.2), both parameterized by the time-varying delays  $\tau_k \in [\tau_{\min}, \tau_{\max}]$ , with  $0 \leq \tau_{\min} \leq \tau_{\max} < h$ . Moreover, consider the equivalent representation of (5.4) that is based on the Jordan form of the continuous-time system matrix  $A$ , given by (4.5). Consider the set of matrices  $\mathcal{H}_{FG}$  as defined in (4.12).*

*If there exist a symmetric matrix  $Y \in \mathbb{R}^{(n+m) \times (n+m)}$ , a matrix  $\bar{Z} \in \mathbb{R}^{m \times n}$ , a matrix  $X = \begin{pmatrix} X_1 & 0 \\ X_2 & X_3 \end{pmatrix}$  with  $X_1 \in \mathbb{R}^{n \times n}$ ,  $X_2 \in \mathbb{R}^{m \times n}$ ,  $X_3 \in \mathbb{R}^{m \times m}$  and a scalar  $0 \leq \gamma < 1$  such that the following LMIs are satisfied:*

$$\begin{pmatrix} (1-\gamma)Y & H_{F,j}X - H_{G,j}(\bar{Z} \ 0) \\ \star & X + X^T - Y \end{pmatrix} > 0, \forall (H_{F,j}, H_{G,j}) \in \mathcal{H}_{FG}, \quad (5.8)$$

*$j = 1, 2, \dots, 2^\nu$ , and  $\star$  defined such that the obtained LMI is symmetric, then  $\bar{K} = \bar{Z}X_1^{-1}$  gives a control gain that renders system (5.3), (5.2) GAS and  $V(\xi_k) = \xi_k^T P \xi_k$ , with  $P = Y^{-1}$  is a Lyapunov function for (5.4), (5.2).*

**Proof** The proof is analogous to the proof of Theorem 5.1.1, in combination with a state-feedback controller instead of an extended state-feedback controller, and the proof of Theorem 3 in [19]. There, it is used that the following two conditions are equivalent to prove global asymptotic stability of a system, e.g. (5.4), (5.1) (for a known controller):

- (i) There exists a symmetric matrix  $P$  such that

$$\begin{pmatrix} P & (H_{F,j} - H_{G,j}K)^T P \\ P(H_{F,j} - H_{G,j}K) & P \end{pmatrix} > 0, \forall (H_{F,j}, H_{G,j}) \in \mathcal{H}_{FG},$$

and  $j = 1, 2, \dots, 2^\nu$ .

- (ii) There exists a symmetric matrix  $P$  and a matrix  $X$  such that

$$\begin{pmatrix} P & (H_{F,j} - H_{G,j}K)^T X^T \\ X(H_{F,j} - H_{G,j}K) & X + X^T - P \end{pmatrix} > 0, \forall (H_{F,j}, H_{G,j}) \in \mathcal{H}_{FG},$$

and  $j = 1, 2, \dots, 2^\nu$ .

In both cases, the Lyapunov function that is exploited to prove GAS of (5.4), (5.1) (or equivalently for (5.2), with  $K = (\bar{K} \ 0_{m,m})$ ) is given by  $V(\xi_k) = \xi_k^T P \xi_k$ .

Based on a similar reasoning it is proven in [17; 19] that for GAS of (5.4), (5.2), it is sufficient if there exists a symmetric matrix  $P$  and a matrix  $X$  such that  $\begin{pmatrix} P & H_{F,j}X - H_{G,j}Z \\ X^T H_{F,j}^T - Z^T H_{G,j}^T & X + X^T - P \end{pmatrix} > 0, \forall (H_{F,j}, H_{G,j}) \in \mathcal{H}_{FG}$ , and  $j = 1, 2, \dots, 2^\nu$ . Here, the controller is obtained from  $K = ZX^{-1}$  and the Lyapunov function is given by  $V(\xi_k) = \xi_k^T P \xi_k$ . Note that for Theorem 5.1.3, it is used that  $Z = (\bar{Z} \ 0)$  and  $X = \begin{pmatrix} X_1 & 0 \\ X_2 & X_3 \end{pmatrix}$ , such that  $K = ZX^{-1}$  gives indeed the state-feedback controller. Note that to determine  $\bar{K}$  there is no difference between using  $\bar{K} = \bar{Z}X_1^{-1}$  and  $K = (\bar{K} \ 0) = (\bar{Z} \ 0)X^{-1}$ , due to the specific shape of  $X$ .  $\square$

To determine whether the use of a Lyapunov-Krasovskii (L-K) functional can result in less conservative controller synthesis conditions for the state-feedback controller (5.2) than Theorem 5.1.3, the candidate L-K functional of Chapter 4 will be considered in the next section. However, it is not expected that the L-K functional results in less conservative results, because Theorem 5.1.3 has a similar conservatism as the stability conditions based on the common quadratic Lyapunov function in Theorem 4.3.1 that was slightly less conservative than the approach based on the L-K functional, as presented in Theorem 4.3.2.

Before exploiting the synthesis conditions based on the L-K functional, the transient performance of the system including the controller designs as can be derived with the previous theorems will be discussed.

**Transient performance** To obtain a performance measure of the derived controller in terms of the transient behavior of the closed-loop system, the convergence bound based on the obtained matrix  $P = Y^{-1}$  and the corresponding value  $\gamma$  can be obtained<sup>1</sup>. Recall that, if the conditions of Theorems 5.1.1 or 5.1.3 are satisfied, then (4.11) holds; i.e. it holds that  $\Delta V(\xi_k) := V(\xi_{k+1}) - V(\xi_k) < -\gamma V(\xi_k)$ . We adopt the notation  $|\xi_k|_P^2 = \xi_k^T P \xi_k$ . Using the fact that  $\lambda_{\min}(P)|\xi_k|^2 \leq |\xi_k|_P^2 \leq \lambda_{\max}(P)|\xi_k|^2$  and  $|x_k|^2 \leq \|C_x P^{-\frac{1}{2}}\|^2 |\xi_k|_P^2$ , with  $C_x$  obtained from  $x_k = C_x \xi_k$ , we can derive a lower bound for the transient decay rate of the discrete-time state  $x_k$  as:

$$|x_k|^2 \leq (1 - \gamma)^k \|C_x P^{-\frac{1}{2}}\|^2 |\xi_0|_P^2 \leq (1 - \gamma)^k \|C_x P^{-\frac{1}{2}}\|^2 \lambda_{\max}(P) |\xi_0|^2. \quad (5.9)$$

It is obvious that the lower bound on the decay rate depends both on  $P$  and  $\gamma$ . An optimization algorithm that derives a control gain  $K$  (or  $\bar{K}$  according to (5.5) ((5.7), or (5.8)), with the optimum decay rate (i.e. the largest possible value of  $\gamma$ ) as defined in (5.9), results in a control design tool that combines stability and transient performance (settling-time) in the face of time-varying delays  $\tau_k \in [\tau_{\min}, \tau_{\max}]$ .

---

<sup>1</sup>Note that  $P = \begin{pmatrix} \bar{Y}_1^{-1} & 0 \\ 0 & \bar{Y}_2^{-1} \end{pmatrix}$  needs to be applied if Corollary 5.1.2 is applied to derive a state-feedback controller.

### 5.1.2 A Lyapunov-Krasovskii functional

To derive a controller synthesis approach for the state-feedback controller, using the candidate Lyapunov-Krasovskii (L-K) functional defined in (4.17) as  $V(\chi_k) = x_k^T \tilde{P} x_k + x_{k-1}^T R x_{k-1} + (x_k - x_{k-1})^T T (x_k - x_{k-1})$ , a slightly different approach is followed. In Chapter 4, this candidate Lyapunov function was used to determine stability of (5.3), (5.2). Recall that in this candidate Lyapunov function the matrices  $\tilde{P}$ ,  $R$ , and  $T$  are chosen to be positive definite, similar to Theorem 4.3.2. Moreover, the discrete-time NCS description of (5.3) is given by (4.19):

$$\chi_{k+1} = \begin{pmatrix} e^{Ah} x_k - \int_0^{h-\tau_k} e^{As} ds B \bar{K} & - \int_{h-\tau_k}^h e^{As} ds B \bar{K} \\ I & 0 \end{pmatrix} \chi_k, \quad (5.10)$$

with  $\chi_k = (x_k^T \ x_{k-1}^T)^T$ . Let us now introduce an additional equation that is used to derive the controller synthesis conditions. This function is used as a relaxation function and is needed to obtain LMIs instead of nonlinear matrix inequalities, as will be shown in the proof of Theorem 5.1.4 in Appendix A.11.

$$\Psi_1(x_k, x_{k-1}) = 2(x_k^T N_1 + x_{k-1}^T N_2)((x_k - x_{k-1}) - (x_k - x_{k-1})) = 0. \quad (5.11)$$

In Theorem 5.1.4 sufficient conditions are proposed that characterize a stabilizing state-feedback controller for (5.3), (5.2), based on the candidate L-K functional (4.17) in combination with the additional function  $\Psi_1$ .

**Theorem 5.1.4 (SF-LK)** *Consider the NCS of (5.3), (5.2) and its discrete-time representation (5.10), (5.2), both parameterized by  $\tau_k \in [\tau_{\min}, \tau_{\max}]$ ,  $0 \leq \tau_{\min} \leq \tau_{\max} < h$ . Moreover, consider the equivalent representation based on the Jordan form of the continuous-time system matrix  $A$ , defined in (4.22), and the set of matrices  $\mathcal{H}_{FG}^x$  as defined in (4.23). If there exist symmetric positive definite matrices  $\tilde{Y} \in \mathbb{R}^{n \times n}$ ,  $\hat{R} \in \mathbb{R}^{n \times n}$ ,  $\hat{N}_1 \in \mathbb{R}^{n \times n}$ ,  $\hat{N}_2 \in \mathbb{R}^{n \times n}$ , a matrix  $Z \in \mathbb{R}^{m \times n}$ , and scalars  $0 \leq \gamma < 1$ ,  $\theta_1 > 0$  that satisfy:*

$$\begin{pmatrix} (1-\gamma)\tilde{Y} - \hat{R} - \hat{N}_1 - \hat{N}_1^T & \star & \star & \star & \star \\ \hat{N}_1^T - \hat{N}_2 & (1-\gamma)\hat{R} + \hat{N}_2 + \hat{N}_2^T & \star & \star & \star \\ \Theta_1 \tilde{Y} - H_{G,j}^x Z & -H_{F,j}^x Z & \tilde{Y} & \star & \star \\ \Theta_1 \tilde{Y} - H_{G,j}^x Z - \tilde{Y} & -H_{F,j}^x Z & 0 & \theta_1 \tilde{Y} & \star \\ \frac{1}{\sqrt{1-\gamma}} \theta_1 \hat{N}_1^T & \frac{1}{\sqrt{1-\gamma}} \theta_1 \hat{N}_2^T & 0 & 0 & \theta_1 \tilde{Y} \end{pmatrix} > 0, \quad (5.12)$$

for all  $(H_{F,j}^x, H_{G,j}^x) \in \mathcal{H}_{FG}^x$ ,  $j = 1, 2, \dots, 2^\nu$ , then the controller (5.2), with the controller gain matrix  $\bar{K} = Z\tilde{Y}^{-1}$  renders system (5.3) GAS. Moreover, (4.17) is a Lyapunov function for (5.10), (5.2), with parameters that can be retrieved from  $\tilde{Y} := \tilde{P}^{-1}$ ,  $\hat{R} := \tilde{P}^{-1} R \tilde{P}^{-1}$ ,  $\hat{N}_1 := \tilde{P}^{-1} N_1 \tilde{P}^{-1}$ ,  $\hat{N}_2 := \tilde{P}^{-1} N_2 \tilde{P}^{-1}$ ,  $\bar{K} = Z\tilde{Y}^{-1}$ , and  $T^{-1} := \theta_1 \tilde{P}^{-1}$ .

**Proof** The proof of Theorem 5.1.4 is given in Appendix A.11.  $\square$

It should be noted that once  $\theta_1$  and  $\gamma$  are chosen, (5.12) is a LMI. Moreover, compared to the stability analysis conditions in Theorem 4.3.2, a relation between the matrices  $T$  and  $\tilde{P}$  ( $T := \frac{1}{\theta_1} \tilde{P}$ ) is introduced to obtain LMI conditions. This will result in additional conservatism compared to Theorem 4.3.2. Moreover, due to this imposed structure, Theorem 5.1.4 will be more conservative than Theorem 5.1.3 (SF-CQLF\*), especially if the same state vector ( $\chi_k$ ) is considered.

**Transient performance** The performance in terms of the transient decay rate can be obtained analogous to (5.9), if  $\xi_0$  is replaced by  $\chi_0$  and if  $P$  is replaced by  $\overline{P_{RT}} = \begin{pmatrix} \tilde{P} + T & -T \\ -T & R + T \end{pmatrix}$  to account for the used candidate L-K functional. Then, it holds that

$$|x_k|^2 \leq (1 - \gamma)^k \|C_x \overline{P_{RT}}^{-\frac{1}{2}}\|^2 |\chi_0|_{\overline{P_{RT}}}^2, \quad (5.13)$$

with  $|\chi_0|_{\overline{P_{RT}}}^2 = \chi_0^T \overline{P_{RT}} \chi_0$ . Note that, compared to (5.9), the matrix  $C_x$  has to be adapted, such that it corresponds to the dimension of  $\chi_k$ , i.e.  $x_k = C_x \chi_k$ , with  $C_x \in \mathbb{R}^{n \times 2n}$ .

## 5.2 Variable sampling intervals, large delays, and packet dropouts

In this section, the previously derived controller synthesis approaches are extended, such that they are applicable for systems with variations in the sampling interval, time-varying delays larger than the sampling interval, and packet dropouts. Recall that in the case of time-varying sampling intervals, the sampling instants  $s_k$  are defined according to (3.19):

$$s_k = \sum_{i=0}^{k-1} h_i \quad \forall k \geq 1, \quad s_0 = 0.$$

The possible sequences of sampling instants, delays, and packet dropouts are denoted by  $\sigma \in \mathcal{S}$ , with  $\mathcal{S}$  defined in (3.20) as:

$$\mathcal{S} := \left\{ \{(s_k, \tau_k, m_k)\}_{k \in \mathbb{N}} : h_{\min} \leq s_{k+1} - s_k \leq h_{\max}, \tau_{\min} \leq \tau_k \leq \tau_{\max}, \sum_{v=k-\bar{\delta}}^k m_v \leq \bar{\delta}, \forall k \in \mathbb{N} \right\}, \quad (5.14)$$

and  $\bar{\delta}$  the maximum number of subsequent packet dropouts. Recall, from Chapter 3, that the continuous-time NCS model for delays larger than the sampling interval, packet dropouts, and time-varying sampling intervals is described by

(3.12):

$$\begin{aligned} \dot{x}(t) &= Ax(t) + Bu^*(t) \\ y(t) &= Cx(t), \end{aligned} \quad (5.15)$$

where the controller is defined according to (3.21):

$$u^*(t) = u_j \text{ for } t \in [s_k + t_j^k, s_k + t_{j+1}^k), \quad (5.16)$$

with  $t_j^k$  defined in (3.22) as:

$$\begin{aligned} t_j^k &= \min \left\{ \max\{0, \tau_j - \sum_{l=j}^{k-1} h_l\} + m_j h_{\max}, \right. \\ &\quad \max\{0, \tau_{j+1} - \sum_{l=j+1}^{k-1} h_l\} + m_{j+1} h_{\max}, \dots, \\ &\quad \left. \max\{0, \tau_{k-\underline{d}} - \sum_{l=k-\underline{d}}^{k-1} h_l\} + m_{k-\underline{d}} h_{\max}, h_k \right\}, \end{aligned} \quad (5.17)$$

and  $t_j^k \leq t_{j+1}^k$ ,  $j \in [k - \bar{d} - \bar{\delta}, k - \bar{d} - \bar{\delta} + 1, \dots, k - \underline{d}]$ .

### 5.2.1 A common quadratic Lyapunov function based on the extended state vector $\xi_k$

In this section, constructive conditions are presented for state-feedback controllers (5.2) and for extended state-feedback controllers of the form (4.29):

$$u_k = -K\xi_k = -\bar{K}x_k - K_1 u_{k-1} - K_2 u_{k-2} \dots - K_{\bar{d}+\bar{\delta}} u_{k-\bar{d}-\bar{\delta}}, \quad (5.18)$$

with  $K \in \mathbb{R}^{m \times (\bar{d}+\bar{\delta})m+n}$ ,  $\bar{d} = \lceil \frac{\tau_{\max}}{h_{\min}} \rceil$ , and  $\bar{\delta}$  the maximum number of subsequent packet dropouts, analogous to Lemma 3.4.1. Similar to Theorem 5.1.1, in first instance, the focus is on the use of the extended state-feedback controller. Then, the structured control synthesis problem that occurs for the state-feedback controller (5.2) is avoided. Recall that the control law (5.1), and therefore also (5.18), is only applicable if Assumption 4.4.1 holds, which states that packet dropouts and message rejection between the sensor and the controller do not occur.

Analogous to the previous section, the discrete-time representation of (5.15) is used to derive constructive conditions. Recall that this discrete-time model is given by (3.24):

$$\begin{aligned} \xi_{k+1} &= \tilde{A}(\mathbf{t}^k, h_k) \xi_k + \tilde{B}(\mathbf{t}^k, h_k) u_k \\ y_k &= \tilde{C} \xi_k, \end{aligned} \quad (5.19)$$

where  $\mathbf{t}^k$  denotes the combination of all time-varying parameters, i.e.  $\mathbf{t}^k = (t_{k-\bar{d}-\bar{\delta}+1}^k, \dots, t_{k-\underline{d}}^k)$ . Based on the same overapproximation procedure as exploited in Theorem 4.4.4, constructive LMI conditions for the design of a controller that ensures the GAS of system (5.15), (5.16), (5.17), (5.18) are given in



Theorem 5.2.1. Herein, a stability characterization using a common quadratic Lyapunov function based on the extended state  $\xi_k$  is used.

**Theorem 5.2.1 (ESF-CQLF)** Consider the NCS model (5.15), (5.16), (5.17), (5.18), and its discrete-time representation (5.19), for sequences of sampling instants, delays, and packet dropouts  $\sigma \in \mathcal{S}$ , with  $\mathcal{S}$  as in (5.14). Consider the equivalent representation (4.7) based on the Jordan form of  $A$  and the set of matrices  $\mathcal{H}_{FG}$  defined in (4.35).

If there exist a symmetric matrix  $Y \in \mathbb{R}^{(n+(\bar{d}+\bar{\delta})m) \times (n+(\bar{d}+\bar{\delta})m)}$ , a matrix  $Z \in \mathbb{R}^{m \times (n+(\bar{d}+\bar{\delta})m)}$ , and a scalar  $0 \leq \gamma < 1$  that satisfy

$$\begin{pmatrix} (1-\gamma)Y & YH_{F,j}^T - Z^TH_{G,j}^T \\ H_{F,j}Y - H_{G,j}Z & Y \end{pmatrix} > 0, \forall (H_{F,j}, H_{G,j}) \in \mathcal{H}_{FG}, \quad (5.20)$$

and  $j = 1, 2, \dots, 2^\zeta$ , then  $x = 0$  is a GAS equilibrium point of the closed-loop NCS (5.15), (5.16), (5.17), (5.18) with  $K = ZY^{-1}$ . Moreover, the function  $V(\xi_k) = \xi_k^T P \xi_k$ , with  $P = Y^{-1}$ , is a Lyapunov function for the discrete-time NCS (5.19), (5.18).

**Proof** The proof is similar to the proof of Theorem 5.1.1 □

For the state-feedback controller, similar to the small delay case, structure in the matrix  $Y$  and  $Z$  is needed. A possible structure is to use  $Y = \text{diag}(\bar{Y}_0, \dots, \bar{Y}_{\bar{d}+\bar{\delta}})$  and  $Z = \begin{pmatrix} \bar{Z} & 0_{(\bar{d}+\bar{\delta})m, (\bar{d}+\bar{\delta})m} \end{pmatrix}$  instead of  $Y$  and  $Z$  as defined in Theorem 5.2.1. Note that the Lyapunov function is in this case given by  $V(\xi_k) = \xi_k^T P \xi_k$ , with  $P = \text{diag}(\bar{Y}_0^{-1}, \dots, \bar{Y}_{\bar{d}+\bar{\delta}}^{-1})$ .

Analogous to the small delay case, the use of the approach in [17; 19], avoids requiring a particular structure in the matrix  $Y$  (or  $P$ ) as it is transferred into a slack variable. The equivalent of Theorem 5.1.3 (SF-CQLF\*) for time-varying sampling intervals, large delays, and packet dropouts is given in the following theorem.

**Theorem 5.2.2 (SF-CQLF\*)** Consider the NCS model (5.15), (5.16), (5.17), (5.2), and its discrete-time representation (5.19), (5.2) for sequences of sampling instants, delays, and packet dropouts  $\sigma \in \mathcal{S}$ , with  $\mathcal{S}$  as in (5.14). Consider the equivalent representation (4.7) based on the Jordan form of  $A$  and the set of matrices  $\mathcal{H}_{FG}$  defined in (4.35).

If there exist a symmetric matrix  $Y \in \mathbb{R}^{(n+(\bar{d}+\bar{\delta})m) \times (n+(\bar{d}+\bar{\delta})m)}$ , a matrix  $\bar{Z} \in \mathbb{R}^{m \times n}$ , a matrix  $X = \begin{pmatrix} X_1 & 0 \\ X_2 & X_3 \end{pmatrix}$ , with  $X_1 \in \mathbb{R}^{n \times n}$ ,  $X_2 \in \mathbb{R}^{(\bar{d}+\bar{\delta})m \times n}$ ,  $X_3 \in \mathbb{R}^{(\bar{d}+\bar{\delta})m \times (\bar{d}+\bar{\delta})m}$ , and a scalar  $0 \leq \gamma < 1$  that satisfy

$$\begin{pmatrix} (1-\gamma)Y & H_{F,j}X - H_{G,j}(\bar{Z} \ 0) \\ \star & X + X^T - Y \end{pmatrix} > 0, \forall (H_{F,j}, H_{G,j}) \in \mathcal{H}_{FG}, \quad (5.21)$$

and  $j = 1, 2, \dots, 2^\zeta$ , then  $x = 0$  is a GAS equilibrium point of the closed-loop NCS (5.15), (5.16), (5.17), (5.2) with  $\bar{K} = \bar{Z}X_1^{-1}$ . Moreover, the function

$V(\xi_k) = \xi_k^T P \xi_k$ , with  $P = Y^{-1}$ , is a Lyapunov function for the discrete-time NCS (5.19), (5.2), (5.2).

**Proof** The proof can be derived analogously to the proof of Theorem 5.1.3, which is based on the proof of Theorem 3 in [19].  $\square$

The synthesis conditions based on the L-K functional can be derived analogously to the small delay case in Theorem 5.1.4 (SF-LK). However, the results are not discussed here, because, based on the restrictions on the structure, as used in Theorem 5.1.4 and based on Lemma 4.3.4 it is to be expected that the results will be more conservative than the results of Theorem 5.2.2 (SF-CQLF\*). The illustrative examples, in Section 5.3, will reveal this observation on the conservatism. For the sake of completeness, the LMI conditions for the L-K functional for time-varying delays, time-varying sampling intervals and packet dropouts are given in Appendix C.

**Transient performance** The performance measure in terms of the transient decay rate, as described in (5.9), holds if the matrix  $C_x$  is adapted to the new definition of  $\xi_k$ , with  $\xi_k = \begin{pmatrix} x_k^T & u_{k-1}^T & \dots & u_{k-\bar{d}-\bar{\delta}}^T \end{pmatrix}^T$  and  $\bar{d}$  defined in Lemma 3.4.1.

### 5.3 Illustrative examples

To illustrate the applicability of the proposed controller synthesis conditions and to make a comparison between the different approaches, the obtained controller synthesis conditions are applied to the motor-roller example, as has been considered in Chapter 4. In this example, a motor drives a roller that is used to transport a sheet of paper through the paper path of an industrial printer (see also the schematic overview of the motor and roller in Figure 4.1). For the sake of simplicity, the system does not follow a prescribed trajectory, but has to move towards zero, i.e. the reference trajectory is assumed to be equal to zero. Such a simplification allows to study the stability of the controllers that are obtained from the different presented controller synthesis conditions in this chapter. Note that in Chapter 6, the tracking problem of this motor-roller system, where the reference signal may be unequal to zero, is studied.

Moreover, a fourth-order motion control example is considered to show the usefulness of the control design approach for more complex systems. This system consists of two rotating discs that are coupled via a spring and a damper. Only one disc is actuated, while, for both discs, the position and the velocity are measured.

In both the second-order and the fourth-order example, the performance in terms of the predicted transient decay rate is compared to the transient decay rate obtained with simulations.

Table 5.1: Obtained controllers for Theorem 5.1.1 (ESF-CQLF) and 5.1.2 (SF-CQLF) for different values of  $\gamma$  and  $\tau_{\max}$  for  $h = 1\text{ms}$ .

$\gamma$	$\tau_{\max}$	$K$ (Theorem 5.1.1)	$\bar{K}$ (Corollary 5.1.2)
0	$0.4h$	(0.041 0.264 -0.030)	(0.034 0.191)
0	$0.6h$	(0.039 0.255 -0.029)	(0.0003 0.004)
0	$h$	(0.041 0.263 -0.036)	-
0.01	$0.4h$	(3.715 0.578 -0.005)	(13.716 1.681)
0.01	$0.49h$	(3.724 0.573 -0.004)	(80.989 11.321)
0.01	$h$	(4.716 0.617 0.008)	-
0.1	$0.4h$	(197.892 2.829 0.267)	(403.624 6.845)
0.1	$0.44h$	(197.175 2.825 0.273)	(619.878 11.604)
0.1	$h$	(165.030 2.52 0.306)	-

### 5.3.1 Motor-roller example

For the sake of comparison, the different proposed controller synthesis methods are used to construct stabilizing controllers, using LMITOOL. First, the small delay case is considered. The results for several maximum delays  $\tau_{\max}$ , with  $\tau_{\min} = 0$  and  $\tau_{\max} < h$  and several values of  $\gamma$  for Theorem 5.1.1 (ESF-CQLF) and Corollary 5.1.2 (SF-CQLF) are given in Table 5.1. Here, the maximum delay for which Corollary 5.1.2 gives a stabilizing controller is given for different values of  $\gamma$ . For Theorem 5.1.1, stabilizing controllers are derived for all delays up to the sampling interval, as is given in Table 5.1. Then, from the number of cases for which a stabilizing controller is derived, it can be concluded that the results of Theorem 5.1.1 (ESF-CQLF) are less conservative than those of Theorem 5.1.2 (SF-CQLF), which was expected, due to the structure used in the Lyapunov function in the latter case. In Table 5.2 some stabilizing controllers obtained from Theorem 5.1.3 (SF-CQLF\*) are given. It is obvious, by comparing Tables 5.1 and 5.2 that the avoidance of the demands on the structure of the  $P$ -matrix, as proposed in Theorem 5.1.3, results in less conservative results than Corollary 5.1.2, where the structure on the  $P$ -matrix was needed. The difference between the use of Theorems 5.1.1 (ESF-CQLF) and 5.1.3 (SF-CQLF\*) cannot be determined based on the presented results. Moreover, in Table 5.2, some stabilizing controllers obtained from Theorem 5.1.4 (SF-LK), including the value of the parameter  $\theta_1$ , are given. Here, the maximum value of  $\tau_{\max}$ , in combination with  $\gamma$ , for which a stabilizing controller can be obtained is included (e.g. for  $\gamma = 0$ , only for  $\tau_{\max} \leq 0.99h$  and for  $\gamma = 0.1$  only for  $\tau_{\max} \leq 0.81h$  a stabilizing controller can be obtained). Based on these results, it can be seen that the use of the L-K functional results in more conservative results than the use of the common quadratic Lyapunov function without demands on the structure of the  $P$ -matrix, because for increasing demands on the transient response (an increase of the parameter  $\gamma$ ) Theorem 5.1.4 (SF-LK) is not able to find a stabilizing controller, while Theorem 5.1.3 (SF-CQLF\*) still finds one. Some difference in conservatism between Theorems 5.1.3 and 5.1.4

Table 5.2: Obtained controllers for Theorems 5.1.3 (SF-CQLF\*) and 5.1.4 (SF-LK) for different values of  $\gamma$  and  $\tau_{\max}$  for  $h = 1\text{ms}$ .

$\gamma$	$\tau_{\max}$	$\bar{K}$ (Theorem 5.1.3)	$\bar{K}$ (Theorem 5.1.4)	$\theta_1$
0	$0.4h$	(0.045 0.280)	(0.891 4.307)	1
0	$0.4h$	(0.045 0.280)	(2.812 6.985)	10
0	$0.4h$	(0.045 0.280)	(4.711 7.878)	20
0	$0.99h$	(0.041 0.252)	(0.939 2.931)	1
0	$h$	(0.412 0.252)	-	1
0.01	$0.4h$	(3.419 0.577)	(42.466 5.927)	1
0.01	$0.98h$	(3.200 0.525)	(28.522 5.002)	1
0.01	$h$	(3.221 0.527)	-	1
0.1	$0.4h$	(196.366 2.598)	(329.252 5.252)	1
0.1	$0.81h$	(171.015 2.338)	(286.395 5.328)	1
0.1	$h$	(156.703 2.188)	-	1

is indeed expected, because in the latter theorem, the matrix  $T$  cannot be chosen independently of  $\tilde{P}$ , due to the assumption that  $T^{-1} = \theta_1 \tilde{P}^{-1}$  (which was needed to obtain LMI conditions). Note that the results of Theorem 5.1.4 (SF-LK) are slightly better than those obtained with Corollary 5.1.2 (SF-CQLF), where a specific structure on the  $P$ -matrix is needed. Finally, from the last two columns of Table 5.2 it is concluded that for  $\theta_1$  many possible values exist (in Theorem 5.1.4). Here, the choice of  $\theta_1$  is made based on trial and error. It can be seen that the choice of  $\theta_1$  has an influence on the obtained controller, although it is hard to provide a systematic procedure for how to select  $\theta_1$ . This is another disadvantage of Theorem 5.1.4 (SF-LK).

The applicability of Theorems 5.2.1 (ESF-CQLF) and 5.2.2 (SF-CQLF\*) for systems with time-delays larger than the sampling interval is studied using the results depicted in Table 5.3. Note that the equivalent of Theorem 5.1.4 (SF-LK) for large delays, as given in Appendix C, does not give feasible solutions, as was expected, because for  $\tau = h$  in Table 5.2 no feasible solution was found. In Table 5.3, it is assumed that there are no packet dropouts, i.e.  $\bar{\delta} = 0$ , and that the sampling interval is constant ( $h = 1\text{ms}$ ). Note that, due to the similarity between packet dropouts and delays, it holds that e.g.  $\tau_{\max} = 1.2h$  and  $\bar{\delta} = 0$  can be replaced by  $\tau_{\max} = 0.2h$  and  $\bar{\delta} = 1$ . Clearly, Theorems 5.2.1 and 5.2.2 are applicable for delays larger than the sampling interval. However, Theorem 5.2.2 (SF-CQLF\*) gives less freedom in the controller design which results in the fact that for  $\tau_{\max} = 2h$  and  $\gamma = 0.1$  no stabilizing controller is found, while using Theorem 5.2.1 (ESF-CQLF) we still find a stabilizing controller. Note that for this specific example a large value of  $\gamma$  was considered. For smaller values of  $\gamma$  both theorems obtain stabilizing controllers. Although Theorem 5.2.1 (ESF-CQLF) is applicable for a slightly larger range of delays, one limitation has to be considered, because it is only applicable if Assumption 4.4.1 holds. This limits the applicability for NCSs with, firstly, large delays if message rejection between the sensor and controller needs to be taken into

Table 5.3: Obtained controllers for Theorems 5.2.1 (ESF-CQLF) and 5.2.2 (SF-CQLF\*) for different values of  $\gamma$  and  $\tau_{\max}$  for  $h = 1\text{ms}$ .

$\gamma$	$\tau_{\max}$	$K$ (Theorem 5.2.1)	$K$ (Theorem 5.2.2)
0	$1.2h$	(0.014 0.181 -0.007 0.001)	(0.011 0.147)
0	$1.4h$	(0.014 0.188 -0.009 0.005)	(0.011 0.152)
0	$2h$	(0.012 0.229 -0.028 0.023)	(0.010 0.184)
0.01	$1.2h$	(15.499 1.672 0.393 0.270)	(9.446 1.013)
0.01	$1.4h$	(15.147 1.641 0.397 0.297)	(9.687 1.037)
0.01	$2h$	(15.802 1.699 0.387 0.242)	(8.658 0.937)
0.1	$1.2h$	(146.322 2.519 0.395 0.143)	(96.050 1.641)
0.1	$1.4h$	(158.951 2.724 0.436 0.193)	(86.867 1.541)
0.1	$2h$	(159.036 2.836 0.460 0.313)	-
0.05	$2.8h$	(42.231 1.446 0.209 0.224 0.142)	(19.432 0.741)

account, and secondly, packet dropouts, because in general, it is expected that the occurrence of packet dropouts in the network between the controller and actuator and between the sensor and controller is similar (hence, packet dropouts between the sensor and controller may occur). Note that this assumption is not necessary for the state-feedback controller for which Theorem 5.1.3 (SF-CQLF\*) holds, which is applicable for packet dropouts and message rejection occurring anywhere in the network.

In the previous examples, it was assumed that the sampling interval was constant. Next, some examples with a time-varying sampling interval will be described. First, consider system (4.1) without delays. Then, the extended state vector  $\xi_k$  does not contain past control inputs, i.e.  $\xi_k = x_k$ , because the only control input that can be active in the sampling interval  $[s_k, s_{k+1})$  is given by  $u_k$ . Therefore, the structured control synthesis problem does not occur if Theorem 5.2.1 is used to design a state-feedback controller. However, Theorems 5.2.1 (ESF-CQLF) and 5.2.2 (SF-CQLF\*) will not give the same results, because only one feasible controller is obtained when solving the controller synthesis LMIs, while many stabilizing controllers exist. For the sake of brevity, the L-K functionals are not used here, because the past control inputs (or past states) are not part of the system description itself, which makes the use of L-K functionals unnecessary (and leads to too complex LMIs). For different values of  $h_{\min}$ ,  $h_{\max}$ , and  $\gamma$ , the stabilizing controllers obtained from both common quadratic Lyapunov based theorems are given in Table 5.4. Note that for increasing values of  $\gamma$ , the controller gains increase rapidly.

If variation in the delay is added, the state vector  $\xi_k$  contains past control inputs. Therefore, Theorem 5.2.1 (ESF-CQLF) is used to design an extended state-feedback controller and Theorems 5.2.2 (SF-CQLF\*) and C.0.1 (SF-LK) are used to design a state-feedback controller. Some results are given in Table 5.5 for  $h \in [0.8, 1.2]\text{ms}$  and  $\tau \in [0.08, 0.72]\text{ms}$ . For  $\gamma = 0.05$ , Theorem C.0.1 (SF-LK) does not give a feasible solution, while Theorems 5.2.1 (ESF-CQLF) and 5.2.2 (SF-CQLF\*) still give a stabilizing controller. This shows that,

Table 5.4: Obtained controllers for Theorems 5.2.1 (ESF-CQLF) and 5.2.2 (SF-CQLF\*) for different values of  $\gamma$ , variable sampling intervals, and no delays.

$\gamma$	$h_{\min}$ [ms]	$h_{\max}$ [ms]	$K$ (Theorem 5.2.1)	$K$ (Theorem 5.2.2)
0.02	1.0	10.0	(22.75 0.89)	(19.57 0.88)
0.02	0.8	1.2	(89.46 6.36)	(101.20 7.57)
0.08	0.8	1.2	(767.06 10.8)	(573.72 8.07)
0.2	0.8	1.2	(2090.00 11.52)	(1427.26 8.50)

Table 5.5: Obtained controllers for Theorems 5.2.1 (ESF-CQLF), 5.2.2 (SF-CQLF\*), and C.0.1 (SF-LK) for different values of  $\gamma$ , with  $h \in [0.8, 1.2]$  ms and  $\tau \in [0.08, 0.72]$  ms.

$\gamma$	$K$ (Theorem 5.2.1)	$\bar{K}$ (Theorem 5.2.2)	$\bar{K}$ (Theorem C.0.1)	$\theta_1$
0.01	(10.66 1.13 0.12)	(7.76 0.89)	(40.47 5.42)	2
0.02	(17.07 1.07 0.07)	(11.21 0.79)	(72.36 4.94)	2
0.03	(21.34 1.01 0.05)	(15.81 0.81)	-	2
0.03	(21.34 1.01 0.05)	(15.81 0.81)	(150.89 6.76)	5
0.05	(33.56 1.07 0.04)	(28.33 0.91)	-	-

analogous to the case with constant sampling intervals, Theorems 5.2.1 (ESF-CQLF) and 5.2.2 (SF-CQLF\*) are less conservative and therefore applicable for a larger range of delays than Theorem C.0.1 (SF-LK). Moreover, analogous to the small delay case with constant sampling intervals, the choice of the parameter  $\theta_1$  has an influence on the stabilizing controller and a suboptimal choice may even result in the fact that no stabilizing controller is found, while for other values of  $\theta_1$  a stabilizing controller is obtained, see  $\gamma = 0.03$  in Table 5.5. We note that, for time-varying delays and sampling intervals, Theorem C.0.1 (SF-LK) gives a feasible solution if the following configuration is used:  $\tau_{\min} = 0$ ,  $\tau_{\max} = 0.98h_{\min}$ ,  $h_{\min} = 0.8$  ms,  $h_{\max} = 1.2$  ms and  $\gamma = 0$ . The obtained controller is given by  $\bar{K} = (1.53 \ 3.46)$ . This means that adding variation in the sampling interval leads to a slightly smaller value of  $\tau_{\max}$  for which a stabilizing state-feedback controller can be designed, compared to the constant sampling interval case, see the results in Table 5.2. Therefore, the additional variables, which are introduced to describe the variation in the sampling interval, do not result in more conservatism, compared to the constant sampling interval case.

It is clear that for increasing values of the parameter  $\gamma$ , it is more difficult to design a stabilizing controller. Moreover, a larger value of  $\gamma$  results in larger controller gains. The next paragraph will give examples to determine the usefulness of the parameter  $\gamma$  to predict the transient decay rate of the NCS.

**Transient performance analysis** In this paragraph, the prediction of the transient decay rate for the different controller synthesis conditions is used, based on a comparison with the obtained value of  $\gamma$  based on Theorems 5.1.1 (ESF-CQLF) and 5.1.4 (SF-LK) for the small delay case and Theorem 5.2.1

(ESF-CQLF) for the large delay case. Corollary 5.1.2 is not considered here, because its applicability is rather limited as concluded in the previous paragraph. For the sake of brevity, Theorem 5.1.3 (SF-CQLF\*) and 5.2.2 (SF-CQLF\*) are not considered. However, their results will be comparable to the results presented in the remaining of this paragraph.

First, the transient decay rate obtained from Theorems 5.1.1 (ESF-CQLF) and 5.2.1 (ESF-CQLF) and (5.9) is investigated. To show the applicability for delays larger than the sampling interval and packet dropouts, controllers are designed that guarantee stability for  $\tau_{\min} = 0$ ,  $\tau_{\max} = 0.8h$ , and  $\bar{\delta} = 2$ , for the constant sampling intervals  $h = 0.01\text{s}$  and  $h = 0.001\text{s}$ . For the sampling interval  $h = 0.01\text{s}$  and  $\gamma = 0.1$ , the controller  $K = (2.137 \ 0.326 \ 0.067 \ 0.180 \ 0.159)$  is obtained using the LMI conditions (5.5) and Theorem 5.2.1. The corresponding time-response of the position signal is depicted in the upper plot of Figure 5.1 for the initial condition  $\xi_0 = (1 \ 0 \ 0 \ 0 \ 0)^T$ . To obtain this response, a randomly time-varying delay is chosen (see the second plot in Figure 5.1) and the moment of packet dropout is determined in a random fashion, but it is guaranteed that at maximum  $\bar{\delta}$  subsequent packet dropouts occur. The occurrence of the packet dropouts is depicted by means of  $m_k$ , see (3.11), in the lower plot of Figure 5.1. For  $h = 0.001\text{s}$  and  $\gamma = 0.05$ , the controller  $K = (42.231 \ 1.446 \ 0.209 \ 0.224 \ 0.142)$  is obtained, using the LMI conditions in Theorem 5.2.1. Note that this controller is equal to the last controller in Table 5.3, due to the fact that the same controller can be applied as long as  $\tau_{\max} + \bar{\delta} = \text{constant}$ , as was concluded in Remark 4.4.6 in Chapter 4. The corresponding time-response, the delays, and the values of  $m_k$ , denoting whether a packet is lost or not, are depicted in Figure 5.2 for the initial condition  $\xi_0 = (1 \ 0 \ 0 \ 0 \ 0)^T$ . The analytical transient decay rate of both controllers, based on  $(1 - \gamma)$  according to (5.9), is given by the dashed lines in the figures. Note that for a fast transient decay rate, the value of  $1 - \gamma$ , which we will denote as the optimum transient decay rate, should be small. Figures 5.1 and 5.2 show that the analytical transient decay rate is not an overly conservative estimate of the transient decay rate of the time-response itself. To obtain an improved understanding of the accuracy of the prediction of the analytical transient decay rate, the optimum decay rate, i.e. the smallest value of  $1 - \gamma$ , for which Theorem 5.1.1 (ESF-CQLF) gives a feasible solution, i.e. a controller design, and the transient decay rate based on simulations of (4.1), (5.18), in combination with the designed controller are compared in Figure 5.3 for time-delays smaller than the constant sampling interval and no packet dropouts. This shows that the analytical transient decay rate  $(1 - \gamma)$  has a slightly larger value, i.e. a slightly slower time-response, than the transient decay rate based on simulations of the time-response of (4.1), (5.18), but the prediction is sufficiently accurate to use it for controller design. Indeed, (5.9) gives a lower bound on the transient decay rate of the system, which means that the transient response of the system is at least equally fast or faster than the analytically obtained bound on the response.

For Theorem 5.1.4 (SF-LK) the transient decay rate is obtained in a similar



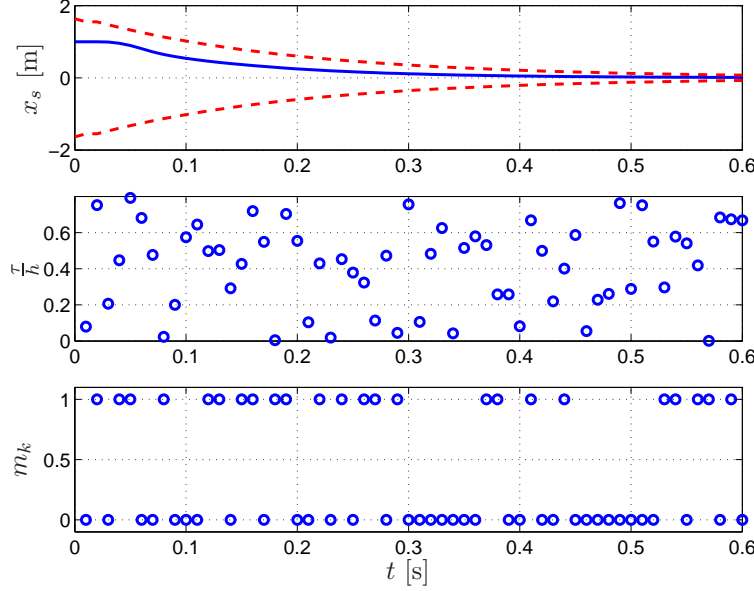


Figure 5.1: Time-response (solid line) of (4.1) and lower bound for transient decay rate (dashed line) obtained from (5.20) (ESF-CQLF) and (5.9), with time-delays and packet dropouts, for  $h = 0.01s$ ,  $\gamma = 0.1$ ,  $\tau_{\min} = 0$ ,  $\tau_{\max} = 0.8h$ , and  $\bar{\delta} = 2$ .

fashion. An example that shows a comparison between the analytical transient decay rate based on (5.13) and the transient response obtained from simulations of (4.1), (5.2) is given in Figure 5.4. The solid line in the upper plot of Figure 5.4 depicts the time-response of (4.1), (5.2) for  $\tau_k \in [0, 0.6h]$ , with the controller  $\bar{K} = (293.121 \quad 3.598)^T$  obtained with Theorem 5.1.4 and the initial condition  $\chi_0 = (0.1 \quad 0 \quad 0.1 \quad 0)^T$ . Here,  $\gamma = 0.15$  is used in combination with  $\theta_1 = 5$ . The dashed line depicts the analytical transient decay rate based on (5.13). The lower plot gives the time-delay during the simulations. Figure 5.4 shows that the bound on the transient response based on (5.13) is not overly conservative compared to the time-response of system (4.1), (5.2). Similar to Figure 5.3, Figure 5.5 depicts a comparison between the optimum decay rate, i.e. the smallest value of  $1 - \gamma$ , for which Theorem 5.1.4 gives a feasible solution and the transient decay rate obtained from the time-response of (4.1), (5.2). For Theorem 5.1.4 (SF-LK) the parameter  $\theta_1 = 5$  is considered. Figure 5.5 shows that the predicted analytical transient decay rate  $1 - \gamma$  is a useful estimation of the practical transient decay rate that is based on the simulations. Again, the transient decay rate, based on the simulations, is slightly smaller, i.e. the transient response is slightly faster, than the analytical transient decay rate  $1 - \gamma$ , with  $\gamma$  obtained from Theorem C.0.1 (SF-LK) in Appendix C.

Summarizing, relations (5.9) and (5.13) are useful to predict the transient de-



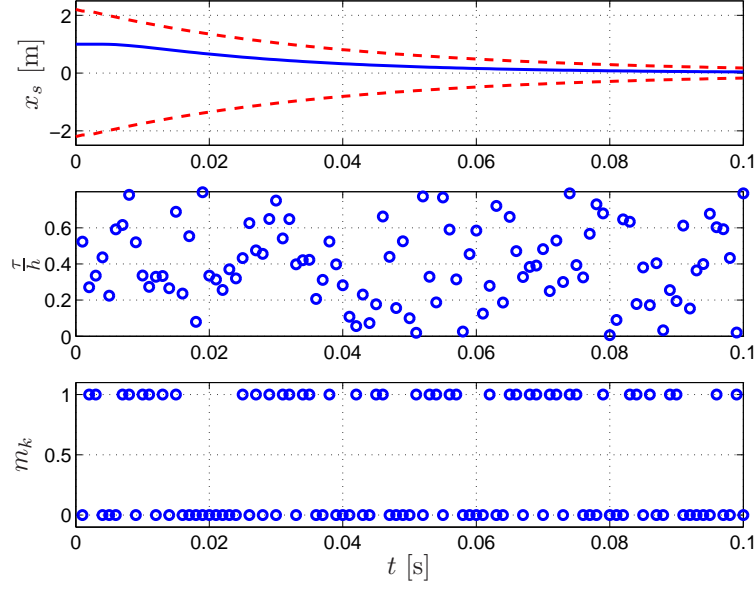


Figure 5.2: Time-response of (4.1) (solid line) and lower bound for transient decay rate (dashed line) obtained from (5.20) (ESF-CQLF) and (5.9), with time-delays and packet dropouts, for  $h = 0.001\text{s}$ ,  $\gamma = 0.05$ ,  $\tau_{\min} = 0$ ,  $\tau_{\max} = 0.8h$ , and  $\bar{\delta} = 2$ .

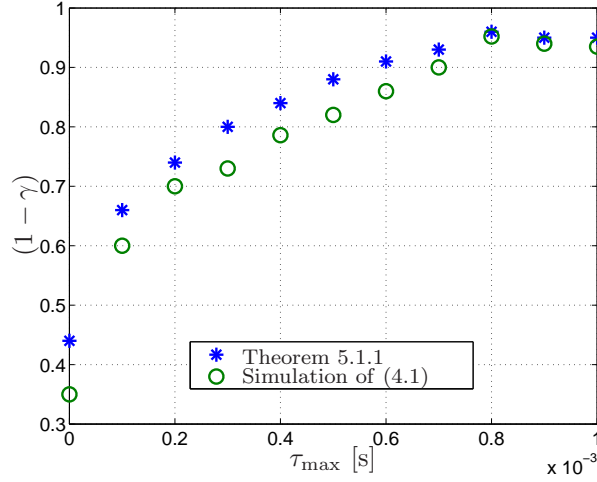


Figure 5.3: Comparison of the transient decay rate of controllers obtained with Theorem 5.1.1 (ESF-CQLF), (5.9) and based on simulations of (4.1), (5.18) (with  $h = 1\text{ms}$ ).

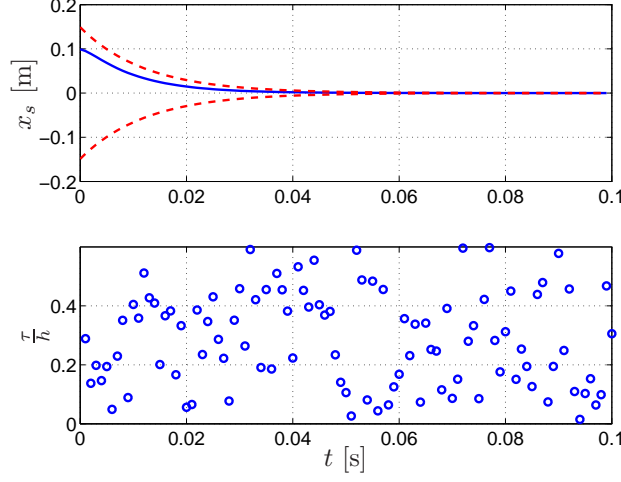


Figure 5.4: Time-response (solid line) of system 4.1 and lower bound of transient decay rate (dashed line) obtained from (5.12) (SF-LK) and (5.13), for time-varying delays, with  $\tau_{\min} = 0$ ,  $\tau_{\max} = 0.6h$ ,  $\gamma = 0.15$ ,  $\theta_1 = 5$ , and  $h = 1\text{ms}$ .

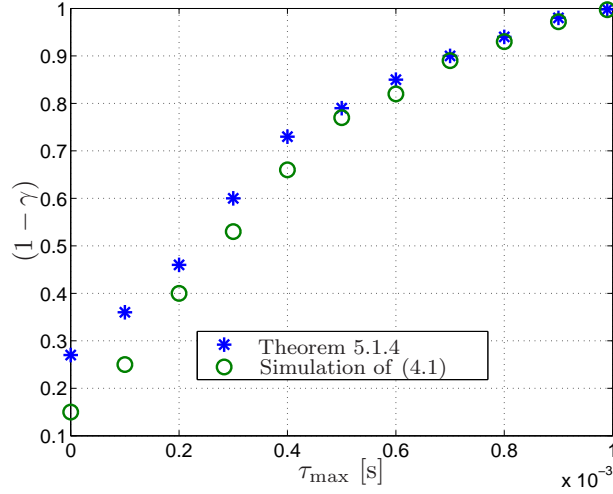


Figure 5.5: Comparison of the transient decay rate of controllers obtained with Theorem 5.1.4 (SF-LK) and based on simulations of (4.1) (with  $h = 1\text{ms}$ ).

cay rate of the NCS. Moreover, solving Theorems 5.1.1 (ESF-CQLF), 5.1.2 (SF-CQLF), 5.1.3 (SF-CQLF\*), or 5.1.4 (SF-LK) for the small delay case, or Theorems 5.2.1 (ESF-CQLF), 5.2.2 (SF-CQLF\*), or C.0.1 (SF-LK) for the case with time-varying delays, packet dropouts and/or time-varying sampling intervals, for a maximum value of  $\gamma$  is useful to design a controller that, firstly, guaran-

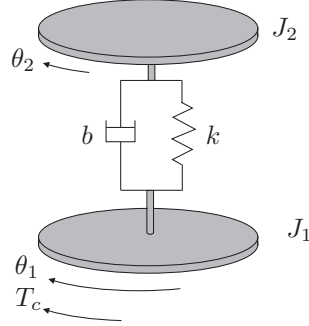


Figure 5.6: Schematic overview of the spring-damper model [22].

tees stability for time-varying delays and packet dropouts and, secondly, has an optimal time-response in terms of the transient decay rate. Note that, in general, the maximum value of  $\gamma$  will result in infinite controller gains, therefore an extension to optimal control (see e.g. [60; 64; 84; 85; 97; 121], and the overview papers [35; 77; 96]), where the control input is accounted for as well, is recommended.

### 5.3.2 Fourth-order motion control system

To show the applicability of the presented results to more complex systems, the controller synthesis approach of Theorems 5.1.1 (ESF-CQLF, small delays), 5.2.1 (ESF-CQLF, large delays) and 5.2.2 (SF-CQLF\*, large delays) are applied to a fourth-order model, obtained from [22] describing two rotating discs that are coupled via a spring and a damper. A schematic overview is given in Figure 5.6. The state-space model is given by:

$$\dot{x} = Ax + Bu = \begin{pmatrix} 0 & 1 & 0 & 0 \\ -\frac{k}{J_2} & -\frac{b}{J_2} & \frac{k}{J_2} & \frac{b}{J_2} \\ 0 & 0 & 0 & 1 \\ \frac{k}{J_1} & \frac{b}{J_1} & -\frac{k}{J_1} & -\frac{b}{J_1} \end{pmatrix} x + \begin{pmatrix} 0 \\ 0 \\ 0 \\ \frac{1}{J_1} \end{pmatrix} u, \quad (5.22)$$

with  $\dot{x} = (\theta_2 \quad \dot{\theta}_2 \quad \theta_1 \quad \dot{\theta}_1)^T$ , the state vector,  $u$  the control input, that is equal to the control torque  $T_c$ ,  $J_1 = 1\text{kgm}^2$ ,  $J_2 = 0.1\text{kgm}^2$ , the inertias of the discs around their respective centers,  $k = 0.091\text{N/m}$  the torsional spring stiffness, and  $b = 0.0036\text{Ns/m}$  the torsional damping coefficient. The output data of the system is obtained based on a constant sampling interval. Moreover, it is assumed that packet dropouts do not occur. The eigenvalues of the matrix  $A$  in (5.22) are  $\lambda_{1,2} = 0$  and  $\lambda_{3,4} = -0.0198 \pm 1.0003i$ . Therefore, the Real Jordan form, as described in Appendix B, is applied to rewrite the NCS in the form of (4.5) or (4.6).

For a constant sampling interval of  $h = 2\text{ms}$ ,  $\gamma = 0.01$ , and  $\tau_k \in [0, h]$ , we

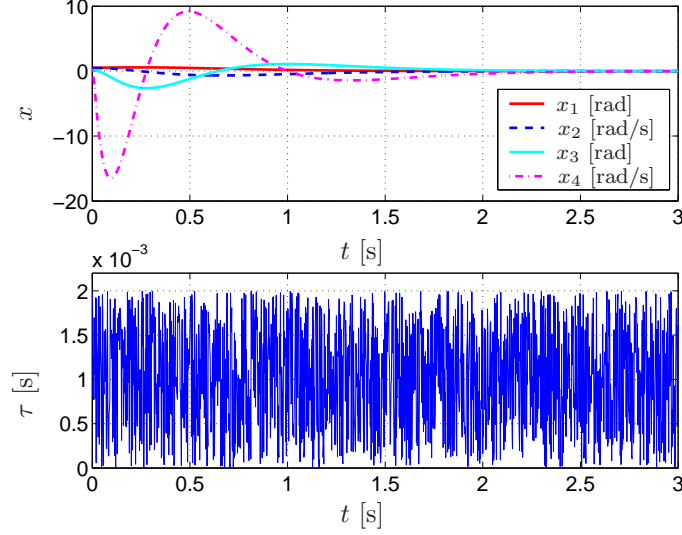


Figure 5.7: Time-responses of (5.22), (5.18), (5.23) for  $\tau_{\min} = 0$ ,  $\tau_{\max} = h$ ,  $\bar{\delta} = 0$ , and  $h = 2\text{ms}$ .

obtain the stabilizing controller (5.1), with

$$K = (118.279 \quad 113.887 \quad 31.348 \quad 5.141 \quad -0.706), \quad (5.23)$$

based on Theorem 5.1.1. The corresponding time-response is depicted in the upper plot of Figure 5.7 for the initial condition  $x_0 = (0.5 \quad 0.5 \quad 0.1 \quad 0)^T$  and  $u_{-1} = 0$ . This shows that the system is indeed stable. The variation in the delays is depicted in the lower plot of this figure.

For the large delay case, with  $\tau_k \in [0, 1.4h]$  and  $h = 2\text{ms}$ , the value  $\gamma$  has to be decreased to 0.001 to obtain a feasible solution based on Theorem 5.2.1, with  $h_k := h$  and  $\bar{\delta} := 0$ . The extended state-feedback controller (5.18), with  $\bar{d} = 2$  and

$$K = (-1.346 \quad 0.768 \quad 2.784 \quad 2.792 \quad 0.299 \quad 0.133), \quad (5.24)$$

stabilizes system (5.22) for delays  $\tau_k \in [0, 1.4h]$ . The corresponding time-response is depicted in the upper plot of Figure 5.8 for the initial condition  $x_0 = (0.5 \quad 0.5 \quad 0.1 \quad 0)^T$ ,  $u_{-1} = 0$ , and  $u_{-2} = 0$ . The corresponding variation in the delays is depicted in the lower plot. Here, for the sake of simplicity, the delay is only implemented between the controller and the actuator, thereby avoiding the possibility of message rejection between the sensor and the controller. The system is stable, but the transient decay rate is smaller than in the upper plot of Figure 5.7, which corresponds to the decrease of the parameter  $\gamma$  from 0.01 for the small delay case to 0.001 for this large delay case.

Analogously, for the state-feedback controller with  $\tau_k \in [0, 1.4h]$ ,  $h = 2\text{ms}$  and  $\gamma = 0.001$  a feasible solution based on Theorem 5.2.2, with  $h_k := h$  and

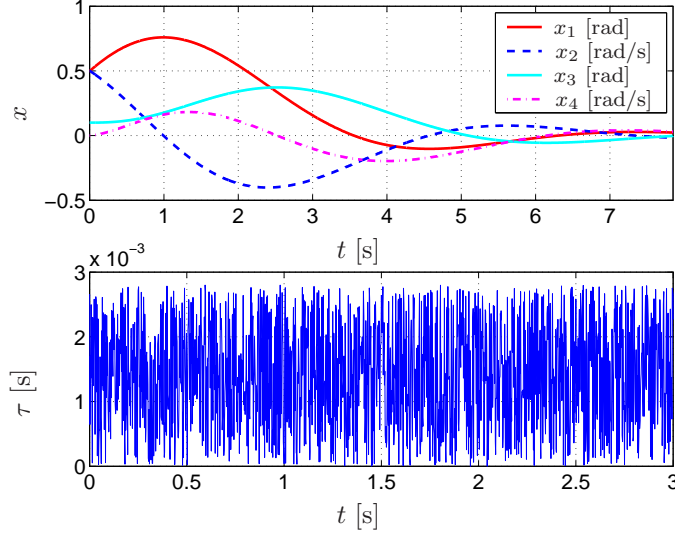


Figure 5.8: Time-responses of (5.22), (5.18), (5.24) for  $\tau_{\min} = 0$ ,  $\tau_{\max} = 1.4h$ ,  $\bar{\delta} = 0$ , and  $h = 2ms$ .

$\bar{\delta} := 0$ , is obtained. The state-feedback controller (5.2), with  $\bar{d} = 2$  and

$$\bar{K} = \begin{pmatrix} -1.008 & 0.678 & 2.139 & 2.042 \end{pmatrix}, \quad (5.25)$$

stabilizes system (5.22) for delays  $\tau_k \in [0, 1.4h]$ .

## 5.4 Discussion

To solve the controller synthesis problem, we have proposed different types of control laws: an extended state-feedback controller that considers both the state and past control inputs as feedback variable and a state-feedback controller. Different candidate Lyapunov functions are used to study the stability of the resulting closed-loop systems. For the extended state-feedback controller a candidate common quadratic Lyapunov function that is parameterized by a single unknown matrix  $P$  with its dimension equal to the extended state vector  $\xi_k$  can be used. For the presented motion control examples feasible solutions and thus stabilizing controllers are obtained, both for the small delay case and the large delay case with and without packet dropouts. Note that for the state-feedback controller, the same approach, with a common quadratic Lyapunov function with a single unknown matrix  $P$ , results in a structured control synthesis problem. However, an improvement, based on the results of [17; 19] is presented that avoids this structured control synthesis problem. The conservatism of the obtained results is comparable to the conservatism in the case of the extended state-feedback controller. The second approach to avoid the structured control synthesis problem for the state-feedback controller is the use of

the candidate Lyapunov-Krasovskii (L-K) functional. However, here, additional conservatism is introduced to obtain LMIs instead of BMIs, which are generally more complicated to solve. Due to this additional conservatism, only feasible solutions for the small delay case are obtained. Therefore, the conservatism of the L-K approach is worse than the conservatism in the case of, firstly, the common quadratic Lyapunov function, based on the approach presented in [17; 19], with the same state-feedback controller, or secondly, the common quadratic Lyapunov function in combination with the extended state-feedback controller. Note that the L-K functional gives in less conservative results than the use of the common quadratic Lyapunov function that contains the structured control synthesis problem.

In general, looking back at the different approaches for the state-feedback controller, it is concluded that, analogous to Chapter 4, the L-K functional can be rewritten as a common quadratic Lyapunov function, which can be used in Sections 5.1.1 and 5.2.1. Compared to Corollary 5.1.2, that includes the structured control synthesis problem, the L-K functional reduces the conservatism. However, it is shown that this structured control synthesis problem can be entirely avoided by exploiting the approach presented in [17; 19], as used in Theorems 5.1.3 and 5.2.2, resulting in less conservative conditions for the common quadratic Lyapunov function based on the extended state vector than for the L-K functional.

The advantage of the extended state-feedback controller that contains the control input history is the fact that the structured control synthesis problem is avoided. This gives the possibility to use a common quadratic Lyapunov approach to solve the control synthesis problem, without adding additional terms to the LMIs, as is the case in e.g. Theorem 5.1.3 (SF-CQLF\*). Recall, from Chapter 4, that this extended state-feedback controller is only applicable if Assumption 4.4.1 (which states that message rejection and packet dropouts between the sensor and controller do not occur) is valid, which is a disadvantage compared to the state-feedback controller that is always valid.

The lower bound on the transient decay rate, as provided by e.g. (5.9) or (5.13), is a useful tool to predict the transient performance of the controlled system. For the motor-roller example it is shown that this theoretical decay rate, both for the extended state-feedback controller and the state-feedback controller, is not extremely conservative. This is concluded based on a comparison of the theoretical decay rate and the transient decay rate of the system, as obtained from simulations. Optimization the LMI conditions with respect to  $\gamma$  in the different controller synthesis conditions gives a controller that guarantees stability in combination with the fastest transient decay rate. Note that, for the stability conditions in Chapter 4, the use of the parameter  $\gamma$ , results in the same transient decay rate conditions. A disadvantage of optimizing  $\gamma$  in the stability or controller synthesis conditions is that the controller gains become large. The use of optimal control strategies that consider both the transient response as well as the control input, based on weighting functions, would be useful to avoid unrealistically high control inputs.

## 6

# *Tracking control*<sup>1</sup>

---

6.1	Small delays	6.3	Tracking control performance
6.2	Variable sampling intervals, large delays, and packet dropouts	6.4	Illustrative examples
		6.5	Discussion

---

The previous chapters discussed the stability and stabilization of equilibria for NCSs. In practical applications, it is often desired that the dynamical system tracks a prescribed *time-varying* reference signal. Within the context of NCSs, we study these tracking problems in this chapter, where we allow for the most general case including time-varying delays, time-varying sampling intervals, and packet dropouts. A typical tracking controller consists of a feedforward part, which induces the desired solution, and a feedback part, which should induce asymptotic stability of the desired solution. The uncertain, time-varying sampling intervals, time-varying delays, and packet dropouts cause inexact feedforward, which induces a perturbation on the tracking error dynamics. As a consequence, exact reference tracking can never be obtained. Therefore, we consider an *approximate* tracking problem in terms of input-to-state stability (ISS) of the tracking error dynamics with respect to this perturbation. We will present sufficient conditions for ISS, which provide bounds on the steady-state tracking error as a function of the plant properties, the control design, and the network properties.

To study the tracking behavior of NCSs, a distinction is made between the small delay case and the case with time-varying sampling intervals, packet dropouts, and delays larger than the sampling interval. To present the sufficient conditions for ISS for both cases, we illustrate the results by a mechanical motion control example showing the effectiveness of the proposed strategy and providing insight in the differences and commonalities between the modeling approach considered in this thesis and the modeling approach based on delay impulsive differential equations in [74], [111], where the tracking problem was also considered.

The outline of the chapter is as follows. In Section 6.1 the tracking problem for a NCS with time-varying delays smaller than the constant sampling interval

---

<sup>1</sup>This chapter is based on [110] and [111] that consider time-varying sampling intervals in combination with delays smaller than the sampling interval. In these papers, besides ISS conditions based on the discrete-time NCS model as proposed in this thesis, ISS conditions based on a model in terms of delay impulsive differential equations for NCSs are proposed in relation to the tracking problem of NCSs.

is described. In Section 6.2 the tracking problem for a NCS with time-varying delays larger than the uncertain and time-varying sampling intervals and packet dropouts is described. In Section 6.3, the tracking control performance, in terms of an ultimate bound on the tracking error is described. In Section 6.4, illustrative examples are presented and in Section 6.5 the obtained results are summarized.

## 6.1 Small delays

In this section, the tracking problem for a NCS with time-varying delays smaller than the constant sampling interval is studied. Recall that the NCS is described by:

$$\begin{aligned} \dot{x}(t) &= Ax(t) + Bu^*(t), \\ y(t) &= Cx(t) \\ u^*(t) &= u_k, \quad \text{for } t \in [s_k + \tau_k, s_{k+1} + \tau_{k+1}) \end{aligned} \quad (6.1)$$

with  $A \in \mathbb{R}^{n \times n}$ ,  $B \in \mathbb{R}^{n \times m}$ , and  $C \in \mathbb{R}^{r \times n}$ , the system matrices,  $u^*(t) \in \mathbb{R}^m$  the continuous-time control input,  $x(t) \in \mathbb{R}^n$  the state at time  $t \in \mathbb{R}$ ,  $y(t) \in \mathbb{R}^r$  the output,  $s_k$  the sampling instants with  $s_k := kh$ ,  $k \in \mathbb{N}$ ,  $u_k := u(s_k) \in \mathbb{R}^m$  the discrete-time control input based on the measurement data at (sensor) sampling instant  $s_k$ , and  $\tau_k$  the time-varying delay. The feedback part of the controller is based on (4.9), which is a state feedback controller  $u_k = -Kx_k$ . Of course, (4.9) will be adapted to include the reference signal in the feedback law. The extended state-feedback controller (4.8) ( $u_k = -K\xi_k$ ) is not considered in this chapter to avoid the limitations of Assumption 4.4.1 (i.e. no message rejection and packet dropouts between the sensor and controller). To study the tracking problem for the small delay case, firstly, the tracking problem and the tracking controller are discussed in Section 6.1.1 and, secondly, certain ISS properties of the tracking error dynamics are discussed in Section 6.1.2.

### 6.1.1 Tracking problem

To study the tracking problem of NCSs with delays smaller than the constant sampling interval, the tracking control design, closed-loop system, and tracking error dynamics are discussed, subsequently.

**Tracking control design** We want the system to asymptotically track a desired trajectory  $x_d(t)$ . The proposed control law consists of a feedforward part and a feedback part. To determine the feedforward signal, and the error that is caused by the difference between the zero-order-hold implementation of the feedforward signal and the ideal feedforward signal, the control signal construction is studied in more detail. Here, we assume that there exists a feedforward  $u_e^{ff}(t)$  that induces the desired trajectory  $x_d(t)$ ; in other words for a given  $x_d(t)$ , there exists a feedforward  $u_e^{ff}(t)$  that satisfies

$$\dot{x}^d(t) = Ax^d(t) + Bu_e^{ff}(t). \quad (6.2)$$



Additionally, we assume that  $x^d(t)$  is at least  $\mathcal{C}^2$ , guaranteeing that  $u_e^{ff}(t)$  is at least  $\mathcal{C}^1$ , which we will need in Section 6.3.1. We propose the following tracking control law for (6.1):

$$u_k(x_k, x^d(s_k), u_e^{ff}(s_k)) = u_e^{ff}(s_k) - \overline{K}(x_k - x^d(s_k)), \quad (6.3)$$

which consists of the superposition of a sampled feedforward component  $u_e^{ff}(s_k)$  with a linear tracking error feedback component with feedback gain matrix  $\overline{K} \in \mathbb{R}^{m \times n}$ . Due to the constant and known sampling interval, the controller can compute the control law (6.3) at time  $s_k + \tau_k^{sc}$ . An alternative control law, although not considered in this chapter, could be:

$$u_k = u_e^{ff}(s_k + \tau_k^{sc}) - \overline{K}(x_k - x^d(s_k)), \quad (6.4)$$

if the delay  $\tau_k^{sc}$  is known to the controller due to the use of time stamping of the measurement data.

Clearly, the implemented continuous-time feedforward  $u^{ff}(t)$  in (6.1), (6.3) is given by

$$u^{ff}(t) = u_e^{ff}(s_k) \quad \text{for } t \in [s_k + \tau_k, s_{k+1} + \tau_{k+1}), \quad (6.5)$$

and differs from the exact feedforward  $u_e^{ff}(t)$  due to the zero-order-hold and the delays. Therefore, the implemented feedforward is decomposed in an exact feedforward part  $u_e^{ff}(t)$  and a feedforward error  $\Delta u^{ff}(t)$ :

$$u^{ff}(t) = u_e^{ff}(t) + \Delta u^{ff}(t), \quad (6.6)$$

where the feedforward error is simply defined by

$$\Delta u^{ff}(t) = u_e^{ff}(s_k) - u_e^{ff}(t) \quad \text{for } t \in [s_k + \tau_k, s_{k+1} + \tau_{k+1}). \quad (6.7)$$

**Closed-loop system** Applying the control law (6.3) to system (6.1) yields the following closed-loop NCS dynamics:

$$\dot{x}(t) = Ax(t) + B_1(x_k - x^d(s_k)) + B_2 u_e^{ff}(t) + B_2 \Delta u^{ff}(t), \quad (6.8)$$

for  $t \in [s_k + \tau_k, s_{k+1} + \tau_{k+1})$ , and with  $B_1 := -B\overline{K}$  and  $B_2 := B$ . The initial condition  $\bar{x}(0) := (x^T(0) \quad x^T(s_{-1}))^T$  for this system consists of both the initial state at time  $s_0 = 0$ , i.e.  $x(0) = x_0$ , and the *hold* state  $x(s_{-1})$  at time  $s_{-1} < 0$  due to the fact that in the time interval  $t \in [0, \tau_0]$ , the feedback part of the control action is given by  $u_{-1} = -\overline{K}(x(s_{-1}) - x^d(s_{-1}))$ . So, the network delays cause the initial state to involve a past state.

**Tracking error dynamics** The tracking error  $e$  is defined by  $e = x - x^d$ . By combining (6.2) and (6.8), the continuous-time tracking error dynamics can be formulated as follows:

$$\dot{e}(t) = Ae(t) + B_1 e(s_k) + B_2 \Delta u^{ff}(t), \quad \text{for } t \in [s_k + \tau_k, s_{k+1} + \tau_{k+1}), \quad (6.9)$$

with initial condition  $\bar{e}(0) := (e^T(0) \ e^T(s_{-1}))^T$ .

As the exact tracking  $\lim_{t \rightarrow \infty} e(t) = 0$  is almost impossible to obtain, due to the presence of a nonzero  $\Delta u^{ff}(t)$ , we consider the approximate tracking problem. In approximate tracking, the aim is to ensure ultimate boundedness of the tracking error, i.e.  $\lim_{t \rightarrow \infty} |e(t)| \leq \varepsilon$ , with  $|e(t)| = |x(t) - x^d(t)|$  and some small  $\varepsilon > 0$ . Some tracking error is to be expected in the NCS setting, as the implemented feedforward signal  $u_e^{ff}(t)$  in (6.5) will never equal the exact feedforward  $u_e^{ff}(t)$ . The reasons for non-exact feedforward are, firstly, the fact that the control signal (and therefore also the feedforward signal) will be passed through a zero-order hold and, secondly, the fact that the network delays (in particular the controller-to-actuator delay  $\tau_k^{ca}$ ) in general cause the feedforward to be implemented too late. Thereby, a feedforward error  $\Delta u^{ff}(t)$  is introduced. However, as we will show in the next sections, for  $h \rightarrow 0$  and  $\tau \rightarrow 0$ , the feedforward error tends to zero, and therefore, the tracking error tends to zero (i.e.  $\varepsilon \rightarrow 0$ ). In the next section, sufficient conditions for the input-to-state stability (ISS) of the continuous-time tracking error dynamics (6.9) with respect to the input  $\Delta u^{ff}(t)$  are proposed. The ISS property of the tracking error dynamics will be used to guarantee that the controller solves an approximate tracking problem.

Moreover, since such ISS properties of linear sampled-data systems with time-varying delays are of interest in a wider context, we consider systems of the form

$$\dot{z}(t) = Az(t) + B_1 z(s_k) + B_2 w(t) \quad \text{for } t \in [s_k + \tau_k, s_{k+1} + \tau_{k+1}), \quad (6.10)$$

with initial condition  $\bar{z}(0) := (z^T(0) \ z^T(s_{-1}))^T$ . Herein, the time-varying input  $w(t)$  may be the feedforward error (as above). Alternatively, in the scope of the disturbance rejection problem one may consider it to represent external perturbations or, in the scope of the design of observer-based output-feedback schemes, it may represent the observer error perturbing the closed-loop system (where the ISS-property is shown to be instrumental in providing a separation principle) [91].

### 6.1.2 Input-to-state stability

In this section, sufficient conditions for the ISS of the continuous-time dynamics of the form (6.10) with respect to the input  $w(t)$  (including the continuous-time tracking error dynamics (6.9)) are proposed. The approach followed in this chapter is based on an analysis using a discrete-time NCS model. Another approach, where the dynamics are analyzed using delay impulsive differential equations is described in [110; 111], and [74].

Analogous to Definition 2.2.4, we will call system (6.10) *uniformly* ISS if its solutions satisfy

$$|z(t)| \leq \beta(|\bar{z}(0)|, t) + \gamma\left(\sup_{0 \leq s \leq t} |w(s)|\right), \quad (6.11)$$

with functions  $\beta \in \mathcal{KL}$  and  $\gamma \in \mathcal{K}$  that are independent of the choice of the delay  $\tau_k$  and  $\bar{z}(0) := (z^T(0) \ z^T(s_{-1}))^T$ , the initial condition of (6.10). Note

that the term *uniformly* refers to the fact that ISS holds for the same functions  $\beta$  and  $\gamma$  independent of the delay. We would like to have the ISS property for any sequence of delays such that  $\tau_{\min} \leq \tau_k \leq \tau_{\max} < h$ ,  $\forall k \in \mathbb{N}$ .

Under the assumption that  $\tau_k < h$ ,  $\forall k$ , the discretization of (6.10) at the sampling instants  $s_k$  gives the discrete-time system:

$$z_{k+1} = e^{Ah} z_k + \int_0^{h-\tau_k} e^{As} ds B_1 z_k + \int_{h-\tau_k}^h e^{As} ds B_1 z_{k-1} + \bar{w}_k, \quad (6.12)$$

where  $\bar{w}_k := \int_0^h e^{As} B_2 w(h + s_k - s) ds$ . Since  $\tau_k < h$ ,  $\forall k$ , the extended state for the system (6.12) is defined by  $\psi_k := (z_k^T \ z_{k-1}^T)^T$ , similar to  $\chi_k$  in (4.20). The discrete-time state-space model is then given by:

$$\psi_{k+1} = \tilde{A}(h, \tau_k) \psi_k + \tilde{B} \bar{w}_k, \text{ for } \tau_k \in [\tau_{\min}, \tau_{\max}], \tau_{\max} < h, \quad (6.13)$$

with  $\psi_k \in \mathbb{R}^{2n}$ ,

$$\tilde{A}(\tau_k) = \begin{pmatrix} e^{Ah} + \int_0^{h-\tau_k} e^{As} ds B_1 & \int_{h-\tau_k}^h e^{As} ds B_1 \\ I & 0 \end{pmatrix}, \quad \tilde{B} = \begin{pmatrix} I \\ 0 \end{pmatrix}. \quad (6.14)$$

Later, we will use that  $z_k = C_z \psi_k$ , with  $C_z = (I \ 0)$  being an  $n \times 2n$ -matrix. Similar to Chapters 4 and 5, the Jordan form of the continuous-time system matrix  $A$  is considered in the analysis. The equivalent representation of (6.13), (6.14) that is based on the Jordan form of the continuous-time system matrix  $A$  is given by:

$$\psi_{k+1} = F(\tau_k) \psi_k + \tilde{B} \bar{w}_k, \text{ for } \tau_k \in [\tau_{\min}, \tau_{\max}], \tau_{\max} < h, \quad (6.15)$$

with  $F(\tau_k) = F_0 + \sum_{i=1}^{\nu} \alpha_i(\tau_k) F_i$  and the matrices  $F_0$ ,  $F_i$ ,  $i = 1, 2, \dots, \nu$ , given by:

$$F_0 = \begin{pmatrix} Q\Theta_0 Q^{-1} + Q\Xi_0 Q^{-1} B_1 & Q\Theta_1 Q^{-1} B_1 \\ I & 0 \end{pmatrix}, \quad (6.16)$$

$$F_i = \begin{pmatrix} Q\Xi_i Q^{-1} B_1 & Q\Gamma_{1,i} Q^{-1} B_1 \\ 0 & 0 \end{pmatrix},$$

with  $\Theta_0$ ,  $\Xi_0$ ,  $\Theta_1$ ,  $\Xi_i$ ,  $\Gamma_{1,i}$ ,  $i = 1, 2, \dots, \nu$ , defined in Appendix B.2 with  $B_1$  replaced by  $-BK$ . Note that, compared to Appendix B.2 and Theorem 4.3.1, the matrices  $G_0$  and  $G_i$ ,  $i = 1, 2, \dots, \nu$ , as used in (B.35) are equal to zero, because their values are already included in  $F_0$  and  $F_i$ ,  $i = 1, 2, \dots, \nu$ . The matrices  $F(\tau_k)$  in (6.15) form the set of matrices  $\mathcal{F}$

$$\mathcal{F} = \{F(\tau_k) : \tau_k \in [\tau_{\min}, \tau_{\max}]\}, \quad (6.17)$$

analogously to (4.10).

Before the conditions for the ISS of system (6.10) are formulated, recall that global asymptotic stability of the fixed point  $\psi = 0$  of the discrete-time system

(6.13), or equivalently (6.15), for the case that  $\bar{w}_k = 0, \forall k$  can be guaranteed based on the stability results obtained in Theorems 4.3.1, and 4.3.2. Note that for the applicability of Theorems 4.3.1 for (6.13), we need that  $P \in \mathbb{R}^{2n \times 2n}$  instead of  $P \in \mathbb{R}^{(n+m) \times (n+m)}$  and that the matrices  $H_{F,j}, j \in \{1, 2, \dots, 2^\nu\}$ , are based on the matrices  $F_0$  and  $F_i, i = 1, 2, \dots, \nu$ , defined in (6.16) and that the matrices  $H_{G,j}$  are empty. Theorem 4.3.2 can be applied if the matrices  $H_{F,j}^x, j \in \{1, 2, \dots, 2^\nu\}$ , are based on a partitioning of the matrices  $F_0$  and  $F_i, i = 1, 2, \dots, \nu$ , defined in (6.16) and that the matrices  $H_{G,j}^x$  are empty. For the sake of brevity, we consider in this chapter only the common quadratic Lyapunov approach of Theorem 4.3.1, because it gives good results for the stability conditions of the state-feedback controller on which we will focus here. Based on the stability results of Theorem 4.3.1, we will show (see Lemma 6.1.1 and Theorem 6.1.2) that the ISS of (6.10) is guaranteed if the following (infinite) set of matrix inequalities is feasible:

$$P = P^T > 0$$

$$\begin{pmatrix} F(\tau_k)^T P F(\tau_k) - (1 - \gamma)P & F(\tau_k)^T (\tau_k) P \tilde{B} \\ \tilde{B}^T P F(\tau_k) & \tilde{B}^T P \tilde{B} - \kappa I \end{pmatrix} < 0, \forall \tau_k \in [\tau_{\min}, \tau_{\max}], \quad (6.18)$$

with  $\tau_{\max} < h$  and  $F(\tau_k) = F_0 + \sum_{i=1}^{\nu} \alpha_i(\tau_k) F_i$ , for some  $0 < \gamma < 1$  and  $\kappa > 0$ . The following lemma formulates sufficient LMI conditions for the feasibility of (6.18) and shows that these LMI conditions guarantee ISS of the discrete-time NCS model (6.13), (6.14).

**Lemma 6.1.1** *Consider the discrete-time NCS model (6.13), (6.14) and its equivalent model (6.15), (6.16) that is based on the Jordan form of  $A$ , both with delays  $\tau_k \in [\tau_{\min}, \tau_{\max}]$ , with  $\tau_{\max} < h$ . Define the set of matrices  $\mathcal{H}_F$ :*

$$\mathcal{H}_F = \left\{ \bar{F}_0 + \sum_{i=1}^{\nu} \delta_i \bar{F}_i : \delta_i \in \{0, 1\}, i = 1, 2, \dots, \nu \right\}, \quad (6.19)$$

with  $\bar{F}_0 = F_0 + \sum_{i=1}^{\nu} \underline{\alpha}_i F_i$ ,  $\bar{F}_i = (\bar{\alpha}_i - \underline{\alpha}_i) F_i$ ,  $\bar{\alpha}_i = \max_{\tau \in [\tau_{\min}, \tau_{\max}]} \alpha_i(\tau)$ ,  $\underline{\alpha}_i = \min_{\tau \in [\tau_{\min}, \tau_{\max}]} \alpha_i(\tau)$ , and  $F_0, F_i$ , for  $i = 1, 2, \dots, \nu$ , defined in (6.16).

If there exist a symmetric matrix  $P \in \mathbb{R}^{2n \times 2n}$  and scalars  $0 < \gamma < 1$  and  $\kappa > 0$  that satisfy:

$$P = P^T > 0$$

$$\begin{pmatrix} H_{F,j}^T P H_{F,j} - (1 - \gamma)P & H_{F,j}^T P \tilde{B} \\ \tilde{B}^T P H_{F,j} & \tilde{B}^T P \tilde{B} - \kappa I \end{pmatrix} < 0, \forall H_{F,j} \in \mathcal{H}_F, j \in \{1, 2, \dots, 2^\nu\}, \quad (6.20)$$

then the matrix inequalities (6.18) are feasible. Moreover,  $V(\psi_k) = \psi_k^T P \psi_k$  is an ISS-Lyapunov function for system (6.13), (6.14) and, consequently, this system is input-to-state stable for bounded inputs  $\bar{w}_k$ .

**Proof** The proof is given in Appendix A.12. □

Let us now present the result on the ISS of the continuous-time dynamics (6.10).

**Theorem 6.1.2** *Consider the sampled-data system (6.10), with uncertain time-varying delays  $\tau_k \in [\tau_{\min}, \tau_{\max}]$ , with  $\tau_{\max} < h$ . Suppose there exist a matrix  $P$  and scalars  $0 < \gamma < 1$  and  $\kappa > 0$  for which (6.18) is satisfied. Then, the system (6.10) is uniformly input-to-state stable (ISS) for  $\tau_k \in [\tau_{\min}, \tau_{\max}]$ , with  $\tau_{\max} < h$  with respect to the time-varying input  $w(t)$ . The functions  $\beta$  and  $\gamma$  in (6.11) can be obtained from:*

$$\begin{aligned} \beta(|\bar{z}(0)|, t) &= |\bar{z}(0)| \begin{cases} \max\{g_{1,0}, g_{1,1}, g_{1,2}\} & \text{for } t \in [0, s_2) \\ g_{1,k} & \text{for } k \geq 2, t \in [s_k, s_{k+1}) \end{cases} \\ \gamma(\sup_{0 \leq s \leq t} |w(s)|) &= g_2 \sup_{0 \leq s \leq t} |w(s)|, \end{aligned} \quad (6.21)$$

with

$$\begin{aligned} g_{1,0} &= c_1 + c_2, \\ g_{1,1} &= c_1 \|C_z P^{-\frac{1}{2}}\| \sqrt{\bar{\gamma} \lambda_{\max}(P)} + c_2, \\ g_{1,k} &= \|C_z P^{-\frac{1}{2}}\| \left( c_1 \sqrt{\bar{\gamma}^k \lambda_{\max}(P)} + c_2 \sqrt{\bar{\gamma}^{k-1} \lambda_{\max}(P)} \right), \quad k \geq 2, \\ g_2 &= c_w \left( 1 + (c_1 + c_2) \|C_z P^{-\frac{1}{2}}\| \sqrt{\frac{\kappa}{\gamma}} \right), \end{aligned} \quad (6.22)$$

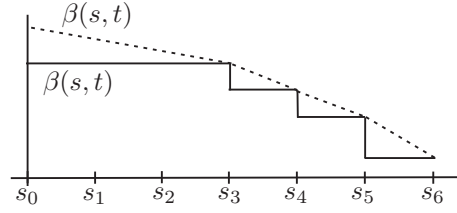
$c_1$ ,  $c_2$ , and  $c_w$  are defined in (A.77), (A.78), (A.80) in Appendix A.13, and  $\bar{\gamma} = 1 - \gamma$ .

**Proof** For the proof, see Appendix A.13.  $\square$

Note that  $\beta(s, t)$  satisfies all the conditions of a class- $\mathcal{KL}$  function except that for fixed  $s$  it is only non-increasing and not continuous everywhere, because for  $s_0 \leq t < s_2$  and  $s_k \leq t < s_{k+1}$ ,  $\forall k \geq 2$  the function  $\beta(s, t)$  is constant and it decreases only at  $t = s_k$ ,  $\forall k \geq 3$ , as depicted by the solid line in Figure 6.1. However, it is easy to construct a  $\bar{\beta}(s, t) \in \mathcal{KL}$  from  $\beta(s, t)$ , as depicted by the dashed line in Figure 6.1. The function  $\gamma(\sup_{0 \leq s \leq t} |w(s)|)$  is a class  $\mathcal{K}$ -function, therefore inequality (6.11) is satisfied.

Clearly, this result implies that the state  $z$  of the sampled-data system is globally uniformly ultimately bounded and the asymptotic bound is given by  $\limsup_{t \rightarrow \infty} |z(t)| \leq g_2 \sup_{t \geq 0} |w(t)|$ , with  $g_2$  as in (6.22). Note that all parameters in (6.22), (A.77), (A.78), and (A.80) are known and depend on the system dynamics (matrices  $A$ ,  $B_1$ , and  $B_2$ ), the constant sampling interval, the maximum and minimum delays  $\tau_{\max}$  and  $\tau_{\min}$ , respectively, and the parameters  $\gamma$ ,  $\kappa$ , and matrix  $P$  obtained from (6.20).

**Remark 6.1.3** An asymptotic bound for the state at the sampling instants can directly be derived from (A.74) in Appendix A.13 and the fact that  $\lim_{k \rightarrow \infty} D_k =$

Figure 6.1: Example of the function  $\beta(s, t)$  and  $\bar{\beta}(s, t)$ 

$\lim_{k \rightarrow \infty} \sum_{i=1}^k \bar{\gamma}^{i-1} = 1/\gamma$ , yielding

$$\begin{aligned} \limsup_{k \rightarrow \infty} |z_k| &\leq \|C_z P^{-\frac{1}{2}}\| \sqrt{\frac{\kappa}{\gamma}} \sup_{k \geq 1} |\bar{w}_k| \leq c_w \|C_z P^{-\frac{1}{2}}\| \sqrt{\frac{\kappa}{\gamma}} \sup_{t \geq 0} |w(t)| \\ &:= \bar{g}_2 \sup_{t \geq 0} |w(t)|. \end{aligned} \quad (6.23)$$

This bound can in many practical cases (e.g. for sufficiently small sampling intervals) be sufficient and it is typically much less conservative than the bound based on the intersample behavior, since  $\bar{g}_2 < g_2$ . The difference between  $g_2$  and  $\bar{g}_2$  originates from the need to upper bound the intersample behavior of  $z(t)$ , thereby introducing additional conservatism.

## 6.2 Variable sampling intervals, large delays, and packet dropouts

The tracking problem and ISS conditions, derived in the previous section for the small delay case, are adapted, such that they are applicable for NCSs with time-varying sampling intervals, delays larger than the sampling interval, and packet dropouts. Recall that the NCS model for this case is given by (3.12)

$$\begin{aligned} \dot{x}(t) &= Ax(t) + Bu^*(t) \\ y(t) &= Cx(t) \\ u^*(t) &= u_j \text{ for } t \in [s_k + t_j^k, s_k + t_{j+1}^k), \end{aligned} \quad (6.24)$$

where  $s_k$  is defined as  $s_k = \sum_{i=0}^{k-1} h_i$ ,  $\forall k \geq 1$ , with  $s_0 = 0$ , and  $t_j^k$  is defined in (3.22) as:

$$\begin{aligned} t_j^k &= \min \left\{ \max\{0, \tau_j - \sum_{l=j}^{k-1} h_l\} + m_j h_{\max}, \right. \\ &\quad \max\{0, \tau_{j+1} - \sum_{l=j+1}^{k-1} h_l\} + m_{j+1} h_{\max}, \dots, \\ &\quad \left. \max\{0, \tau_{k-\underline{d}} - \sum_{l=k-\underline{d}}^{k-1} h_l\} + m_{k-\underline{d}} h_{\max}, h_k \right\}, \end{aligned} \quad (6.25)$$

with  $t_j^k \leq t_{j+1}^k$  and  $j \in [k - \bar{d} - \bar{\delta}, k - \bar{d} - \bar{\delta} + 1, \dots, k - \underline{d}]$ . Moreover,  $0 = t_{k-\bar{d}-\bar{\delta}}^k \leq t_{k-\bar{d}-\bar{\delta}+1}^k \leq \dots \leq t_{k-\underline{d}}^k \leq t_{k-\underline{d}+1}^k := h_k$ .

### 6.2.1 Tracking problem

Similar to the small delay case, the control signal construction, closed-loop system, and tracking error dynamics are described.

**Control signal** Both message rejection and packet dropouts may result in the fact that the control signal, including the feedforward signal is never used to actuate the plant. This requires some adaptation in the control signal construction compared to the small delay case. It is obvious that the desired continuous-time dynamics, as described by (6.2) and the tracking control law (6.3) are not affected by variations in the sampling time, packet dropouts, and message rejection. The implemented feedforward of (6.5) has to be adapted, to allow for message rejection and packet dropouts:

$$u^{ff}(t) = u_e^{ff}(s_j) \quad \text{for } t \in [s_k + t_j^k, s_k + t_{j+1}^k), \quad (6.26)$$

for  $t_j^k$  defined in Lemma 3.4.1. Note that this is not the only possible description for the feedforward signal. In [74], the following notation is used:  $u^{ff}(t) = u_e^{ff}(s_k)$  for  $t \in [t_k, t_{k+1})$ , with  $t_k$  the actuator update times and  $k$  a sequential number that is not changed if a packet is dropped (or rejected). Based on (6.26) and (6.6), the feedforward error is defined as:

$$\Delta u^{ff}(t) = u_e^{ff}(s_j) - u_e^{ff}(t) \quad \text{for } t \in [s_k + t_j^k, s_k + t_{j+1}^k). \quad (6.27)$$

**Closed-loop system** Due to the possibility of delays larger than the sampling interval and the use of packet dropouts, the closed-loop NCS dynamics of (6.8) needs to be modified as well. Applying the control law (6.3) to system (6.24) yields the following closed-loop NCS dynamics:

$$\dot{x}(t) = Ax(t) + B_1 (x_j - x^d(s_j)) + B_2 u_e^{ff}(t) + B_2 \Delta u^{ff}(t), \quad (6.28)$$

for  $t \in [s_k + t_j^k, s_k + t_{j+1}^k)$ ,  $j \in \{k - \bar{d} - \bar{\delta}, \dots, k - \underline{d}\}$  and with  $B_1 := -B\bar{K}$  and  $B_2 := B$ . The initial condition is given by  $\bar{x}(0) := (x^T(0) \ x^T(s_{-1}) \ x^T(s_{-2}) \ \dots \ x^T(s_{-\bar{d}-\bar{\delta}}))^T$ , with  $x(s_{-1}), x(s_{-2}), \dots, x(s_{-\bar{d}-\bar{\delta}})$  the *hold* states at the times  $s_{-\bar{d}-\bar{\delta}} < \dots < s_{-1} < 0$ .

**Tracking error dynamics** Due to the new definition of the feedforward signal and the closed-loop system, the tracking error dynamics (with the tracking error  $e = x - x^d$ ) needs to be redefined. By combining (6.2) and (6.28), the continuous-time tracking error dynamics can be formulated as follows:

$$\dot{e}(t) = Ae(t) + B_1 e(s_j) + B_2 \Delta u^{ff}(t), \quad (6.29)$$

for  $t \in [s_k + t_j^k, s_k + t_{j+1}^k)$ ,  $j \in \{k - \bar{d} - \bar{\delta}, \dots, k - \underline{d}\}$  and with initial condition  $\bar{e}(0) := (e^T(0) \ e^T(s_{-1}) \ e^T(s_{-2}) \ \dots \ e^T(s_{-\bar{d}-\bar{\delta}}))^T$ .

Analogously, the generic form (6.10) for sampled-data systems is, for this extended case, given by

$$\dot{z}(t) = Az(t) + B_1 z(s_j) + B_2 w(t) \quad \text{for } t \in [s_k + t_j^k, s_k + t_{j+1}^k), \quad (6.30)$$

with  $t_j^k$  defined in Lemma 3.4.1 for  $j \in \{k - \bar{d} - \bar{\delta}, \dots, k - \underline{d}\}$  and initial condition  $\bar{z}(0) := (z^T(0) \ z^T(s_{-1}) \ z^T(s_{-2}) \ \dots \ z^T(s_{-\bar{d}-\bar{\delta}}))^T$ .

### 6.2.2 Input-to-state stability

To prove ISS of system (6.30), (6.25) over all admissible sequences of sampling instants, delays, and packet dropouts  $\sigma \in \mathcal{S}$ , the relation (6.11) should hold for functions  $\beta$  and  $\gamma$  that are independent of the choice of the sequence  $\sigma \in \mathcal{S}$ . Recall that it holds that  $\sigma := \{(s_k, \tau_k, m_k)\}_{k \in \mathbb{N}} \in \mathcal{S}$ , with  $\mathcal{S}$  defined in (3.20) as

$$\mathcal{S} := \left\{ \{(s_k, \tau_k, m_k)\}_{k \in \mathbb{N}} : h_{\min} \leq s_{k+1} - s_k \leq h_{\max}, \tau_{\min} \leq \tau_k \leq \tau_{\max}, \sum_{v=k-\bar{\delta}}^k m_v \leq \bar{\delta}, \forall k \in \mathbb{N} \right\}. \quad (6.31)$$

Similar to the previous section, ISS conditions of (6.30), (6.25) will be proven based on a preliminary analysis of the discretized NCS model. The exact discretization of (6.30), (6.25) for sequences of sampling instants, time-delays, and packet dropouts  $\sigma \in \mathcal{S}$  at the sampling instants  $s_k$  can be derived similar to the discrete-time NCS model (3.23), which results in the following discrete-time system:

$$z_{k+1} = e^{Ah_k} z_k + \sum_{j=k-\bar{d}-\bar{\delta}}^{k-\underline{d}} \int_{h_k-t_{j+1}^k}^{h_k-t_j^k} e^{As} ds B_1 z_j + \bar{w}_k, \quad (6.32)$$

where  $\bar{w}_k := \int_0^{h_k} e^{As} B_2 w(h_k + s_k - s) ds$ . Note that the extended state for the system (6.32) is defined by  $\psi_k := (z_k^T \ z_{k-1}^T \ \dots \ z_{k-\bar{d}-\bar{\delta}}^T)^T$ , similar to the definition in  $\chi_k$  in (4.43). The discrete-time state-space model in terms of this extended state is given by:

$$\psi_{k+1} = \tilde{A}(\mathbf{t}^k, h_k) \psi_k + \tilde{B} \bar{w}_k, \quad (6.33)$$

where  $\psi_k \in \mathbb{R}^{(1+\bar{d}+\bar{\delta})n}$ ,  $\mathbf{t}^k = (t_{k-\bar{d}-\bar{\delta}+1}^k, \dots, t_{k-\underline{d}}^k)$ ,  $t_j^k \in [t_{j,\min}^k, t_{j,\max}^k]$  for  $k - \bar{d} - \bar{\delta} + 1 \leq j \leq k - \underline{d}$ ,  $h_k \in [h_{\min}, h_{\max}]$ ,

$$\tilde{A}(\mathbf{t}^k, h_k) = \begin{pmatrix} e^{Ah_k} + \tilde{N}_0 & \tilde{N}_1 & \tilde{N}_2 & \dots & \tilde{N}_{\bar{d}+\bar{\delta}} \\ I & 0 & 0 & \dots & 0 \\ 0 & I & 0 & \dots & 0 \\ \vdots & \vdots & \ddots & & \vdots \\ 0 & 0 & & I & 0 \end{pmatrix}, \quad \tilde{B} = \begin{pmatrix} I \\ 0 \end{pmatrix}, \quad (6.34)$$



$$\tilde{N}_\rho = \begin{cases} \int_{h_k - t_{k-\rho+1}^k}^{h_k - t_{k-\rho}^k} e^{As} ds B_1 & \text{if } \rho \geq \underline{d} \\ 0 & \text{if } \rho < \underline{d}, \end{cases} \quad (6.35)$$

for  $\rho \in \{0, 1, \dots, \bar{d} + \bar{\delta}\}$  and  $t_{k-\rho}^k$  defined in (6.25) with  $j = k - \rho$ . The relation between  $z_k$  and  $\psi_k$  that we will need later is given by  $z_k = C_z \psi_k$ , with  $C_z = (I \ 0 \ \dots \ 0)$  being an  $n \times (\bar{d} + \bar{\delta} + 1)n$ -matrix.

The representation of (6.34) based on the Jordan form of the continuous-time system matrix  $A$  is given by:

$$\begin{aligned} \psi_{k+1} &= F(\mathbf{t}^k, h_k) \psi_k + \tilde{B} \bar{w}_k, \text{ with } \mathbf{t}^k = (t_{k-\bar{d}-\bar{\delta}+1}^k, \dots, t_{k-\underline{d}}^k), \\ t_j^k &\in [t_{j,\min}^k, t_{j,\max}^k], \ k - \bar{d} - \bar{\delta} + 1 \leq j \leq k - \underline{d}, \ h_k \in [h_{\min}, h_{\max}], \end{aligned} \quad (6.36)$$

$F(\mathbf{t}^k, h_k) = F_0 + \sum_{i=1}^{\zeta} \alpha_i(t_j^k, h_k) F_i$  and the matrices  $F_0, F_i, i = 1, 2, \dots, \zeta$ , given by:

$$\begin{aligned} F_0 &= \begin{pmatrix} \hat{\Theta} & Q\Theta_1 Q^{-1} B_1 & \dots & Q\Theta_{\bar{d}+\bar{\delta}-1} Q^{-1} B_1 & Q\Theta_{\bar{d}+\bar{\delta}} Q^{-1} B_1 \\ I & 0 & \dots & 0 & 0 \\ 0 & I & & 0 & 0 \\ \vdots & \vdots & \ddots & & \vdots \\ 0 & 0 & & I & 0 \end{pmatrix}, \\ F_i &= \begin{pmatrix} \hat{\Gamma} & Q\Gamma_{1,i} Q^{-1} B_1 & Q\Gamma_{2,i} Q^{-1} B_1 & \dots & Q\Gamma_{\bar{d}+\bar{\delta},i} Q^{-1} B_1 \\ 0 & 0 & 0 & \dots & 0 \\ \vdots & \vdots & \vdots & & \vdots \\ 0 & 0 & 0 & \dots & 0 \end{pmatrix}, \end{aligned} \quad (6.37)$$

with  $\hat{\Theta} = Q\Theta_0 Q^{-1} + Q\Xi_0 Q^{-1} B_1$  and  $\hat{\Gamma} = Q\Gamma_{0,i} Q^{-1} + Q\Xi_i Q^{-1} B_1$ . The matrices  $\Theta_0, \Xi_0, \Theta_{\hat{i}}, \hat{i} = 1, 2, \dots, \bar{d} + \bar{\delta}, \Gamma_{0,i}, \Gamma_{\hat{i},i}, \hat{i} = 1, 2, \dots, \bar{d} + \bar{\delta}$ , and  $\Xi_i, i = 1, 2, \dots, \zeta$ , are equal to their definitions in Appendix B.3. The matrices  $F_0$  and  $F_i$  in (6.37) are a combination of the matrices  $F_0, F_i, G_0$ , and  $G_i, i = 1, 2, \dots, \zeta$ , in Appendix B.3. Moreover, the matrices  $F(t_j^k, h_k)$  in (6.36) form an infinite set of matrices  $\mathcal{F}$ , analogous to (4.34):

$$\mathcal{F} = \left\{ F(\mathbf{t}^k, h_k) : \mathbf{t}^k = (t_{k-\bar{d}-\bar{\delta}+1}^k, \dots, t_{k-\underline{d}}^k), \ t_j^k \in [t_{j,\min}^k, t_{j,\max}^k], \right. \\ \left. k - \bar{d} - \bar{\delta} + 1 \leq j \leq k - \underline{d}, \ h_k \in [h_{\min}, h_{\max}] \right\}.$$

Stability of this system can be guaranteed based on Theorem 4.4.4 if the matrix  $P \in \mathbb{R}^{(n+(\bar{d}+\bar{\delta})m) \times (n+(\bar{d}+\bar{\delta})m)}$  is replaced by  $P \in \mathbb{R}^{(\bar{d}+\bar{\delta}+1)n \times (\bar{d}+\bar{\delta}+1)n}$ . Moreover, the matrices  $H_{F,j}, j \in \{1, 2, \dots, 2^\zeta\}$ , are based on the matrices  $F_0$  and  $F_i, i = 1, 2, \dots, \zeta$ , defined in (6.37) and the matrices  $H_{G,j}, j \in \{1, 2, \dots, 2^\zeta\}$ , are equal to zero. Similar reasonings hold for Theorem 4.4.7.

The following lemma formulates sufficient LMI conditions for the ISS of (6.36), (6.37) (and equivalently for (6.33), (6.34), (6.35)).

**Lemma 6.2.1** *Consider the discrete-time NCS model (6.33), (6.34), (6.35) and its equivalent (6.36), (6.37) that is based on the Jordan form of  $A$ , both with sequences of sampling instants, delays, and packet dropouts  $\sigma \in \mathcal{S}$ , as defined in (6.31). Define the set of matrices  $\mathcal{H}_F$ :*

$$\mathcal{H}_F = \left\{ \bar{F}_0 + \sum_{i=1}^{\zeta} \delta_i \bar{F}_i : \delta_i \in \{0, 1\}, i = 1, 2, \dots, \zeta \right\}, \quad (6.38)$$

with  $\bar{F}_0 = F_0 + \sum_{i=1}^{\zeta} \underline{\alpha}_i F_i$ ,  $\bar{F}_i = (\bar{\alpha}_i - \underline{\alpha}_i) F_i$ ,

$$\begin{aligned} \bar{\alpha}_i &= \max_{t_j^k \in [t_{j,\min}^k, t_{j,\max}^k], h_k \in [h_{\min}, h_{\max}]} \alpha_i(t_j^k, h_k), \\ \underline{\alpha}_i &= \min_{t_j^k \in [t_{j,\min}^k, t_{j,\max}^k], h_k \in [h_{\min}, h_{\max}]} \alpha_i(t_j^k, h_k), \end{aligned}$$

and  $F_0, F_i$ , for  $i = 1, 2, \dots, \zeta$ , defined in (6.37).

If there exist a symmetric matrix  $P \in \mathbb{R}^{(\bar{d}+\bar{\delta}+1)n \times (\bar{d}+\bar{\delta}+1)n}$  and scalars  $0 < \gamma < 1$  and  $\kappa > 0$  such that the following matrix inequalities are satisfied:

$$\begin{aligned} P &= P^T > 0 \\ \begin{pmatrix} H_{F,j}^T P H_{F,j} - (1 - \gamma)P & H_{F,j}^T P \tilde{B} \\ \tilde{B}^T P H_{F,j} & \tilde{B}^T P \tilde{B} - \kappa I \end{pmatrix} &< 0, \forall H_{F,j} \in \mathcal{H}_F, j \in \{1, 2, \dots, 2\zeta\}, \end{aligned} \quad (6.39)$$

then the discrete-time NCS model (6.33), (6.34), (6.35) is ISS with respect to the input  $\bar{w}_k$ .

**Proof** The proof can be derived analogously to the proof of Lemma 6.1.1 in Appendix A.12.  $\square$

Before the ISS of the continuous-time system (6.30), (6.25) is derived, we present a lemma that gives the upper bound on the intersample behavior of (6.30), (6.25).

**Lemma 6.2.2** *The upper bound on the intersample behavior of (6.30), (6.25) denoted by  $z(s_k + \tilde{t})$  with  $\tilde{t} \in [0, h_k)$ , is given by:*

$$\begin{aligned} |z(s_k + \tilde{t})| &\leq c_0 |z_k| + c_1 |z_{k-1}| + c_2 |z_{k-2}| + \dots + c_{\bar{d}+\bar{\delta}} |z_{k-\bar{d}-\bar{\delta}}| \\ &\quad + c_w \sup_{s_k \leq s < s_{k+1}} |w(s)|, \quad \text{for } \tilde{t} \in [0, h_k), \end{aligned} \quad (6.40)$$

with

$$c_0 = \begin{cases} \max(\bar{c}_0, \tilde{c}_0 + \hat{c}_0) & \text{if } \underline{d} = 0 \\ \max(e^{\lambda_{\max} h_{\max}}, 1) & \text{if } \underline{d} > 0 \end{cases} \quad (6.41)$$

$$\begin{aligned}
\bar{c}_0 &= \begin{cases} \max(e^{\lambda_{\max}\tau_{\max}}, 1) & \text{if } \bar{\delta} = 0 \text{ and } \tau_{\max} < h_{\max} \\ \max(e^{\lambda_{\max}h_{\max}}, 1) & \text{if } (\bar{\delta} = 0 \text{ and } \tau_{\max} \geq h_{\max}) \text{ or } (\bar{\delta} > 0) \end{cases} \\
\tilde{c}_0 &= \begin{cases} \max(e^{\lambda_{\max}h_{\max}}, e^{\lambda_{\max}\tau_{\min}}) & \text{if } \lambda_{\max} \neq 0 \\ 1 & \text{if } \lambda_{\max} = 0 \end{cases} \\
\hat{c}_0 &= \|B_1\| \begin{cases} \frac{e^{\lambda_{\max}(h_{\max}-\tau_{\min})}-1}{\lambda_{\max}} & \text{if } \lambda_{\max} \neq 0 \\ (h_{\max} - \tau_{\min}) & \text{if } \lambda_{\max} = 0 \end{cases}
\end{aligned} \tag{6.42}$$

$c_\rho$ , for  $\rho \in \{1, 2, \dots, \bar{d} + \bar{\delta} - 1\}$ :

$$c_\rho = \|B_1\| \begin{cases} \frac{e^{\lambda_{\max}(h_{\max}-(\tau_{\min}-\underline{d}h_{\max}))}-1}{\lambda_{\max}} & \text{if } \lambda_{\max} \neq 0 \text{ and } \rho = \underline{d} \text{ and } \underline{d} > 0 \\ \frac{e^{\lambda_{\max}h_{\max}}-1}{\lambda_{\max}} & \text{if } \lambda_{\max} \neq 0 \text{ and } \rho > \underline{d} \\ \min(\tau_{\max}^*, h_{\max}) & \text{if } \lambda_{\max} = 0 \text{ and } \rho \in \{\bar{\delta} + \underline{d} + 1, \dots, \bar{d} + \bar{\delta} - 1\} \\ (h_{\max} - (\tau_{\min} - \underline{d}h_{\max})) & \text{if } \lambda_{\max} = 0 \text{ and } \rho = \underline{d} \text{ and } \underline{d} > 0 \\ h_{\max} & \text{if } \lambda_{\max} = 0 \text{ and } \rho \in \{\underline{d} + 1, \dots, \bar{\delta} + \underline{d}\} \\ 0 & \text{if } \rho < \underline{d}, \end{cases} \tag{6.43}$$

with  $\tau_{\max}^* = \tau_{\max} - (\rho - \bar{\delta} - 1)h_{\min}$  and

$$c_{\bar{d}+\bar{\delta}} = \|B_1\| \begin{cases} \frac{e^{\lambda_{\max}h_{\max}}-1}{\lambda_{\max}} & \text{if } \lambda_{\max} \neq 0 \\ (\tau_{\max} - (\bar{d} - 1)h_{\min}) & \text{if } \lambda_{\max} = 0, \end{cases} \tag{6.44}$$

$$c_w = \|B_2\| \begin{cases} \frac{e^{\lambda_{\max}h_{\max}}-1}{\lambda_{\max}} & \text{if } \lambda_{\max} \neq 0 \\ h_{\max} & \text{if } \lambda_{\max} = 0. \end{cases} \tag{6.45}$$

**Proof** The proof is given in Appendix A.14.  $\square$

Let us now present the result on the input-to-state stability of the continuous-time dynamics (6.30), (6.25).

**Theorem 6.2.3** Consider the sampled-data system (6.30), (6.25), with sequences of sampling instants, delays, and packet dropouts  $\sigma \in \mathcal{S}$ . Suppose there exist a matrix  $P$  and scalars  $0 < \gamma < 1$  and  $\kappa > 0$  for which (6.39) is satisfied. Then, the system (6.30), (6.25) is uniformly input-to-state stable (ISS) for  $\sigma \in \mathcal{S}$  with respect to the time-varying input  $w(t)$ . The functions  $\beta$  and  $\gamma$  in (6.11) can be obtained from

$$\begin{aligned}
\bar{\beta}(|\bar{z}(0)|, t) &= \\
|\bar{z}(0)| &\begin{cases} \max\{g_{1,0}, g_{1,1}, g_{1,2}, \dots, g_{1,\bar{d}+\bar{\delta}+1}\} & \text{for } t \in [0, s_{\bar{d}+\bar{\delta}+1}), \\ g_{1,k} & \text{for } t \in [s_k, s_{k+1}), \quad k \geq \bar{d} + \bar{\delta} + 1, \end{cases} \\
\gamma(\sup_{0 \leq s \leq t} |w(s)|) &= g_2 \sup_{0 \leq s \leq t} |w(s)|,
\end{aligned} \tag{6.46}$$

with

$$\begin{aligned}
g_{1,0} &= c_0 + c_1 + c_2 + \dots + c_{\bar{d}+\bar{\delta}}, \\
g_{1,1} &= c_0 \|C_z P^{-\frac{1}{2}}\| \sqrt{\bar{\gamma} \lambda_{\max}(P)} + c_1 + \dots + c_{\bar{d}+\bar{\delta}}, \\
&\vdots \\
g_{1,\bar{d}+\bar{\delta}} &= \|C_z P^{-\frac{1}{2}}\| \left( c_0 \sqrt{\bar{\gamma}^k \lambda_{\max}(P)} + c_1 \sqrt{\bar{\gamma}^{k-1} \lambda_{\max}(P)} + \dots \right. \\
&\quad \left. + c_{\bar{d}+\bar{\delta}-1} \sqrt{\bar{\gamma} \lambda_{\max}(P)} \right) + c_{\bar{d}+\bar{\delta}}, \\
g_{1,k} &= \|C_z P^{-\frac{1}{2}}\| \left( c_0 \sqrt{\bar{\gamma}^k \lambda_{\max}(P)} + c_1 \sqrt{\bar{\gamma}^{k-1} \lambda_{\max}(P)} + \dots \right. \\
&\quad \left. + c_{\bar{d}+\bar{\delta}} \sqrt{\bar{\gamma}^{k-\bar{d}-\bar{\delta}} \lambda_{\max}(P)} \right), \quad k \geq \bar{d} + \bar{\delta} + 1, \\
g_2 &= c_w \left( 1 + (c_0 + c_1 + \dots + c_{\bar{d}+\bar{\delta}}) \|C_z P^{-\frac{1}{2}}\| \sqrt{\frac{\kappa}{\gamma}} \right),
\end{aligned} \tag{6.47}$$

$c_0, c_1, \dots, c_{\bar{d}+\bar{\delta}}$  defined in (6.41), (6.42), (6.43), (6.44),  $c_w$  defined in (6.45), and  $\bar{\gamma} = 1 - \gamma$ .

**Proof** For the proof, see Appendix A.15.  $\square$

Note that  $\bar{\beta}(s, t)$  satisfies all the conditions of a class- $\mathcal{KL}$  function except that for fixed  $s$  it is only non-increasing and not continuous everywhere, because for  $s_0 \leq t < s_{\bar{d}+\bar{\delta}+1}$  and  $s_k \leq t < s_{k+1}$ ,  $\forall k \geq \bar{d} + \bar{\delta} + 1$  the function  $\bar{\beta}(s, t)$  is flat and it decreases at  $t = s_k$ ,  $\forall k \geq \bar{d} + \bar{\delta} + 2$ . However, it is easy to construct a  $\beta(s, t) \in \mathcal{KL}$  from  $\bar{\beta}(s, t)$ . The function  $\gamma(\sup_{0 \leq s \leq t} |w(s)|)$  belongs to the class  $\mathcal{K}$ , thus inequality (6.11) is satisfied.

Theorem 6.2.3 implies that the state  $z$  of the sampled-data system is globally uniformly ultimately bounded and that the asymptotic bound is given by  $\limsup_{t \rightarrow \infty} |z(t)| \leq g_2 \sup_{t \geq 0} |w(t)|$ , with  $g_2$  as in (6.47).

**Remark 6.2.4** Analogous to the small delay case, an asymptotic bound for the state at the sampling instants can directly be derived from (A.108) and the fact that  $\lim_{k \rightarrow \infty} D_k = 1/\gamma$ . This results in exactly the same relation as for the small delay case, given in (6.23).

The ISS-conditions obtained in this section depend explicitly on the values of  $h_{\min}$  and  $\tau_{\min}$ . The ISS-conditions proposed in [74], [111] for the model based on delay impulsive differential equations do not explicitly depend on the values of  $h_{\min}$  and  $\tau_{\min}$ . Consequently, the latter approach towards modeling NCSs may result in more conservative conditions in comparison to those obtained using the discrete-time approach as proposed in this thesis, when  $0 \ll h_{\min} \simeq h_{\max}$  or  $0 \ll \tau_{\min} \simeq \tau_{\max}$ . A comparison between the approach described in [74] and the approach of Theorems 6.1.2 and 6.2.3 will be given in Section 6.4, based on the motor-roller example.

### 6.3 Tracking control performance

The results in Theorem 6.1.2 and Theorem 6.2.3 on the ISS property of NCSs (or equivalently sampled-data systems) can directly be used in the scope of the tracking problem of NCSs as stated in Sections 6.1.1 and 6.2.1. Namely, when applied to the tracking error dynamics (6.9) for the small delay case and (6.29) for the case with time-varying sampling intervals, large delays, and packet dropouts, the satisfaction of the conditions of Theorems 6.1.2 and 6.2.3 guarantees that the approximate tracking problem is solved and an ultimate bound on the tracking error can be provided. In Section 6.3.1, a bound on  $|\Delta u^{ff}(t)|$ , i.e.  $\sup_{t \in \mathbb{R}} |\Delta u^{ff}(t)|$ , based on the properties of the exact feedforward  $\Delta u_e^{ff}(t)$ ,  $\tau_{\min}$ ,  $\tau_{\max}$ ,  $h_{\min}$ ,  $h_{\max}$ , and  $\bar{\delta}$  is provided. Using this knowledge, the results of the previous section are used to solve the approximate tracking problem and to explicitly construct the bound on the tracking error in Section 6.3.2.

#### 6.3.1 Feedforward error

In Section 6.1.2, it is shown that the ultimate bound on the tracking error depends linearly on the bound on the feedforward error. Let us therefore study how the feedforward error depends on the properties of the exact feedforward, the network delays, the packet dropouts, and the sampling intervals.

For the sake of simplicity, we start with the small delay case. Each scalar component of the exact feedforward  $u_e^{ff}(t)$  is denoted by  $u_{e,i}^{ff}(t)$ ,  $i = 1, \dots, m$ . In the time interval  $t \in [s_k + \tau_k, s_{k+1} + \tau_{k+1})$ , the delayed zero-order hold feedforward signal is given by  $u^{ff}(t) = u_e^{ff}(s_k)$ . Consequently, each component of the feedforward error  $\Delta u_i^{ff}(t)$  in this time interval satisfies:

$$\Delta u_i^{ff}(t) = u_{e,i}^{ff}(s_k) - u_{e,i}^{ff}(t) \quad \forall t \in [s_k + \tau_k, s_{k+1} + \tau_{k+1}), \quad (6.48)$$

$i = 1, \dots, m$ , analogous to (6.7). Using the mean value theorem, we can write

$$\Delta u_i^{ff}(t) = u_{e,i}^{ff}(s_k) - u_{e,i}^{ff}(t) = \frac{\partial u_{e,i}^{ff}}{\partial t} \Big|_{t^*} (s_k - t), \quad (6.49)$$

$$\Rightarrow |\Delta u_i^{ff}(t)| \leq \vartheta_{1,i} |s_k - t|, \quad \forall t \in [s_k + \tau_k, s_{k+1} + \tau_{k+1}),$$

with  $t^* \in [s_k, t]$ , since  $t \geq s_k$  and

$$\vartheta_{1,i} = \sup_{t \in \mathbb{R}} \left| \frac{du_{e,i}^{ff}(t)}{dt} \right|, \quad i = 1, \dots, m. \quad (6.50)$$

Note that such  $\vartheta_{1,i}$ ,  $i = 1, \dots, m$ , are well-defined due to the assumption that  $\dot{x}_d(t)$  is at least  $\mathcal{C}^2$ , guaranteeing that  $u_e^{ff}(t)$  is at least  $\mathcal{C}^1$ . Moreover,  $\vartheta_{1,i}$ ,  $i = 1, \dots, m$  is a bounded value.

Based on (6.49), we can provide the following bound for each component of the feedforward error on  $\mathbb{R}$ :

$$\begin{aligned}
|\Delta u_i^{ff}(t)| &\leq \vartheta_{1,i} \max(|\tau_k + h|), \quad i \in \{1, \dots, m\}, \quad \forall t \in \mathbb{R}, \\
\Rightarrow |\Delta u_i^{ff}(t)| &\leq \vartheta_{1,i}(\tau_{\max} + h) =: R_{0,i}, \quad i \in \{1, \dots, m\}, \quad \forall t \in \mathbb{R}. \\
\Rightarrow |\Delta u^{ff}(t)| &\leq \sqrt{\sum_{i=1}^m R_{0,i}^2} =: R_0, \quad \forall t \in \mathbb{R}.
\end{aligned} \tag{6.51}$$

For the case with time-varying sampling intervals, large delays, and packet dropouts the definition of the feedforward error can be derived analogously. The duration of the feedforward signal  $u^{ff}(t) = u_e^{ff}(s_k)$  is more complicated to derive than in the small delay case, because it is possible that  $u_e^{ff}(s_k)$  or the next feedforward signal  $u_e^{ff}(s_{k+1})$  is not implemented due to packet dropout or message rejection. Because we are interested in an upper bound of the feedforward signal, we will consider the worst case scenario. Then, the longest duration of the feedforward signal  $u_e^{ff}(s_k)$  needs to be considered, because this results in the largest feedforward error. Note that if  $u_e^{ff}(s_k)$  is not implemented, an older feedforward signal, e.g.  $u_e^{ff}(s_{k-1})$  is active until the next input is implemented, resulting in the fact that  $\Delta u_e^{ff}(s_{k-1})$  needs to be considered instead of  $\Delta u_e^{ff}(s_k)$ . The longest period during which  $u^{ff}(t) = u_e^{ff}(s_k)$  may hold, is given by  $t \in [s_k + \tau_k, s_{k+\bar{\delta}+1} + \tau_{k+\bar{\delta}+1})$ , which includes the maximum number of packet dropouts after  $t = s_k$ . Note that in the case of message rejection it is possible that  $s_{k+\bar{\delta}+1} + \tau_{k+\bar{\delta}+1} > s_{k+\bar{\delta}+2} + \tau_{k+\bar{\delta}+2}$ , but then still  $s_{k+\bar{\delta}+1} + \tau_{k+\bar{\delta}+1}$  needs to be considered to derive the upper bound on the feedforward error, because it represents the worst case situation. Based on this worst case duration of the control signal, the feedforward error  $\Delta u^{ff}(t)$  will be derived.

Analogously to the small delay case, each component of the feedforward error  $\Delta u_i^{ff}(t)$  satisfies:

$$\Delta u_i^{ff}(t) = u_{e,i}^{ff}(s_k) - u_{e,i}^{ff}(t) \quad \forall t \in [s_k + \tau_k, s_{k+\bar{\delta}+1} + \tau_{k+\bar{\delta}+1}), \tag{6.52}$$

$i = 1, \dots, m$ , analogous to (6.48) and (6.7). Using the mean value theorem, we can derive

$$|\Delta u_i^{ff}(t)| \leq \vartheta_{1,i} |s_k - t|, \quad \forall t \in [s_k + \tau_k, s_{k+\bar{\delta}+1} + \tau_{k+\bar{\delta}+1}), \tag{6.53}$$

with  $t^* \in [s_k, t]$ , since  $t \geq s_k$ , and

$$\vartheta_{1,i} = \sup_{t \in \mathbb{R}} \left| \frac{\partial u_{e,i}^{ff}(t)}{\partial t} \right|, \quad i = 1, \dots, m, \tag{6.54}$$

where  $\vartheta_{1,i}$ ,  $i = 1, 2, \dots, m$ , is bounded. Analogous to (6.51) and based on (6.53), the bound for each component of the feedforward error on  $\mathbb{R}$ , dependent on the

network properties, such as delays, time-varying sampling interval, and packet dropouts, is given by:

$$\begin{aligned}
|\Delta u_i^{ff}(t)| &\leq \vartheta_{1,i} \max(\tau_k + (\bar{\delta} + 1)h_k), \quad i \in \{1, \dots, m\}, \quad \forall t \in \mathbb{R}, \\
\Rightarrow |\Delta u_i^{ff}(t)| &\leq \vartheta_{1,i}(\tau_{\max} + (\bar{\delta} + 1)h_{\max}) =: \bar{R}_{0,i}, \quad i \in \{1, \dots, m\}, \quad \forall t \in \mathbb{R}. \\
\Rightarrow |\Delta u^{ff}(t)| &\leq \sqrt{\sum_{i=1}^m \bar{R}_{0,i}^2} =: \bar{R}_0, \quad \forall t \in \mathbb{R}.
\end{aligned} \tag{6.55}$$

Note that (6.51) can be retrieved from (6.55) by considering  $\bar{\delta} = 0$  and  $h_{\max} = h$ .

### 6.3.2 Solution to the approximate tracking problem

Let us now state the following corollary, based on Theorem 6.2.3 and the bound on the feedforward error defined in the previous section, on the steady-state tracking performance achieved by applying the tracking controller (6.4), and  $u_e^{ff}(t)$  satisfying (6.2), to the NCS (6.24), for time-varying sampling intervals, packet dropouts, and delays that may be larger than the sampling interval.

**Corollary 6.3.1 (Tracking error)** *Consider the NCS (6.24), with sequences of sampling instants, delays, and packet dropouts  $\sigma \in \mathcal{S}$  and  $\mathcal{S}$  defined by (6.31). Moreover, consider the controller (6.4) and  $u_e^{ff}(t)$  satisfying (6.2). If the LMIs (6.39) are feasible, with  $B_1 = -BK$  and  $B_2 = B$ , then the tracking error dynamics (6.29) is uniformly input-to-state stable (ISS) with respect to the feedforward error  $\Delta u^{ff}(t)$  over the class  $\mathcal{S}$  of sampling-delay-packet dropouts sequences (6.31). Moreover, the tracking error is globally uniformly ultimately bounded with the asymptotic bound computed from  $\limsup_{t \geq 0} |e(t)| \leq g_2 \bar{R}_0$ , with  $g_2$  given in (6.47) and  $\bar{R}_0$  given in (6.55).*

Note that this corollary is also valid for the small delay case, where the LMI conditions in (6.39) are replaced by the LMI conditions (6.20). Then, the parameters  $\bar{R}_0$  and  $g_2$  in Corollary 6.3.1 need to be replaced by their definitions in (6.51) and (6.22), respectively.

## 6.4 Illustrative examples

The motor-roller example, as considered in (4.1) in Chapter 4, is used to illustrate the usefulness of the ISS conditions. In this example, a motor drives a roller that is used to transport a sheet of paper through the paper path of an industrial printer. In this section, we apply the proposed results on ISS to upper bound the steady-state tracking error. This information can be used to

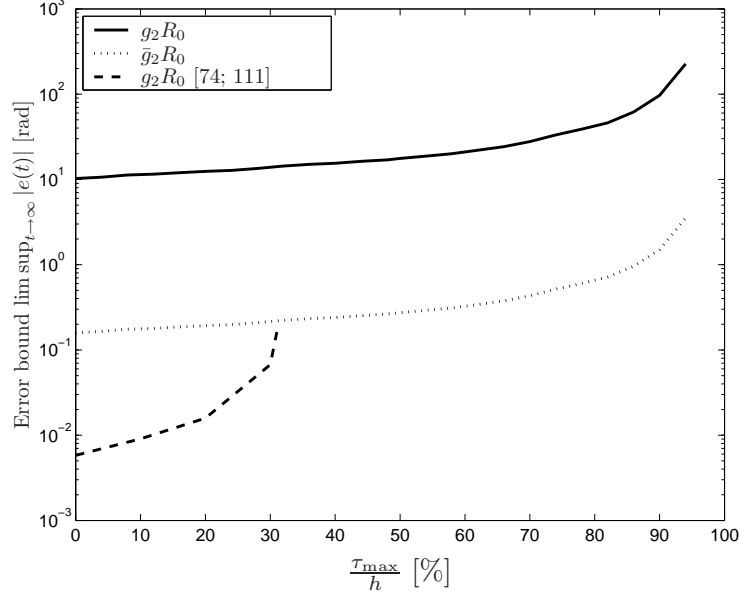


Figure 6.2: Tracking error bounds for a constant sampling interval  $h = 5 \times 10^{-3}s$  and time-varying and uncertain delays in the set  $[0, \tau_{\max}]$ .

derive requirements on e.g. the maximum sampling interval or the maximum delay allowed to guarantee a certain steady-state tracking performance.

Consider the motor-roller system, described by

$$\begin{aligned} \ddot{x}_s(t) &= \frac{nr_R}{J_M + n^2 J_R} u^*(t), \\ u^*(t) &= u_j, \text{ for } t \in [s_k + t_j^k, s_k + t_{j+1}^k), \end{aligned} \quad (6.56)$$

with  $t_j^k$  defined in (6.25), for  $j \in \{k - \bar{d} - \bar{\delta}, \dots, k - \underline{d}\}$ ,  $J_M = 1.95 \cdot 10^{-5} \text{kgm}^2$  the inertia of the motor,  $J_R = 6.5 \cdot 10^{-5} \text{kgm}^2$  the inertia of the roller,  $r_R = 14 \text{mm}$  the radius of the roller,  $n = 0.2$  the transmission ratio between motor and roller,  $x_s$  [m] the position of the sheet of paper, and  $u$  [Nm] the motor torque. Moreover, consider the control law (6.4), with  $\bar{K} = (50 \quad 1.18)$  and a harmonic desired trajectory:  $x_d(t) = (A_d \sin(\omega t) \quad A_d \omega \cos(\omega t))^T$ , with  $A_d = 0.01$  and  $\omega = 2\pi$ . The exact feedforward is given by  $u_e^{ff}(t) = -\frac{A_d \omega^2}{b} \sin(\omega t)$ , with  $b = \frac{nr_R}{J_M + n^2 J_R}$ .

Consider first the case of a constant sampling interval, but with time-varying and uncertain delays in the set  $[0, \tau_{\max}]$ . Figure 6.2 depicts the error bounds as provided in Corollary 6.3.1 for  $\tau_{\max} \leq h$  and the error bound obtained with the delay impulsive differential model in [74; 111]. Note that for the discrete-time modeling approach also the bound for the tracking error at the sampling times  $s_k$  ( $\bar{g}_2 R_0$ ) is included by means of the dotted line. Figure 6.2



shows that by using the discrete-time approach, ISS can be guaranteed up to  $\tau_{\max} = 0.94h$ , but using the delay impulsive approach ISS can only be guaranteed up to  $\tau_{\max} = 0.33h$ . So, the discrete-time approach allows to prove ISS for a larger range of delays. However, the delay impulsive modeling/analysis approach provides much tighter (ISS) bounds on the tracking error (note that the scale of the vertical axis is logarithmic). Note that the overestimation of the bound on the tracking error for the discrete-time modeling approach is significantly worsened due to upperbounding the intersample behavior (compare the solid and dotted lines in Figure 6.2).

Next, the case in which the sampling interval is variable, i.e.  $h \in [h_{\min}, h_{\max}]$ , and the delay is zero is considered. Figure 6.3 depicts the error bounds as provided in Corollary 6.3.1 and the error bound obtained with the delay impulsive differential model in [74; 111]. Note that, in this example,  $h_{\min} = h_{\max}/1.5$ , so  $h_{\min} \neq 0$  is used. Using the discrete-time modeling approach, ISS almost up to  $h_{\max} = 1.34 \times 10^{-2}\text{s}$ , which is the sampling interval for which the system with a constant sampling interval (and no delay) becomes unstable (see the dashed vertical line in Figure 6.3) can be assured. This fact shows that the proposed ISS conditions are not conservative from a stability perspective. Using the delay impulsive modeling approach, ISS can only be guaranteed up to  $h_{\max} = 9 \times 10^{-3}\text{s}$ . However, the delay impulsive approach clearly provides significantly less conservative bounds on the tracking error. Moreover, Figure 6.3 shows that the bounds on the tracking error increases progressively for increasing  $h_{\max}$  (and  $h_{\min}$ ). This increase is due to, firstly, the fact that the ISS gain  $g_2$  increases for increasing  $h_{\max}$  and, secondly, the fact that the bound on the feedforward error  $\bar{R}_0$  in (6.55) increases for increasing  $h_{\max}$ . This type of plot is instrumental in determining an upper bound on the maximum sampling interval needed to guarantee a minimum level of steady-state tracking performance.

Comparing the two modeling approaches and related ISS results in this example, it is concluded that the discrete-time modeling approach seems to allow to prove ISS for larger ranges of sampling intervals and delays, whereas the delay impulsive modeling approach clearly provides much tighter (ISS) bounds on the tracking error.

## 6.5 Discussion

In this chapter, a solution to the approximate tracking problem of NCSs (or, more general, sampled-data systems) with uncertain, time-varying sampling intervals, packet dropouts, and delays that are allowed to be larger than the sampling interval is presented. The uncertain, time-varying sampling intervals, network delays, and zero-order hold cause an inexact feedforward, which induces a perturbation on the tracking error dynamics. Sufficient conditions in terms of LMIs for the input-to-state stability (ISS) of the tracking error dynamics with respect to this perturbation are given. Note that the LMIs are an adaptation of the stability analysis LMIs as derived in Chapter 4. These ISS results provide bounds on the steady-state tracking error as a function of the plant properties,

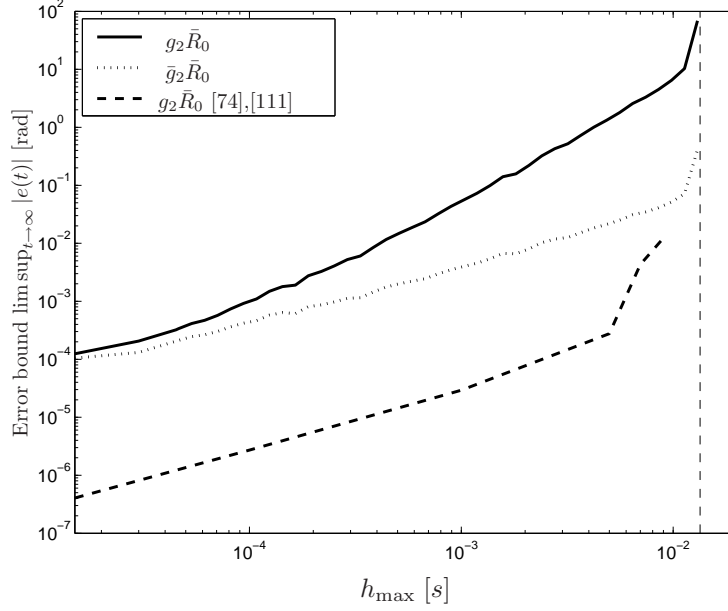


Figure 6.3: Tracking error bounds for variable sampling intervals  $h \in [h_{\min}, h_{\max}]$  and no delays, where  $h_{\max} = 1.5h_{\min}$ .

the control design, and the network properties. Such error bounds can readily be used to formulate design rules regarding the maximum sampling interval, the maximum delay, or the maximum number of packet dropouts allowed to guarantee a certain steady-state tracking performance.

The results are illustrated on a mechanical motion control example showing the effectiveness of the proposed strategy and providing insight in the differences and commonalities between the discrete-time modeling approach and a modeling approach that is based on delay impulsive differential equations, as described in [74; 111]. More specifically, in the presented motion control example, our discrete-time modeling approach allows to prove ISS (and thus a bounded tracking error) for larger ranges of sampling intervals and delays. On the other hand, the delay impulsive modeling approach provides much tighter (ISS) bounds (and therewith tighter bounds on the tracking error).

## ***Experimental validation of the stability of NCSs with delays<sup>1</sup>***

---

7.1 NCS model 7.2 Stability 7.3 The experimental set-up	7.4 Experimental results 7.5 Discussion
---	--

---

This chapter presents a comparison between theoretical and experimental results on the stability and transient performance of NCSs with time-delays that are either constant or time-varying. These delays are allowed to be larger than the *constant* sampling interval, and packet dropouts are not considered. The experimental study is performed on two typical motion control examples: a single inertia system and a motor-load system. Firstly, the single inertia system is used for validation of the stability region for constant delays. This region, e.g. presented in [133], describes the stabilizing controller gains for different constant delays. Secondly, an experimental example, for the single inertia system, is presented showing that the time-varying nature of network delays (even below the sampling time) can induce closed-loop instability (as was previously indicated in theoretical studies in e.g. [118] and in the motivating example in Section 4.1). Thirdly, for both set-ups, validation of the results on the stability and transient performance of NCSs with uncertain, time-varying delays, as derived in Chapters 4 and 5 is performed.

The outline of this chapter is as follows. In Section 7.1, the discrete-time NCS representation of Chapter 3 is adapted for the output-feedback case, since in both setups the entire state cannot be measured. In Section 7.2, the stability conditions of Chapter 4 are adapted such that they are applicable for the output-feedback case. Moreover, stability conditions for both constant and periodic delays are discussed. The two experimental set-ups are introduced in Section 7.3 and measurements for the validation of both stability and transient performance results are presented in Section 7.4. Finally, in Section 7.5 a discussion on the obtained results is given.

### ***7.1 NCS model***

The NCS model, for the static output-feedback case can be obtained from the state-feedback case. Recall that the continuous-time NCS model for any control

---

<sup>1</sup>This chapter is based on [13].

input and for time-varying delays larger than the constant sampling interval and no packet dropouts is given by (3.6):

$$\begin{aligned} \dot{x}(t) &= Ax(t) + Bu^*(t) \\ y(t) &= Cx(t) \\ u^*(t) &= u_j \text{ for } t \in [s_k + t_j^k, s_k + t_{j+1}^k), \end{aligned} \quad (7.1)$$

where  $t_j^k$  is defined, as in (3.7), by

$$t_j^k = \min \left\{ \max\{0, \tau_j - (k-j)h\}, \max\{0, \tau_{j+1} - (k-j-1)h\}, \dots, \max\{0, \tau_{k-\underline{d}} - \underline{d}h\}, h \right\}, \quad (7.2)$$

with  $t_j^k \leq t_{j+1}^k$  and  $j \in [k - \bar{d}, k - \bar{d} + 1, \dots, k - \underline{d}]$ . Moreover,  $0 =: t_{k-\bar{d}}^k \leq t_{k-\bar{d}+1}^k \leq \dots \leq t_{k-\underline{d}}^k \leq t_{k-\underline{d}+1}^k := h$ . The corresponding discrete-time NCS model is given by (3.8), i.e.

$$\begin{aligned} x_{k+1} &= e^{Ah}x_k + \sum_{j=k-\bar{d}}^{k-\underline{d}} \int_{h-t_{j+1}^k}^{h-t_j^k} e^{As} ds Bu_j \\ y_k &= Cx_k, \end{aligned} \quad (7.3)$$

with  $t_j^k$  as defined in (7.2). To make the model of (7.3), in combination with a static output-feedback controller, suitable for the stability analysis, it is rewritten in the following state-space notation that includes the output  $y_k$ :

$$\eta_{k+1} = \bar{A}(\mathbf{t}^k)\eta_k + \bar{B}(\mathbf{t}^k)u_k, \quad (7.4)$$

with

$$\eta_k = (\xi_k^T \ y_{k-1}^T)^T = \begin{pmatrix} x_k^T & u_{k-1}^T & u_{k-2}^T & \dots & u_{k-\bar{d}}^T & y_{k-1}^T \end{pmatrix}^T, \quad (7.5)$$

$$\bar{A}(\mathbf{t}^k) = \begin{pmatrix} \tilde{A}(\mathbf{t}^k) & 0 \\ \tilde{C} & 0 \end{pmatrix}, \quad \bar{B}(\mathbf{t}^k) = \begin{pmatrix} \tilde{B}(\mathbf{t}^k) \\ 0 \end{pmatrix}, \quad (7.6)$$

where  $\tilde{A}(\mathbf{t}^k)$ ,  $\tilde{B}(\mathbf{t}^k)$ , and  $\tilde{C}$  are equal to their definitions in (3.9), which are

$$\tilde{A}(\mathbf{t}^k) = \begin{pmatrix} e^{Ah} & \tilde{M}_1 & \tilde{M}_2 & \dots & \tilde{M}_{\bar{d}} \\ 0 & 0 & 0 & \dots & 0 \\ 0 & I & 0 & \dots & 0 \\ \vdots & & \ddots & & \dots \\ 0 & \dots & 0 & I & 0 \end{pmatrix}, \quad \tilde{B}(\mathbf{t}^k) = \begin{pmatrix} \tilde{M}_0 \\ I \\ 0 \\ \vdots \\ 0 \end{pmatrix}, \quad (7.7)$$

$\tilde{C} = (C \ 0 \ \dots \ 0)$ , and

$$\tilde{M}_\rho = \begin{cases} \int_{h-t_{k-\rho+1}^k}^{h-t_{k-\rho}^k} e^{As} ds B & \text{if } \rho \geq \underline{d}, \\ 0 & \text{if } \rho < \underline{d}, \end{cases} \quad (7.8)$$

for  $\rho \in \{0, 1, \dots, \bar{d}\}$  and  $t_{k-\rho}^k$  defined in (7.2), with  $j = k - \rho$ . Finally,  $\mathbf{t}^k$  denotes the combination of the time-varying parameters, i.e.  $\mathbf{t}^k = (t_{k-\bar{d}+1}^k, \dots, t_{k-\underline{d}}^k)$ .

**Remark 7.1.1** Note that for constant delays  $\tau$ ,  $\bar{A}$  and  $\bar{B}$  are constant matrices and depend on the parameter  $\tau^* := \tau - (\bar{d} - 1)h$ , with  $\bar{d} = \lceil \frac{\tau}{h} \rceil$ . The matrices  $\tilde{M}_\rho$  in  $\bar{A}(\mathbf{t}^k)$  and  $\bar{B}(\mathbf{t}^k)$  are then given by:

$$\tilde{M}_\rho = \begin{cases} \int_0^{h-\tau^*} e^{As} ds B & \text{if } \rho = \bar{d} - 1, \\ \int_{h-\tau^*}^h e^{As} ds B & \text{if } \rho = \bar{d}, \\ 0 & \text{if } \rho < \bar{d} - 1, \end{cases} \quad (7.9)$$

for  $\bar{d} \geq 1$ . These adaptations result in exactly the same constant delay model that is presented in e.g. [4; 133].

## 7.2 Stability

In this section, the stability results for constant, periodic, and arbitrary varying time-delays for a NCS with output-feedback are derived. Consider the control law:

$$u_k = -K\eta_k = K_1 y_k - K_2 y_{k-1}, \quad (7.10)$$

with  $K = (-K_1 C \quad 0 \quad \dots \quad 0 \quad -K_2)$ . For constant time-delays, the stability of the NCS can be derived based on the eigenvalues of the controlled system  $\eta_{k+1} = \hat{A}\eta_k$ , with

$$\hat{A} = \bar{A} - \bar{B}K, \quad (7.11)$$

and  $\bar{A}$ ,  $\bar{B}$  defined in (7.6), (7.7), (7.9).

For periodic delays with a known sequence, the stability can be obtained based on the eigenvalues of the system matrices of the periodic system (i.e. the product of the matrices corresponding to the periodic repetition of the delays), see [31] for more details. Note that in Section 4.1 an example for the periodic delay sequence  $\tau_1, \tau_2, \tau_1, \tau_2, \dots$  is given.

For time-varying delays, Theorem 4.4.4 can be used if the system matrices are adapted such that system (7.4) is evaluated. Below, the adapted version of this theorem will be described. First, the discrete-time NCS representation (7.4) is rewritten based on the Jordan form of the continuous-time system matrix  $A$ . It holds that

$$\xi_{k+1} = \left( F_0 + \sum_{i=1}^{\beta} \alpha_i(t_j^k) F_i \right) \eta_k + \left( G_0 + \sum_{i=1}^{\beta} \alpha_i(t_j^k) G_i \right) u_k, \quad (7.12)$$

with  $\alpha_i(t_j^k)$ ,  $i = 1, 2, \dots, \beta$ , defined in Appendix B.4 by (B.38), (B.39), (B.40), and (B.41) if only  $\beta$  uncertain parameters are considered and  $h_k$  is replaced by  $h$ . The constant matrices  $F_0$ ,  $G_0$ ,  $F_i$ , and  $G_i$ ,  $i = 1, 2, \dots, \beta$ , are also

defined in Appendix B.4. Note that in (7.12) the parameter  $j$  takes values from  $j \in \{k - \bar{d} + 1, k - \bar{d} + 2, \dots, k - \underline{d}\}$ , because  $t_{k-\bar{d}}^k := 0$  and  $t_{k-\underline{d}+1}^k := h$ , as defined in Lemma 3.2.1.

To derive the stability conditions, similar to Theorems 4.3.1 and 4.4.4, where a common quadratic candidate Lyapunov function is used, the set of matrices  $\mathcal{FG}$  is redefined, such that the output dependent part  $\tilde{C}$  is included and the sampling interval is constant, as is the case in the experiments:

$$\mathcal{FG} = \left\{ \left( F(\mathbf{t}^k), G(\mathbf{t}^k) \right) : \mathbf{t}^k = (t_{k-\bar{d}+1}^k, \dots, t_{k-\underline{d}}^k), t_j^k \in [t_{j,\min}^k, t_{j,\max}^k], \right. \\ \left. k - \bar{d} < j \leq k - \underline{d} \right\},$$

with  $F(t_j^k) = F_0 + \sum_{i=1}^{\beta} \alpha_i(t_j^k) F_i$ ,  $G(t_j^k) = G_0 + \sum_{i=1}^{\beta} \alpha_i(t_j^k) G_i$ . Then, analogous to Theorem 4.4.4, Theorem 7.2.1 proposes conditions that guarantee the stability of the continuous-time and discrete-time closed-loop NCS model.

**Theorem 7.2.1** *Consider the continuous-time NCS model (7.1), (7.2) with delays  $\tau_k \in [\tau_{\min}, \tau_{\max}]$  and consider the corresponding discrete-time representation (7.4), (7.6), (7.7), (7.2), and its equivalent representation (7.12) that is based on the Jordan form of the continuous-time system matrix  $A$  of (7.1). Moreover, consider a known controller (7.10). Define the set of matrices  $\mathcal{H}_{FG}$ :*

$$\mathcal{H}_{FG} = \left\{ \left( \bar{F}_0 + \sum_{i=1}^{\beta} \delta_i \bar{F}_i, \bar{G}_0 + \sum_{i=1}^{\beta} \delta_i \bar{G}_i \right) : \delta_i \in \{0, 1\}, i = 1, 2, \dots, \beta \right\},$$

with  $\bar{F}_0 = F_0 + \sum_{i=1}^{\beta} \underline{\alpha}_i F_i$ ,  $\bar{F}_i = (\bar{\alpha}_i - \underline{\alpha}_i) F_i$ ,  $\bar{G}_0 = G_0 + \sum_{i=1}^{\beta} \underline{\alpha}_i G_i$ ,  $\bar{G}_i = (\bar{\alpha}_i - \underline{\alpha}_i) G_i$ , and  $\bar{\alpha}_i = \max_{t_j^k \in [t_{j,\min}^k, t_{j,\max}^k]} \alpha_i(t_j^k)$ ,  $\underline{\alpha}_i = \min_{t_j^k \in [t_{j,\min}^k, t_{j,\max}^k]} \alpha_i(t_j^k)$ , the maximum and minimum value of  $\alpha_i(t_j^k)$ , respectively, with  $t_{j,\min}^k$  and  $t_{j,\max}^k$  defined in (4.32) and (4.33), respectively.

If there exist a matrix  $P \in \mathbb{R}^{(n+\bar{d}m+r) \times (n+\bar{d}m+r)}$  and a scalar  $0 \leq \gamma < 1$ , such that the following LMI conditions are satisfied:

$$\begin{pmatrix} (1-\gamma)P & (H_{F,j} - H_{G,j}K)^T P \\ P(H_{F,j} - H_{G,j}K) & P \end{pmatrix} > 0, \quad (7.13)$$

for all  $(H_{F,j}, H_{G,j}) \in \mathcal{H}_{FG}$ , with  $j = 1, 2, \dots, 2^\beta$ , then (7.1), (7.2), with the controller defined in (7.10), is GAS for  $\tau_k \in [\tau_{\min}, \tau_{\max}]$ .

**Proof** The proof is analogous to the proof of Theorem 4.3.1 and Theorem 4.3.6.  $\square$

**Transient performance** The lower bound on the transient decay rate can be derived analogously to (5.9), with  $\xi_k$  replaced by  $\eta_k$ . This gives:

$$|x_k|^2 \leq (1-\gamma)^k \|C_x P^{-\frac{1}{2}}\|^2 |\eta_0|_P^2, \quad (7.14)$$

with  $|\eta_0|_P^2 = \eta_0^T P \eta_0$  and  $C_x$  defined such that it holds that  $x_k = C_x \eta_k$ .

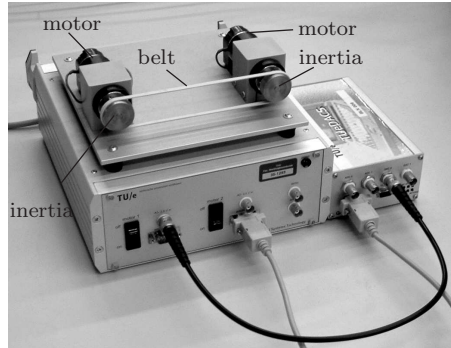


Figure 7.1: Overview of the experimental motion control set-up.

### 7.3 The experimental set-up

Two representative experimental motion control systems, with, respectively, second-order and fourth-order continuous-time dynamics are considered. The experimental set-up, depicted in Figure 7.1, exists of two identical servomotors, with the same inertia mounted on each drive shaft. A rubber belt connects both inertias. The first study is performed on the system with the rubber belt removed (i.e. a single actuated inertia remains, as is encountered in many motion control systems, e.g. the motor-roller example as considered in the previous chapters). The second study is performed with the belt mounted, yielding a typical motor-load motion control setting with a flexible coupling (the belt). Herein, the left motor is used for actuation and the position of the right motor is measured through an incremental encoder with a resolution of 2000 increments per revolution. In both set-ups the angular velocity is estimated by numerical differentiation with a backward difference method. This estimation is explicitly included in the control law, which results in the use of an output-feedback controller. A constant velocity is used as a reference signal.

The time-delays are artificially induced in the control system in order to be able to perform tests with well-defined sequences of delays, needed to validate the output-feedback control designs. This results in an academic experimental setting, where we have known and guaranteed bounds on the variation of the time-delays. To achieve both predictable time-varying and constant delays in the set-up, a high-performance measuring device is used: TUE DACS [109], [1]. The controller is implemented with the Real-Time toolbox of Matlab/Simulink. The time-delays are implemented within Simulink, being fractions of the sampling interval. Hereto, two different sampling rates are used. Firstly, the Simulink block, including the controller, is executed at 5 kHz, which allows for time delays of  $\frac{1}{5000}$ s. Secondly, the plant is effectively sampled at 500 Hz by removing nine out of ten data packets obtained at the 5 kHz rate. This combination of sampling rates allows for time-delays of 10, 20, ..., 90, 100% of the sampling interval of the plant ( $h = 2$ ms). To ensure correct implementation

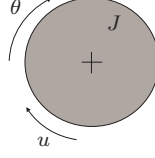


Figure 7.2: Schematic overview of the single inertia set-up.

of the delays, the actuation is performed at 5 kHz again. For constant and periodic time-delays, the constant minimum time-delay that is always present in the set-up is equal to 0.04ms (i.e. 2% of the sampling time). For time-varying delays, this minimum time-delay is equal to 0.28ms (i.e. 14% of the sampling time). Note that this minimum time-delay includes both the controller computation and the transmission of the signals and is derived if no additional possibly time-varying delays are implemented in the Simulink block. The time-variation in the delays is obtained at random, with a discrete uniform distribution, with  $\tau \in \{0, 0.1h, \dots, 2h\}$  or obtained based on a previously defined sequence of these delays. The additionally implemented time-delay is introduced after the control computation, thus it represents the controller-to-actuator delay. Because all delays are combined into one single delay in the NCS model, see Chapter 3, this implementation is suitable to validate the stability results. Note that the total delay, as used in the stability analysis conditions, is thus the combination of both the minimum delay and the bounds on the variation of the delay.

Next, the dynamics of both set-ups will be presented. The single inertia set-up is depicted in Figure 7.2 and it is modeled by (7.1), with  $x = (\theta \ \dot{\theta})^T$ ,  $A = \begin{pmatrix} 0 & 1 \\ 0 & 0 \end{pmatrix}$ ,  $B = \begin{pmatrix} 0 \\ \frac{k_m}{J} \end{pmatrix}$ ,  $C = (1 \ 0)$ ,  $\frac{k_m}{J} = 2.15 \cdot 10^3 \text{ rad/Vs}^2$ ,  $k_m$  the motor constant, and  $J$  the inertia (see [83]).

The motor-load configuration is depicted in Figure 7.3 and it is modeled by (7.1), with the state vector defined as  $x = (\theta_1 \ \dot{\theta}_1 \ \theta_2 \ \dot{\theta}_2)^T$ , and the system matrices defined by

$$A = \begin{pmatrix} 0 & 1 & 0 & 0 \\ -\frac{2kr^2}{J} & -\frac{2br^2}{J} & \frac{2kr^2}{J} & \frac{2br^2}{J} \\ 0 & 0 & 0 & 1 \\ \frac{2kr^2}{J} & \frac{2br^2}{J} & -\frac{2kr^2}{J} & -\frac{2br^2}{J} \end{pmatrix}, \quad B = \begin{pmatrix} 0 \\ \frac{k_m}{J} \\ 0 \\ 0 \end{pmatrix}, \quad C = (0 \ 0 \ 1 \ 0),$$

with  $k_m$  the motor constant,  $J$  the inertia of the first and second motor (i.e. both motors have the same inertia),  $k$  the spring stiffness of the belt,  $b$  the viscous damping coefficient modeling the dissipation in the belt, and  $r$  the radius of the inertias, which are connected via the belt. A frequency domain parameter identification procedure gives the following parameter values:  $\frac{k_m}{J} = 2.04 \cdot 10^3 \text{ rad/Vs}^2$ ,  $\frac{b}{k} = 5.1 \cdot 10^{-3} \text{ s}$ , and  $kr^2 = 0.42 \text{ Nm}$ , see [5].



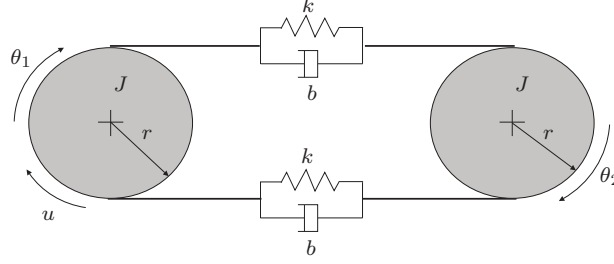


Figure 7.3: Schematic overview of the motor-load set-up.

## 7.4 Experimental results

For both experimental set-ups, the following output-feedback controller is used:

$$u_k = - \begin{pmatrix} K_1 & K_2 \end{pmatrix} \begin{pmatrix} Cx_k \\ \frac{Cx_k - y_{k-1}}{h} \end{pmatrix} = - \left( (K_1 + \frac{K_2}{h})C \quad 0_{1 \times \bar{d}} \quad -\frac{K_2}{h} \right) \eta_k, \quad (7.15)$$

with  $K_1$  and  $K_2$  the controller gains. Let us now discuss the experimental results for the cases of constant delays, periodic delays, and random time-varying delays in the following sections.

### 7.4.1 Constant delays

For the validation of the results for constant delays the focus is, for the sake of simplicity, on the set-up with a single inertia. For a fixed controller gain  $K_1 = 17\text{V/rad}$ , measurements are performed to determine all stabilizing controller gains  $K_2$  that stabilize the NCS of (7.1), (7.15) for constant time-delays. The experimentally obtained minimum and maximum stabilizing controller gains, denoted by  $\underline{K}_2$  and  $\overline{K}_2$ , respectively, are depicted in Figure 7.4 by the star and plus-signs, respectively. For comparison, the border of the analytical stability region obtained by analysis of the eigenvalues of the controlled system is depicted by the solid line, which shows that the analytic model provides an accurate prediction of the stability region in practice.

### 7.4.2 Periodic Delays

The experimental time responses of the position error ( $e = \theta_{ref} - \theta$ , with  $\theta_{ref}$  the reference position) for the constant time-delays  $\tau_1 = 0.02h$  and  $\tau_2 = 0.42h$ , with  $K = (17 \quad 0.23)$ , are depicted in the upper and lower plot of Figure 7.5. Both responses are clearly stable. Note that, on a model level, the eigenvalues of the discrete-time system matrices are given by  $\{\lambda_i\} = \{0.301 \pm 0.715i, -0.0004, 0.854\}$  for  $\hat{A}(\tau_1)$ , and  $\{\lambda_i\} = \{-0.105, 0.529 \pm 0.832i, 0.855\}$  for  $\hat{A}(\tau_2)$ , with  $\hat{A}(\tau)$  defined in (7.11). Clearly all eigenvalues are within the unit circle which confirms the experimentally observed stability properties. In Figure 7.6, the time-response for the periodic delay sequence  $\tau_1, \tau_2, \tau_2, \tau_1, \tau_2, \tau_2, \dots$

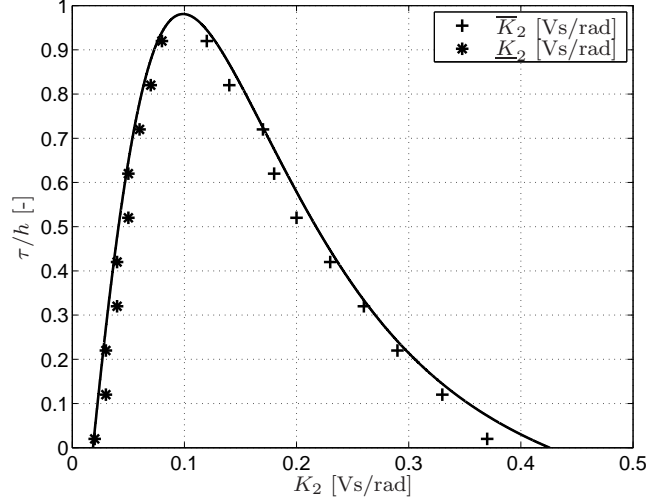


Figure 7.4: Analytical and experimental stability region for the single inertia system with constant time-delays,  $h = 2\text{ms}$ , and  $K_1 = 17\text{V/rad}$ .

is depicted. According to the eigenvalues of the periodic system matrix  $\hat{A}(\tau_2)\hat{A}(\tau_2)\hat{A}(\tau_1)$ , with  $\hat{A}(\cdot)$  defined in (7.11), this system is unstable (the eigenvalues are  $\{\lambda_i\} = \{-1.006, -0.566, 0, 0.624\}$ ). From Figure 7.6, it is observed that the time-response does not converge to zero and remains bounded. However, in the time-interval  $[1.1, 1.3]\text{s}$  a divergent error signal is observed, indicating an unstable behavior of the system. For  $t > 1.3\text{s}$ , the amplitude of the error remains bounded, which is caused by the saturation of the control input (i.e. the control input is limited to  $[-2.5, 2.5]\text{V}$ , as depicted in the lower plot of Figure 7.6). This saturation avoids that the error escapes to infinity. Moreover, the system becomes nonlinear, due to the saturation of the control input, which is not considered in the analysis of Theorem 7.2.1. The divergence of the error for control inputs smaller than the saturation level shows that the original system, without saturation, is indeed unstable.

This example of the destabilizing effect of periodic delays, both analytically and experimentally, motivates the controller design for time-varying delays.

### 7.4.3 Randomly Time-Varying Delays

Figure 7.7 depicts the stability region of the controlled single inertia system for randomly time-varying delays (dashed line), obtained with Theorem 7.2.1, and for constant delays (solid line), with  $K_1 = 1\text{V/rad}$  and  $h = 2\text{ms}$ . The controller gain  $K_1$  is reduced to  $K_1 = 1\text{V/rad}$ , such that stabilizing controllers can be found for delays larger than the sampling interval. Note that the previously used controller gain  $K_1 = 17\text{V/rad}$ , does not allow for delays larger than the sampling interval, because the region for constant delays is already limited to delays

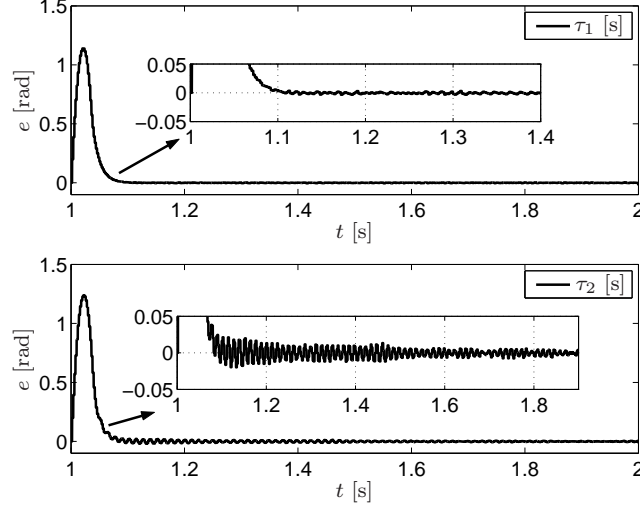


Figure 7.5: Time-response of the single inertia system for  $\tau_1 = 0.02h$  (upper plot) and  $\tau_2 = 0.42h$  (lower plot), with  $K = (17 \ 0.23)$  and  $h = 2\text{ms}$ .

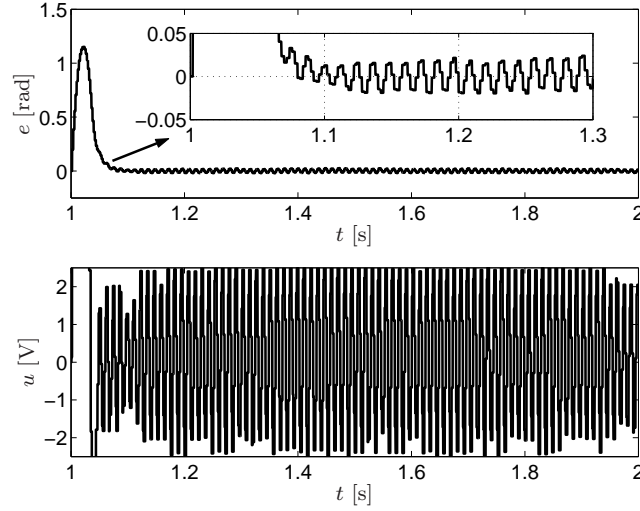


Figure 7.6: Time-response of the single inertia system, for the periodic delay sequence  $\tau_1, \tau_2, \tau_2$ , with  $\tau_1 = 0.02h$ ,  $\tau_2 = 0.42h$ ,  $K = (17 \ 0.23)$ , and  $h = 2\text{ms}$ .

smaller than the sampling interval, as can be seen in Figure 7.4. Figure 7.7 shows that the conservatism of the stability conditions in Theorem 7.2.1 is limited (compare hereto the solid and dashed lines). The gray lines depict the measurements that are performed to validate the stability region. Both random delay sequences with a uniform distribution between  $\tau_{\min}$  and  $\tau_{\max}$

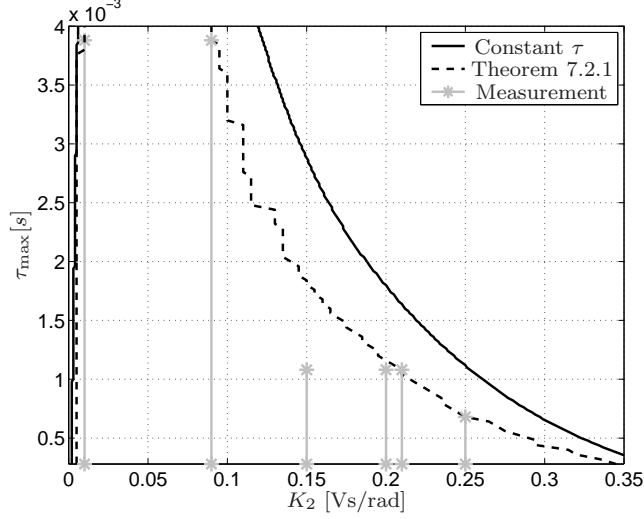


Figure 7.7: Stability region for the single inertia system for constant delays (solid line) and time-varying delays according to Theorem 7.2.1, with  $K_1 = 1 \text{ V/rad}$ ,  $\tau_{\min} = 0.28 \text{ ms}$ ,  $h = 2 \text{ ms}$ .

(denoted by  $\star$ ), and a periodic sequence  $\tau_{\min}, \tau_{\max}, \tau_{\min}, \tau_{\max}, \dots$  are used for validation purposes. These measurements show a stable configuration, which is in agreement with Theorem 7.2.1. Two examples of such time-responses for random variations in the delay are depicted by the solid line in the upper plot of Figure 7.8 and 7.9 in terms of the error. Additionally, the middle plot gives the control input and the lower plot gives, for a smaller time-scale, the delays that are used in the experiments. Note that in Figure 7.9, the control input does not converge to a constant value. This is caused by the measurement error of the encoder in combination with a relatively high value of the controller gain  $K_2$ . In Figure 7.8 this effect is much smaller, due to the choice of the controller that is less close to the largest stabilizing controller gain  $K_2$  that can be found for this delay combination. However, the control input does not converge to zero, due to the presence of Coulomb friction in the motor.

Additionally, several measurements for time-varying delays are performed to evaluate the possible conservatism of the transient decay rate in (7.14). Two time-response measurements are depicted in Figures 7.8 and 7.9. In the upper plots the measured time-response is depicted by the solid line and the estimated decay rate according to (7.14) is depicted by the dashed line. To obtain a better understanding of the relation between the analytical transient decay rate  $(1 - \gamma)$  obtained with (7.13), (7.14) and the experimental decay rate, a range of measurements are compared in Figure 7.10 for varying controller gains  $K_2$ . The plot depicts the analytical and experimental decay rate  $1 - \gamma$ . The experimental decay rate is estimated based on the time-response and the relation  $|e_k|^2 \leq (1 -$

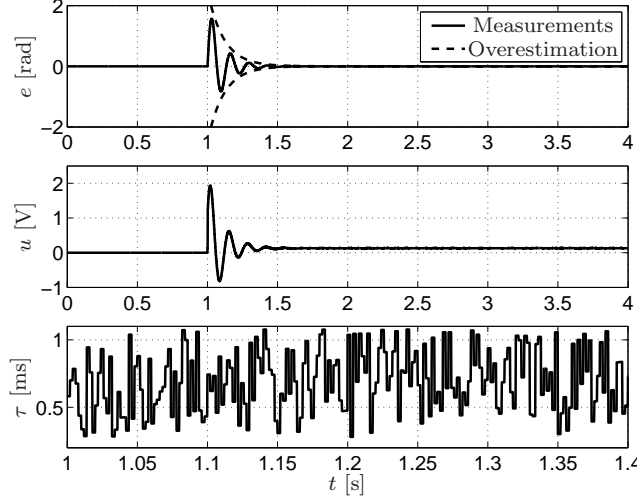


Figure 7.8: Experimental time response of the single inertia system for  $\tau_k \in [0.28, 1.08]\text{ms}$ ,  $K_1 = 1\text{V/rad}$ ,  $K_2 = 0.01\text{Vs/rad}$ ,  $\gamma = 0.034$ ,  $h = 2\text{ms}$  and the corresponding lower bound of the decay rate as in (7.14).

$\gamma)^k |e_0|^2$ . Except for values near the stability boundary, there is a clear match between the experimental results and the model results. Based on this fact, we can claim that the parameter  $\gamma$  represents a useful measure in terms of transient performance, which can be used in the controller design with Theorem 7.2.1.

To show the applicability of Theorem 7.2.1 for more complex systems, the stability region for the motor-load set-up is validated. The analytical stability regions for constant and time-varying delays are depicted in Figure 7.11 for  $K_1 = 0.05\text{V/rad}$ . Similar to the single inertia system, measurements for different uniform and periodic delay configurations are performed (depicted by the gray lines with  $\tau_{\min} = 0.14h$  and  $\tau_{\max} = 0.94h$  denoted by  $\star$ ). Again, it is concluded that no unstable measurements occur inside the stability region for time-varying delays. During the measurements, it is noticed that for  $K_2 = 0.021\text{Vs/rad}$  the system became unstable, which indicates that the upper bound of  $K_2$  obtained from the conditions in Theorem 7.2.1 is not overly conservative. In the experiments, for lower values of  $K_2$  ( $K_2 < 0.021\text{Vs/rad}$ ), no instability was found for either constant or time-varying delays. This indicates that the obtained analytical upper bound on  $K_2$  for constant and time-varying delays show a small difference with their experimental equivalents. This difference is partly caused by an inaccuracy of the estimated parameters, resulting in a difference between the model and the experiments.

As an example, the error signal ( $e = \theta_{2,\text{ref}} - \theta_2$ , with  $\theta_{2,\text{ref}}$  the reference signal and  $\theta_2$  the measured angle of the right motor), the control input, and the delay are depicted in Figure 7.12 for  $K_1 = 0.05\text{V/rad}$ ,  $K_2 = 0.01$ ,  $\gamma = 0.01$ ,  $\tau \in [0.28, 3.88]\text{ms}$ , and  $h = 2\text{ms}$ . This shows that the system is indeed stable.

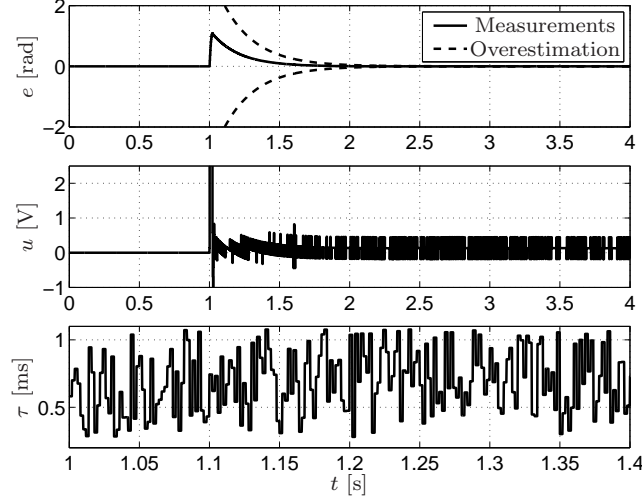


Figure 7.9: Experimental time response of the single inertia system for  $\tau_k \in [0.28, 1.08]ms$ ,  $K_1 = 1V/rad$ ,  $K_2 = 0.2Vs/rad$ ,  $\gamma = 0.019$ ,  $h = 2ms$ , the corresponding lower bound of the decay rate as in (7.14).

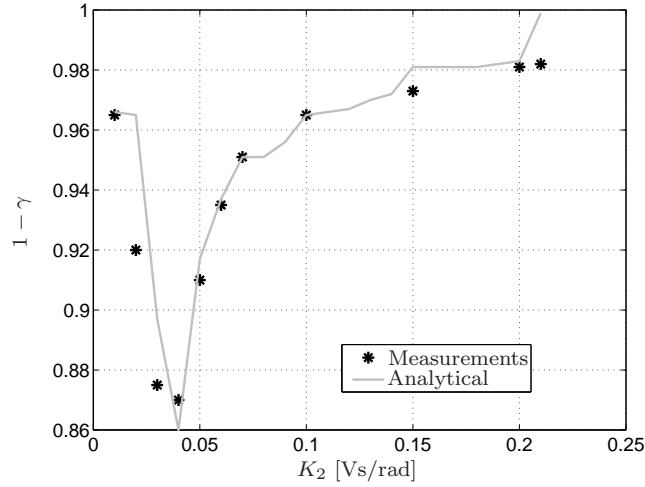


Figure 7.10: Comparison of the analytical and experimental decay rate ( $K_1 = 1V/rad$ ,  $\tau_k \in [0.28, 1.08]ms$ ,  $h = 2ms$ ) of the single inertia system.

Moreover, the analytical transient decay rate, obtained with (7.14), is depicted by the dashed line. This shows that for this configuration, the analytical decay rate is a useful estimate of the transient performance of the system in practice. Analogous to the single inertia system, the convergence ratio based on the analytical results and based on the measurements are compared in Figure 7.13

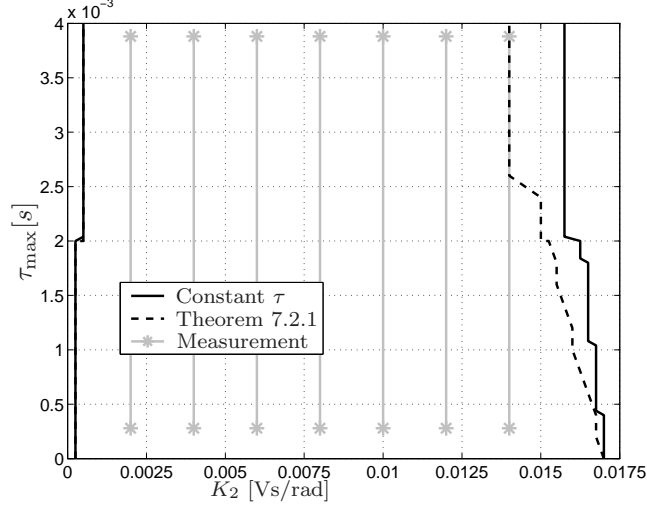


Figure 7.11: Stability region for constant delays  $\tau_{\max}$  (solid line) and time-varying delays according to Theorem 7.2.1 of the motor-load system, with  $K_1 = 0.05$  V/rad,  $\tau_{\min} = 0.28$  ms,  $h = 2$  ms.

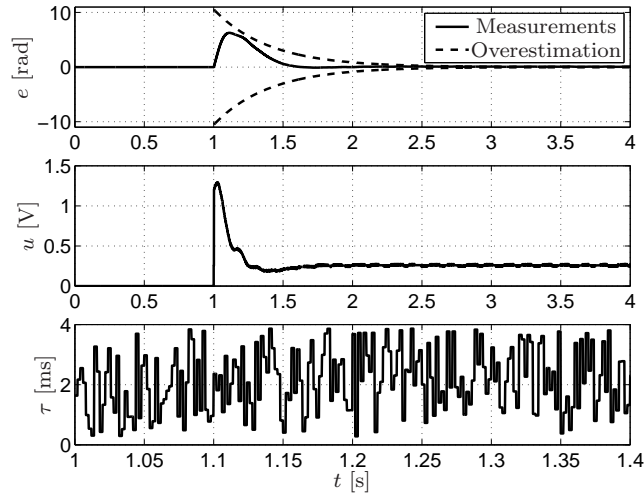


Figure 7.12: Experimental time response of the single inertia system for  $\tau_k \in [0.28, 3.88]$  ms,  $K_1 = 0.05$  V/rad,  $K_2 = 0.01$  Vs/rad,  $\gamma = 0.01$ ,  $h = 2$  ms, the corresponding lower bound of the decay rate as in (7.14).

for different values of  $K_2$  ( $K_1 = 0.05$  V/rad,  $\tau_k \in [0.28, 3.88]$  ms, and  $h = 2$  ms). This shows that for small values of  $K_2$  the analytical transient decay rate is an accurate estimate of the practical transient performance. For larger values of

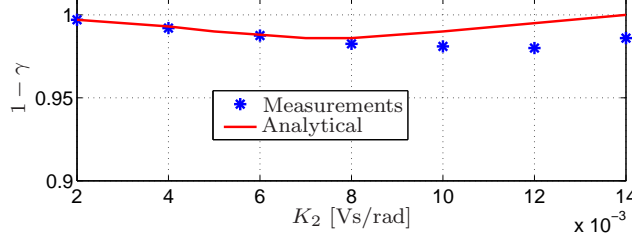


Figure 7.13: Comparison of the analytical and experimental decay rate ( $K_1 = 0.05 \text{ V/rad}$ ,  $\tau_k \in [0.28, 3.88] \text{ ms}$ ,  $h = 2 \text{ ms}$ ) of the motor-load system.

$K_2$ , i.e.  $K_2 > 7 \text{ Vs/rad}$ , the difference between the estimated decay rate and the time-response during the experiments is slightly larger, although still acceptable. The main difference between the analytical and experimental results is found for the values of  $K_2$  for which the smallest value of  $1 - \gamma$ , i.e. the optimum transient decay rate resulting in the smallest settling time, occurs. For the experiments, a larger value of  $K_2$  is obtained than based on the analysis tools. This is caused by the inaccuracy between the model and the experimental set-up, as was already noticed in the validation of the stability region, where the region for constant and time-varying delays is smaller than the stability region in the practical situation. Still, due to the small difference, the analytical decay rate is useful for controller design.

## 7.5 Discussion

In this chapter, the stability of NCSs is experimentally investigated for constant and time-varying delays. To the author's knowledge, this is the first time that the theoretical stability region for constant delays is validated. It is shown that there is a clear match between the measurements and the analytical stability region for constant delays. For time-varying delays, first, the destabilizing effect of time-variations in the delay is validated on the single inertia system for periodic time-delays. This observation shows, in combination with the theoretical example in Section 4.1, the value of the research on the stability of NCSs with time-varying delays, as presented in this thesis. Second, for time-varying delays, the stability conditions of Chapter 4 are adapted for the output-feedback case and validated on two representative motion control examples, i.e. a single inertia and a motor-load set-up. In both cases, the controllers that guarantee stability for time-varying delays are validated on the set-up. Moreover, the performance measure in terms of transient decay rate, as described in Chapter 5, is validated and shown to be predictive if the plant model is an accurate description of the experimental set-up.



## *Conclusions and recommendations*

---

### 8.1 Conclusions

### 8.2 Recommendations

---

In this chapter the main conclusions, regarding the work in this thesis will be presented (Section 8.1) and recommendations for future work will be given (Section 8.2).

### **8.1 Conclusions**

The conclusions are divided in two parts. Firstly, in Section 8.1.1, conclusions regarding Networked Control Systems (NCSs) are presented. Here, the model, stability, controller synthesis, and tracking conditions are discussed, as well as the experimental results. Secondly, in Section 8.1.2, conclusions regarding the design of high-tech systems are presented, based on the obtained results for NCSs.

#### **8.1.1 Networked Control Systems**

In this thesis, NCSs consisting of a linear continuous-time plant and a discrete-time controller are considered. Due to the use of the communication network and a possibly shared processor, the NCS has to deal with time-varying delays, which can be smaller and larger than the sampling interval, time-varying sampling intervals, and packet dropouts. The basis of the thesis is a discrete-time NCS model that includes the combination of these effects. The starting point of the proposed model is the standard discrete-time NCS model that describes a NCS with time-varying delays smaller than the constant sampling interval and no packet dropouts (see e.g. [85; 133]). In the literature, an extension for time-varying delays larger than the sampling interval exists, where it is assumed that all data (both from the sensor and the controller) arrives in a sequential order (see [101; 124]). Note that if the variation of the delays is larger than one sampling interval, the sequential order cannot be guaranteed. Therefore, an improved model that includes message rejection, i.e. the rejection of data if newer data is already available, is presented in this thesis. Moreover, an extension is presented such that the effects of packet dropouts and variations in the sampling interval are included in the NCS model. Due to the assumption that the variation in the delay and sampling interval is bounded and that the number of subsequent packet dropouts is bounded, a time-varying discrete-time

NCS model with a state of finite dimension is obtained. The dimension of the (extended) state of the discrete-time NCS model depends on both the ratio between the maximum time-delay and the minimum sampling interval, and the maximum number of subsequent packet dropouts.

Based on this model, stability conditions are presented. Two different controllers are used, i.e. a state-feedback controller that depends on the state of the continuous-time plant at the sampling instants and an extended state-feedback controller that depends on the extended state vector that contains, besides the current state, a number of past control inputs related to the maximum time-delay and the maximum number of subsequent packet dropouts. A disadvantage of the extended state-feedback controller is, however, that packet dropouts and message rejection between the sensor and the controller are not allowed, to guarantee the existence of all control inputs in the extended state-feedback controller. For the state-feedback controller this restricting assumption is not necessary, due to the dependence of the control law on the most recent state of the continuous-time system only. For both controllers, based on different candidate Lyapunov functions, conditions in terms of linear matrix inequalities (LMIs) are presented that guarantee global asymptotic stability of the NCS. First, a common quadratic candidate Lyapunov function that depends on the extended state vector is considered. This method is applicable for both controllers. Second, a candidate Lyapunov-Krasovskii (L-K) functional is considered to obtain stability conditions for the state-feedback controller. A disadvantage of the L-K approach is the increased conservatism compared to the common quadratic Lyapunov approach, if the same extended state vector is considered. Moreover, the LMIs become more complex; however, the number of LMIs that deal with the uncertain time-variations in the NCS remains the same. The difference in conservatism is explained, based on the structure of the Lyapunov functions. It is shown that the L-K functional can be rewritten as a common quadratic Lyapunov function, if the same state vector is considered. An illustrative example, where a comparison of the two candidate Lyapunov functions, with respect to the state-feedback controller is given, confirms this observation.

The obtained stability conditions are adapted, such that controller synthesis conditions are obtained. The advantages and disadvantages of the different control laws and both Lyapunov-based approaches are studied. First, the common quadratic candidate Lyapunov function that depends on the extended state vector is considered to derive synthesis conditions for both controllers. For the extended state-feedback controller, constructive LMI conditions are obtained, where the conservatism is comparable to the stability analysis results. Illustrative examples show that both for small delays, large delays and packet dropouts stabilizing controllers are obtained. For the state-feedback controller, analogous to the extended state-feedback controller, stabilizing conditions are derived, however, the results are extremely conservative due to the demands on the structure of the Lyapunov matrix in the Lyapunov function. This structure is needed to guarantee that a state-feedback controller is obtained. The illustrative example confirms this fact, because only for a limited number of small delays stabilizing controllers can be derived. An improvement that avoids the

structure in the Lyapunov matrix, but still allows to derive a state-feedback controller is presented based on the results of [19]. The conservatism is in this case comparable to the conservatism for the stability analysis results for the state-feedback controller. The illustrative example confirms this fact, because stabilizing controllers for small delays, large delays, and packet dropouts are obtained. Second, the Lyapunov-Krasovskii functional is also considered to characterize stabilizing controllers. Again, the structured control synthesis problem is avoided. However, additional assumptions are needed to obtain synthesis LMIs instead of nonlinear matrix inequalities. Therefore, compared to the stability analysis results for the L-K approach, the conservatism is increased. The illustrative examples show that only for the small delay case stabilizing controllers are obtained. Comparing the different approaches for the state-feedback controller shows that the L-K approach is less conservative than the standard synthesis conditions, based on the common quadratic Lyapunov function, but more conservative than the synthesis conditions, where the structure in the Lyapunov matrix is avoided by applying the results presented in [19]. Therefore, the use of the L-K functional to derive stabilizing controllers is not advisable, even more because the conditions are more complex than the approaches based on a common quadratic Lyapunov function.

The approximate tracking control problem is solved for NCSs with time-varying delays, time-varying sampling intervals, and packet dropouts. These effects cause an error in the feedforward signal, which perturbs the tracking error dynamics. Sufficient conditions in terms of LMIs for input-to-state stability (ISS) of the tracking error dynamics with respect to this feedforward error are given. Based on these LMI conditions, we formulated an ultimate bound for the tracking error that depends on, firstly, the plant properties, secondly, the controller, thirdly, the desired trajectory and, fourthly, the network properties, such as delays, dropouts, and the sampling interval. Such conditions can be used as a design tool during the multi-disciplinary design of high-tech systems, because it gives a bound on the tracking error depending on several factors that can be influenced by the design, such as bounds on the delays, sampling interval, and the occurrence of packet dropouts, or for a given desired tracking error, it gives the demands on the variation in the delays and sampling interval and the bounds on the occurrence of packet dropouts. Using illustrative examples, a comparison between the proposed discrete-time model and a model based on impulsive differential equations, as described in [74; 111], is given. It is shown that, for a typical motion control example, the discrete-time modeling approach allows to prove a bounded tracking error for larger ranges of sampling intervals and delays than the impulsive differential equations. On the other hand, the delay impulsive modeling approach provides much tighter bounds on the tracking error.

Experiments are performed on a single motor set-up and on a motor-load set-up. For the first time, an example is shown where a periodic variation in the delays destabilizes the system, while the system is stable for the constant upper and lower bound of these delays. This example motivates the necessity to include variations in the delays during the controller design. Moreover, the sta-

bility analysis results, as proposed in this thesis, are validated on both set-ups for time-varying delays, constant sampling intervals, and no packet dropouts. Note that in the literature, hardly any experimental validation of stability analysis and controller synthesis results is available. The performed experiments show that the stability results, as proposed in this thesis, are useful in practical applications to design stabilizing controllers that can deal with variations in the delay. Additionally, it is shown that the transient decay rate, that can be obtained based on the LMI conditions is a useful prediction of the transient decay rate in practice.

### 8.1.2 High-tech systems design

The previous conclusions are related to Networked Control Systems. As mentioned in the introduction, the analysis and design conditions are also useful in the broader scope of the design of high-tech systems, such as wafersteppers, electron microscopes, and copiers in which control systems operating over communication networks play an important role. The bounds on the variation of the sampling interval, the variation of the time-delays, and the number of subsequent packet dropouts can be obtained from measurements on the network, but also from measurements on the software implementation in the high-tech system or from models of the software implementation, see e.g. [21; 112]. Recall that the processor that is used for the control computation under consideration, may be used for other software tasks leading to variations in the starting moment of the control computation and therefore to delays in the control loop. Moreover, the processor may be shared between multiple controllers, resulting in the use of a communication network between the processor and the plants. This may lead to above mentioned variations in the delay and sampling interval or packet dropouts. During the design process of high-tech systems that include these aspects, the bounds on the time-variation in the delays and sampling interval (or bounds on the latency and jitter in software engineering terms) can be used to decide if the controller should be adapted such that it can handle these variations or that adaptations in the software (and its architecture) are needed to decrease these variations. For the software related adaptations, one can think of using multiple processors instead of one shared processor (i.e. a change in the architecture) or using a faster processor. A comparison between different architectures is discussed for instance in [112]. An adaptation in the controller may, based on control engineering knowledge, lead to a decrease of the performance (e.g. a larger tracking error or a slower transient response), while a change in the software architecture is often related to the cost-price, especially if the number of processors is changed. The approach presented in this thesis is helpful to make these tradeoffs more explicitly.

## 8.2 Recommendations

First, recommendations concerning the stability analysis and controller synthesis results, as presented in this thesis will be discussed. We will discuss the number of LMI conditions that are needed, possible solutions to decrease the conservatism of the stability and synthesis conditions, and ideas to avoid the assumptions on delays and packet dropouts between the sensor and controller that are needed for the extended state-feedback controller.

- Although the number of LMIs that need to be solved for stability analysis and controller synthesis is reduced compared to previous results in [16], still many LMIs need to be solved, especially when packet dropouts and delay variations larger than two times the minimum sampling interval occur (because the number of LMIs increase exponentially with  $\nu$  that depends on the dimension of the continuous-time system matrix  $A$ ). A reduction of the number of LMIs would be favorable in terms of numerical tractability with reasonable computation time. Moreover, a further reduction of the conservatism is still advantageous. In [28], a reduction of the number of LMIs is proposed, based on a geometric study that contains a comparison between the region where the system may be active due to the variations in the delays and the region enclosed by the generators. This leads to a removal of the generators that describe the region where the system can never be active for the given variations. Due to the analogy with the model proposed in this thesis, such a reduction may be possible for the analysis and synthesis results proposed in this thesis. This will, due to the removal of part of the generators, result in less LMIs that need to be solved for and a reduction of the computation time. Moreover, the conservatism will be decreased, or, if none of the removed generators was limiting for conservatism, remain the same.
- In this thesis, all results are based on the use of a common quadratic Lyapunov function, or Lyapunov-Krasovskii functionals that can be rewritten as a common quadratic Lyapunov function. A delay-dependent quadratic Lyapunov approach, where a different quadratic Lyapunov function is used for each generator, leads, in general, to less conservative results. However, the number of LMIs increases rapidly, because, for each generator all possible combinations of subsequent Lyapunov functions need to be considered. This may lead to numerical problems in the LMI solver, due to the large number of equations that need to be solved for. Especially for delays larger than the sampling interval and a number of subsequent packet dropouts, this problem may arise, due to the number of generators that are needed to describe these uncertainties. Due to the increase of the number of LMIs it is unclear, if for this kind of systems, delay-dependent quadratic Lyapunov functions give indeed results that are computationally feasible. Here, we focussed on a common quadratic approach exactly for this latter reason.

- A solution to overcome the assumption for the extended state-feedback controller, which states that, firstly, all data is received by the controller in a sequential order (i.e. no message rejection) or that you have to wait until all  $x_l$ ,  $l \leq k$  have arrived, and secondly, that no packet dropouts occur between the sensor and controller, can be the use of a model based predictor that determines the unavailable states if a packet is dropped (or rejected) between the sensor and the controller. Then, the extended state-feedback controller can always be computed and the assumption on the validity of this controller can be avoided. If such a model based predictor is used, one should decide if the predictor behaves in an event-driven fashion or in a time-driven fashion (possibly with a time-skew between the sensor and the processor, where this predictor and the controller are evaluated). If the predictor acts in an event-driven fashion, besides the computation of possibly lost (or rejected) data, it can be used to estimate the current state of the system, based on the received measurement data and their known delay (which can be achieved by means of time-stamping). This may improve the accuracy of the control input if the delays are large, compared to the response-time of the system. However, the performance of the predictor needs to be considered as well. If the predictor acts in a time-driven fashion, its prediction of the states can be used by the controller to derive a new control input if a certain time (e.g. the average delay) has passed, without receiving new measurement data (due to large delays or packet dropouts). This may result in a better performance. Note that in both cases the stability of the system, including the predictor, needs to be studied as well.

Additionally, recommendations concerning the use of NCSs in general can be given. These recommendations deal with possible extensions in the model, and therefore also in the analysis and synthesis results, that are needed to apply NCSs in practice. Moreover, possible improvements to the experiments are mentioned briefly.

- In this thesis, the focus is on the network effects, however, the effect of quantization is not included. Analogous to the deteriorating effect of delays, it is well known that a controller that is globally asymptotically stabilizing for a system without quantization, may fail if a quantization with a finite number of quantization levels is used, see e.g. [58] and the references therein. The combination of the network effects, as considered in this thesis, and quantization are needed to get a complete overview of the different aspects that occur in NCSs and guarantee stability in practical applications. Note that in [79] quantization and protocol design are combined, however without delays.
- In this thesis, the bounds on the variation of the delay and the sampling interval and the maximum number of subsequent packet dropouts are assumed to be known. These bounds need to be obtained based on measurements or models of the software and communication network. If protocol

design is included in the control design, it will be possible to find a stabilizing controller, in combination with a protocol, that guarantees that data is transmitted within some bounds on the delay, sampling interval, and the number of subsequent packet dropouts, such that the overall system is stable. Note that the approaches discussed in e.g. [18; 80; 81; 104] consider already this combination, however, without delays.

- The approach presented in this thesis is limited to a system that has one actuator and all sensor data is obtained at the same sampling instant and sent in one packet. In practice, multiple actuators and sensors can be present. Then, data from different sending sources needs to be combined to derive the control inputs. The effect that the data is obtained at different time-instances, or that only part of the data is available, need to be accounted for. In this case the use of an observer that derives the state of the system at one time-instant, based on the part of the data that is available, would be of interest. In the literature such effects are studied in e.g. [76; 80].
- The experiments in this thesis are limited to a NCS with network delays. Experimental validation of the stability and tracking results for NCSs with network delays, packet dropouts, and variations in the sampling interval is advisable. A next step could be to apply to proposed results to a real NCS, instead of the set-ups that are considered in the Chapter 7, where the delays are added artificially. Then, before validation, measurements need to be performed to derive the upper and lower bounds on the variation of the sampling interval and the delays and the maximum number of subsequent packet dropouts, as these are needed in the stability analysis and controller design.

The above presented recommendations focussed on the field of NCSs. However, the presented results may be applicable for sensor-based event-driven control, as studied in e.g. [94]. For this kind of controllers, the sampling interval is in general not equidistantly spaced. Consider for instance a controller that is evaluated at every encoder pulse. Then, the sampling instants are velocity dependent, which results in an uncertain, and time-varying sampling interval. The analysis of the achievable tracking error, as proposed in this thesis, based on the variations in the sampling interval, may be useful during the design of such a sensor-based event-driven controller. For event-driven controllers, in general, the sampling interval is one of the design parameters. Applying the analysis and synthesis conditions proposed in this thesis is possible, however, the results will be rather conservative, because no additional demands on the tracking error can be taken into account. An example of such a demand is that no new control input is computed if the tracking error is inside a specified error bound (see e.g. [3]), which may result in large sampling intervals.

Finally, for high-tech systems design, one can think of combining the proposed discrete-time model with a software model that predicts the latency and jitter. However, this may be complicated, because then all the software, includ-

ing non-control related tasks, that are executed on the same processor, need to be modeled, or accounted for otherwise. Probably, an approach as considered in TrueTime [9] can be helpful to achieve this. Such a combination would show much correspondence with combining the proposed NCS model and analysis techniques with protocol design, because the protocol design is part of the software implementation.

The list of recommendations indicates that there are still many issues to be resolved before all the advantages, such as ease of maintenance and flexibility of wired and wireless networked control systems can be harvested. Part of the solution will lie in the improvement of the employed communication networks and protocols, resulting in increased reliability and reduction of the end-to-end latencies and packet dropouts. However, the solution cannot be obtained in a (cost-effective) manner by only improving the communication infrastructure. It is important to take a systems perspective on reliability and to develop control algorithms that are robust to communications imperfections. This requires developing models of network characteristics which are compatible with controller analysis and synthesis methods, which lead to controllers that can deal with unreliable communication. This latter aspect is recognized widely in academia, which makes the networked control a lively research area at present. The results presented in this thesis form a significant contribution to this exciting and challenging research field, which will expand over the years to come, both in theory as in applications.



# A

## Proofs of theorems and lemmas

---

A.1 Proof of Lemma 3.2.1	A.9 Proof of Theorem 4.4.7
A.2 Proof of Lemma 3.3.1	A.10 Proof of Theorem 5.1.1
A.3 Proof of Lemma 3.4.1	A.11 Proof of Theorem 5.1.4
A.4 Proof of Theorem 4.3.2	A.12 Proof of Lemma 6.1.1
A.5 Proof of Lemma 4.3.4	A.13 Proof of Theorem 6.1.2
A.6 Proof of Lemma 4.3.5	A.14 Proof of Lemma 6.2.2
A.7 Proof of Theorem 4.3.6	A.15 Proof of Theorem 6.2.3
A.8 Proof of Lemma 4.4.2	

---

### A.1 Proof of Lemma 3.2.1

From the definition of  $\bar{d}$  in the lemma, we have that the control input  $u_{k-\bar{d}}$  is always available before or exactly at  $t = s_k := kh$  as  $s_{k-\bar{d}} + \tau_{k-\bar{d}} \leq s_{k-\bar{d}} + \tau_{\max} \leq s_k$ . Moreover,  $u_{k-\bar{d}}$  is the oldest control input that can be active in the sampling interval  $[s_k, s_{k+1})$ . To prove this, consider any previous input  $u_j$  for some  $j < k - \bar{d}$ . From the definition of  $\bar{d}$ , we have that  $\bar{d}h \geq \tau_{\max}$  and thus:

$$(j+1)h + \tau_{j+1} \leq (j+1)h + \tau_{\max} \leq s_{k-\bar{d}} + \tau_{\max} \leq s_k.$$

This implies that the control input  $u_{j+1}$  arrives before time  $s_k$  and thus  $u_j$  will not be active in the sampling interval  $[s_k, s_{k+1})$ . To prove that newer inputs  $u_j$ ,  $j > k - \bar{d}$  are not necessarily available before  $s_k$ , we determine the latest time at which  $u_{k-\bar{d}+1}$  might be implemented, which is equal to  $s_{k-\bar{d}+1} + \tau_{\max}$ . Based on the definition of  $\bar{d}$  it holds that  $\bar{d}h - \tau_{\max} \in [0, h)$ , i.e.  $\tau_{\max} > (\bar{d}-1)h$ . Using this fact and that fact that  $s_{k-\bar{d}+1} = s_k - (\bar{d}-1)h$  gives:

$$s_{k-\bar{d}+1} + \tau_{\max} > s_k.$$

This proves that  $u_{k-\bar{d}+1}$  might be implemented after  $s_k$ , implying that the older input  $u_{k-\bar{d}}$  might indeed be active in  $[s_k, s_{k+1})$ .

From the definition of  $\underline{d}$  in the lemma, it follows that the input  $u_{k-\underline{d}}$  represents the most recent control input that might be implemented during the sampling interval  $[s_k, s_{k+1})$ . Indeed, as  $\underline{d}h \leq \tau_{\min}$ , we have that  $s_{k-\underline{d}} + \tau_{\min} < s_{k+1}$ , which implies that the input  $u_{k-\underline{d}}$  might be available for implementation before time  $s_{k+1}$ . To show that there is no more recent control input that might be

active in the interval  $[s_k, s_{k+1})$ , consider the control input  $u_j$ , for some  $j > k - \underline{d}$ . From the definition of  $\underline{d}$ , we have that:

$$s_j + \tau_j \geq s_j + \tau_{\min} \geq s_{k+1} \quad \forall j > k - \underline{d}.$$

Therefore, the control input  $u_j$ ,  $j > k - \underline{d}$ , cannot be implemented in the sampling interval  $[s_k, s_{k+1})$ . Hence, the control inputs  $u_{k-\underline{d}}, \dots, u_{k-\underline{d}}$  are the only control inputs that can be active in the sampling interval  $[s_k, s_{k+1})$ .

The times  $t_j^k$  with  $j \in [k - \underline{d}, \dots, k - \underline{d}]$  will be constructed in such a manner that  $s_k + t_j^k$  is the time at which the control input  $u_j$  becomes active in the sampling interval  $[s_k, s_{k+1})$ . Hence,  $t_{k-\underline{d}}^k$  is given by:

$$t_{k-\underline{d}}^k = \min [h, \tau_{k-\underline{d}} - \underline{d}h]. \quad (\text{A.1})$$

Note that, by definition,  $\tau_{k-\underline{d}} - \underline{d}h \geq 0$ ,  $\forall k$ . In principle, if  $\tau_{k-\underline{d}} - \underline{d}h \in [0, h]$  then  $s_k + \tau_{k-\underline{d}}$  is the time at which  $u_{k-\underline{d}}$  is implemented. If  $\tau_{k-\underline{d}} - \underline{d}h > h$ , then  $u_{k-\underline{d}}$  might be active after  $s_{k+1}$ . Since, we are only interested in the interval  $[s_k, s_{k+1})$  we take the minimum of this value and  $h$  in (A.1). Next, as  $u_{k-\underline{d}-1}$  can only be active before  $u_{k-\underline{d}}$  is available (otherwise message rejection will occur),  $t_{k-\underline{d}-1}^k$  is given by:

$$t_{k-\underline{d}-1}^k = \min [t_{k-\underline{d}}^k, \max\{0, \tau_{k-\underline{d}-1} - (\underline{d} + 1)h\}]. \quad (\text{A.2})$$

Similarly to  $t_{k-\underline{d}}^k$ , if  $\tau_{k-\underline{d}-1} - (\underline{d} + 1)h \in [0, t_{k-\underline{d}}^k]$  then  $s_k - (\underline{d} + 1)h + \tau_{k-\underline{d}-1}$  is the time at which  $u_{k-\underline{d}-1}$  is implemented. In case  $\tau_{k-\underline{d}-1} - (\underline{d} + 1)h < 0$ , then  $u_{k-\underline{d}-1}$  might be active before  $s_k$ . Since, we are only interested, here, in the interval  $[s_k, s_{k+1})$ , we take the maximum of this value and 0 in (A.2). For the other values of  $t_j^k$ , the recursion can be derived similarly, yielding:

$$t_j^k = \min [t_{j+1}^k, \max\{0, \tau_j - (k - j)h\}], \quad \text{for } k - \bar{d} \leq j \leq k - \underline{d},$$

with  $t_{k-\underline{d}+1}^k := h$ . Recursive substitution of these relations yields the characterization of (3.7).

## A.2 Proof of Lemma 3.3.1

To prove that  $u_{k-\bar{d}-\bar{\delta}}$  is the oldest input that can be active during the sampling interval  $[s_k, s_{k+1})$  we consider, firstly, the case without packet dropouts and, secondly, the case with the maximum number of subsequent dropped packets. From the definition of  $\bar{d}$  in Lemma 3.3.1, we have that the control input  $u_{k-\bar{d}}$  is always available before or exactly at  $t = s_k := kh$ , provided  $u_{k-\bar{d}}$  is not dropped (i.e.  $m_{k-\bar{d}} = 0$ ), as  $s_{k-\bar{d}} + \tau_{k-\bar{d}} \leq s_{k-\bar{d}} + \tau_{\max} \leq s_k$ . Hence, in the case that  $u_{k-\bar{d}}$  is not dropped, no control inputs  $u_j$  with  $j < k - \bar{d}$  will be active in  $[s_k, s_{k+1})$ , as also stated in Lemma 3.2.1. To prove that newer inputs  $u_j$ ,  $j > k - \bar{d}$  are not necessarily available before  $s_k$ , the same reasoning as in

the proof of Lemma 3.2.1 in Appendix A.1 can be used. This implies that the older input  $u_{k-\bar{d}}$  might indeed be active in  $[s_k, s_{k+1})$ . Next, we consider the case with packet dropouts and we will show that  $u_{k-\bar{d}-\bar{\delta}}$  is the oldest input that can possibly be active in  $[s_k, s_{k+1})$ . Note hereto that, from (3.13), it follows that at least one of the control inputs  $u_{k-\bar{d}-\bar{\delta}}, u_{k-\bar{d}-\bar{\delta}+1}, \dots, u_{k-\bar{d}}$  is not lost. If  $u_{k-\bar{d}+1}$  is indeed implemented after  $s_k$  (which is possible as just shown), then at least one of the inputs  $u_{k-\bar{d}-\bar{\delta}}, u_{k-\bar{d}-\bar{\delta}+1}, \dots, u_{k-\bar{d}}$  will be active in the sampling interval  $[s_k, s_{k+1})$ . The fact that the maximum number of subsequent packet dropouts equals  $\bar{\delta}$  implies that  $u_{k-\bar{d}-\bar{\delta}}$  is the oldest control input that might be implemented in the sampling interval  $[s_k, s_{k+1})$ .

The proof that  $u_{k-\underline{d}}$  represents the most recent control input that might be implemented during the sampling interval  $[s_k, s_{k+1})$  is equal to the corresponding part of the proof of Lemma 3.2.1 in Appendix A.1. Hence, the control inputs  $u_{k-\bar{d}-\bar{\delta}}, \dots, u_{k-\underline{d}}$  are the only control inputs that can be active in the sampling interval  $[s_k, s_{k+1})$ .

The times  $t_j^k$  with  $j \in [k - \bar{d} - \bar{\delta}, \dots, k - \underline{d}]$  will be constructed in such a manner that  $s_k + t_j^k$  is the time at which the control input  $u_j$  becomes active in the sampling interval  $[s_k, s_{k+1})$ . Hence,  $t_{k-\underline{d}}^k$  is given by:

$$t_{k-\underline{d}}^k = \min [h, \tau_{k-\underline{d}} - \underline{d}h + m_{k-\underline{d}}h]. \quad (\text{A.3})$$

Indeed, as in the proof of Lemma 3.2.1, if  $m_{k-\underline{d}} = 0$ , then  $s_k + \tau_{k-\underline{d}} - \underline{d}h$  is the time at which  $u_{k-\underline{d}}$  is available at the plant. If  $\tau_{k-\underline{d}} - \underline{d}h > h$ , then  $u_{k-\underline{d}}$  might be active after  $s_{k+1}$ , but not in  $[s_k, s_{k+1})$ . Since, we are only interested in the interval  $[s_k, s_{k+1})$  we take the minimum of this value and  $h$  in (A.3). Note that, by definition,  $\tau_{k-\underline{d}} - \underline{d}h \geq 0$ . Finally, if  $u_{k-\underline{d}}$  is lost, i.e.  $m_{k-\underline{d}} = 1$ , then the expression for  $t_{k-\underline{d}}^k$  in (A.3) becomes  $h$ , which means that the input is not used in  $[s_k, s_{k+1})$ . Next, as  $u_{k-\underline{d}-1}$  can only be active before  $u_{k-\underline{d}}$  is available,  $t_{k-\underline{d}-1}^k$  is given by:

$$t_{k-\underline{d}-1}^k = \min [t_{k-\underline{d}}^k, \max\{0, \tau_{k-\underline{d}-1} - (\underline{d}+1)h\} + m_{k-\underline{d}-1}h]. \quad (\text{A.4})$$

Similarly to  $t_{k-\underline{d}}^k$ , if  $\max\{0, \tau_{k-\underline{d}-1} - (\underline{d}+1)h\} + m_{k-\underline{d}-1}h \in [0, t_{k-\underline{d}}^k)$  (note that if the packet belonging to  $s_{k-\underline{d}-1}$  is dropped, the value of  $\max\{0, \tau_{k-\underline{d}-1} - (\underline{d}+1)h\} + m_{k-\underline{d}-1}h$  becomes  $h \geq t_{k-\underline{d}}^k$ ) then  $s_k + \tau_{k-\underline{d}-1} - (\underline{d}+1)h$  is the time at which  $u_{k-\underline{d}-1}$  is available at the actuator. In case  $\tau_{k-\underline{d}-1} - (\underline{d}+1)h < 0$ , then  $u_{k-\underline{d}-1}$  might already be active before  $s_k$ . Since, we are only interested, here, in the interval  $[s_k, s_{k+1})$ , we take the maximum of this value and zero in (A.4). For the other values of  $t_j^k$ , the recursion can be derived similarly, yielding:

$$t_j^k = \min [t_{j+1}^k, \max\{0, \tau_j - (k-j)h\} + m_jh],$$

for  $k - \bar{d} - \bar{\delta} \leq j \leq k - \underline{d}$ ,  $m_j$  satisfying (3.13) and with  $t_{k-\underline{d}+1}^k := h$ . The elaboration of this recursive relation yields the characterization of (3.15).

### A.3 Proof of Lemma 3.4.1

This proof follows the same reasoning as the proof of Lemma 3.3.1 in Appendix A.2. To prove that  $u_{k-\bar{d}-\bar{\delta}}$  is the oldest control input that might be active during the sampling interval  $[s_k, s_{k+1})$ , we consider, firstly, the case without packet dropouts, and secondly, the case with packet dropouts. From the definition of  $\bar{d}$  in Lemma 3.4.1, we have that the control input  $u_{k-\bar{d}}$  is always available before or exactly at  $s_k$ , if  $u_{k-\bar{d}}$  is not dropped. To prove this, we use the relation  $s_k := s_{k-\bar{d}} + \sum_{l=k-\bar{d}}^{k-1} h_l$ , which provides the upper and lower bounds on  $s_k$ , given by  $s_{k-\bar{d}} + \bar{d}h_{\min} \leq s_k \leq s_{k-\bar{d}} + \bar{d}h_{\max}$ . Combining the lower bound on  $s_k$  and  $s_{k-\bar{d}} + \tau_{k-\bar{d}} \leq s_{k-\bar{d}} + \tau_{\max}$  gives:  $s_{k-\bar{d}} + \tau_{k-\bar{d}} \leq s_{k-\bar{d}} + \tau_{\max} \leq s_k - \bar{d}h_{\min} + \tau_{\max} \leq s_k$ , due to the definition of  $\bar{d} = \lceil \frac{\tau_{\max}}{h_{\min}} \rceil$ . Hence, in the case that the control input  $u_{k-\bar{d}}$  is not dropped (i.e.  $m_{k-\bar{d}} = 0$ ), it might be active before  $s_k$  and no older control inputs  $u_j$ , with  $j < k - \bar{d}$  will be active in the sampling interval  $[s_k, s_{k+1})$ . To show that  $u_{k-\bar{d}}$  can be active in the sampling interval  $[s_k, s_{k+1})$ , we need to show that  $u_{k-\bar{d}+1}$  can become active after  $s_k$  if no packets are dropped.

To do so, note that the upper and lower bounds of  $s_k$  in terms of  $s_{k-\bar{d}+1}$  are given by  $s_{k-\bar{d}+1} + (\bar{d}-1)h_{\min} \leq s_k \leq s_{k-\bar{d}+1} + (\bar{d}-1)h_{\max}$  and both the upper and lower bound can be achieved. The largest time at which  $u_{k-\bar{d}+1}$  can be implemented is equal to  $s_{k-\bar{d}+1} + \tau_{\max}$ . Combining the largest implementation time of  $u_{k-\bar{d}+1}$  and the smallest value of  $s_k$  gives  $s_{k-\bar{d}+1} + \tau_{\max} \geq s_{k-\bar{d}+1} + (\bar{d}-1)h_{\min}$ . Based on the definition of  $\bar{d}$ , it holds that  $\bar{d}-1 < \frac{\tau_{\max}}{h_{\min}} \leq \bar{d}$ , which gives that  $u_{k-\bar{d}+1}$  might be implemented after  $s_k$ . This proves that in the case without packet dropouts  $u_{k-\bar{d}}$  can indeed be active in the sampling interval  $[s_k, s_{k+1})$ . To prove that  $u_{k-\bar{d}-\bar{\delta}}$  is the oldest control input that can possibly be active in  $[s_k, s_{k+1})$ , the case with packet dropouts needs to be considered. This proof follows the same reasoning as the proof of Lemma 3.3.1 in Appendix A.2.

From the definition of  $\underline{d}$  in Lemma 3.4.1, it follows that the input  $u_{k-\underline{d}}$  represents the most recent control input that might be implemented during the sampling interval  $[s_k, s_{k+1})$ . To prove this, consider the smallest time at which  $u_{k-\underline{d}}$  might be implemented, which is given by  $s_{k-\underline{d}} + \tau_{\min}$ . Based on the definition of  $\underline{d}$ , which gives that  $\tau_{\min} < (\underline{d}+1)h_{\max}$ , we can conclude that  $s_{k-\underline{d}} + \tau_{\min} < s_{k-\underline{d}} + (\underline{d}+1)h_{\max}$ . Combining this with the tight bounds on  $s_{k+1}$ , given by:

$$s_{k-\underline{d}} + (\underline{d}+1)h_{\min} \leq s_{k+1} \leq s_{k-\underline{d}} + (\underline{d}+1)h_{\max}$$

yields that it might hold that  $s_{k-\underline{d}} + \tau_{\min} \leq s_{k+1}$ . Consequently,  $u_{k-\underline{d}}$  might be implemented before  $s_{k+1}$ . More recent control inputs always arrive after  $s_{k+1}$ , as we will show next. Consider  $j > k - \underline{d}$ . Then, we have that  $s_j + \tau_{\min}$  is the earliest time at which  $u_j$  might be implemented. To determine if this moment may occur before  $s_{k+1}$ , consider the upper bound on  $s_{k+1}$ , in terms of  $s_j$ , given by  $s_{k+1} \leq s_j + (k-j+1)h_{\max}$ . Combining these results gives that

$$s_j + \tau_{\min} < s_j + (k-j+1)h_{\max} \tag{A.5}$$

should hold if  $u_j$ ,  $j > k - \underline{d}$ , is implemented in the interval  $[s_k, s_{k+1})$ . Due to the definition of  $\underline{d} = \lfloor \frac{\tau_{\min}}{h_{\max}} \rfloor$ , (A.5) is never correct for  $j > k - \underline{d}$ . This proves that  $u_{k-\underline{d}}$  is indeed the most recent control input that can be active in the sampling interval  $[s_k, s_{k+1})$ .

The times  $t_j^k$  with  $j \in \{k - \bar{d} - \bar{\delta}, \dots, k - \underline{d}\}$  are constructed in the same way as in Appendix A.2. The time  $t_{k-\underline{d}}^k$  is given by

$$t_{k-\underline{d}}^k = \min \left[ h_k, \tau_{k-\underline{d}} - \sum_{l=k-\underline{d}}^{k-1} h_l + m_{k-\underline{d}} h_{\max} \right]. \quad (\text{A.6})$$

Indeed, if  $m_{k-\underline{d}} = 0$ , then  $s_k + \tau_{k-\underline{d}} - \sum_{l=k-\underline{d}}^{k-1} h_l$  is the time at which  $u_{k-\underline{d}}$  is available at the plant. If  $\tau_{k-\underline{d}} - \sum_{l=k-\underline{d}}^{k-1} h_l > h_k$ , then  $u_{k-\underline{d}}$  might be active after  $s_{k+1}$ , but not in  $[s_k, s_{k+1})$ . Since, we are only interested in the interval  $[s_k, s_{k+1})$  we take the minimum of this value and  $h_k$  in (A.6). Note that, by the definition of  $\underline{d}$ ,  $\tau_{k-\underline{d}} - \sum_{l=k-\underline{d}}^{k-1} h_l \geq 0$ . Finally, if  $u_{k-\underline{d}}$  is lost, i.e.  $m_{k-\underline{d}} = 1$ , then the expression in (A.6) gives  $h_k$ , which means that the input is not used in  $[s_k, s_{k+1})$ . Next, as  $u_{k-\underline{d}-1}$  can only be active before  $u_{k-\underline{d}}$  is available,  $t_{k-\underline{d}-1}^k$  is given by

$$t_{k-\underline{d}-1}^k = \min \left[ t_{k-\underline{d}}^k, \max \left\{ 0, \tau_{k-\underline{d}-1} - \sum_{l=k-\underline{d}-1}^{k-1} h_l \right\} + m_{k-\underline{d}-1} h_{\max} \right]. \quad (\text{A.7})$$

Similarly to  $t_{k-\underline{d}}^k$ , if  $\max\{0, \tau_{k-\underline{d}-1} - \sum_{l=k-\underline{d}-1}^{k-1} h_l\} + m_{k-\underline{d}-1} h_{\max} \in [0, t_{k-\underline{d}}^k)$ , then  $s_k + \tau_{k-\underline{d}-1} - \sum_{l=k-\underline{d}-1}^{k-1} h_l$  is the time at which  $u_{k-\underline{d}-1}$  is available at the actuator. In case  $\tau_{k-\underline{d}-1} - \sum_{l=k-\underline{d}-1}^{k-1} h_l < 0$ , then  $u_{k-\underline{d}-1}$  might be active before  $s_k$ . Since, we are only interested, here, in the interval  $[s_k, s_{k+1})$ , we take the maximum of this value and zero in (A.7). For the other values of  $t_j^k$ , the recursion can be derived similarly, which leads to

$$t_j^k = \min \left[ t_{j+1}^k, \max \left\{ 0, \tau_j - \sum_{l=j}^{k-1} h_l \right\} + m_j h_{\max} \right],$$

for  $k - \bar{d} - \bar{\delta} \leq j \leq k - \underline{d}$ ,  $m_j$  satisfying (3.13), and with  $t_{k-\underline{d}+1}^k := h_k$ . The elaboration of this recursive relation yields the characterization of (3.22).

## A.4 Proof of Theorem 4.3.2

The proof of Theorem 4.3.2 consists of two parts. First the convex overestimation of the set  $\mathcal{FG}^x$ , defined in (4.21), is explained, and, second, the stability of the discrete-time NCS model (4.5), (4.9) is proven. Similar to the proof of Theorem 4.3.1 an overapproximation of the set  $\mathcal{FG}^x$  can be made. Therefore,

define the set  $\overline{\mathcal{FG}}^x$

$$\overline{\mathcal{FG}}^x = \left\{ \left( \overline{F}_0^x + \sum_{i=1}^{\nu} \delta_i \overline{F}_i^x, \overline{G}_0^x + \sum_{i=1}^{\nu} \delta_i \overline{G}_i^x \right) : \delta_i \in [0, 1], i = 1, 2, \dots, \nu \right\}, \quad (\text{A.8})$$

with  $\overline{F}_0^x = F_0^x + \sum_{i=1}^{\nu} \underline{\alpha}_i F_i^x$ ,  $\overline{F}_i^x = (\overline{\alpha}_i - \underline{\alpha}_i) F_i^x$ ,  $\overline{G}_0^x = G_0^x + \sum_{i=1}^{\nu} \underline{\alpha}_i G_i^x$ , and  $\overline{G}_i^x = (\overline{\alpha}_i - \underline{\alpha}_i) G_i^x$ , with  $\overline{\alpha}_i = \max_{\tau \in [\tau_{\min}, \tau_{\max}]} \alpha_i(\tau)$  and  $\underline{\alpha}_i = \min_{\tau \in [\tau_{\min}, \tau_{\max}]} \alpha_i(\tau)$ . Similar to the proof of Theorem 4.3.1, the set  $\overline{\mathcal{FG}}$  is still an infinite set of matrices. However, each matrix in this set can be written as a convex combination of the generators of the corresponding set, which are defined as the set  $\mathcal{H}_{FG}^x$  in (4.23). The separate matrices in  $\mathcal{H}_{FG}^x$  are denoted individually by  $(H_{F,j}^x, H_{G,j}^x)$ ,  $j = 1, 2, \dots, 2^\nu$ . Moreover,  $H_{F,j}^x$  and  $H_{G,j}^x$  occur always in combination, because they depend on the same values of  $\alpha_i$ . Based on these generators,  $\overline{\mathcal{FG}}^x$  can be written as:

$$\text{co}(\mathcal{H}_{FG}^x) = \left\{ \left( \sum_{j=1}^{2^\nu} (\phi_j H_{F,j}^x), \sum_{j=1}^{2^\nu} (\phi_j H_{G,j}^x) \right) : \sum_{j=1}^{2^\nu} \phi_j = 1, \phi_j \in [0, 1], j = 1, 2, \dots, 2^\nu \right\}. \quad (\text{A.9})$$

Then, the following relation between the different defined sets holds

$$\mathcal{FG}^x \subseteq \overline{\mathcal{FG}}^x = \text{co}(\mathcal{H}_{FG}^x). \quad (\text{A.10})$$

Based on the system model (4.22), with  $\chi_k = (x_k^T \ x_{k-1}^T)^T$  and the candidate Lyapunov function  $V(\chi_k) = \chi_k^T \begin{pmatrix} \tilde{P} + T & -T \\ -T & R + T \end{pmatrix} \chi_k$ , the satisfaction of the LMIs:

$$\begin{aligned} \begin{pmatrix} \tilde{P} + T & -T \\ -T & R + T \end{pmatrix} &= \begin{pmatrix} \tilde{P} + T & -T \\ -T & R + T \end{pmatrix}^T > 0 \\ \tilde{C}^T(\tau_k) \begin{pmatrix} \tilde{P} + T & -T \\ -T & R + T \end{pmatrix} \tilde{C}(\tau_k) - (1 - \gamma) \begin{pmatrix} \tilde{P} + T & -T \\ -T & R + T \end{pmatrix} &< 0, \end{aligned} \quad (\text{A.11})$$

with  $\tilde{C}(\tau_k) = \begin{pmatrix} \hat{\Theta}_0 - G^x(\tau_k) \overline{K} & -F^x(\tau_k) \overline{K} \\ I & 0 \end{pmatrix}$  for all possible values of  $\alpha_i$ ,  $i = 1, 2, \dots, \nu$ , is sufficient for the GES of the fixed point  $x = 0$  of (4.22). Since (4.24) holds for all  $(H_{F,j}^x, H_{G,j}^x) \in \mathcal{H}_{FG}^x$  with  $j = 1, 2, \dots, 2^\nu$ , we have that, by using the Schur complement:

$$\begin{pmatrix} -R + (1 - \gamma)(\tilde{P} + T) & \star & \star & \star \\ -(1 - \gamma)T & (1 - \gamma)(R + T) & \star & \star \\ \tilde{P}(\hat{\Theta}_0 - H_{G,j}^x \overline{K}) & -\tilde{P}(H_{F,j}^x \overline{K}) & \tilde{P} & \star \\ T(\hat{\Theta}_0 - H_{G,j}^x \overline{K} - I) & -T(H_{F,j}^x \overline{K}) & 0 & T \end{pmatrix} > 0,$$

for all  $(H_{F,j}^x, H_{G,j}^x) \in \mathcal{H}_{FG}^x$  and with  $0 \leq \gamma < 1$ . Note that  $\star$  denotes matrices that render the overall matrix symmetric. Since  $\phi_j \geq 0$  for all  $j \in \{1, 2, \dots, 2^\nu\}$  and  $\sum_{j=1}^{2^\nu} \phi_j = 1$ , it holds that

$$\begin{aligned} 0 &< \sum_{j=1}^{2^\nu} \phi_j \begin{pmatrix} -R + (1-\gamma)(\tilde{P} + T) & \star & \star & \star \\ -(1-\gamma)T & (1-\gamma)(R+T) & \star & \star \\ \tilde{P}(\hat{\Theta}_0 - H_{G,j}^x \bar{K}) & -\tilde{P}(H_{F,j}^x \bar{K}) & \tilde{P} & \star \\ T(\hat{\Theta}_0 - H_{G,j}^x \bar{K} - I) & -T(H_{F,j}^x \bar{K}) & 0 & T \end{pmatrix} \\ &= \begin{pmatrix} -R + (1-\gamma)(\tilde{P} + T) & \star & \star & \star \\ -(1-\gamma)T & (1-\gamma)(R+T) & \star & \star \\ \tilde{P}(\hat{\Theta}_0 - \sum_{j=1}^{2^\nu} \phi_j H_{G,j}^x \bar{K}) & -\tilde{P} \sum_{j=1}^{2^\nu} \phi_j H_{F,j}^x \bar{K} & \tilde{P} & \star \\ T(\hat{\Theta}_0 - \sum_{j=1}^{2^\nu} \phi_j H_{G,j}^x \bar{K} - I) & -T \sum_{j=1}^{2^\nu} \phi_j H_{F,j}^x \bar{K} & 0 & T \end{pmatrix}. \end{aligned}$$

Consequently, it holds that

$$\begin{pmatrix} -R + (1-\gamma)(\tilde{P} + T) & \star & \star & \star \\ -(1-\gamma)T & (1-\gamma)(R+T) & \star & \star \\ \tilde{P}(\hat{\Theta}_0 - \bar{H}_G^x \bar{K}) & -\tilde{P}(\bar{H}_F^x \bar{K}) & \tilde{P} & \star \\ T(\hat{\Theta}_0 - \bar{H}_G^x \bar{K} - I) & -T(\bar{H}_F^x \bar{K}) & 0 & T \end{pmatrix} > 0, \quad (\text{A.12})$$

for all  $(\bar{H}_F^x, \bar{H}_G^x) \in \text{co}(\mathcal{H}_{FG}^x)$ . Based on the fact that (A.10) holds, we have that (A.12) implies that:

$$\begin{pmatrix} -R + (1-\gamma)(\tilde{P} + T) & \star & \star & \star \\ -(1-\gamma)T & (1-\gamma)(R+T) & \star & \star \\ \tilde{P}(\hat{\Theta}_0 - G^x(\tau_k) \bar{K}) & -\tilde{P}(F^x(\tau_k) \bar{K}) & \tilde{P} & \star \\ T(\hat{\Theta}_0 - G^x(\tau_k) \bar{K} - I) & -T(F^x(\tau_k) \bar{K}) & 0 & T \end{pmatrix} > 0,$$

for all  $\tau_k \in [\tau_{\min}, \tau_{\max}]$ . Applying the Schur complement again gives (A.11), which shows that  $V(\chi_k) = \chi_k^T \begin{pmatrix} \tilde{P} + T & -T \\ -T & R + T \end{pmatrix} \chi_k$  is a common quadratic Lyapunov function for (4.19), (4.9) which proves that the origin  $\chi = 0$  of (4.19), (and equivalently of (3.3), (4.9)) is GES. However, to apply the Schur complement it is needed that both  $\tilde{P}$  and  $T$  are positive definite instead of  $\begin{pmatrix} \tilde{P} + T & -T \\ -T & R + T \end{pmatrix} > 0$ . (Note that this demand is indeed included in the theorem.)

## A.5 Proof of Lemma 4.3.4

To compare the stability characterization of the adapted common quadratic Lyapunov approach in Corollary 4.3.3 and the L-K approach in Theorem 4.3.2, we exploit that the candidate L-K functional (4.17) can be rewritten as  $V(\chi_k) =$

$\chi_k^T \begin{pmatrix} \tilde{P} + T & -T \\ -T & R + T \end{pmatrix} \chi_k$ . This shows that every L-K functional of this form actually is a common quadratic Lyapunov function of the form  $V(\chi_k) = \chi_k^T \bar{P} \chi_k$ , with  $\bar{P} = \begin{pmatrix} \tilde{P} + T & -T \\ -T & R + T \end{pmatrix}$ . Due to the fact that in the L-K approach it is demanded that  $\tilde{P} = \tilde{P}^T > 0$ ,  $R = R^T > 0$ , and  $T = T^T > 0$ , while in the common quadratic Lyapunov approach we would then demand only that  $\begin{pmatrix} \tilde{P} + T & -T \\ -T & R + T \end{pmatrix} > 0$ , slightly more conservative results may be obtained, using the L-K approach.

## A.6 Proof of Lemma 4.3.5

To prove the bounds on the intersample behavior, both the case with  $\tilde{t} < \tau_k$  and the case with  $\tilde{t} \geq \tau_k$  will be considered. First the case  $\tilde{t} \geq \tau_k$  is described. Note that, (4.27) implies:

$$|x(s_k + \tilde{t})| \leq |e^{A\tilde{t}} x_k| + \left| \int_0^{\tilde{t}-\tau_k} e^{As} ds B u_k \right| + \left| \int_{\tilde{t}-\tau_k}^{\tilde{t}} e^{As} ds B u_{k-1} \right|. \quad (\text{A.13})$$

Using Wazewski's inequalities, see [116], and [117]:

$$|e^{A\tilde{t}} x| \leq |x| e^{\lambda_{\max} \tilde{t}}, \quad (\text{A.14})$$

with  $\lambda_{\max} = \frac{1}{2} \max(\text{eig}(A + A^T))$ , the terms in the above inequality can be upper bounded to obtain an inequality of the form:

$$|x(s_k + \tilde{t})| \leq \hat{c}_0 |x_k| + \hat{c}_1 |u_k| + \hat{c}_2 |u_{k-1}|. \quad (\text{A.15})$$

For  $\tau_k \in [\tau_{\min}, \tau_{\max}]$  and  $\tau_k < \tilde{t} \leq h$ , the first term in (A.13) can be rewritten as:

$$|e^{A\tilde{t}} x_k| \leq \hat{c}_0 |x_k|, \text{ with } \hat{c}_0 := \begin{cases} \max\{e^{\lambda_{\max} h}, e^{\lambda_{\max} \tau_{\min}}\} & \text{for } \lambda_{\max} \neq 0 \\ 1 & \text{for } \lambda_{\max} = 0. \end{cases} \quad (\text{A.16})$$

To rewrite the second term in the right-hand side of (A.13), the integrals are rewritten as follows:

$$\left| \int_0^{\tilde{t}-\tau_k} e^{As} B u_k ds \right| \leq \|B\| |u_k| \int_0^{\tilde{t}-\tau_k} e^{\lambda_{\max} s} ds.$$

The integral in the right-hand side of this inequality can be solved exactly, because  $\lambda_{\max}$  is a real number, yielding:

$$\begin{aligned} \left| \int_0^{\tilde{t}-\tau_k} e^{As} B u_k ds \right| &\leq \hat{c}_1 |u_k|, \\ \text{with } \hat{c}_1 &:= \begin{cases} \|B\| \frac{1}{\lambda_{\max}} (e^{\lambda_{\max}(h-\tau_{\min})} - 1) & \text{if } \lambda_{\max} \neq 0 \\ \|B\| (h - \tau_{\min}) & \text{if } \lambda_{\max} = 0. \end{cases} \end{aligned} \quad (\text{A.17})$$



The upper bound of the last term of (A.13) can be derived in a similar fashion:

$$\left| \int_{\tilde{t}-\tau_k}^{\tilde{t}} e^{As} ds B u_{k-1} \right| \leq \hat{c}_2 |u_{k-1}|, \quad (\text{A.18})$$

$$\text{with } \hat{c}_2 := \begin{cases} \|B\| \frac{1}{\lambda_{\max}} (e^{\lambda_{\max} h} - 1) & \text{if } \lambda_{\max} \neq 0 \\ \|B\| \tau_{\max} & \text{if } \lambda_{\max} = 0. \end{cases}$$

Next the second case ( $\tilde{t} < \tau_k$ ) has to be studied. The norm of  $|x(s_k + \tilde{t})|$  in (4.26) can be upper bounded as follows:

$$|x(s_k + \tilde{t})| \leq |e^{A\tilde{t}} x_k| + \left| \int_0^{\tilde{t}} (e^{As}) B u_{k-1} ds \right|. \quad (\text{A.19})$$

Based on Wazewski's inequalities (A.14), we obtain an inequality of the form:

$$|x(s_k + \tilde{t})| \leq \bar{c}_0 |x_k| + \bar{c}_2 |u_{k-1}|. \quad (\text{A.20})$$

The first term in the right-hand side of (A.19) is given by:

$$|e^{A\tilde{t}} x_k| \leq \bar{c}_0 |x_k|, \quad \text{with } \bar{c}_0 := \max\{1, e^{\lambda_{\max} \tau_{\max}}\}. \quad (\text{A.21})$$

The upper bound of the second term in the right-hand side of (A.19) can be derived analogously to (A.17):

$$\left| \int_0^{\tilde{t}} e^{As} B u_{k-1} ds \right| \leq \bar{c}_2 |u_{k-1}|, \quad \text{with } \bar{c}_2 := \begin{cases} \|B\| \frac{e^{\lambda_{\max} \tau_{\max}} - 1}{\lambda_{\max}} & \text{if } \lambda_{\max} \neq 0 \\ \|B\| \tau_{\max} & \text{if } \lambda_{\max} = 0. \end{cases} \quad (\text{A.22})$$

Consequently, the inequality in (A.13), (A.19) can be replaced by:

$$|x(s_k + \tilde{t})| \leq c_0 |x_k| + c_1 |u_k| + c_2 |u_{k-1}|, \quad \forall \tilde{t} \in [0, h), \quad (\text{A.23})$$

with

$$c_0 = \max\{\hat{c}_0, \bar{c}_0\}, \quad c_1 = \hat{c}_1, \quad c_2 = \max\{\hat{c}_2, \bar{c}_2\} = \hat{c}_2. \quad (\text{A.24})$$

## A.7 Proof of Theorem 4.3.6

In this proof, we combine the results of Theorem 4.3.1 (or Theorem 4.3.2) and Lemma 4.3.5. First, the proof is given for Theorem 4.3.1 in combination with the extended state feedback controller (4.8). Second, the proof for the state feedback controller (4.9) in combination with Theorems 4.3.1 and 4.3.2 is given.

**Extended state feedback controller and the common quadratic Lyapunov approach** Based on Lemma 4.3.5, in combination with the boundedness of the control input from (4.8), i.e.  $|u_k| \leq \|K\| |\xi_k|$ , it holds that:

$$|x(s_k + \tilde{t})| \leq c_0 |x_k| + c_1 \|K\| |\xi_k| + c_2 |u_{k-1}|, \quad (\text{A.25})$$

with  $c_0$ ,  $c_1$ , and  $c_2$  defined in (A.24), (A.22), (A.21), (A.18), (A.17), and (A.16). Note that the initial condition of (3.1), (4.8), applicable for (A.25) is given by  $\bar{\xi}_0 = (x_0^T \ u_{-1}^T)^T$  such that it includes both the current state  $x_0$  and the past control input  $u_{-1}$ . To prove asymptotic stability of the intersample behavior, it needs to be proven that the second condition in Lemma 2.2.2 holds. If Theorem 4.3.1 is satisfied, then based on  $|\xi_k|_P^2 = \xi_k^T P \xi_k$  and (4.13) it holds that:

$$|\xi_{k+1}|_P^2 < (1 - \gamma)|\xi_k|_P^2 \Rightarrow |\xi_k|_P^2 < (1 - \gamma)^k |\xi_0|_P^2, \quad (\text{A.26})$$

with  $0 < \gamma < 1$ . To rewrite (A.25) in terms of the initial condition  $\bar{\xi}_0$ , the following relation between  $x_k$  and  $\xi_k$  is used:  $x_k = C_x \xi_k$ , with  $C_x = (I \ 0)$ . Moreover, the following relation between  $u_{k-1}$  and  $\xi_k$  is needed:  $u_{k-1} = C_u \xi_k$ , with  $C_u = (0 \ I)$ . Using the fact that  $\lambda_{\min}(P)|\xi_k|^2 \leq |\xi_k|_P^2 \leq \lambda_{\max}(P)|\xi_k|^2$ , the fact that  $|x_k|^2 \leq \|C_x P^{-\frac{1}{2}}\|^2 |\xi_k|_P^2$ ,  $|u_{k-1}|^2 \leq \|C_u P^{-\frac{1}{2}}\|^2 |\xi_k|_P^2$ , and relation (A.26), the bound on the intersample behavior, described by (A.25), can be rewritten as follows:

- for  $k = 0$ :

$$|x(s_k + \tilde{t})| \leq (c_0 + c_1 \|K\| + c_2) |\bar{\xi}_0|, \quad (\text{A.27})$$

- for  $k \geq 1$ :

$$\begin{aligned} |x(s_k + \tilde{t})| &\leq \left( \|C_x P^{-\frac{1}{2}}\| c_0 + \sqrt{\frac{1}{\lambda_{\min}(P)}} c_1 \|K\| \right) \sqrt{\lambda_{\max}(P)(1 - \gamma)^k} |\bar{\xi}_0| \\ &\quad + c_2 \|C_u P^{-\frac{1}{2}}\| \sqrt{\lambda_{\max}(P)(1 - \gamma)^k} |\bar{\xi}_0|, \end{aligned} \quad (\text{A.28})$$

for  $0 \leq \tilde{t} \leq h$ . Since  $\gamma \in (0, 1)$ , (A.28) decreases for increasing values of  $k$ ,  $\forall k \geq 1$ . Then, the following upper bound for  $x(t)$  can be found:

$$|x(t)| \leq \bar{\beta}(t) |\bar{\xi}_0|, \quad (\text{A.29})$$

with  $\bar{\beta}(t)$  a non-increasing function of  $t$  according to

$$\bar{\beta}(t) = \begin{cases} \max\{\beta_0, \beta_1\} & \text{for } t \in [0, s_1), \\ \beta_k & \text{for } k \geq 1 \text{ and } t \in [s_k, s_{k+1}), \end{cases} \quad (\text{A.30})$$

with

$$\begin{aligned} \beta_0 &= c_0 + c_1 \|K\| + c_2, \\ \beta_k &= \left( \|C_x P^{-\frac{1}{2}}\| c_0 + \sqrt{\frac{1}{\lambda_{\min}(P)}} c_1 \|K\| \right) \sqrt{\lambda_{\max}(P)(1 - \gamma)^k} \\ &\quad + c_2 \|C_u P^{-\frac{1}{2}}\| \sqrt{\lambda_{\max}(P)(1 - \gamma)^k} \quad \text{for } k \geq 1. \end{aligned} \quad (\text{A.31})$$

Note that  $\bar{\beta}(t)$  is a non-increasing function, because it decreases at the sampling instants  $s_k$ ,  $\forall k \geq 1$ . It is not difficult to find a function  $\beta(t) \in \mathcal{KL}$ , such that  $\beta(t) \geq \bar{\beta}(t)$ . Therefore, it is concluded that, based on Lemma 2.2.2, the NCS denoted by (3.1), (4.8) is GAS if the conditions of Theorem 4.3.1 are satisfied.

**State-feedback controller and the common quadratic Lyapunov approach** If the state feedback controller is considered, a slightly different bound for the control input is used:  $|u_k| \leq \|\bar{K}\| |x_k|$ . Then, (A.25) is rewritten as:

$$|x(s_k + \tilde{t})| \leq c_0 |x_k| + c_1 \|\bar{K}\| |x_k| + c_2 |u_{k-1}|. \quad (\text{A.32})$$

Analogous to the previous paragraph, it can be proven that (A.29) holds, with  $\bar{\beta}(t)$  defined in (A.30) and (A.31), where  $\|K\|$  is replaced by  $\|\bar{K}\|$ . Then, a function  $\beta(t) \geq \bar{\beta}(t)$ , with  $\beta(t) \in \mathcal{KL}$  can be derived. According to Lemma 2.2.2, the continuous-time NCS (3.1), (4.9) is GAS.

**State-feedback controller and the L-K functional** For the Lyapunov-Krasovskii based functional in Theorem 4.3.2, another state vector is considered, i.e.  $\chi_k = (x_k^T \ x_{k-1}^T)^T$ . Therefore, the derivation of the class  $\mathcal{KL}$ -function  $\beta(t)$  is slightly different. Based on  $|u_k| \leq \|\bar{K}\| |x_k|$ , it holds for the intersample behavior, defined in (4.28), that:

$$|x(s_k + \tilde{t})| \leq c_0 |x_k| + c_1 \|\bar{K}\| |x_k| + c_2 \|\bar{K}\| |x_{k-1}|, \quad (\text{A.33})$$

with  $c_0$ ,  $c_1$ , and  $c_2$  defined in (A.24), (A.22), (A.21), (A.18), (A.17), and (A.16). Note that the initial condition of (3.1), (4.8), applicable for (A.25) is given by  $\bar{\chi}_0 = (x_0^T \ x_{-1}^T)^T$  such that it includes both the current state  $x_0$  and the past state  $x_{-1}$ . To prove global asymptotic stability of (A.25), it needs to be proven that the third condition in Lemma 2.2.2 holds. If Theorem 4.3.2 is satisfied, then for the extended state  $\chi_k$  it holds that:

$$|\chi_{k+1}|_{\overline{P_{RT}}}^2 < (1 - \gamma) |\chi_k|_{\overline{P_{RT}}}^2 \Rightarrow |\chi_k|_{\overline{P_{RT}}}^2 < (1 - \gamma)^k |\chi_0|_{\overline{P_{RT}}}^2, \quad (\text{A.34})$$

with  $0 < \gamma < 1$  and  $\overline{P_{RT}} = \begin{pmatrix} \tilde{P} + T & -T \\ -T & R + T \end{pmatrix}$ . To prove that  $x_k$  converges to zero, the following relation between  $x_k$  and  $\chi_k$  is used:  $x_k = C_x \chi_k$ , with  $C_x = (I \ 0)$ . Using the fact that  $\lambda_{\min}(\overline{P_{RT}}) |\chi_k|^2 \leq |\chi_k|_{\overline{P_{RT}}}^2 \leq \lambda_{\max}(\overline{P_{RT}}) |\chi_k|^2$  and relation (A.34), the bound on the intersample behavior, described by (A.33), can be rewritten:

- for  $k = 0$ :

$$|x(s_k + \tilde{t})| \leq (c_0 + (c_1 + c_2) \|\bar{K}\|) |\bar{\chi}_0|, \quad (\text{A.35})$$

- for  $k \geq 1$ :

$$\begin{aligned} |x(s_k + \tilde{t})| &\leq \|C_x \overline{P_{RT}}^{-\frac{1}{2}}\| (c_0 + c_1 \|\bar{K}\|) \sqrt{\lambda_{\max}(\overline{P_{RT}}) (1 - \gamma)^k} |\bar{\chi}_0| \\ &\quad + c_2 \|\bar{K}\| \|C_x \overline{P_{RT}}^{-\frac{1}{2}}\| \sqrt{\lambda_{\max}(\overline{P_{RT}}) (1 - \gamma)^{k-1}} |\bar{\chi}_0|, \end{aligned} \quad (\text{A.36})$$

for  $0 \leq \tilde{t} \leq h$ . Since  $\gamma \in (0, 1)$ , (A.36) decreases for increasing values of  $k$ ,  $\forall k \geq 1$ . Then, the following upper-bound for  $x(t)$  can be found:

$$|x(t)| \leq \bar{\beta}(t) |\bar{\chi}_0|, \quad (\text{A.37})$$

with  $\bar{\beta}(t)$  a decreasing function of  $t$  according to

$$\bar{\beta}(t) = \begin{cases} \max\{\beta_0, \beta_1\} & \text{for } t \in [0, s_1), \\ \beta_1 & \text{for } k \geq 1 \text{ and } t \in [s_k, s_{k+1}), \end{cases} \quad (\text{A.38})$$

with

$$\begin{aligned} \beta_0 &= c_0 + (c_1 + c_2)\|\bar{K}\|, \\ \beta_k &= (c_0 + c_1\|K\|)\|C_x \overline{P_{RT}}^{-\frac{1}{2}}\| \sqrt{\lambda_{\max}(\overline{P_{RT}})(1-\gamma)^k} \\ &\quad + c_2\|\bar{K}\|\|C_x \overline{P_{RT}}^{-\frac{1}{2}}\| \sqrt{\lambda_{\max}(\overline{P_{RT}})(1-\gamma)^k} \quad \text{for } k \geq 1. \end{aligned}$$

Note that  $\bar{\beta}(t)$  is a decreasing function, but not of class  $\mathcal{KL}$ , because it decreases only at the sampling instants  $s_k$ ,  $\forall k \geq 1$ . However, it is not difficult to find a function  $\beta(t) \in \mathcal{KL}$ , such that  $\beta(t) \geq \bar{\beta}(t)$ . Therefore, it is concluded that, based on the conditions in Lemma 2.2.2, the NCS denoted by (3.1), (4.9) is GAS if the conditions of Theorem 4.3.2 are satisfied.

## A.8 Proof of Lemma 4.4.2

To determine the minimum and maximum values of the parameter  $t_j^k$ , the definition of  $t_j^k$  in (3.22) is considered. First, the lower bound of  $t_j^k$  will be derived. Based on (3.22), it holds for  $j = k - \underline{d}$  that:

$$t_{k-\underline{d}}^k = \min \left\{ \max \left\{ 0, \tau_{k-\underline{d}} - \sum_{l=k-\underline{d}}^{k-1} h_l \right\} + m_{k-\underline{d}} h_{\max}, h_k \right\}. \quad (\text{A.39})$$

To obtain the smallest value,  $m_{k-\underline{d}} = 0$  needs to be considered. In general, the minimum value of  $t_{k-\underline{d}}^k$  is given by:

$$t_{k-\underline{d},\min}^k = \min \{ \tau_{\min} - \underline{d} h_{\max}, h_{\min} \}, \quad (\text{A.40})$$

where it is used that  $\tau_{k-\underline{d}} - \underline{d} h_{\max} \geq 0$ , due to the definition of  $\underline{d}$ . Next, consider  $j < k - \underline{d}$ . To determine the minimum value of  $t_j^k$ , as defined in (3.22), it is used that:  $\min(\tau_j - \sum_{l=j}^{k-1} h_l) = \tau_{\min} - (k-j)h_{\max}$ ,  $j \in \{k - \bar{d} - \bar{\delta} + 1, \dots, k - \underline{d} - 1\}$ . Moreover, to obtain the smallest value of  $t_j^k$ ,  $m_j = 0$  needs to be considered for the corresponding value of  $j$  with  $j \in \{k - \bar{d} - \bar{\delta} + 1, \dots, k - \underline{d} - 1\}$ . Then, (3.22) reduces to

$$\begin{aligned} t_{j,\min}^k &= \min \left\{ \max\{0, \tau_{\min} - (k-j)h_{\max}\}, \max\{0, \tau_{\min} - (k-j+1)h_{\max}\}, \right. \\ &\quad \left. \dots, \tau_{\min} - \underline{d} h_{\max}, h_{\min} \right\}, \end{aligned} \quad (\text{A.41})$$

for  $j \in \{k - \bar{d} - \bar{\delta}, \dots, k - \underline{d} - 1\}$ . Based on the definition of  $\underline{d}$ , it holds that  $\tau_{\min} - (k-j)h_{\max} \leq 0$ , for  $j \in \{k - \bar{d} - \bar{\delta}, \dots, k - \underline{d} - 1\}$ . Then, (A.41) reduces to  $t_{j,\min}^k = 0$  for  $j < k - \underline{d}$ , because  $h_{\min} \geq 0$  and  $\tau_{\min} - \underline{d} h_{\max} \geq 0$ .

Second, consider the upper bound of  $t_j^k$ ,  $j \in \{k - \bar{d} - \bar{\delta} + 1, \dots, k - \underline{d}\}$ . Note that, by definition, it holds that  $t_{k-\bar{d}-\bar{\delta}}^k = 0$ . Before a generic solution is derived, first two specific cases of  $t_j^k$  are considered, i.e.  $t_{k-\underline{d}}^k$  and  $t_{k-\underline{d}-1}^k$  to show the differences between a situation with and without packet dropouts. The upper bound of  $t_{k-\underline{d}}^k$  can be obtained from (A.39). Two cases are distinguished, i.e. the case with and without packet dropouts.

- If packet dropouts occur,  $m_{k-\underline{d}} = 1$  is allowed. The maximum value of  $t_{k-\underline{d}}^k$  is then given by  $h_{\max}$ , because  $\tau_{k-\underline{d}} - \sum_{l=k-\underline{d}}^{k-1} h_{\min} + m_{k-\underline{d}} h_{\max}$  is always larger than (or equal to)  $h_{\max}$ .
- In the case without packet dropouts, thus  $m_{k-\underline{d}} := 0$  the maximum value can be obtained from:  $t_{k-\underline{d},\max}^k = \min\{\tau_{\max} - \underline{d}h_{\min}, h_{\max}\}$ .

For  $j = k - \underline{d} - 1$ , the upper bound of  $t_j^k$  can be determined, based on:

$$t_{k-\underline{d}-1,\max}^k = \min\left\{\max\{0, \tau_{\max} - (\underline{d} + 1)h_{\min}\} + m_{k-\underline{d}-1}h_{\max}, \tau_{\max} - \underline{d}h_{\min} + m_{k-\underline{d}}h_{\max}, h_{\max}\right\}. \quad (\text{A.42})$$

The cases with and without packet dropouts are considered separately to determine the upper bound:

- In the case of packet dropouts, the largest value of  $t_{k-\underline{d}-1}^k$  occurs for  $m_{k-\underline{d}-1} = 1$ . Then, the maximum value of  $t_{k-\underline{d}-1}^k$  is given by:

$$\min\{\tau_{\max} - \underline{d}h_{\min} + m_{k-\underline{d}}h_{\max}, h_{\max}\},$$

because  $\max\{0, \tau_{\max} - (\underline{d} + 1)h_{\min}\} + h_{\max} \geq h_{\max}$ . The two following cases can be distinguished:

- if also  $m_{k-\underline{d}} = 1$  (which is allowed if  $\bar{\delta} > 1$ ), the maximum value is  $t_{k-\underline{d}-1,\max}^k = h_{\max}$ ,
- if  $m_{k-\underline{d}} = 0$ , which is necessary if  $\bar{\delta} = 1$ , then the maximum is given by:

$$t_{k-\underline{d}-1,\max}^k = \begin{cases} \min(\tau_{\max} - \underline{d}h_{\min}, h_{\max}) & \text{if } \bar{d} > \underline{d} \\ 0 & \text{if } \bar{d} = \underline{d}. \end{cases} \quad (\text{A.43})$$

For  $\bar{d} > \underline{d}$ , it is used that  $\tau_{\max} - \underline{d}h_{\min} \geq 0$ , due to the definition of  $\underline{d}$ .

- For the case without packet dropouts i.e.  $m_{k-\underline{d}-1} = 0$  and  $m_{k-\underline{d}} = 0$ , the maximum of  $t_{k-\underline{d}-1}^k$  is given by:

$$t_{k-\underline{d}-1,\max}^k = \begin{cases} \min(\tau_{\max} - (\underline{d} + 1)h_{\min}, h_{\max}) & \text{if } \bar{d} > \underline{d} + 1 \\ 0 & \text{if } \bar{d} = \underline{d} + 1. \end{cases} \quad (\text{A.44})$$

Due to the definition of  $\bar{d}$  and  $\underline{d}$ , it holds that  $\tau_{\max} - (\underline{d} + 1)h_{\min} \in (0, h_{\min}]$ . Note that if  $\bar{d} = \underline{d}$  and  $\bar{\delta} = 0$ , i.e. no packet dropouts and no delays,  $t_{k-\underline{d}-1}^k$  does not exist, due to the definition of  $j$  in (3.22).

These examples show that a distinction between the case with and without packet dropouts needs to be made. Moreover, the maximum number of subsequent packet dropouts  $\bar{\delta}$  needs to be considered in the computation of the upper bound of  $t_j^k$  for  $j \in \{k - \bar{d} - \bar{\delta} + 1, \dots, k - \underline{d}\}$ . The value of  $t_{k - \bar{d} - \bar{\delta}}^k$  is not included, because it is by definition, see (3.22), equal to zero. To derive a generic solution for the upper bound, consider the definition of  $t_j^k$  in (3.22). To obtain the maximum value of  $t_j^k$ , (3.22) can be replaced by the following relation:

$$\begin{aligned} \max(t_j^k) = \min \left\{ \begin{aligned} &\max\{0, \tau_{\max} - (k - j)h_{\min}\} + m_j h_{\max}, \\ &\max\{0, \tau_{\max} - (k - j - 1)h_{\min}\} + m_{j+1} h_{\max}, \dots, \\ &\max\{0, \tau_{\max} - \underline{d}h_{\min}\} + m_{k - \underline{d}} h_{\max}, h_{\max} \end{aligned} \right\}, \end{aligned} \quad (\text{A.45})$$

for  $j \in \{k - \bar{d} - \bar{\delta} + 1, \dots, k - \underline{d}\}$ . Analogous to the two described examples, the cases with and without packet dropouts are considered.

- If packet dropouts occur, i.e.  $\bar{\delta} > 0$ , at maximum  $\bar{\delta}$  subsequent times  $m_j = 1$  occurs. Thus, according to (A.45), as long as  $j > k - \bar{\delta} - \underline{d}$ , all values from  $m_j$  until  $m_{k - \underline{d}}$  can be equal to one. Then  $t_{j, \max}^k$  is equal to  $h_{\max}$ .

For  $j = k - \bar{\delta} - \underline{d}$  it holds that at least one of the values of  $m_{k - \bar{\delta} - \underline{d}}, \dots, m_{k - \underline{d}}$  has to be equal to zero. It is easy to see that the largest value of  $t_{k - \bar{\delta} - \underline{d}}^k$  is obtained if  $m_{k - \underline{d}} = 0$  and all other values of  $m_j$ ,  $j \in \{k - \bar{\delta} - \underline{d}, \dots, k - \underline{d} - 1\}$ , are equal to one. Then for  $t_{k - \bar{\delta} - \underline{d}, \max}^k$  is given by

$$t_{k - \bar{\delta} - \underline{d}, \max}^k = \min\{\tau_{\max} - \underline{d}h_{\min}, h_{\max}\}.$$

Due to the definition of  $\underline{d}$  it is indeed possible that  $\tau_{\max} - \underline{d}h_{\min} > h_{\max}$ . Then,  $t_{k - \bar{\delta} - \underline{d}, \max}^k$  is given by  $h_{\max}$ , because  $t_j^k$  is derived in the interval  $[s_k, s_{k+1})$ , with  $s_{k+1} - s_k \leq h_{\max}$ . Moreover, note that it holds that  $\tau_{\max} - \underline{d}h_{\min} > 0$ , due to the definition of  $\underline{d}$ .

For smaller values of  $j$ , i.e.  $j \in \{k - \bar{d} - \bar{\delta} + 1, \dots, k - \bar{\delta} - \underline{d} - 1\}$ , a similar reasoning holds, where the largest value of  $t_j^k$  is obtained if  $m_{j + \bar{\delta}} = 0$ , i.e.  $\bar{\delta}$  subsequent packets are dropped, denoted by  $m_j = 1, m_{j+1} = 1, \dots, m_{j + \bar{\delta} - 1} = 1$ , if  $j \in \{k - \bar{d} - \bar{\delta} + 1, \dots, k - \bar{\delta} - \underline{d} - 1\}$  is considered. Note that it holds that  $\tau_{\max} - (k - j - \bar{\delta})h_{\min} > 0$ , for  $j \in \{k - \bar{d} - \bar{\delta} + 1, \dots, k - \bar{\delta} - \underline{d}\}$ . To prove this, consider the smallest value of  $j$ , i.e.  $j = k - \bar{d} - \bar{\delta} + 1$ , which results in the largest value of  $(k - j - \bar{\delta})h_{\min}$ :

$$\begin{aligned} \tau_{\max} - (\bar{d} - 1)h_{\min} &= \tau_{\max} - \left( \left\lceil \frac{\tau_{\max}}{h_{\min}} \right\rceil - 1 \right) h_{\min} \\ \Rightarrow \tau_{\max} - (\bar{d} - 1)h_{\min} &\in (0, h_{\min}]. \end{aligned} \quad (\text{A.46})$$

Then, analogous to  $j = k - \bar{\delta} - \underline{d}$ , it holds that

$$t_{j, \max}^k = \min\{\tau_{\max} - (k - j - \bar{\delta})h_{\min}, h_{\max}\},$$

for  $j \in \{k - \bar{d} - \bar{\delta} + 1, \dots, k - \bar{\delta} - \underline{d} - 1\}$ . Note that  $\tau_{\max} - (k - j - \bar{\delta})h_{\min} > h_{\max}$  may occur, except for  $j = k - \bar{d} - \bar{\delta} + 1$ . To prove this, first consider  $j = k - \bar{d} - \bar{\delta} + 1$ , for which (A.46) proves that the upper bound of  $t_{k-\bar{d}-\bar{\delta}+1}^k$  is given by  $h_{\min}$ . Second, for larger values of  $j$ , i.e.  $j \in \{k - \bar{d} - \bar{\delta} + 2, \dots, k - \bar{\delta} - \underline{d} - 1\}$  it holds, based on a similar reasoning as in (A.46), that  $t_j^k > h_{\min}$ , which allows for  $t_j^k > h_{\max}$ , with  $h_{\max} \geq h_{\min}$ . Summarizing,  $t_{j,\max}^k$  is given by:

$$t_{j,\max}^k = \begin{cases} \min\{\tau_{\max} - (k - j - \bar{\delta})h_{\min}, h_{\max}\} & \text{if } j \in \{k - \bar{d} - \bar{\delta} + 1, \dots, k - \bar{\delta} - \underline{d}\} \\ h_{\max} & \text{if } j \in \{k - \bar{\delta} - \underline{d} + 1, \dots, k - \underline{d}\}. \end{cases} \quad (\text{A.47})$$

Note that  $j = k - \bar{d} - \bar{\delta}$  gives by definition, see (3.22),  $t_{k-\bar{d}-\bar{\delta}}^k = 0$ .

- If no packet dropouts occur,  $t_{j,\max}^k$  is given by:

$$t_{j,\max}^k = \min\{\tau_{\max} - (k - j)h_{\min}, h_{\max}\}, \text{ for } j \in \{k - \bar{d} + 1, \dots, k - \underline{d}\}. \quad (\text{A.48})$$

Note that for  $j = k - \underline{d}$  it is indeed possible that  $\tau_{\max} - \underline{d}h_{\min} < h_{\max}$ . Moreover, it holds that  $\tau_{\max} - (k - j)h_{\min} > 0$  for  $j \in \{k - \bar{d} + 1, \dots, k - \underline{d}\}$ . To prove this consider the smallest value of  $j$ , which gives  $\tau_{\max} - (\bar{d} - 1)h_{\min}$  that was considered in (A.46).

Concluding, there is no difference between the case with and without packet dropouts, because (A.48) can be obtained from (A.47) for  $\bar{\delta} = 0$ . Note that the previous presented examples are indeed described by (A.47).

## A.9 Proof of Theorem 4.4.7

To prove Theorem 4.4.7, let us repeat the system description based on the Jordan form of the continuous-time system matrix  $A$  in (4.43):

$$\chi_{k+1} = \begin{pmatrix} \mathbf{F} & -F_1^x(\mathbf{t}^k, h_k)\bar{K} & -F_2^x(\mathbf{t}^k, h_k)\bar{K} & \dots & -F_{\bar{d}+\bar{\delta}}^x(\mathbf{t}^k, h_k)\bar{K} \\ I & 0 & 0 & \dots & 0 \\ 0 & I & 0 & \dots & 0 \\ \vdots & \vdots & \ddots & \ddots & \vdots \\ 0 & \dots & 0 & I & 0 \end{pmatrix} \chi_k, \quad (\text{A.49})$$

with  $\mathbf{F} = F_0^x(\mathbf{t}^k, h_k) - G^x(\mathbf{t}^k, h_k)\bar{K}$ , for all  $(F_0^x(\mathbf{t}^k, h_k), F_1^x(\mathbf{t}^k, h_k), \dots, F_{\bar{d}+\bar{\delta}}^x(\mathbf{t}^k, h_k), G^x(\mathbf{t}^k, h_k)) \in \mathcal{FG}^x$ , and  $\mathcal{FG}^x$  defined in (4.42). Recall that the candidate Lyapunov-Krasovskii functional is given by (4.40):

$$V(\chi_k) = x_k^T \tilde{P} x_k + \sum_{\hat{i}=1}^{\bar{d}+\bar{\delta}} x_{k-\hat{i}}^T R_{\hat{i}} x_{k-\hat{i}} + \sum_{\hat{i}=1}^{\bar{d}+\bar{\delta}} (x_{k-\hat{i}+1} - x_{k-\hat{i}})^T T_{\hat{i}} (x_{k-\hat{i}+1} - x_{k-\hat{i}}). \quad (\text{A.50})$$

To prove global asymptotic stability, it needs to be shown that

$$\Delta V(\chi_k) := V(\chi_{k+1}) - V(\chi_k) < -\gamma V(\chi_k),$$

for all  $\chi_k \neq 0$  and with  $\gamma \in [0, 1)$ . Based on (A.49) and (A.50), in combination with the control law (4.9) ( $u_k = -\bar{K}x_k$ ), we can write

$$\begin{aligned} V(\chi_{k+1}) - (1 - \gamma)V(\chi_k) = & x_{k+1}^T \tilde{P}x_{k+1} - (1 - \gamma)x_k^T \tilde{P}x_k + \sum_{\hat{i}=1}^{\bar{d}+\bar{\delta}} x_{k-\hat{i}+1}^T R_{\hat{i}} x_{k-\hat{i}+1} \\ & - (1 - \gamma) \sum_{\hat{i}=1}^{\bar{d}+\bar{\delta}} x_{k-\hat{i}}^T R_{\hat{i}} x_{k-\hat{i}} + \sum_{\hat{i}=1}^{\bar{d}+\bar{\delta}} (x_{k-\hat{i}+2} - x_{k-\hat{i}+1})^T T_{\hat{i}} (x_{k-\hat{i}+2} - x_{k-\hat{i}+1}) \\ & - (1 - \gamma) \sum_{\hat{i}=1}^{\bar{d}+\bar{\delta}} (x_{k-\hat{i}+1} - x_{k-\hat{i}})^T T_{\hat{i}} (x_{k-\hat{i}+1} - x_{k-\hat{i}}) < 0 \end{aligned} \quad (\text{A.51})$$

for  $\chi_k \neq 0$ . For the sake of transparency, this equation is divided in three parts that depend on the matrices  $\tilde{P}$ ,  $R_{\hat{i}}$ , or  $T_{\hat{i}}$ ,  $\hat{i} \in \{1, 2, \dots, \bar{d}+\bar{\delta}\}$ . First, consider the part that depends on the matrix  $\tilde{P}$ . Rewriting this part in a matrix notation, after implementation of the dynamics of (A.49), gives:

$$\begin{aligned} x_{k+1}^T \tilde{P}x_{k+1} - (1 - \gamma)x_k^T \tilde{P}x_k = & \chi_k^T \left( \begin{array}{ccc} \mathbf{F}^T \tilde{P} \mathbf{F} - (1 - \gamma)\tilde{P} & -\mathbf{F}^T \tilde{P} F_1^x \bar{K} & -\mathbf{F}^T \tilde{P} F_2^x \bar{K} \\ \star & (F_1^x \bar{K})^T \tilde{P} F_1^x \bar{K} & (F_1^x \bar{K})^T \tilde{P} F_2^x \bar{K} \\ \star & \star & (F_2^x \bar{K})^T \tilde{P} F_2^x \bar{K} \\ \vdots & \vdots & \\ \star & \star & \star \\ \star & \star & \star \\ \dots & -\mathbf{F}^T \tilde{P} F_{\bar{d}+\bar{\delta}-1}^x \bar{K} & -\mathbf{F}^T \tilde{P} F_{\bar{d}+\bar{\delta}}^x \bar{K} \\ \dots & (F_1^x \bar{K})^T \tilde{P} F_{\bar{d}+\bar{\delta}-1}^x \bar{K} & (F_1^x \bar{K})^T \tilde{P} F_{\bar{d}+\bar{\delta}}^x \bar{K} \\ \dots & (F_2^x \bar{K})^T \tilde{P} F_{\bar{d}+\bar{\delta}-1}^x \bar{K} & (F_2^x \bar{K})^T \tilde{P} F_{\bar{d}+\bar{\delta}}^x \bar{K} \\ \ddots & \vdots & \\ \star & (F_{\bar{d}+\bar{\delta}-1}^x \bar{K})^T \tilde{P} F_{\bar{d}+\bar{\delta}-1}^x \bar{K} & (F_{\bar{d}+\bar{\delta}-1}^x \bar{K})^T \tilde{P} F_{\bar{d}+\bar{\delta}}^x \bar{K} \\ \star & \star & (F_{\bar{d}+\bar{\delta}}^x \bar{K})^T \tilde{P} F_{\bar{d}+\bar{\delta}}^x \bar{K} \end{array} \right) \chi_k, \end{aligned} \quad (\text{A.52})$$

with  $\mathbf{F} = F_0^x(\mathbf{t}^k, h_k) - G^x(\mathbf{t}^k, h_k)\bar{K}$ . Note that for the sake of brevity  $F_{\hat{i}}^x$  is used instead of  $F_{\hat{i}}^x(\mathbf{t}^k, h_k)$ ,  $\hat{i} = 1, 2, \dots, \bar{d}+\bar{\delta}$ , and  $\mathbf{t}^k = (t_{k-\bar{d}-\bar{\delta}+1}^k, \dots, t_{k-\bar{d}}^k)$ . Second, consider the part of (A.51) that depends on the matrices  $R_{\hat{i}}$ ,  $\hat{i} \in \{1, 2, \dots, \bar{d}+\bar{\delta}\}$ .



Rewriting this part in a matrix notation gives:

$$\sum_{\hat{i}=1}^{\bar{d}+\bar{\delta}} x_{k-\hat{i}+1}^T R_{\hat{i}} x_{k-\hat{i}+1} - (1-\gamma) \sum_{\hat{i}=1}^{\bar{d}+\bar{\delta}} x_{k-\hat{i}}^T R_{\hat{i}} x_{k-\hat{i}} = \chi_k^T \begin{pmatrix} R_1 & 0 & 0 & \dots & 0 \\ 0 & R_2 - (1-\gamma)R_1 & 0 & \dots & 0 \\ \vdots & & \ddots & & \vdots \\ 0 & 0 & R_{\bar{d}+\bar{\delta}} - (1-\gamma)R_{\bar{d}+\bar{\delta}-1} & 0 & 0 \\ 0 & 0 & \dots & 0 & -(1-\gamma)R_{\bar{d}+\bar{\delta}} \end{pmatrix} \chi_k. \quad (\text{A.53})$$

Third, consider the part of (A.51) depending on the matrices  $T_{\hat{i}}$ ,  $\hat{i} \in \{1, 2, \dots, \bar{d}+\bar{\delta}\}$ . Implementing the dynamics of (A.49) and rewriting in a matrix notation gives:

$$\begin{aligned} & \sum_{\hat{i}=1}^{\bar{d}+\bar{\delta}} (x_{k-\hat{i}+2} - x_{k-\hat{i}+1})^T T_{\hat{i}} (x_{k-\hat{i}+2} - x_{k-\hat{i}+1}) \\ & - (1-\gamma) \sum_{\hat{i}=1}^{\bar{d}+\bar{\delta}} (x_{k-\hat{i}+1} - x_{k-\hat{i}})^T T_{\hat{i}} (x_{k-\hat{i}+1} - x_{k-\hat{i}}) = \\ & (x_{k+1} - x_k)^T T_1 (x_{k+1} - x_k) + \\ & \sum_{\hat{i}=1}^{\bar{d}+\bar{\delta}-1} (x_{k-\hat{i}+1} - x_{k-\hat{i}})^T (T_{\hat{i}+1} - (1-\gamma)T_{\hat{i}}) (x_{k-\hat{i}+1} - x_{k-\hat{i}}) - \\ & (1-\gamma) (x_{k-\bar{d}-\bar{\delta}+1} - x_{k-\bar{d}-\bar{\delta}})^T T_{\bar{d}+\bar{\delta}} (x_{k-\bar{d}-\bar{\delta}+1} - x_{k-\bar{d}-\bar{\delta}}) = \\ & \chi_k^T \begin{pmatrix} \mathbf{A}_0^T T_1 \mathbf{A}_0 & -\mathbf{A}_0^T T_1 \mathbf{A}_1 & -\mathbf{A}_0^T T_1 \mathbf{A}_2 & \dots & -\mathbf{A}^T T_1 \mathbf{A}_{\bar{d}+\bar{\delta}-1} & -\mathbf{A}^T T_1 \mathbf{A}_{\bar{d}+\bar{\delta}} \\ * & \mathbf{A}_1^T T_1 \mathbf{A}_1 & \mathbf{A}_1^T T_1 \mathbf{A}_2 & \dots & \mathbf{A}_1^T \tilde{P} \mathbf{A}_{\bar{d}+\bar{\delta}-1} & \mathbf{A}_1^T \tilde{P} \mathbf{A}_{\bar{d}+\bar{\delta}} \\ * & * & \mathbf{A}_2^T T_1 \mathbf{A}_2 & & \mathbf{A}_2^T T_1 \mathbf{A}_{\bar{d}+\bar{\delta}-1} & \mathbf{A}_2^T T_1 \mathbf{A}_{\bar{d}+\bar{\delta}} \\ \vdots & \vdots & & & \vdots & \\ * & * & * & * & \mathbf{A}_{\bar{d}+\bar{\delta}-1}^T T_1 \mathbf{A}_{\bar{d}+\bar{\delta}-1} & \mathbf{A}_{\bar{d}+\bar{\delta}-1}^T T_1 \mathbf{A}_{\bar{d}+\bar{\delta}} \\ * & * & * & * & * & \mathbf{A}_{\bar{d}+\bar{\delta}}^T T_1 \mathbf{A}_{\bar{d}+\bar{\delta}} \end{pmatrix} \chi_k + \\ & \chi_k^T \begin{pmatrix} -(1-\gamma)T_1 + T_2 & +(1-\gamma)T_1 - T_2 & 0 & \dots \\ * & -(1-\gamma)T_1 + \gamma T_2 + T_3 & -T_3 + (1-\gamma)T_2 & 0 \\ * & * & -(1-\gamma)T_2 + \gamma T_3 + T_4 & 0 \\ \vdots & \vdots & & \\ * & * & * & * \\ * & * & * & * \end{pmatrix} \chi_k, \\ & \begin{pmatrix} 0 & 0 & 0 & \vdots \\ 0 & 0 & 0 & 0 \\ 0 & 0 & 0 & 0 \\ * & \mathbf{B} & (1-\gamma)T_{\bar{d}+\bar{\delta}-1} - T_{\bar{d}+\bar{\delta}} & 0 \\ * & * & -(1-\gamma)T_{\bar{d}+\bar{\delta}-1} + \gamma T_{\bar{d}+\bar{\delta}} & (1-\gamma)T_{\bar{d}+\bar{\delta}} \\ * & * & * & -(1-\gamma)T_{\bar{d}+\bar{\delta}} \end{pmatrix} \chi_k, \quad (\text{A.54}) \end{aligned}$$

with

$$\begin{aligned}
\mathbf{A}_0 &= F_0^x(\mathbf{t}^k, h_k) - G^x(\mathbf{t}^k, h_k)\overline{K} - I, \\
\mathbf{A}_1 &= F_1^x(\mathbf{t}^k, h_k)\overline{K}, \\
\mathbf{A}_2 &= F_2^x(\mathbf{t}^k, h_k)\overline{K}, \\
&\vdots \\
\mathbf{A}_{\overline{d}+\overline{\delta}} &= F_{\overline{d}+\overline{\delta}}^x(\mathbf{t}^k, h_k)\overline{K}, \\
\mathbf{B} &= -(1-\gamma)T_{\overline{d}+\overline{\delta}-2} + \gamma T_{\overline{d}+\overline{\delta}-1} + T_{\overline{d}+\overline{\delta}}.
\end{aligned}$$

Note that analogous to (A.9) in the proof of Theorem 4.3.2 in Appendix A.4, the following overapproximations can be considered:

$$\mathcal{FG}^x \subset \text{co}\{\mathcal{H}_{FG}^x\},$$

with  $\mathcal{FG}^x$  defined in (4.42) and  $\mathcal{H}_{FG}^x$  defined in (4.44). Combining (A.52), (A.53), and (A.54) into one equation and applying the same overapproximation procedure as in the proof of Theorem 4.3.2 in Appendix A.4, proves the LMI conditions (4.45), (4.46) in Theorem 4.4.7.

### A.10 Proof of Theorem 5.1.1

Pre- and post-multiplying of the LMI (5.5) with  $\text{diag}(Y^{-1}, Y^{-1})$  gives (4.15), after the linearizing change of variables  $Y^{-1} = P$  and  $ZY^{-1} = K$ . Then, the proof of Theorem 4.3.1 can be exploited to prove that (5.5) guarantees GES of (4.5), (5.1). The proof for the fact that (5.3), (5.1) is GAS as well, follows from the same reasoning as used in the proof of Theorem 4.3.6, which shows that satisfaction of (5.5) is sufficient to guarantee GAS of (5.3) for the obtained controller  $K$  in (5.1).

### A.11 Proof of Theorem 5.1.4

The same overapproximation procedure as in the proof for the stability analysis in Appendix A.4 is considered. Therefore, this proof deals with rewriting the stability analysis results such that they are applicable for controller synthesis. Consider the candidate Lyapunov function

$$V(\chi_k) = x_k^T \tilde{P} x_k + x_{k-1}^T R x_{k-1} + (x_k - x_{k-1})^T T (x_k - x_{k-1}).$$

The following inequality is sufficient for the global exponential stability of the discrete-time NCS model (5.10):

$$\Delta V(\chi_k) = V(\chi_{k+1}) - V(\chi_k) < -\gamma V(\chi_k), \text{ for } \chi_k \neq 0,$$

which is equivalent to:

$$\Delta V(\chi_k) + \gamma V(\chi_k) + \Psi_1 < 0, \text{ for } \chi_k \neq 0 \quad (\text{A.55})$$

due to the fact that  $\Psi_1 = 0$ , as defined in (5.11). Next, we will consider the different parts in (A.55). It holds that

$$\begin{aligned} \Delta V(\chi_k) + \gamma V(\chi_k) = & \\ & x_{k+1}^T \tilde{P} x_{k+1} - (1 - \gamma) x_k^T \tilde{P} x_k + x_k^T R x_k - (1 - \gamma) x_{k-1}^T R x_{k-1} + \\ & (x_{k+1} - x_k)^T T (x_{k+1} - x_k) - (1 - \gamma) (x_k - x_{k-1})^T T (x_k - x_{k-1}). \end{aligned} \quad (\text{A.56})$$

Combining (A.56), with the dynamics of (4.22) (which represent equivalent dynamics to (4.19) or (5.10)) based on the Jordan form of the continuous-time system matrix  $A$ , gives

$$\begin{aligned} \Delta V(\chi_k) + \gamma V(\chi_k) = & (\mathbf{G}_0 x_k - F^x(\tau_k) \bar{K} x_{k-1})^T \tilde{P} (\mathbf{G}_0 x_k - F^x(\tau_k) \bar{K} x_{k-1}) \\ & - (1 - \gamma) x_k^T \tilde{P} x_k + x_k^T R x_k - (1 - \gamma) x_{k-1}^T R x_{k-1} \\ & + (\mathbf{H}_0 x_k - F^x(\tau_k) \bar{K} x_{k-1})^T T (\mathbf{H}_0 x_k - F^x(\tau_k) \bar{K} x_{k-1}) \\ & - (1 - \gamma) (x_k - x_{k-1})^T T (x_k - x_{k-1}), \end{aligned} \quad (\text{A.57})$$

with  $\mathbf{G}_0 = \hat{\Theta}_0 - G^x(\tau_k) \bar{K}$ ,  $\mathbf{H}_0 = \hat{\Theta}_0 - G^x(\tau_k) \bar{K} - I$ .

Next, the third term in (A.55), i.e.  $\Psi_1$ , that should lead to a relaxation of the LMI conditions, is rewritten. Using the fact that for any two vectors  $x$  and  $y$  and a positive definite matrix  $G$  it holds that:

$$2x^T y \leq x^T G x + y^T G^{-1} y, \quad (\text{A.58})$$

and that  $\chi_k^T = (x_k^T \quad x_{k-1}^T)^T$ , the following upper bound on the quadratic function  $\Psi_1$ , as defined in (5.11), can be derived:

$$\begin{aligned} \Psi_1 &= 2\chi_k^T N (x_k - x_{k-1} - (x_k - x_{k-1})) \\ &\leq 2\chi_k^T N (x_k - x_{k-1}) + \frac{1}{1-\gamma} \chi_k^T N T^{-1} N^T \chi_k \\ &\quad + (1 - \gamma) (x_k - x_{k-1})^T T (x_k - x_{k-1}), \end{aligned} \quad (\text{A.59})$$

with  $N = \begin{pmatrix} N_1 \\ N_2 \end{pmatrix}$ ,  $N_1, N_2 \in \mathbb{R}^{n \times n}$  positive definite symmetric matrices. Moreover, it holds that

$$2\chi_k^T N (x_k - x_{k-1}) = \chi_k^T \begin{pmatrix} N_1 + N_1^T & -N_1 + N_2^T \\ N_2 - N_1^T & -N_2 - N_2^T \end{pmatrix} \chi_k.$$

Combining (A.55), (A.57) and (A.59), gives:

$$\begin{aligned} \Delta V(\chi_k) + \gamma V(\chi_k) + \Psi_1 \leq & \\ & (\mathbf{G}_0 x_k - F^x(\tau_k) \bar{K} x_{k-1})^T \tilde{P} (\mathbf{G}_0 x_k - F^x(\tau_k) \bar{K} x_{k-1}) \\ & - (1 - \gamma) x_k^T \tilde{P} x_k + x_k^T R x_k - (1 - \gamma) x_{k-1}^T R x_{k-1} \\ & + (\mathbf{H}_0 x_k - F^x(\tau_k) \bar{K} x_{k-1})^T T (\mathbf{H}_0 x_k - F^x(\tau_k) \bar{K} x_{k-1}) \\ & + 2\chi_k^T N (x_k - x_{k-1}) + \frac{1}{1-\gamma} \chi_k^T N T^{-1} N^T \chi_k < 0, \end{aligned} \quad (\text{A.60})$$

for all  $\chi_k \neq 0$ . Rewriting (A.60) in a matrix notation with  $\chi_k = \begin{pmatrix} x_k^T & x_{k-1}^T \end{pmatrix}^T$ , gives:

$$\chi_k^T \begin{pmatrix} \mathbf{S}_0 & \mathbf{S}_1 \\ \star & \mathbf{S}_2 \end{pmatrix} \chi_k < 0,$$

with

$$\begin{aligned} \mathbf{S}_0 &= \mathbf{G}_0^T \tilde{P} \mathbf{G}_0 - (1 - \gamma) \tilde{P} + R + \mathbf{H}_0^T T \mathbf{H}_0 + N_1 + N_1^T + \frac{1}{1 - \gamma} N_1 T^{-1} N_1^T, \\ \mathbf{S}_1 &= -(\mathbf{G}_0^T \tilde{P} + \mathbf{H}_0^T T) F^x(\tau_k) \bar{K} + N_2^T - N_1 + \frac{1}{1 - \gamma} N_1 T^{-1} N_2^T, \\ \mathbf{S}_2 &= -(1 - \gamma) R + (F^x(\tau_k) \bar{K})^T (\tilde{P} + T) F^x(\tau_k) \bar{K} - N_2 - N_2^T + \frac{1}{1 - \gamma} N_2 T^{-1} N_2^T. \end{aligned}$$

Based on the same overapproximation procedure as in the proof of Theorem 4.3.2 in Appendix A.4, it is sufficient if it holds that:

$$\chi_k^T \begin{pmatrix} \bar{\mathbf{S}}_0 & \bar{\mathbf{S}}_1 \\ \star & \bar{\mathbf{S}}_2 \end{pmatrix} \chi_k < 0,$$

with

$$\begin{aligned} \bar{\mathbf{S}}_0 &= \bar{\mathbf{G}}_{0,j}^T \tilde{P} \bar{\mathbf{G}}_{0,j} - (1 - \gamma) \tilde{P} + R + \bar{\mathbf{H}}_{0,j}^T T \bar{\mathbf{H}}_{0,j} + N_1 + N_1^T + \frac{1}{1 - \gamma} N_1 T^{-1} N_1^T, \\ \bar{\mathbf{S}}_1 &= -(\bar{\mathbf{G}}_{0,j}^T \tilde{P} + \bar{\mathbf{H}}_{0,j}^T T) H_{F,j}^x \bar{K} + N_2^T - N_1 + \frac{1}{1 - \gamma} N_1 T^{-1} N_2^T, \\ \bar{\mathbf{S}}_2 &= -(1 - \gamma) R + (H_{F,j}^x \bar{K})^T (\tilde{P} + T) H_{F,j}^x \bar{K} - N_2 - N_2^T + \frac{1}{1 - \gamma} N_2 T^{-1} N_2^T, \end{aligned}$$

and  $\bar{\mathbf{G}}_{0,j} = \hat{\Theta}_0 - H_{G,j}^x \bar{K}$ ,  $\bar{\mathbf{H}}_{0,j} = \hat{\Theta}_0 - H_{G,j}^x \bar{K} - I$ . Applying the Schur complement for the inequality  $-\begin{pmatrix} \bar{\mathbf{S}}_0 & \bar{\mathbf{S}}_1 \\ \star & \bar{\mathbf{S}}_2 \end{pmatrix} > 0$ , gives:

$$\begin{pmatrix} \mathbf{T}_0 & N_1 - N_2^T - \frac{1}{1 - \gamma} N_1 T^{-1} N_2^T & \bar{\mathbf{G}}_{0,j}^T & \bar{\mathbf{H}}_{0,j}^T \\ \star & \mathbf{T}_1 & -(H_{F,j}^x \bar{K})^T & -(H_{F,j}^x \bar{K})^T \\ \star & \star & \tilde{P}^{-1} & 0 \\ \star & \star & \star & T^{-1} \end{pmatrix} > 0,$$

with  $\mathbf{T}_0 = (1 - \gamma) \tilde{P} - R - N_1 - N_1^T - \frac{1}{1 - \gamma} N_1 T N_1^T$  and  $\mathbf{T}_1 = (1 - \gamma) R + N_2 + N_2^T - \frac{1}{1 - \gamma} N_2 T^{-1} N_2^T$ . Applying the Schur complement on  $T$  a second time to remove the multiplications of  $N_1$  with  $T$ , and  $N_2$  with  $T$ , gives:

$$\begin{pmatrix} \mathbf{U}_0 & N_1 - N_2^T & \bar{\mathbf{G}}_{0,j}^T & \bar{\mathbf{H}}_{0,j}^T & \frac{1}{\sqrt{1 - \gamma}} N_1 T^{-1} \\ \star & (1 - \gamma) R + N_2 + N_2^T & -(H_{F,j}^x \bar{K})^T & -(H_{F,j}^x \bar{K})^T & \frac{1}{\sqrt{1 - \gamma}} N_2 T^{-1} \\ \star & \star & \tilde{P}^{-1} & 0 & 0 \\ \star & \star & \star & T^{-1} & 0 \\ \star & \star & \star & \star & T^{-1} \end{pmatrix} > 0,$$

with  $U_0 = (1 - \gamma)\tilde{P} - R - N_1 - N_1^T$ . Pre- and postmultiplication with  $\text{diag}(\tilde{P}^{-1}, \tilde{P}^{-1}, I, I, I)$ , with  $I$  the identity matrix of size  $n \times n$ , in combination with the following linearizing change of variables:  $\tilde{Y} := \tilde{P}^{-1}$ ,  $\tilde{R} := \tilde{P}^{-1}R\tilde{P}^{-1}$ ,  $\tilde{N}_1 := \tilde{P}^{-1}N_1\tilde{P}^{-1}$ ,  $\tilde{N}_2 := \tilde{P}^{-1}N_2\tilde{P}^{-1}$ ,  $Z := \tilde{K}\tilde{P}^{-1}$ , and  $T^{-1} := \theta_1\tilde{P}^{-1}$  gives the expression (5.12) in Theorem 5.1.4.

## A.12 Proof of Lemma 6.1.1

The proof of Lemma 6.1.1 follows partly the same reasoning as the proof of Theorem 4.3.1. Firstly, the relations between the different defined sets of matrices are explained. Secondly, based on these relations, it is proven that the conditions of (6.20) are sufficient for (6.18). Thirdly, it is proven that the conditions of (6.18) are sufficient to prove input-to-state stability of (6.13).

First, let us consider the time-varying parameters  $\alpha_i(\tau_k)$ ,  $i = 1, 2, \dots, \nu$ , that result in the fact that the number of LMIs in (6.18) are infinite (namely  $\tau_k \in [\tau_{\min}, \tau_{\max}]$ ). With  $\bar{\alpha}_i$  and  $\underline{\alpha}_i$ , as defined in the lemma (as well as in Theorem 4.3.1), we can write any  $\alpha_i \in [\underline{\alpha}_i, \bar{\alpha}_i]$  as  $\alpha_i = \underline{\alpha}_i + \delta_i(\bar{\alpha}_i - \underline{\alpha}_i)$ , for some  $\delta_i \in [0, 1]$  and  $i = 1, 2, \dots, \nu$ . Hence, the set  $\bar{\mathcal{F}}$ , defined as

$$\bar{\mathcal{F}} = \left\{ \bar{F}_0 + \sum_{i=1}^{\nu} \delta_i \bar{F}_i : \delta_i \in [0, 1], i = 1, 2, \dots, \nu \right\}, \quad (\text{A.61})$$

with  $\bar{F}_0 = F_0 + \sum_{i=1}^{\nu} \underline{\alpha}_i F_i$ ,  $\bar{F}_i = (\bar{\alpha}_i - \underline{\alpha}_i)F_i$  is an overapproximation of the set  $\mathcal{F}$ , as in (6.17), in the sense that  $\mathcal{F} \subseteq \bar{\mathcal{F}}$ . Due to the definition of the new uncertainty parameters  $\delta_i$ , the set  $\bar{\mathcal{F}}$  is still infinite. However, each matrix in this set can be written as a convex combination of the generators of the corresponding set, which are defined by the set of generators  $\mathcal{H}_F$  in (6.19). Note that  $\mathcal{H}_F$  consists of  $2^\nu$  matrices, which we denote individually by  $H_{F,j}$ ,  $j = 1, 2, \dots, 2^\nu$ . Based on these generators, a convex overapproximation of  $\bar{\mathcal{F}}$  is given by:

$$\text{co}(\mathcal{H}_F) = \left\{ \sum_{j=1}^{2^\nu} \phi_j H_{F,j} : \sum_{j=1}^{2^\nu} \phi_j = 1, \phi_j \in [0, 1], j = 1, 2, \dots, 2^\nu \right\}, \quad (\text{A.62})$$

in the sense that

$$\mathcal{F} \subseteq \bar{\mathcal{F}} = \text{co}(\mathcal{H}_F). \quad (\text{A.63})$$

Next, we show that indeed (6.20) is sufficient to guarantee the satisfaction of (6.18). Since (6.20) holds for all  $H_{F,j} \in \mathcal{H}_F$  with  $j = 1, 2, \dots, 2^\nu$ , we have that, by using the Schur complement:

$$\begin{pmatrix} (1 - \gamma)P & 0 & H_{F,j}^T \\ 0 & \kappa I & \tilde{B}^T \\ H_{F,j} & \tilde{B} & P^{-1} \end{pmatrix} > 0, \quad (\text{A.64})$$

with  $0 < \gamma < 1$ . Since  $\phi_j \geq 0 \ \forall j \in \{1, 2, \dots, 2^\nu\}$  and  $\sum_{j=1}^{2^\nu} \phi_j = 1$ , (A.64) implies

$$\begin{aligned} 0 &< \sum_{j=1}^{2^\nu} \phi_j \begin{pmatrix} (1-\gamma)P & 0 & H_{F,j}^T \\ 0 & \kappa I & \tilde{B}^T \\ H_{F,j} & \tilde{B} & P^{-1} \end{pmatrix} \\ &= \begin{pmatrix} (1-\gamma)P & 0 & \sum_{j=1}^{2^\nu} \phi_j H_{F,j}^T \\ 0 & \kappa I & \tilde{B}^T \\ \sum_{j=1}^{2^\nu} \phi_j H_{F,j} & \tilde{B} & P^{-1} \end{pmatrix}, \end{aligned} \quad (\text{A.65})$$

with  $\phi_j \in [0, 1]$ ,  $j = 1, 2, \dots, 2^\nu$ . Consequently, it holds that:

$$\begin{pmatrix} (1-\gamma)P & 0 & \overline{H_F}^T \\ 0 & \kappa I & \tilde{B}^T \\ \overline{H_F} & \tilde{B} & P^{-1} \end{pmatrix} > 0, \ \forall \overline{H_F} \in \text{co}(\mathcal{H}_{\mathcal{F}}). \quad (\text{A.66})$$

Based on (A.63), we have that (A.66) implies:

$$\begin{pmatrix} (1-\gamma)P & 0 & F(\tau_k)^T \\ 0 & \kappa I & \tilde{B}^T \\ F(\tau_k) & \tilde{B} & P^{-1} \end{pmatrix} > 0, \ \forall \tau_k \in [\tau_{\min}, \tau_{\max}] \quad (\text{A.67})$$

with  $F(\tau_k) = F_0 + \sum_{i=1}^{\nu} \alpha_i(\tau_k) F_i$  and  $F_0, F_i, i \in \{1, 2, \dots, \nu\}$ , defined in (6.16). Applying the Schur complement again gives (6.18).

Finally, we prove that the LMIs of (6.18) are sufficient to prove input-to-state stability of (6.13). Therefore, we consider the discrete-time system (6.15) (which is equivalent to (6.13), due to the use of the Jordan form) and the candidate ISS Lyapunov function  $V(\psi_k) = \psi_k^T P \psi_k$ , with  $P = P^T > 0$ . The increment of  $V(\psi_k)$  along solutions of (6.15), (6.16) satisfies

$$\begin{aligned} \Delta V(\psi_k) &= V(\psi_{k+1}) - V(\psi_k) = \psi_{k+1}^T P \psi_{k+1} - \psi_k^T P \psi_k \\ &= \psi_k^T (F^T(\tau_k) P F(\tau_k) - P) \psi_k + 2 \psi_k^T F^T(\tau_k) P \tilde{B} \bar{w}_k + \bar{w}_k^T \tilde{B}^T P \tilde{B} \bar{w}_k. \end{aligned} \quad (\text{A.68})$$

Rewriting of this equation, gives:

$$\Delta V(\psi_k) = \bar{\psi}_k^T \begin{pmatrix} F^T(\tau_k) P F(\tau_k) - P & F^T(\tau_k) P \tilde{B} \\ \tilde{B}^T P F(\tau_k) & \tilde{B}^T P \tilde{B} \end{pmatrix} \bar{\psi}_k, \quad (\text{A.69})$$

with  $\bar{\psi}_k = (\psi_k^T \ \bar{w}_k^T)^T$ . To prove ISS, we require that  $\Delta V(\psi_k) < -\gamma V(\psi_k) + \kappa \bar{w}_k^T \bar{w}_k$ . Then, based on (A.69) it holds that:

$$\begin{aligned} \Delta V(\psi_k) + \gamma V(\psi_k) - \kappa \bar{w}_k^T \bar{w}_k &= \\ \bar{\psi}_k^T \begin{pmatrix} F^T(\tau_k) P F(\tau_k) - (1-\gamma)P & F(\tau_k) P \tilde{B} \\ \tilde{B}^T P F(\tau_k) & \tilde{B}^T P \tilde{B} - \kappa I \end{pmatrix} \bar{\psi}_k &< 0, \end{aligned} \quad (\text{A.70})$$

which gives exactly the LMI conditions that are presented in (6.18). Thus, if the LMIs in (6.18) are feasible (which is the case if the LMIs in (6.20) are

satisfied), then it holds that  $\Delta V(\psi_k) < -\gamma V(\psi_k) + \kappa \bar{w}_k^T \bar{w}_k$ , which proves that Condition (2.18) in Definition 2.3.5 holds. Note that the first condition (2.17) in Definition 2.3.5 is satisfied due to the fact that  $P = P^T > 0$  holds in (6.18) and (6.20), which proves that  $V(\psi_k) = \psi_k^T P \psi_k > 0$ . Consequently,  $V$  is an ISS Lyapunov function and the application of Proposition 2.3.6 guarantees that (6.13) is ISS with respect to the input  $\bar{w}_k$ . This completes the proof that (6.13) (due to the equivalence with (6.15)) is ISS if the LMI conditions in (6.20) are feasible.

### A.13 Proof of Theorem 6.1.2

From Lemma 6.1.1 it follows that the discrete-time NCS model (6.13) is ISS and that  $V(\psi_k) = \psi_k^T P \psi_k$  is a quadratic ISS Lyapunov function for this system. By denoting  $|\psi_k|_P^2 = \psi_k^T P \psi_k$ , we can rewrite  $\Delta V(\psi_k) < -\gamma \psi_k^T P \psi_k + \kappa \bar{w}_k^T \bar{w}_k$  as

$$|\psi_{k+1}|_P^2 - |\psi_k|_P^2 < -\gamma |\psi_k|_P^2 + \kappa \sup_{1 \leq l \leq k} |\bar{w}_l|^2. \quad (\text{A.71})$$

This implies that

$$|\psi_{k+1}|_P^2 < \bar{\gamma} |\psi_k|_P^2 + \kappa \sup_{1 \leq l \leq k} |\bar{w}_l|^2 \Rightarrow |\psi_k|_P^2 < \bar{\gamma}^k |\psi_0|_P^2 + \kappa D_k \sup_{1 \leq l \leq k} |\bar{w}_l|^2, \quad k \geq 1, \quad (\text{A.72})$$

with  $0 < \bar{\gamma} = 1 - \gamma < 1$  and  $D_k = \sum_{i=1}^k \bar{\gamma}^{i-1}$ . Using (A.72), the fact that  $\lambda_{\min}(P) |\psi_k|^2 \leq |\psi_k|_P^2 \leq \lambda_{\max}(P) |\psi_k|^2$  and  $|z_k|^2 \leq \|C_z P^{-\frac{1}{2}}\|^2 |\psi_k|_P^2$ , the following inequality on regarding the norms of the tracking error  $z_k$  at the sampling instants can be established:

$$\begin{aligned} \frac{|z_k|^2}{\|C_z P^{-\frac{1}{2}}\|^2} &\leq |\psi_k|_P^2 \\ &< \bar{\gamma}^k |\psi_0|_P^2 + \kappa D_k \sup_{1 \leq l \leq k} |\bar{w}_l|^2 \\ &\leq \bar{\gamma}^k \lambda_{\max}(P) |\psi_0|^2 + \kappa D_k \sup_{1 \leq l \leq k} |\bar{w}_l|^2, \quad k \geq 1. \end{aligned} \quad (\text{A.73})$$

Now, using the fact that  $|\psi_0|^2 = |z_0|^2 + |z_{-1}|^2$  in (A.73), gives

$$\begin{aligned} \frac{|z_k|^2}{\|C_z P^{-\frac{1}{2}}\|^2} &< \bar{\gamma}^k \lambda_{\max}(P) (|z_0|^2 + |z_{-1}|^2) + \kappa D_k \sup_{1 \leq l \leq k} |\bar{w}_l|^2 \\ \Rightarrow |z_k| &< \|C_z P^{-\frac{1}{2}}\| \left( \sqrt{\bar{\gamma}^k \lambda_{\max}(P)} \sqrt{|z_0|^2 + |z_{-1}|^2} + \sqrt{\kappa D_k} \sup_{1 \leq l \leq k} |\bar{w}_l| \right), \quad k \geq 1. \end{aligned} \quad (\text{A.74})$$

Let us now revert to the continuous-time sampled-data system (6.10) and study its evolution for  $t \in [s_k, s_{k+1})$ :

$$z(s_k + \tilde{t}) = e^{A\tilde{t}} z_k + \int_0^{\tilde{t}} e^{As} ds B_1 z_{k-1} + \int_0^{\tilde{t}} e^{As} B_2 w(s_k + \tilde{t} - s) ds, \quad \text{for } 0 \leq \tilde{t} < \tau_k,$$

$$\begin{aligned}
z(s_k + \tilde{t}) &= e^{A\tilde{t}} z_k + \int_{\tilde{t}+\tau_k}^{\tilde{t}} e^{As} ds B_1 z_{k-1} + \int_0^{\tilde{t}-\tau_k} e^{As} ds B_1 z_k \\
&\quad + \int_0^{\tilde{t}} e^{As} B_2 w(s_k + \tilde{t} - s) ds, \quad \text{for } \tau_k \leq \tilde{t} < h.
\end{aligned}$$

Consequently, the following bounds on the tracking error in this time interval can be established:

$$\begin{aligned}
|z(s_k + \tilde{t})| &\leq |e^{A\tilde{t}} z_k| + \left| \int_0^{\tilde{t}} e^{As} ds B_1 z_{k-1} \right| \\
&\quad + \left| \int_0^{\tilde{t}} e^{As} ds B_2 \right| \sup_{s_k \leq s \leq t_k} |w(s)|, \quad \text{for } 0 \leq \tilde{t} < \tau_k,
\end{aligned} \tag{A.75}$$

$$\begin{aligned}
|z(s_k + \tilde{t})| &\leq |e^{A\tilde{t}} z_k| + \left| \int_{\tilde{t}-\tau_k}^{\tilde{t}} e^{As} ds B_1 z_{k-1} \right| + \left| \int_0^{\tilde{t}-\tau_k} e^{As} ds B_1 z_k \right| \\
&\quad + \left| \int_0^{\tilde{t}} e^{As} ds B_2 \right| \sup_{s_k \leq s < s_{k+1}} |w(s)|, \quad \text{for } \tau_k \leq \tilde{t} < h.
\end{aligned}$$

Using Wazewski's inequalities, see (A.14) (i.e.  $|e^{A\tilde{t}} z| \leq |z| e^{\lambda_{\max} \tilde{t}}$ , with  $\lambda_{\max} = \frac{1}{2} \max(\text{eig}(A + A^T))$ ), the terms in the above inequality can be upperbounded to obtain:

$$|z(s_k + \tilde{t})| \leq \bar{c}_1 |z_k| + \bar{c}_2 |z_{k-1}| + \bar{c}_w \sup_{s_k \leq s \leq t_k} |w(s)|, \quad \text{for } 0 \leq \tilde{t} < \tau_k,$$

$$|z(s_k + \tilde{t})| \leq (\hat{c}_1 + \hat{c}_2) |z_k| + \tilde{c}_2 |z_{k-1}| + \hat{c}_w \sup_{s_k \leq s < s_{k+1}} |w(s)|, \quad \text{for } \tau_k \leq \tilde{t} < h. \tag{A.76}$$

with

$$\begin{aligned}
\bar{c}_1 &= \max(1, e^{\lambda_{\max} \tau_{\max}}) \\
\bar{c}_2 &= \|B_1\| \begin{cases} \frac{e^{\lambda_{\max} \tau_{\max}} - 1}{\lambda_{\max}} & \text{if } \lambda_{\max} \neq 0 \\ \tau_{\max} & \text{if } \lambda_{\max} = 0 \end{cases} \\
\bar{c}_w &= \|B_2\| \begin{cases} \frac{e^{\lambda_{\max} \tau_{\max}} - 1}{\lambda_{\max}} & \text{if } \lambda_{\max} \neq 0 \\ \tau_{\max} & \text{if } \lambda_{\max} = 0 \end{cases}
\end{aligned} \tag{A.77}$$



$$\begin{aligned}
\hat{c}_1 &= \begin{cases} \max(e^{\lambda_{\max} h}, e^{\lambda_{\max} \tau_{\min}}) & \text{if } \lambda_{\max} \neq 0 \\ 1 & \text{if } \lambda_{\max} = 0 \end{cases} \\
\hat{c}_2 &= \|B_1\| \begin{cases} \frac{e^{\lambda_{\max}(h-\tau_{\min})}-1}{\lambda_{\max}} & \text{if } \lambda_{\max} \neq 0 \\ h - \tau_{\min} & \text{if } \lambda_{\max} = 0 \end{cases} \\
\tilde{c}_2 &= \|B_1\| \begin{cases} \frac{e^{\lambda_{\max} h}-1}{\lambda_{\max}} & \text{if } \lambda_{\max} \neq 0 \\ \tau_{\max} & \text{if } \lambda_{\max} = 0 \end{cases} \\
\hat{c}_w &= \|B_2\| \begin{cases} \frac{e^{\lambda_{\max} h}-1}{\lambda_{\max}} & \text{if } \lambda_{\max} \neq 0 \\ h & \text{if } \lambda_{\max} = 0 \end{cases}.
\end{aligned} \tag{A.78}$$

Consequently, the inequality in (A.75) can be replaced by

$$|z(s_k + \tilde{t})| \leq c_1 |z_k| + c_2 |z_{k-1}| + c_w \sup_{s_k \leq s \leq s_{k+1}} |w(s)|, \text{ for } 0 \leq \tilde{t} < h, \forall k \tag{A.79}$$

with  $c_1$ ,  $c_2$ , and  $c_w$  defined by

$$\begin{aligned}
c_1 &= \max(\bar{c}_1, \hat{c}_1 + \hat{c}_2), \\
c_2 &= \max(\bar{c}_2, \tilde{c}_2), \\
c_w &= \max(\bar{c}_w, \hat{c}_w) = \hat{c}_w.
\end{aligned} \tag{A.80}$$

The next step is to exploit (A.74) in (A.79); however in order to do so, first the following upper bound on  $\sup_{1 \leq l \leq k} |\bar{w}_l|$  needs to be formulated:

$$\begin{aligned}
\sup_{1 \leq l \leq k} |\bar{w}_l| &= \sup_{1 \leq l \leq k} \left| \int_0^h e^{As} B_2 w(h + s_l - s) ds \right| \\
&\leq \sup_{1 \leq l \leq k} \int_0^h \|e^{As}\| \|B_2\| |w(h + s_l - s)| ds \\
&\leq \|B_2\| \sup_{0 \leq s \leq t} |w(s)| \begin{cases} \frac{e^{\lambda_{\max} h}-1}{\lambda_{\max}} & \text{if } \lambda_{\max} \neq 0 \\ h & \text{if } \lambda_{\max} = 0 \end{cases} \\
&= c_w \sup_{0 \leq s < s_{k+1}} |w(s)|, \quad \text{for } k \geq 1,
\end{aligned} \tag{A.81}$$

with  $c_w$  defined in (A.77), (A.78), (A.80). Now, using (A.74), (A.81), and the fact that  $\sqrt{|z_0|^2 + |z_{-1}|^2} = |\bar{z}(0)|$  in (A.79) yields

$$\begin{aligned}
|z(s_k + \tilde{t})| &\leq \|C_z P^{-\frac{1}{2}}\| \left( c_1 \sqrt{\gamma^k \lambda_{\max}(P)} + c_2 \sqrt{\gamma^{k-1} \lambda_{\max}(P)} \right) |\bar{z}(0)| \\
&\quad + c_w \left( 1 + \left( c_1 \sqrt{\kappa D_k} + c_2 \sqrt{\kappa D_{k-1}} \right) \|C_z P^{-\frac{1}{2}}\| \right) \sup_{0 \leq s \leq s_{k+1}} |w(s)|,
\end{aligned} \tag{A.82}$$

for  $0 \leq \tilde{t} < h$ ,  $k \geq 2$ . If  $k < 2$ , different relations are needed. Analogously, from (A.79) it can be derived that

$$\begin{aligned}
|z(s_0 + \tilde{t})| &\leq c_1 |z_0| + c_2 |z_{-1}| + c_w \sup_{s_0 \leq s \leq s_1} |w(s)|, \\
&\leq (c_1 + c_2) |\bar{z}(0)| + c_w \sup_{s_0 \leq s \leq s_1} |w(s)|,
\end{aligned} \tag{A.83}$$

and

$$\begin{aligned}
|z(s_1 + \tilde{t})| &\leq c_1|z_1| + c_2|z_0| + c_w \sup_{s_0 \leq s \leq s_2} |w(s)|, \\
&\leq (c_1 \|C_z P^{-\frac{1}{2}}\| \sqrt{\bar{\gamma} \lambda_{\max}(P)} + c_2) |\bar{z}(0)| \\
&\quad + c_w (1 + \sqrt{\kappa} \|C_z P^{-\frac{1}{2}}\|) \sup_{s_0 \leq s \leq s_2} |w(s)|.
\end{aligned} \tag{A.84}$$

Now, note that  $D_k$  is a strictly increasing (since  $0 < \bar{\gamma} < 1$ ) geometric series which exhibits a limit for  $k \rightarrow \infty$ :  $\lim_{k \rightarrow \infty} D_k = \lim_{k \rightarrow \infty} \sum_{i=1}^{\infty} \bar{\gamma}^{i-1} = 1/(1 - \bar{\gamma}) = 1/\gamma$ . Concluding, it can be shown that the continuous-time tracking error dynamics is ISS with respect to the time-varying input  $w(t)$ , since

$$|z(t)| \leq g_1(t) |\bar{z}(0)| + g_2 \sup_{0 \leq s \leq t} |w(s)|, \text{ for } t \geq 0, \tag{A.85}$$

with  $g_1(t)$  a decreasing function of  $t$  according to

$$g_1(t) = \begin{cases} \max\{g_{1,0}, g_{1,1}, g_{1,2}\} & \text{for } t \in [0, s_2) \\ g_{1,k} & \text{for } k \geq 2, t \in [s_k, s_{k+1}) \end{cases} \tag{A.86}$$

with

$$\begin{aligned}
g_{1,0} &= c_1 + c_2, \\
g_{1,1} &= c_1 \|C_z P^{-\frac{1}{2}}\| \sqrt{\bar{\gamma} \lambda_{\max}(P)} + c_2, \\
g_{1,k} &= \|C_z P^{-\frac{1}{2}}\| \left( c_1 \sqrt{\bar{\gamma}^k \lambda_{\max}(P)} + c_2 \sqrt{\bar{\gamma}^{k-1} \lambda_{\max}(P)} \right), \quad k \geq 2.
\end{aligned} \tag{A.87}$$

Note that  $g_1(t)$  is a decreasing function, with  $\lim_{t \rightarrow \infty} g_1(t) = 0$ , because  $g_{1,k}$ ,  $k \geq 2$ , is a strictly decreasing sequence, with  $\lim_{k \rightarrow \infty} g_{1,k} = 0$ . Moreover,  $g_2$  in (A.85) is given by

$$g_2 = c_w \left( 1 + (c_1 + c_2) \|C_z P^{-\frac{1}{2}}\| \sqrt{\frac{\kappa}{\gamma}} \right). \tag{A.88}$$

Note that (A.88) is larger than  $c_w$  that was obtained for  $|z(s_0 + \tilde{t})|$  and  $c_w(1 + \sqrt{\kappa D_1}) = c_w(1 + \sqrt{\kappa})$  that was obtained for  $|z(s_1 + \tilde{t})|$ , which proves that  $g_2$  holds for all  $k$ .

### A.14 Proof of Lemma 6.2.2

To obtain an upper bound on the intersample behavior of (6.30), its state evolution for  $t \in [s_k, s_{k+1})$ , denoted by  $z(s_k + \tilde{t})$ , with  $\tilde{t} \in [0, h_k)$ , is studied in detail. The evolution of  $z(s_k + \tilde{t})$  depends on the number of different states  $z(s_j)$  that are active in the time-interval  $t \in [s_k, \tilde{t})$ . To determine the control inputs that are active, we define the parameter  $f$ :

$$f := \max \left\{ j \in \{k - \bar{d} - \bar{\delta}, k - \bar{d} - \bar{\delta} + 1, \dots, k - \underline{d}\} \mid t_j^k \leq \tilde{t} \right\}, \tag{A.89}$$

with  $t_j^k$  defined in Lemma 3.4.1. The intersample behavior for  $t \in [s_k, s_k + \tilde{t})$  is given by:

$$z(s_k + \tilde{t}) = e^{A\tilde{t}} z_k + \sum_{j=k-\underline{d}-\bar{\delta}}^f \int_{\tilde{t}-\bar{t}_{j+1}^k}^{\tilde{t}-\bar{t}_j^k} e^{As} ds B_1 z_j + \int_0^{\tilde{t}} e^{As} B_2 w(s_k + \tilde{t} - s) ds, \quad (\text{A.90})$$

for  $\tilde{t} \in [0, h_k)$ . Herein, we slightly adapted  $t_j^k$  in (5.17) to  $\bar{t}_j^k$  to account for  $f < k - \underline{d}$ . It holds that

$$\bar{t}_j^k = t_j^k, \text{ for } j \leq f, \quad (\text{A.91})$$

with  $f$  defined in (A.89),  $\bar{t}_{f+1}^k := \tilde{t}$  if  $\bar{t}_f^k < \tilde{t}$  and, based on (A.91),  $\bar{t}_{k-\underline{d}-\bar{\delta}}^k := 0$ , which corresponds to the definition of  $t_{k-\underline{d}-\bar{\delta}}^k$ . The upper bound on the intersample behavior (A.90), can now be given by:

$$\begin{aligned} |z(s_k + \tilde{t})| &\leq |e^{A\tilde{t}} z_k| + \left| \sum_{j=k-\underline{d}-\bar{\delta}}^f \int_{\tilde{t}-\bar{t}_{j+1}^k}^{\tilde{t}-\bar{t}_j^k} e^{As} ds B_1 z_j \right| \\ &\quad + \left| \int_0^{\tilde{t}} e^{As} B_2 w(s_k + \tilde{t} - s) ds \right|, \quad \text{for } \tilde{t} \in [0, h_k). \end{aligned} \quad (\text{A.92})$$

The upper bound will be determined by upperbounding each term  $\int_{\tilde{t}-\bar{t}_{j+1}^k}^{\tilde{t}-\bar{t}_j^k} e^{As} ds B_1 z_j$ ,  $j \in \{k - \underline{d} - \bar{\delta}, \dots, f\}$ , individually. For the maximum value of  $f$ , i.e.  $\max(f) = k - \underline{d}$ , which corresponds to the largest number of different control inputs that can be active in the interval  $[s_k, s_k + \tilde{t})$ , this results in

$$\begin{aligned} |z(s_k + \tilde{t})| &\leq c_0 |z_k| + c_1 |z_{k-1}| + c_2 |z_{k-2}| + \dots + c_{\bar{d}+\bar{\delta}} |z_{k-\bar{d}-\bar{\delta}}| \\ &\quad + c_w \sup_{s_k \leq s < s_{k+1}} |w(s)|, \quad \text{for } \tilde{t} \in [0, h_k), \end{aligned} \quad (\text{A.93})$$

which corresponds to the bound as given in (6.40) in Lemma 6.2.2. Next, the different parameters  $c_0, \dots, c_{\bar{d}+\bar{\delta}}$ , and  $c_w$  will be determined, based on the largest contribution of the corresponding term related to  $|z_j|$ ,  $j \in \{k - \bar{d} - \bar{\delta}, \dots, k - \underline{d}\}$ , in the interval  $[s_k, s_k + \tilde{t})$ .

**Remark A.14.1** The easiest way to find the largest contribution of each  $|z_j|$ -related term in (A.92) is to use

$$\left( \max_{\tilde{t}}(\bar{t}_{j+1}^k) - \min_{\tilde{t}}(\bar{t}_j^k) \right) \max_{s \in [\bar{t}_{j+1}^k, \bar{t}_j^k]} |e^{As} B_1 z_j|,$$

for  $0 \leq \tilde{t} < h_k \leq h_{\max}$  and therefore for  $j \in \{k - \bar{d} - \bar{\delta}, \dots, k - \underline{d}\}$ . However, this result will be rather conservative.

To obtain a less conservative result than proposed in the remark, Wazewski's inequalities, see (A.14), with  $\lambda_{\max} = \frac{1}{2} \max(\text{eig}(A + A^T))$ , are used to find an upper bound for the integrals in (A.92), based on the matrix exponential of

A. This strategy is analogous to that used in the proof of Lemma 4.3.5 in Appendix A.6, where the intersample behavior for NCSs with delays smaller than the constant sampling interval and no packet dropouts is studied. Still, the upper and lower bounds of  $\bar{t}_j^k$  and  $\bar{t}_{j+1}^k$ , for  $j \in \{k - \bar{d} - \bar{\delta}, \dots, f\}$ , with  $f \leq k - \underline{d}$ , are needed. For the different values of  $f$  these bounds need to be determined. This derivation of the bounds on  $\bar{t}_j^k$  will be combined with the derivation of the parameters  $c_\rho$ ,  $\rho \in \{0, 1, \dots, \bar{d} + \bar{\delta}\}$  as needed in (A.93).

#### A.14.1 Determination of $c_0$

To determine the parameter  $c_0$ , besides the possible contribution of the integral  $\int_{\bar{t}-\bar{t}_{k+1}^k}^{\bar{t}-\bar{t}_k^k} e^{As} ds B_1 z_k$ , the contribution of  $|e^{A\bar{t}} z_k|$  needs to be taken into account. For  $c_0$ , three cases can be distinguished that depend on the value of  $\underline{d}$  and the size of  $\bar{t}$  compared to  $t_{k-\underline{d}}^k$ . In each of these cases, the possibility of packet dropouts will be included.

- $\underline{d} = 0$  and  $\bar{t} < t_{k-\underline{d}}^k = t_k^k$ :

In this case, the relation  $\int_{\bar{t}-\bar{t}_{k+1}^k}^{\bar{t}-\bar{t}_k^k} e^{As} ds B_1 z_k$  does not have to be considered, because  $f < k - \underline{d} = k$ . Note that

$$t_k^k \in \begin{cases} [\min(h_{\min}, \tau_{\min}), \min(\tau_{\max}, h_{\max})], & \text{if } \bar{\delta} = 0, \\ [\min(h_{\min}, \tau_{\min}), h_{\max}], & \text{if } \bar{\delta} > 0, \end{cases} \quad (\text{A.94})$$

as can be obtained from Lemma 4.4.2. Hence, the maximum value for  $\bar{t}$  for which  $\bar{t} < t_k^k$  is given by:

$$\begin{aligned} \bar{t} &< \min(\tau_{\max}, h_{\max}), & \text{if } \bar{\delta} = 0, \\ \bar{t} &< h_{\max}, & \text{if } \bar{\delta} > 0. \end{aligned}$$

In this relation a distinction is made, between the situation with and without packet dropouts, analogous to Lemma 4.4.2. Based on these upper bounds on  $\bar{t}$ , the maximum contribution of  $|z_k|$  (which is only related to the term  $|e^{A\bar{t}} z_k|$ ) on the intersample behavior for this specific case is given by:

$$|e^{A\bar{t}} z_k| \leq |z_k| \begin{cases} e^{\lambda_{\max} \tau_{\max}} & \text{if } \lambda_{\max} > 0 \text{ and } (\tau_{\max} < h_{\max} \text{ and } \bar{\delta} = 0) \\ e^{\lambda_{\max} h_{\max}} & \text{if } \lambda_{\max} > 0 \text{ and } (\tau_{\max} \geq h_{\max} \text{ and } \bar{\delta} = 0) \\ & \text{or } (\bar{\delta} > 0) \\ 1 & \text{if } \lambda_{\max} \leq 0, \end{cases}$$

which can be simplified to:

$$\begin{aligned} |e^{A\bar{t}} z_k| &\leq \bar{c}_0 |z_k|, \text{ with} \\ \bar{c}_0 &:= \begin{cases} \max(e^{\lambda_{\max} \tau_{\max}}, 1) & \text{if } \bar{\delta} = 0 \text{ and } \tau_{\max} < h_{\max} \\ \max(e^{\lambda_{\max} h_{\max}}, 1) & \text{if } (\bar{\delta} = 0 \text{ and } \tau_{\max} \geq h_{\max}) \text{ or } (\bar{\delta} > 0). \end{cases} \end{aligned} \quad (\text{A.95})$$

- $\underline{d} = 0$  and  $\tilde{t} \geq t_{k-\underline{d}}^k = t_k^k$ :

Here, the parameter  $f$  is given by  $f = k - \underline{d} = k$ , if  $t_k^k < h_k$ , because, it holds that  $\tilde{t} \in [0, h_k)$ , analogous to (A.90). If  $t_k^k = h_k$ , then the parameter  $f$  is given by  $f = k - \underline{d} - 1 = k - 1$ . In the first case, the relation  $\int_{\tilde{t}-\bar{t}_{k+1}^k}^{\tilde{t}-\bar{t}_k^k} e^{As} ds B_1 z_k = \int_0^{\tilde{t}-t_k^k} e^{As} ds B_1 z_k$  has to be considered to derive the value of  $c_0$ . Note that in the second case, this relation does not have to be considered, see (A.90). In order to account for this integral, we first study the minimum and maximum value of  $\tilde{t}$ , based on the parameters  $t_k^k$  and  $\bar{t}_k^k$ . For  $t_{k,\min}^k$ , the definition is given in Lemma 4.4.2. Analogous to (A.91), it holds that  $\bar{t}_{k,\min}^k = t_{k,\min}^k$  for  $j = k \leq f$ . However, due to the dependence on the value of  $f$ , this relation cannot be applied straightforwardly to compute the value of  $c_0$ , as we will show now. According to Lemma 4.4.2, it holds that  $t_{k,\min}^k = \min(\tau_{\min}, h_{\min})$  (using  $\underline{d} = 0$ ). If it holds that  $t_k^k \in [h_{\min}, \tau_{\min})$ , which is possible if  $h_{\min} < \tau_{\min}$ , then  $t_k^k$  is, due to its definition in Lemma 3.4.1 ( $t_k^k = \min(\tau_k, h_k)$ ), equal to  $h_k$ . It is easy to see that  $\bar{t}_k^k = \tilde{t}$  for any value of  $\tilde{t} \in [t_{k-1}^k, h_k)$ . Then, as mentioned above, the integral  $\int_{\tilde{t}-\bar{t}_{k+1}^k}^{\tilde{t}-\bar{t}_k^k} e^{As} ds B z_k$ , does not need to be considered. If  $t_k^k \geq \tau_{\min}$ , it holds that  $\bar{t}_k^k = t_k^k$  if  $t_k^k \leq \tilde{t}$ . Then, for  $\tilde{t} > t_k^k$ , the integral  $\int_{\tilde{t}-\bar{t}_{k+1}^k}^{\tilde{t}-\bar{t}_k^k} e^{As} ds B z_j$ , needs to be considered, with  $\bar{t}_{k+1}^k = \tilde{t}$ . Then, to obtain the upper bound on the contribution of the integral related to  $|z_k|$  on the intersample behavior, we can limit ourselves to the values of  $\tilde{t} \geq \tau_{\min}$ . Note that the upper bound of  $\tilde{t}$  is given by  $h_{\max}$ . Based on this lower and upper bound of  $\tilde{t}$ , the minimum and maximum value of  $\bar{t}_k^k$ , for which the contribution of the integral related to  $z_k$  is larger than zero, is given by:

$$\bar{t}_k^k \in \begin{cases} [\tau_{\min}, \min(\tau_{\max}, h_{\max})], & \text{if } \bar{\delta} = 0, \\ [\tau_{\min}, h_{\max}], & \text{if } \bar{\delta} > 0, \end{cases} \quad (\text{A.96})$$

where it is used that  $\tilde{t} > \tau_{\min}$ . In the above reasoning, the occurrence of packet dropouts was not included explicitly. Packet dropouts result in the fact that the integral  $\int_0^{\tilde{t}-\bar{t}_k^k} e^{As} ds B_1 z_k$  does not have to be considered in the contribution of  $z_k$  on the intersample behavior. In the case of a packet dropout, it holds, according to Lemma 3.4.1, that  $t_k^k = h_k$ . Then, the integral  $\int_{h_k-t_{k+1}^k}^{h_k-t_k^k} e^{As} ds B_1 z_k = \int_0^{h_k-t_k^k} e^{As} ds B_1 z_k = 0$ . Moreover, it holds that  $f < k$ , resulting in  $\bar{t}_k^k := \tilde{t}$  and  $\bar{t}_{k+1}^k$  not defined. Therefore, it holds that  $\int_{\tilde{t}-\bar{t}_{k+1}^k}^{\tilde{t}-\bar{t}_k^k} e^{As} ds B_1 z_k$  is not defined. This proves that, in the case of packet dropouts, this integral does not have to be taken into account. Then, the largest contribution of the integral related to  $z_k$  on the bound on the intersample behavior is, for  $\tilde{t} \geq t_k^k$ , obtained if  $m_k = 0$  (no packet dropout) is used. Clearly, the bounds on  $\bar{t}_k^k$  as defined in (A.96), and  $\tilde{t} \in [\tau_{\min}, h_{\max})$  still hold.

Based on these observations, it holds that:

$$|e^{A\tilde{t}} z_k| \leq \tilde{c}_0 |z_k|, \quad (A.97)$$

$$\text{with } \tilde{c}_0 := \begin{cases} e^{\lambda_{\max} h_{\max}} & \text{if } \lambda_{\max} > 0 \\ e^{\lambda_{\max} \tau_{\min}} & \text{if } \lambda_{\max} < 0 \\ 1 & \text{if } \lambda_{\max} = 0, \end{cases}$$

and

$$\begin{aligned} \left| \int_{\tilde{t}-\tilde{t}_k^k-\underline{d}+1}^{\tilde{t}-\tilde{t}_k^k-\underline{d}} e^{As} ds B_1 z_k \right| &= \left| \int_0^{\tilde{t}-\tilde{t}_k^k} e^{As} ds B_1 z_k \right| \\ &\leq \begin{cases} |z_k| \|B_1\| \frac{e^{\lambda_{\max}(\tilde{t}-\tilde{t}_k^k)} - 1}{\lambda_{\max}} & \text{if } \lambda_{\max} \neq 0 \\ |z_k| \|B_1\| (\tilde{t} - \tilde{t}_k^k) & \text{if } \lambda_{\max} = 0 \end{cases} \\ &\leq \hat{c}_0 |z_k|, \end{aligned} \quad (A.98)$$

$$\text{with } \hat{c}_0 := \begin{cases} |z_k| \|B_1\| \frac{e^{\lambda_{\max}(h_{\max}-\tau_{\min})} - 1}{\lambda_{\max}} & \text{if } \lambda_{\max} \neq 0 \\ |z_k| \|B_1\| (h_{\max} - \tau_{\min}) & \text{if } \lambda_{\max} = 0. \end{cases}$$

- $\underline{d} > 0$ :

In this case it holds, by the definition of  $\underline{d}$ , that  $\tau_{\min} > h_{\max}$ . The upper bound on  $|z(s_k + \tilde{t})|$ , as far as it relates to terms concerning  $|z_k|$ , then only depends on  $|e^{A\tilde{t}} z_k|$ , with:

$$|e^{A\tilde{t}} z_k| \leq \check{c}_0 |z_k|, \text{ with } \check{c}_0 := \begin{cases} e^{\lambda_{\max} h_{\max}} & \text{if } \lambda_{\max} > 0 \\ 1 & \text{if } \lambda_{\max} \leq 0. \end{cases} \quad (A.99)$$

Summarizing, it holds that

$$c_0 = \begin{cases} \max(\bar{c}_0, \tilde{c}_0 + \hat{c}_0) & \text{if } \underline{d} = 0 \\ \check{c}_0 & \text{if } \underline{d} > 0, \end{cases} \quad (A.100)$$

with  $\bar{c}_0$ ,  $\tilde{c}_0$ ,  $\hat{c}_0$ , and  $\check{c}_0$  defined in (A.95), (A.97), (A.98), and (A.99), respectively.

### A.14.2 Determination of $c_\rho$

To obtain the parameters  $c_\rho$ ,  $\rho \in \{1, 2, \dots, \bar{d} + \bar{\delta}\}$  in (A.93), the maximum value of  $|\int_{\tilde{t}-\tilde{t}_j^k}^{\tilde{t}-\tilde{t}_j^k} e^{As} ds B_1 z_j|$  needs to be considered for each  $j$ . The values of  $j$  in this relation are given by  $j \in \{k - \bar{d} - \bar{\delta}, \dots, k - \underline{d} - 1\}$  for  $\underline{d} = 0$  and given by  $j \in \{k - \bar{d} - \bar{\delta}, \dots, k - \underline{d}\}$  for  $\underline{d} > 0$ . Note that the value of  $\tilde{t}$  is chosen such that for each  $j$  the input  $z_j$  is indeed implemented in the interval  $[s_k, s_k + \tilde{t})$ . To

derive the maximum value of each  $c_\rho$ , with  $\rho \in \{\underline{d}+1, \underline{d}+2, \dots, \bar{d}+\bar{\delta}\}$  if  $\underline{d} = 0$  and with  $\rho \in \{\underline{d}, \underline{d}+1, \dots, \bar{d}+\bar{\delta}\}$  if  $\underline{d} > 0$ , the following general bound on the integral  $\int_{\tilde{t}-\bar{t}_{j+1}^k}^{\tilde{t}-\bar{t}_j^k} e^{As} ds B_1 z_j$ , which is based on Wazewski's inequalities (A.14), is instrumental:

$$\left| \int_{\tilde{t}-\bar{t}_{j+1}^k}^{\tilde{t}-\bar{t}_j^k} e^{As} ds B_1 z_j \right| \leq |z_j| \begin{cases} \|B_1\| \frac{e^{\lambda_{\max}(\tilde{t}-\bar{t}_j^k)} - e^{\lambda_{\max}(\tilde{t}-\bar{t}_{j+1}^k)}}{\lambda_{\max}} & \text{if } \lambda_{\max} \neq 0 \\ \|B_1\| (\bar{t}_{j+1}^k - \bar{t}_j^k) & \text{if } \lambda_{\max} = 0, \end{cases} \quad (\text{A.101})$$

if  $\tilde{t} > \bar{t}_j^k$  (such that  $\bar{t}_j^k$  exists) and with  $\bar{t}_j^k$  defined in (3.22). To determine an upper bound for the right-hand side of this inequality, the minimum and maximum values of  $\bar{t}_j^k, \bar{t}_{j+1}^k$  in combination with  $\tilde{t}$  need to be considered. Recall that the lower bound and upper bound of  $\bar{t}_j^k$  are given by  $\bar{t}_{j,\min}^k$  and  $\bar{t}_{j,\max}^k$ , respectively, as derived in Lemma 4.4.2. Based on this knowledge, the upper and lower bounds of  $\bar{t}_j^k$  can be derived. For  $\bar{t}_{j,\min}^k$  it holds, based on (A.91), that  $\bar{t}_{j,\min}^k = \bar{t}_{j,\min}^k$ , for  $j \leq f$ , with  $\bar{t}_{j,\min}^k$  defined in (4.30). Analogous to the case  $\bar{d} = 0$  and  $\tilde{t} \geq \bar{t}_k^k$ , the dependence of  $\bar{t}_{j,\min}^k$  on  $f$  needs to be accounted for. Based on the same reasoning, it can be proven that for  $\tilde{t} > \bar{t}_j^k, j \in \{k-\bar{d}-\bar{\delta}, \dots, k-\underline{d}\}$ , that:

$$\bar{t}_{j,\min}^k = \begin{cases} \tau_{\min} - \underline{d}h_{\max} & \text{if } j = k - \underline{d} \\ 0 & \text{if } j < k - \underline{d}. \end{cases} \quad (\text{A.102})$$

Again, it is used that  $\tilde{t} \geq \tau_{\min}$  (see  $\underline{d} = 0$  and  $\tilde{t} \geq \bar{t}_{k-\underline{d}}^k = \bar{t}_k^k$  in the determination of  $c_0$ ). For  $\tilde{t} < \bar{t}_j^k$ , the parameter  $\bar{t}_j^k = \tilde{t}$ . Then, the integral related to  $z_j$  is not considered in the computation of  $z(s_k + \tilde{t})$  and does not contribute to the upper bound on  $z(s_k + \tilde{t})$ . To derive  $\bar{t}_{j,\max}^k$  it holds, based on (A.91) and analogous to (A.45), that:

$$\bar{t}_{j,\max}^k = \min \left\{ \begin{aligned} &\max\{0, \tau_{\max} - (k-j)h_{\min}\} + m_j h_{\max}, \\ &\max\{0, \tau_{\max} - (k-j-1)h_{\min}\} + m_{j+1} h_{\max}, \dots, \\ &\max\{0, \tau_{\max} - (k-f)h_{\min}\} + m_f h_{\max}, \tilde{t}_{\max} \end{aligned} \right\}, \quad (\text{A.103})$$

for  $j \in \{k-\bar{d}-\bar{\delta}+1, \dots, f\}$ . Because  $\tilde{t}_{\max} := \sup_{h_k} \tilde{t} = h_{\max}$  (due to the fact that  $\tilde{t} \in [0, h_k)$ ), it holds that (A.103) can be replaced by (A.45) (for  $\tilde{t} \rightarrow h_{\max}$ ). Then, the upper bound  $\bar{t}_{j,\max}^k$ , corresponds to  $\bar{t}_{j,\max}^k$ , defined in (4.31), if  $\tilde{t} \geq \bar{t}_j^k, j \in \{k-\bar{d}-\bar{\delta}, \dots, k-\underline{d}\}$ :

$$\bar{t}_{j,\max}^k = \begin{cases} \min\{\tau_{\max} - (k-j-\bar{\delta})h_{\min}, h_{\max}\} & \text{if } j \in \{k-\bar{d}-\bar{\delta}+1, \dots, k-\bar{\delta}-\underline{d}\}, \\ h_{\max} & \text{if } j \in \{k-\bar{\delta}-\underline{d}+1, \dots, k-\underline{d}\}. \end{cases} \quad (\text{A.104})$$

Based on the obtained upper and lower bounds of  $\bar{t}_j^k$ , the parameters  $c_\rho, \rho \in \{1, 2, \dots, \bar{d}+\bar{\delta}\}$ , in (A.93) can be derived. The upper bound of the first expression in the right-hand side of (A.101) is, for  $\tilde{t} \geq \bar{t}_j^k$ , obtained if  $\tilde{t}-\bar{t}_j^k$  is maximal, while  $\tilde{t}-\bar{t}_{j+1}^k$  is minimal. This results in  $e^{\lambda_{\max}(h_{\max}-\bar{t}_{j,\min}^k)}$  and  $e^{\lambda_{\max}(\tilde{t}-\bar{t}_{j+1}^k)} = 1$ ,

because  $\tilde{t}$  can be chosen such that  $\tilde{t} = \bar{t}_{j+1}^k$ . In combination with (A.102), this leads to the following bounds:

$$\|B_1\| \frac{e^{\lambda_{\max}(\tilde{t} - \bar{t}_j^k)} - e^{\lambda_{\max}(\tilde{t} - \bar{t}_{j+1}^k)}}{\lambda_{\max}} \leq \begin{cases} \|B_1\| \frac{e^{\lambda_{\max} h_{\max}} - 1}{\lambda_{\max}} & \text{if } j < k - \underline{d} \\ \|B_1\| \frac{e^{\lambda_{\max}(h_{\max} - (\tau_{\min} - \underline{d} h_{\max}))} - 1}{\lambda_{\max}} & \text{if } j = k - \underline{d}. \end{cases} \quad (\text{A.105})$$

The upper bound of the second equation of (A.101) is obtained if  $\bar{t}_{j+1}^k$  is maximal, while  $\bar{t}_j^k$  is minimal. This results, based on (A.102) and (A.104) in:

$$\|B_1\| (\bar{t}_{j+1}^k - \bar{t}_j^k) \leq \begin{cases} \min(\tau_{\max} - (k - j - 1 - \bar{\delta})h_{\min}, h_{\max}) & \text{if } j \in \{k - \bar{\delta} - \underline{d}, \dots, k - \bar{\delta} - \underline{d} - 1\} \\ h_{\max} & \text{if } j \in \{k - \bar{\delta} - \underline{d}, \dots, k - \underline{d} - 1\} \\ h_{\max} - (\tau_{\min} - \underline{d} h_{\max}) & \text{if } j = k - \underline{d}. \end{cases} \quad (\text{A.106})$$

Note that  $\tilde{t} < \bar{t}_j^k$ ,  $j \in \{k - \bar{\delta} - \underline{d}, \dots, k - \underline{d}\}$ , leads to the situation that  $z_j$  is not active in the interval  $[s_k, s_k + \tilde{t})$ , resulting in  $c_\rho = 0$ ,  $\rho \in \{\underline{d}, \dots, \bar{d} + \bar{\delta}\}$ . Then, from (A.105) and (A.106) in combination with  $\rho = k - j$ , the parameter  $c_\rho$ ,  $\rho \in \{1, 2, \dots, \bar{d} + \bar{\delta} - 1\}$  can be obtained. Note that  $c_\rho := 0$  if  $\rho \in \{1, 2, \dots, \underline{d} - 1\}$ . This gives the following relation for  $c_\rho$

$$c_\rho = \|B_1\| \begin{cases} \frac{e^{\lambda_{\max}(h_{\max} - (\tau_{\min} - \underline{d} h_{\max}))} - 1}{\lambda_{\max}} & \text{if } \lambda_{\max} \neq 0 \text{ and } \rho = \underline{d} \text{ and } \underline{d} > 0 \\ \frac{e^{\lambda_{\max} h_{\max}} - 1}{\lambda_{\max}} & \text{if } \lambda_{\max} \neq 0 \text{ and } \rho > \underline{d} \\ \min(\tau_{\max}^*, h_{\max}) & \text{if } \lambda_{\max} = 0 \text{ and } \\ & \rho \in \{\bar{\delta} + \underline{d} + 1, \dots, \bar{d} + \bar{\delta} - 1\} \\ (h_{\max} - (\tau_{\min} - \underline{d} h_{\max})) & \text{if } \lambda_{\max} = 0 \text{ and } \rho = \underline{d} \text{ and } \underline{d} > 0 \\ h_{\max} & \text{if } \lambda_{\max} = 0 \text{ and } \\ & \rho \in \{\underline{d} + 1, \dots, \bar{\delta} + \underline{d}\} \\ 0 & \text{if } \rho < \underline{d}, \end{cases}$$

with  $\tau_{\max}^* = \tau_{\max} - (\rho - \bar{\delta} - 1)h_{\min}$ . This proves (6.43).

The value for  $c_{\bar{d} + \bar{\delta}}$  can be obtained based on (A.101), (A.102), and (A.104). It holds that  $\bar{t}_{k - \bar{d} - \bar{\delta}}^k := 0$  and  $\bar{t}_{k - \bar{d} - \bar{\delta} + 1, \max}^k := \tau_{\max} - (\bar{d} - 1)h_{\min}$ , because



$\tau_{\max} - (\bar{d} - 1)h_{\min} \leq h_{\max}$ , due to the definition of  $\bar{d} := \lceil \frac{\tau_{\max}}{h_{\min}} \rceil$ . This gives

$$c_{\bar{d}+\bar{\delta}} = \begin{cases} \|B_1\| \frac{e^{\lambda_{\max} h_{\max}} - 1}{\lambda_{\max}} & \text{if } \lambda_{\max} \neq 0 \\ \|B_1\| (\tau_{\max} - (\bar{d} - 1)h_{\min}) & \text{if } \lambda_{\max} = 0, \end{cases}$$

which proves (6.44).

Finally, the value for  $c_w$  can be proven by:

$$|\int_0^{\tilde{t}} e^{As} B_2 w(s_k + \tilde{t} - s) ds| \leq \|B_2\| \sup_{s_k \leq s < s_{k+1}} |w(s)| \begin{cases} \frac{e^{\lambda_{\max} h_{\max}} - 1}{\lambda_{\max}} & \text{if } \lambda_{\max} \neq 0 \\ h_{\max} & \text{if } \lambda_{\max} = 0. \end{cases}$$

### A.15 Proof of Theorem 6.2.3

To prove input-to-state stability of the continuous-time NCS (6.30), (3.22) first the bound on the discrete-time state  $z_k$  is determined, based on the relations considered in Lemma 6.2.1. Second, the bound on the intersample behavior as discussed in Lemma 6.2.2 is combined with the bound on  $z_k$ .

In Lemma 6.2.1, it is proven that  $\Delta V(\psi_k) < -\gamma \psi_k^T P \psi_k + \kappa \bar{w}_k^T \bar{w}_k$  holds for the discrete-time NCS model (6.33). Similar to the small delay case (see relations (A.71) and (A.72)) it holds for  $|\psi_k|_P^2 = \psi_k^T P \psi_k$  that:

$$|\psi_{k+1}|_P^2 < \bar{\gamma} |\psi_k|_P^2 + \kappa \sup_{1 \leq l \leq k} |\bar{w}_l|^2 \Rightarrow |\psi_k|_P^2 < \bar{\gamma}^k |\psi_0|_P^2 + \kappa D_k \sup_{1 \leq l \leq k} |\bar{w}_l|^2, \quad k \geq 1,$$

with  $0 < \bar{\gamma} = 1 - \gamma < 1$ ,  $D_k = \sum_{i=1}^k \bar{\gamma}^{i-1}$ , and  $P$  satisfying the conditions in (6.39). Analogous to the small delay case, (A.73) holds:

$$\frac{|z_k|^2}{\|C_z P^{-\frac{1}{2}}\|^2} \leq \bar{\gamma}^k \lambda_{\max}(P) |\psi_0|^2 + \kappa D_k \sup_{1 \leq l \leq k} |\bar{w}_l|^2, \quad k \geq 1. \quad (\text{A.107})$$

Now, we use the fact that  $|\psi_0|^2 = |z_0|^2 + |z_{-1}|^2 + \dots + |z_{-\bar{d}-\bar{\delta}}|^2$  in (A.107) to obtain

$$\begin{aligned} \frac{|z_k|^2}{\|C_z P^{-\frac{1}{2}}\|^2} &< \bar{\gamma}^k \lambda_{\max}(P) (|z_0|^2 + |z_{-1}|^2 + \dots + |z_{-\bar{d}-\bar{\delta}}|^2) + \kappa D_k \sup_{1 \leq l \leq k} |\bar{w}_l|^2. \\ \Rightarrow |z_k| &< \|C_z P^{-\frac{1}{2}}\| \left( \sqrt{\bar{\gamma}^k \lambda_{\max}(P)} \sqrt{|z_0|^2 + |z_{-1}|^2 + \dots + |z_{-\bar{d}-\bar{\delta}}|^2} \right. \\ &\quad \left. + \sqrt{\kappa D_k} \sup_{1 \leq l \leq k} |\bar{w}_l| \right), \quad \forall k \geq 1. \end{aligned} \quad (\text{A.108})$$

As a second step, we consider the continuous-time system (6.30) and its evolution for  $t \in [s_k, s_{k+1})$  as described in Lemma 6.2.2. Combining (6.40) and

(A.108) gives:

$$\begin{aligned}
|z(s_k + \tilde{t})| &\leq \\
&c_0 \|C_z P^{-\frac{1}{2}}\| \sqrt{\bar{\gamma}^k \lambda_{\max}(P)} \sqrt{|z_0|^2 + |z_{-1}|^2 + \dots + |z_{-\bar{d}-\bar{\delta}}|} \\
&+ c_1 \|C_z P^{-\frac{1}{2}}\| \sqrt{\bar{\gamma}^{k-1} \lambda_{\max}(P)} \sqrt{|z_0|^2 + |z_{-1}|^2 + \dots + |z_{-\bar{d}-\bar{\delta}}|} \\
&+ \dots \\
&+ c_{\bar{d}+\bar{\delta}} \|C_z P^{-\frac{1}{2}}\| \sqrt{\bar{\gamma}^{k-\bar{d}-\bar{\delta}} \lambda_{\max}(P)} \sqrt{|z_0|^2 + |z_{-1}|^2 + \dots + |z_{-\bar{d}-\bar{\delta}}|} \\
&+ \|C_z P^{-\frac{1}{2}}\| \left( c_0 \sqrt{\kappa D_k} + c_1 \sqrt{\kappa D_{k-1}} + \dots + c_{\bar{d}+\bar{\delta}} \sqrt{\kappa D_{k-\bar{d}-\bar{\delta}}} \right) \sup_{1 \leq l \leq k} |\bar{w}_l| \\
&+ c_w \sup_{s_k \leq s < s_{k+1}} |w(s)|,
\end{aligned} \tag{A.109}$$

for  $0 \leq \tilde{t} < h_k$ ,  $k \geq \bar{d} + \bar{\delta} + 1$ . Recall that the upper bound of  $\sup_{1 \leq l \leq k} |\bar{w}_l|$  can be derived analogously to (A.81) with  $h$  replaced by  $h_{\max}$ . Then, using (A.81) and the fact that  $\sqrt{|z_0|^2 + |z_{-1}|^2 + \dots + |z_{-\bar{d}-\bar{\delta}}|} = |\bar{z}(0)|$ , (A.109) can be rewritten as:

$$\begin{aligned}
|z(s_k + \tilde{t})| &\leq \\
&\|C_z P^{-\frac{1}{2}}\| \left( c_0 \sqrt{\bar{\gamma}^k \lambda_{\max}(P)} + c_1 \sqrt{\bar{\gamma}^{k-1} \lambda_{\max}(P)} + \dots \right. \\
&\quad \left. + c_{\bar{d}+\bar{\delta}} \sqrt{\bar{\gamma}^{k-\bar{d}-\bar{\delta}} \lambda_{\max}(P)} \right) |\bar{z}(0)| \\
&+ c_w \left( 1 + \left( c_0 \sqrt{\kappa D_k} + c_1 \sqrt{\kappa D_{k-1}} + \dots \right. \right. \\
&\quad \left. \left. + c_{\bar{d}+\bar{\delta}} \sqrt{\kappa D_{k-\bar{d}-\bar{\delta}}} \right) \|C_z P^{-\frac{1}{2}}\| \right) \sup_{s_k \leq s < s_{k+1}} |w(s)|,
\end{aligned} \tag{A.110}$$

for  $0 \leq \tilde{t} < h_k$ ,  $k \geq \bar{d} + \bar{\delta} + 1$ . For  $k < \bar{d} + \bar{\delta} + 1$ , the upper bound of  $|z(s_k + \tilde{t})|$  can be derived analogously. For  $k = 0$ , i.e.  $s_0 := 0$  it holds that:

$$\begin{aligned}
|z(s_0 + \tilde{t})| &\leq c_0 |z_0| + c_1 |z_{-1}| + c_2 |z_{-2}| + \dots + c_{\bar{d}+\bar{\delta}} |z_{-\bar{d}-\bar{\delta}}| \\
&+ c_w \sup_{s_0 \leq s < s_1} |w(s)|, \text{ for } \tilde{t} \in [0, h_0) \\
&\leq (c_0 + c_1 + c_2 + \dots + c_{\bar{d}+\bar{\delta}}) |\bar{z}_0| + c_w \sup_{s_0 \leq s < s_1} |w(s)|, \text{ for } \tilde{t} \in [0, h_0).
\end{aligned}$$

For  $k = 1$  it holds that:

$$\begin{aligned}
|z(s_1 + \tilde{t})| &\leq c_0|z_1| + c_1|z_0| + c_2|z_{-1}| + \dots + c_{\bar{d}+\bar{\delta}}|z_{-\bar{d}-\bar{\delta}+1}| \\
&\quad + c_w \sup_{s_0 \leq s < s_1} |w(s)|, \text{ for } \tilde{t} \in [0, h_1) \\
&\leq (c_0 \|C_z P^{-\frac{1}{2}}\| \sqrt{\bar{\gamma} \lambda_{\max}(P)} + c_1 + c_2 + \dots + c_{\bar{d}+\bar{\delta}}) |\bar{z}_0| \\
&\quad + c_w (1 + c_0 \sqrt{\kappa} \|C_z P^{-\frac{1}{2}}\|) \sup_{s_0 \leq s < s_1} |w(s)|, \text{ for } \tilde{t} \in [0, h_1).
\end{aligned}$$

For  $k = 2$  it holds that:

$$\begin{aligned}
|z(s_2 + \tilde{t})| &\leq c_0|z_2| + c_1|z_1| + c_2|z_0| + \dots + c_{\bar{d}+\bar{\delta}}|z_{-\bar{d}-\bar{\delta}+2}| + c_w \sup_{s_0 \leq s < s_1} |w(s)|, \\
&\quad \text{for } \tilde{t} \in [0, h_2) \\
&\leq \left( \|C_z P^{-\frac{1}{2}}\| (c_0 \sqrt{\bar{\gamma}^2 \lambda_{\max}(P)} + c_1 \sqrt{\bar{\gamma} \lambda_{\max}(P)}) + c_2 + \dots + c_{\bar{d}+\bar{\delta}} \right) |\bar{z}_0| \\
&\quad + c_w \left( 1 + (c_0 \sqrt{\kappa D_2} + c_1 \sqrt{\kappa}) \|C_z P^{-\frac{1}{2}}\| \right) \sup_{s_1 \leq s < s_2} |w(s)|, \text{ for } \tilde{t} \in [0, h_2).
\end{aligned}$$

Similar relations can be derived for larger values of  $k < \bar{d} + \bar{\delta} + 1$ . The last value of  $k$  for which (A.110) does not hold is  $k = \bar{d} + \bar{\delta}$ . Then, the intersample behavior in the sampling interval  $[s_{\bar{d}+\bar{\delta}}, s_{\bar{d}+\bar{\delta}+1})$  denoted by  $|z(s_{\bar{d}+\bar{\delta}} + \tilde{t})|$  is given by:

$$\begin{aligned}
|z(s_{\bar{d}+\bar{\delta}} + \tilde{t})| &\leq c_0|z_{\bar{d}+\bar{\delta}}| + c_1|z_{\bar{d}+\bar{\delta}-1}| + c_2|z_{\bar{d}+\bar{\delta}-2}| + \dots + c_{\bar{d}+\bar{\delta}}|z_0| \\
&\quad + c_w \sup_{s_{\bar{d}+\bar{\delta}} \leq s < s_{\bar{d}+\bar{\delta}+1}} |w(s)|, \text{ for } \tilde{t} \in [0, h_{\bar{d}+\bar{\delta}}) \\
&\leq \left( \|C_z P^{-\frac{1}{2}}\| (c_0 \sqrt{\bar{\gamma}^{\bar{d}+\bar{\delta}} \lambda_{\max}(P)} + c_1 \sqrt{\bar{\gamma}^{\bar{d}+\bar{\delta}-1} \lambda_{\max}(P)} + \dots \right. \\
&\quad \left. + c_{\bar{d}+\bar{\delta}-1} \sqrt{\bar{\gamma} \lambda_{\max}(P)}) + c_{\bar{d}+\bar{\delta}} \right) |\bar{z}_0| \\
&\quad + c_w \left( 1 + \|C_z P^{-\frac{1}{2}}\| (c_0 \sqrt{\kappa D_{\bar{d}+\bar{\delta}}} + c_1 \sqrt{\kappa D_{\bar{d}+\bar{\delta}-1}} + \dots \right. \\
&\quad \left. + c_{\bar{d}+\bar{\delta}-1} \sqrt{\kappa}) \right) \sup_{s_{\bar{d}+\bar{\delta}} \leq s < s_{\bar{d}+\bar{\delta}+1}} |w(s)| \text{ for } \tilde{t} \in [0, h_{\bar{d}+\bar{\delta}}).
\end{aligned}$$

Similar to the small delay case,  $D_k$  is a strictly increasing (since  $0 < \bar{\gamma} < 1$ ) geometric series which exhibits a limit for  $k \rightarrow \infty$ :  $\lim_{k \rightarrow \infty} D_k = \lim_{k \rightarrow \infty} \sum_{i=1}^{\infty} \bar{\gamma}^{i-1} = 1/(1 - \bar{\gamma}) = 1/\bar{\gamma}$ . Concluding, we can show that the continuous-time tracking error dynamics is ISS with respect to the time-varying input  $w(t)$ , since

$$|z(t)| \leq g_1(t) |\bar{z}(0)| + g_2 \sup_{0 \leq s \leq t} |w(s)|, \text{ for } t \geq 0, \quad (\text{A.111})$$

with  $g_1(t)$  a decreasing function of  $t$  according to

$$g_1(t) = \begin{cases} \max(g_{1,0} \dots, g_{1,\bar{d}+\bar{\delta}}, g_{1,\bar{d}+\bar{\delta}+1}), & \text{for } t \in [0, s_{\bar{d}+\bar{\delta}+1}) \\ g_{1,k} & \text{for } t \in [s_k, s_{k+1}), k \geq \bar{d} + \bar{\delta} + 1, \end{cases} \quad (\text{A.112})$$

with

$$\begin{aligned} g_{1,0} &= c_0 + c_1 + c_2 + \dots + c_{\bar{d}+\bar{\delta}}, \\ g_{1,1} &= c_0 \|C_z P^{-\frac{1}{2}}\| \sqrt{\gamma \lambda_{\max}(P)} + c_1 + \dots + c_{\bar{d}+\bar{\delta}}, \\ g_{1,2} &= \|C_z P^{-\frac{1}{2}}\| (c_0 \sqrt{\gamma^2 \lambda_{\max}(P)} + c_1 \sqrt{\gamma \lambda_{\max}(P)}) + c_2 + \dots + c_{\bar{d}+\bar{\delta}}, \\ &\vdots \\ g_{1,\bar{d}+\bar{\delta}} &= \|C_z P^{-\frac{1}{2}}\| (c_0 \sqrt{\gamma^{\bar{d}+\bar{\delta}} \lambda_{\max}(P)} + c_1 \sqrt{\gamma^{\bar{d}+\bar{\delta}-1} \lambda_{\max}(P)} + \dots \\ &\quad + c_{\bar{d}+\bar{\delta}-1} \sqrt{\gamma \lambda_{\max}(P)}) + c_{\bar{d}+\bar{\delta}} \\ g_{1,k} &= \|C_z P^{-\frac{1}{2}}\| \left( c_0 \sqrt{\gamma^k \lambda_{\max}(P)} + c_1 \sqrt{\gamma^{k-1} \lambda_{\max}(P)} + \dots \right. \\ &\quad \left. + c_{\bar{d}+\bar{\delta}} \sqrt{\gamma^{k-\bar{d}-\bar{\delta}} \lambda_{\max}(P)} \right), \text{ for } k \geq \bar{d} + \bar{\delta} + 1. \end{aligned} \quad (\text{A.113})$$

Note that  $g_1(t)$  is a decreasing function, with  $\lim_{t \rightarrow \infty} g_1(t) = 0$ , because  $g_{1,k}$ ,  $k \geq \bar{d} + \bar{\delta} + 1$ , is a strictly decreasing sequence, with  $\lim_{k \rightarrow \infty} g_{1,k} = 0$ . Moreover,  $g_2$  in (A.111) is given by

$$g_2 = c_w \left( 1 + (c_0 + c_1 + \dots + c_{\bar{d}+\bar{\delta}}) \|C_z P^{-\frac{1}{2}}\| \sqrt{\frac{\kappa}{\gamma}} \right). \quad (\text{A.114})$$

Note that (A.114) is larger than  $c_w$  that was obtained for  $|z(s_0 + \tilde{t})|$ ,  $|z(s_1 + \tilde{t})|$ ,  $\dots$ ,  $|z(s_{\bar{d}+\bar{\delta}+\tilde{t}})|$ , which proves that  $g_2$  holds for all  $k$ .

# ***B***

## ***Jordan form***

---

B.1	Jordan Canonical form and Real Jordan form	B.3	Time-varying sampling intervals
B.2	Jordan forms of the NCS model	B.4	Output-feedback

---

This appendix describes the use of the Jordan form to reformulate the discrete-time Networked Control System models. The advantage of the use of the Jordan form is that a generic solution can be derived for the integrals that are used in the discrete-time NCS model, see e.g. (3.2) and (3.23). This solution allows to rewrite the right-hand side of the discrete-time NCS model as a combination of time-varying parameters in combination with constant matrices, such that stability analysis conditions can be derived. The use of time-varying parameters instead of time-varying matrices simplifies the derivation of the stability analysis conditions.

In Section B.1 the Jordan form is introduced. In Section B.2 the Jordan form of the continuous-time system matrix  $A$  is applied to rewrite the discrete-time NCS model for small delays of Section 3.1. In Section B.3, the model including time-varying sampling intervals, packet dropouts, and delays larger than the sampling interval is rewritten based on the Jordan form of the continuous-time system matrix  $A$ . Note that the models for the large delay case with or without packet dropouts and for constant sampling intervals can be derived from the model that includes time-varying sampling intervals. Finally, Section B.4 gives the formulation of the NCS model, based on the Jordan form, for the output-feedback case as considered in the experiments of Chapter 7.

### ***B.1 Jordan Canonical form and Real Jordan form***

For every square matrix  $A \in \mathbb{R}^{n \times n}$ , there exists a Jordan form  $J \in \mathbb{R}^{n \times n}$ , given by [108], [67]:

$$J = Q^{-1}AQ, \quad (\text{B.1})$$

with  $Q \in \mathbb{R}^{n \times n}$  a matrix that contains the generalized eigenvectors of  $A$  and

$$J = \text{diag}(J_1, \dots, J_p), \quad (\text{B.2})$$

where  $J_{\tilde{i}}$ ,  $\tilde{i} = 1, 2, \dots, p$ , is called a Jordan block, which has a block diagonal form and  $p$  denotes the number of distinct eigenvalues. Dependent on the

eigenvalues, two different cases are distinguished: the Jordan Canonical form that is applied for real eigenvalues and the Real Jordan form that is applied for complex eigenvalues. First, we consider the Jordan Canonical form, which we denote by  $J_R$  (real eigenvalues). The Jordan block  $J_{R,\tilde{i}}$ , which is the Jordan block for the  $\tilde{i}^{th}$  distinct eigenvalue ( $\lambda_{\tilde{i}}$ ) of the matrix  $A$  is represented by one of the following matrices:

$$\lambda_{\tilde{i}}, \begin{pmatrix} \lambda_{\tilde{i}} & 1 \\ 0 & \lambda_{\tilde{i}} \end{pmatrix}, \begin{pmatrix} \lambda_{\tilde{i}} & 1 & 0 \\ 0 & \lambda_{\tilde{i}} & 1 \\ 0 & 0 & \lambda_{\tilde{i}} \end{pmatrix}, \begin{pmatrix} \lambda_{\tilde{i}} & 1 & 0 & \dots & 0 \\ 0 & \lambda_{\tilde{i}} & 1 & \dots & 0 \\ \vdots & & \ddots & & \vdots \\ 0 & 0 & \dots & \lambda_{\tilde{i}} & 1 \\ 0 & 0 & \dots & 0 & \lambda_{\tilde{i}} \end{pmatrix}. \quad (\text{B.3})$$

Note that (B.2) is still valid, which gives for real eigenvalues:  $J_R = \text{diag}(J_{R,1}, \dots, J_{R,p})$ . If the geometric multiplicity  $g_{\tilde{i}} \in \mathbb{Z}^+$  of the eigenvalue  $\lambda_{\tilde{i}}$  of  $A$  is equal to one, then the dimension of the  $\tilde{i}^{th}$  Jordan block  $J_{R,\tilde{i}}$  is equal to the algebraic multiplicity  $m_{\tilde{i}}$  of the eigenvalue  $\lambda_{\tilde{i}}$ , with  $\tilde{i} = 1, 2, \dots, p$ . If the geometric multiplicity is unequal to one, then  $g_{\tilde{i}}$  Jordan blocks describe the Jordan block associated with  $\lambda_{\tilde{i}}$ :  $J_{R,\tilde{i}} = \text{diag}(J_{R,\tilde{i},1}, \dots, J_{R,\tilde{i},g_{\tilde{i}}})$ . The dimension of these combined  $g_{\tilde{i}}$  Jordan blocks is equal to the algebraic multiplicity  $m_{\tilde{i}}$  of the  $\tilde{i}^{th}$  distinct eigenvalue ( $\tilde{i} = 1, 2, \dots, p$ ). Note that the geometric multiplicity can never exceed the algebraic multiplicity of  $\lambda_{\tilde{i}}$ , so  $g_{\tilde{i}} \leq m_{\tilde{i}}$ , see [11], and [78].

In the discrete-time NCS models, e.g. (3.2), (3.16), (3.23), the exponential functions of the continuous-time system matrix  $A$ , such as  $e^{Ah}$  or  $e^{Ah_k}$  and  $e^{As}$ , are considered. For the exponential of  $A$  it holds that:

$$e^{As} = Q \text{diag}(e^{J_{R,1}s}, \dots, e^{J_{R,p}s}) Q^{-1}. \quad (\text{B.4})$$

The exponential functions  $e^{J_{R,\tilde{i}}s}$  are, based on the Jordan blocks given in (B.3), given by:

$$e^{\lambda_{\tilde{i}}s}, e^{\lambda_{\tilde{i}}s} \begin{pmatrix} 1 & s \\ 0 & 1 \end{pmatrix}, e^{\lambda_{\tilde{i}}s} \begin{pmatrix} 1 & s & \frac{s^2}{2!} \\ 0 & 1 & s \\ 0 & 0 & 1 \end{pmatrix}, e^{\lambda_{\tilde{i}}s} \begin{pmatrix} 1 & s & \frac{s^2}{2!} & \dots & \frac{s^{(k-1)}}{(k-1)!} \\ 0 & 1 & s & \dots & \frac{s^{(k-2)}}{(k-2)!} \\ \vdots & & \ddots & & \vdots \\ 0 & 0 & 1 & s \\ 0 & 0 & 0 & 1 \end{pmatrix}, \quad (\text{B.5})$$

for the  $\tilde{i}^{th}$  distinct real eigenvalue  $\lambda_{\tilde{i}}$ . The parameter  $k$  in (B.5) denotes the size of the Jordan block  $J_{R,\tilde{i},j}$ , with  $j \in \{1, 2, \dots, g_{\tilde{i}}\}$ . The number of different parameters in the Jordan block  $J_{R,\tilde{i}}$ , where the parameters are denoted by e.g.  $e^{\lambda_{\tilde{i}}s}$ ,  $se^{\lambda_{\tilde{i}}s}$ ,  $\frac{s^2}{2}e^{\lambda_{\tilde{i}}s}$  is equal to the algebraic multiplicity  $m_{\tilde{i}}$  if  $g_{\tilde{i}} = 1$ . If the Jordan block  $J_{R,\tilde{i}}$  consists of different Jordan blocks i.e.  $g_{\tilde{i}} > 1$ , the number of different parameters that depend on  $\lambda_{\tilde{i}}$  depends on the largest Jordan block, because the parameters of the other blocks are a subset of the parameters of this largest Jordan block (each block has the form of (B.5)). The number of

different time-varying parameters that is related to the  $\tilde{i}^{th}$  distinct eigenvalue is given by:

$$q_{\tilde{i}} = \max_{\tilde{j}=1,2,\dots,g_{\tilde{i}}} \dim J_{R,\tilde{i},\tilde{j}}, \quad (\text{B.6})$$

with  $J_{R,\tilde{i},\tilde{j}}$  the  $\tilde{j}^{th}$  Jordan block of the  $\tilde{i}^{th}$  distinct real eigenvalue  $\lambda_{\tilde{i}}$ . Second, if the matrix exhibits complex eigenvalues  $\lambda_{\tilde{i}} = a_{\tilde{i}} \pm b_{\tilde{i}}j$ , the Real Jordan form is more useful, because it avoids the occurrence of complex matrices  $J$  and  $Q$  in (B.1). A Jordan block  $J_{\tilde{i}}(a_{\tilde{i}} + b_{\tilde{i}}j)$  with complex eigenvalues can be replaced by a real Jordan block  $J_{C,\tilde{i}}(a_{\tilde{i}}, b_{\tilde{i}})$  (complex eigenvalues), of the form:

$$D, \begin{pmatrix} D & I \\ 0 & D \end{pmatrix}, \begin{pmatrix} D & I & 0 \\ 0 & D & I \\ 0 & 0 & D \end{pmatrix}, \begin{pmatrix} D & I & 0 & \dots & 0 \\ 0 & D & I & \dots & 0 \\ \vdots & & \ddots & & \vdots \\ 0 & 0 & \dots & D & I \\ 0 & 0 & \dots & 0 & D \end{pmatrix}, \quad (\text{B.7})$$

with the matrix  $D(a_{\tilde{i}}, b_{\tilde{i}})$ , defined as

$$D = \begin{pmatrix} a_{\tilde{i}} & -b_{\tilde{i}} \\ b_{\tilde{i}} & a_{\tilde{i}} \end{pmatrix} = a_{\tilde{i}}I + b_{\tilde{i}}L_r, \quad (\text{B.8})$$

with  $I$  the identity matrix,  $L_r = \begin{pmatrix} 0 & -1 \\ 1 & 0 \end{pmatrix}$  and  $L_r^2 = -I$ . Analogous to the Jordan Canonical form, it holds that each Jordan block  $J_{C,\tilde{i}}(a_{\tilde{i}}, b_{\tilde{i}})$  exists of different Jordan blocks if the geometric multiplicity  $g_{\tilde{i}}$  of the  $\tilde{i}^{th}$  distinct complex eigenvalue with positive imaginary part  $\lambda_{\tilde{i}} = a_{\tilde{i}} + b_{\tilde{i}}j$  is larger than one. The number of Jordan blocks for the  $\tilde{i}^{th}$  distinct pair of complex eigenvalues  $a_{\tilde{i}} \pm b_{\tilde{i}}j$  is equal to  $g_{\tilde{i}}$ , the geometric multiplicity of the eigenvalue with the positive imaginary part of the  $\tilde{i}^{th}$  pair of complex eigenvalues. Therefore it holds that:

$$J_{C,\tilde{i}} = \text{diag}(J_{C,\tilde{i},1}, J_{C,\tilde{i},2}, \dots, J_{C,\tilde{i},g_{\tilde{i}}}),$$

with  $J_{C,\tilde{i},1}, \dots, J_{C,\tilde{i},g_{\tilde{i}}}$ ,  $g_{\tilde{i}}$  Jordan blocks for the  $\tilde{i}^{th}$  distinct pair of complex eigenvalues  $\lambda_{\tilde{i}}$ . Similar to (B.5), the exponential function of the Real Jordan block  $J_{C,\tilde{i}}$ , described by one of the forms in (B.7), is given by:

$$e^{Ds}, \begin{pmatrix} e^{Ds} & se^{Ds} \\ 0 & e^{Ds} \end{pmatrix}, e^{Ds} \begin{pmatrix} e^{Ds} & se^{Ds} & \frac{s^2}{2!}e^{Ds} \\ 0 & e^{Ds} & se^{Ds} \\ 0 & 0 & e^{Ds} \end{pmatrix}, \quad (\text{B.9})$$

$$e^{Ds} \begin{pmatrix} I & se^{Ds} & \frac{s^2}{2!}e^{Ds} & \dots & \frac{s^{k-1}}{(k-1)!}e^{Ds} \\ 0 & e^{Ds} & se^{Ds} & \dots & \frac{s^{k-2}}{(k-2)!}e^{Ds} \\ \vdots & & \ddots & & \vdots \\ 0 & 0 & \dots & e^{Ds} & se^{Ds} \\ 0 & 0 & \dots & 0 & e^{Ds} \end{pmatrix},$$

with

$$e^{Ds} = e^{a_{\tilde{i}}s} \begin{pmatrix} \cos b_{\tilde{i}}s & -\sin b_{\tilde{i}}s \\ \sin b_{\tilde{i}}s & \cos b_{\tilde{i}}s \end{pmatrix}. \quad (\text{B.10})$$

Analogous to the Jordan Canonical form,  $q_{C,\tilde{i}}$  denotes the number of different parameters that are related to the  $\tilde{i}^{th}$  distinct pair of complex eigenvalues

$$q_{C,\tilde{i}} = \max_{\tilde{j}=1,2,\dots,g_{\tilde{i}}} \dim J_{C,\tilde{i},\tilde{j}}, \quad (\text{B.11})$$

where  $g_{\tilde{i}}$  denotes the geometric multiplicity of the  $\tilde{i}^{th}$  distinct complex eigenvalue with a positive imaginary part. Obviously, if both real and complex eigenvalues occur, combinations of the exponential of the Real Jordan blocks (B.7) and Jordan blocks (B.3) are used:  $J := \text{diag}(J_R, J_C)$ . Note that for real eigenvalues the Real Jordan form is equal to the Jordan Canonical form.

## B.2 Jordan forms of the NCS model

In this section, the general NCS description for small delays (4.5), used for the stability analysis and control synthesis, will be derived. Note that in Section B.3 the general NCS description for time-varying sampling intervals, delays larger than this sampling interval, and packet dropouts is discussed. As a starting point, consider the NCS model for small delays, as derived in Chapter 3, see (3.3):

$$\xi_{k+1} = \begin{pmatrix} e^{Ah} & \int_{h-\tau_k}^h e^{As} ds B \\ 0 & 0 \end{pmatrix} \xi_k + \begin{pmatrix} \int_0^{h-\tau_k} e^{As} ds B \\ I \end{pmatrix} u_k, \quad \forall \tau_k \in [\tau_{\min}, \tau_{\max}].$$

A general solution of the integrals in this equation in terms of the time-varying parameter  $h - \tau_k$  will be derived. To solve these integrals, we adopt the Jordan form of the continuous-time state matrix  $A$ , according to  $A = QJQ^{-1}$ , with  $J$  the Jordan Canonical form, Real Jordan form, or a combination. This gives:

$$\xi_{k+1} = \begin{pmatrix} Qe^{Jh}Q^{-1} & \int_{h-\tau_k}^h Qe^{Js}dsQ^{-1}B \\ 0 & 0 \end{pmatrix} \xi_k + \begin{pmatrix} \int_0^{h-\tau_k} Qe^{Js}dsQ^{-1}B \\ I \end{pmatrix} u_k, \quad (\text{B.12})$$

for all  $\tau_k \in [\tau_{\min}, \tau_{\max}]$ .

### Real eigenvalues

If  $A$  has only real eigenvalues that can be multiplicative (i.e. there may be eigenvalues  $\lambda_{\tilde{i}}$  with  $m_{\tilde{i}} > 1$ ), the exponential of  $A$  can be rewritten as:

$$e^{As} = Qe^{Js}Q^{-1} = Q \left( \sum_{\tilde{i}=1}^p \sum_{\hat{j}=0}^{q_{\tilde{i}}-1} \frac{s^{\hat{j}}}{\hat{j}!} e^{\lambda_{\tilde{i}}s} S_{\tilde{i},\hat{j}} \right) Q^{-1}, \quad (\text{B.13})$$



with  $S_{\bar{i},\hat{j}}$  a matrix with a one at the positions that correspond to the position in  $J$  at which the value  $\frac{s^{\hat{j}}}{\hat{j}!}e^{\lambda_{\bar{i}}s}$  appears (see e.g. (B.5)) and a zero at all other matrix positions and  $q_{\bar{i}}$  defined in (B.6). To explain  $S_{\bar{i},\hat{j}}$ , we give two examples.

Firstly, if  $J = \begin{pmatrix} \lambda_1 & 1 & 0 \\ 0 & \lambda_1 & 1 \\ 0 & 0 & \lambda_1 \end{pmatrix}$ , it holds that  $p = 1$ ,  $q_1 = 3$ , which gives:

$$e^{Js} = e^{\lambda_1 s} S_{1,0} + s e^{\lambda_1 s} S_{1,1} + \frac{s^2}{2} e^{\lambda_1 s} S_{1,2},$$

with

$$S_{1,0} = \begin{pmatrix} 1 & 0 & 0 \\ 0 & 1 & 0 \\ 0 & 0 & 1 \end{pmatrix}, S_{1,1} = \begin{pmatrix} 0 & 1 & 0 \\ 0 & 0 & 1 \\ 0 & 0 & 0 \end{pmatrix}, \text{ and } S_{1,2} = \begin{pmatrix} 0 & 0 & 1 \\ 0 & 0 & 0 \\ 0 & 0 & 0 \end{pmatrix}.$$

Secondly, if  $J = \begin{pmatrix} \lambda_1 & 0 & 0 \\ 0 & \lambda_2 & 1 \\ 0 & 0 & \lambda_2 \end{pmatrix}$ , it holds that  $p = 2$ ,  $q_1 = 1$ , and  $q_2 = 2$ , which gives:

$$e^{Js} = e^{\lambda_1 s} S_{1,0} + e^{\lambda_2 s} S_{2,0} + s e^{\lambda_2 s} S_{2,1},$$

with

$$S_{1,0} = \begin{pmatrix} 1 & 0 & 0 \\ 0 & 0 & 0 \\ 0 & 0 & 0 \end{pmatrix}, S_{2,0} = \begin{pmatrix} 0 & 0 & 0 \\ 0 & 1 & 0 \\ 0 & 0 & 1 \end{pmatrix}, \text{ and } S_{2,1} = \begin{pmatrix} 0 & 0 & 0 \\ 0 & 0 & 1 \\ 0 & 0 & 0 \end{pmatrix}.$$

From these examples, it is clear that  $S_{\bar{i},\hat{j}}$  depends on the combination of the Jordan blocks.

To rewrite the NCS model of (B.12), the integral  $\int e^{As} ds$  needs to be solved. If none of the eigenvalues is equal to zero, then  $J = J_{NZ}$  is invertible and a general solution for the integral can be obtained:

$$\int e^{As} ds = \int Q e^{Js} Q^{-1} ds = Q J_{NZ}^{-1} \left( \sum_{\bar{i}=1}^{p_{NZ}} \sum_{\hat{j}=0}^{q_{\bar{i}}-1} \frac{s^{\hat{j}}}{\hat{j}!} e^{\lambda_{\bar{i}} s} S_{\bar{i},\hat{j}} \right) Q^{-1}, \quad (\text{B.14})$$

with  $p_{NZ}$  the number of distinct real, non-zero eigenvalues. The NCS model (B.12) can be written as:

$$\begin{aligned} \xi_{k+1} = & \begin{pmatrix} Q e^{J_{NZ} h} Q^{-1} & Q J_{NZ}^{-1} (e^{J_{NZ} h} - e^{J_{NZ} (h-\tau_k)}) Q^{-1} B \\ 0 & 0 \end{pmatrix} \xi_k + \\ & \begin{pmatrix} Q J_{NZ}^{-1} (e^{J_{NZ} (h-\tau_k)} - I) Q^{-1} B \\ I \end{pmatrix} u_k, \forall \tau_k \in [\tau_{\min}, \tau_{\max}], \end{aligned}$$

with  $e^{J_{NZ} (h-\tau_k)} = \sum_{\bar{i}=1}^{p_{NZ}} \sum_{\hat{j}=0}^{q_{\bar{i}}-1} \frac{(h-\tau_k)^{\hat{j}}}{\hat{j}!} e^{\lambda_{\bar{i}} (h-\tau_k)} S_{\bar{i},\hat{j}}$ .

If eigenvalues equal to zero occur, the inverse of the Jordan matrix  $J = J_Z$  does not exist and the description as in (B.14) cannot be used. The equivalent for (B.14) for the case of eigenvalues equal to zero is given by:

$$\int e^{As} ds = \int Q e^{J_Z s} Q^{-1} ds = Q \left( \sum_{\tilde{i}=1}^{p_Z} \sum_{\hat{j}=1}^{q_{\tilde{i}}} \frac{s^{\hat{j}}}{\hat{j}!} e^{\lambda_{\tilde{i}} s} S_{\tilde{i}, \hat{j}-1} \right) Q^{-1}, \quad (\text{B.15})$$

with  $p_Z := 1$  the number of distinct eigenvalues equal to zero. Note that it holds for real eigenvalues that  $p = p_{NZ} + p_Z$ , with  $p$  the number of distinct real eigenvalues. The corresponding NCS model is written as:

$$\begin{aligned} \xi_{k+1} = & \begin{pmatrix} Q e^{J_Z h} Q^{-1} & \sum_{\hat{j}=1}^{q_Z} \left( \frac{h^{\hat{j}}}{\hat{j}!} - \frac{(h-\tau_k)^{\hat{j}}}{\hat{j}!} \right) Q S_{1, \hat{j}-1} Q^{-1} B \\ 0 & 0 \end{pmatrix} \xi_k + \\ & \begin{pmatrix} \sum_{\hat{j}=1}^{q_Z} \frac{(h-\tau_k)^{\hat{j}}}{\hat{j}!} Q S_{1, \hat{j}-1} Q^{-1} B \\ I \end{pmatrix} u_k, \quad \forall \tau_k \in [\tau_{\min}, \tau_{\max}], \end{aligned} \quad (\text{B.16})$$

with  $q_Z$  the size of the maximum Jordan block for the eigenvalues equal to zero as defined in (B.6),  $S_{1, \hat{j}}$  defined according to (B.13), with  $\tilde{i} := 1$ , because  $p_Z := 1$ .

### Complex eigenvalues

If  $A$  has only complex eigenvalues, the Real Jordan form (denoted by  $J_C$ ) is applied to avoid the occurrence of complex values of the matrix entries in the system matrices. A general solution for the matrix exponential  $e^{As}$ , similar to (B.13), is given by:

$$\begin{aligned} e^{As} &= Q e^{J_C s} Q^{-1} \\ &= Q \left( \sum_{\tilde{i}=1}^{p_C} \sum_{\hat{j}=0}^{q_{C, \tilde{i}}-1} \frac{s^{\hat{j}}}{\hat{j}!} e^{a_{\tilde{i}} s} (\cos(b_{\tilde{i}} s) S_{\tilde{i}, \hat{j}, 1} + \sin(b_{\tilde{i}} s) S_{\tilde{i}, \hat{j}, 2}) \right) Q^{-1}, \end{aligned} \quad (\text{B.17})$$

with  $p_C$  the number of distinct complex pairs of eigenvalues. A general expression for  $S_{\tilde{i}, \hat{j}, 1}$  and  $S_{\tilde{i}, \hat{j}, 2}$  is complicated to derive; therefore we give two examples. The first example deals with one complex pair of eigenvalues and the second example deals with a complex pair of eigenvalues that occurs twice. If we assume that  $J_C = \begin{pmatrix} a & -b \\ b & a \end{pmatrix}$ , which corresponds to one complex pair of eigenvalues (i.e.  $p_C = 1$  and  $q_{C,1} = 2$ ), the exponential of the Real Jordan matrix  $e^{J_C s}$  is given by:  $e^{J_C s} = e^{as} \begin{pmatrix} \cos(bs) & -\sin(bs) \\ \sin(bs) & \cos(bs) \end{pmatrix}$ . Then it holds that

$$S_{1,0,1} = \begin{pmatrix} 1 & 0 \\ 0 & 1 \end{pmatrix}, \quad S_{1,0,2} = \begin{pmatrix} 0 & -1 \\ 1 & 0 \end{pmatrix}. \quad (\text{B.18})$$

To solve the integrals in (B.12), the following relations are used:

$$\int e^{as} \cos(bs) ds = \frac{e^{as}}{a^2 + b^2} (a \cos(bs) + b \sin(bs)), \quad (\text{B.19})$$

and

$$\int e^{as} \sin(bs) ds = \frac{e^{as}}{a^2 + b^2} (a \sin(bs) - b \cos(bs)). \quad (\text{B.20})$$

Then, system (B.12) can be rewritten as  $\xi_{k+1} = \begin{pmatrix} \bar{\Phi}_0 & \bar{\Phi}_1 \\ 0 & 0 \end{pmatrix} \xi_k + \begin{pmatrix} \bar{\Gamma} \\ I \end{pmatrix} u_k$ , with

$$\bar{\Phi}_0 = e^{ah} Q \begin{pmatrix} \cos(bh) & -\sin(bh) \\ \sin(bh) & \cos(bh) \end{pmatrix} Q^{-1},$$

$$\begin{aligned} \bar{\Phi}_1 = & \frac{e^{ah}}{a^2 + b^2} Q \begin{pmatrix} a \cos(bh) + b \sin(bh) & -a \sin(bh) + b \cos(bh) \\ a \sin(bh) - b \cos(bh) & a \cos(bh) + b \sin(bh) \end{pmatrix} Q^{-1} B \\ & - e^{a(h-\tau_k)} Q (\cos(b(h-\tau_k)) S_{1,0,1} + \sin(b(h-\tau_k)) S_{1,0,2}) Q^{-1} B, \end{aligned}$$

$$\begin{aligned} \bar{\Gamma} = & -Q \frac{1}{a^2 + b^2} \begin{pmatrix} a & b \\ -b & a \end{pmatrix} Q^{-1} B \\ & + e^{a(h-\tau_k)} Q (\cos(b(h-\tau_k)) S_{1,0,1} + \sin(b(h-\tau_k)) S_{1,0,2}) Q^{-1} B, \end{aligned}$$

and

$$S_{1,0,1} = \frac{1}{a^2 + b^2} \begin{pmatrix} a & b \\ -b & a \end{pmatrix}, \quad S_{1,0,2} = \frac{1}{a^2 + b^2} \begin{pmatrix} b & -a \\ a & b \end{pmatrix}. \quad (\text{B.21})$$

If a pair of complex eigenvalues occurs twice, another Real Jordan matrix needs to be used:  $J_C = \begin{pmatrix} a & -b & 1 & 0 \\ b & a & 0 & 1 \\ 0 & 0 & a & -b \\ 0 & 0 & b & a \end{pmatrix}$ . It holds that in (B.17):

$$S_{1,0,1} = \begin{pmatrix} I & 0 \\ 0 & I \end{pmatrix}, \quad S_{1,1,1} = \begin{pmatrix} 0 & I \\ 0 & 0 \end{pmatrix}, \quad S_{1,0,2} = \begin{pmatrix} \Psi & 0 \\ 0 & \Psi \end{pmatrix}, \quad S_{1,1,2} = \begin{pmatrix} 0 & \Psi \\ 0 & 0 \end{pmatrix}, \quad (\text{B.22})$$

with  $I$  a  $2 \times 2$  identity matrix and  $\Psi = \begin{pmatrix} 0 & -1 \\ 1 & 0 \end{pmatrix}$ . In this case, besides the integral in (B.19) and (B.20), two additional integrals need to be solved to find a general solution for (B.12):

$$\begin{aligned} \int s e^{as} \cos(bs) ds = & \frac{s e^{as}}{a^2 + b^2} (a \cos(bs) + b \sin(bs)) + \\ & \frac{e^{as}}{(a^2 + b^2)^2} ((b^2 - a^2) \cos(bs) - 2ab \sin(bs)), \end{aligned} \quad (\text{B.23})$$

and

$$\begin{aligned} \int s e^{as} \sin(bs) ds = & \frac{s e^{as}}{a^2 + b^2} (a \sin(bs) - b \cos(bs)) + \\ & \frac{e^{as}}{(a^2 + b^2)^2} ((b^2 - a^2) \sin(bs) + 2ab \cos(bs)). \end{aligned} \quad (\text{B.24})$$

System (B.12) can now be formulated as:  $\xi_{k+1} = \begin{pmatrix} \bar{\Phi}_0 & \bar{\Phi}_1 \\ 0 & 0 \end{pmatrix} \xi_k + \begin{pmatrix} \bar{\Gamma} \\ I \end{pmatrix} u_k$ , with

$$\begin{aligned} \bar{\Phi}_0 &= Q e^{ah} \begin{pmatrix} \cos bh & -\sin bh & h \cos bh & -h \sin bh \\ \sin bh & \cos bh & h \sin bh & h \cos bh \\ 0 & 0 & \cos bh & -\sin bh \\ 0 & 0 & \sin bh & \cos bh \end{pmatrix} Q^{-1}, \\ \bar{\Phi}_1 &= \frac{e^{ah}}{a^2 + b^2} Q L Q^{-1} B \\ &\quad - e^{a(h-\tau_k)} Q (\cos(b(h-\tau_k)) S_{1,0,1} + \sin(b(h-\tau_k)) S_{1,0,2}) Q^{-1} B \\ &\quad - (h-\tau_k) \frac{e^{a(h-\tau_k)}}{a^2 + b^2} Q (\cos(b(h-\tau_k)) S_{1,1,1} + \sin(b(h-\tau_k)) S_{1,1,2}) Q^{-1} B, \\ \bar{\Gamma} &= -Q \frac{1}{a^2 + b^2} \begin{pmatrix} a & b & \frac{b^2-a^2}{a^2+b^2} & -\frac{2ab}{a^2+b^2} \\ -b & a & \frac{2ab}{a^2+b^2} & \frac{b^2-a^2}{a^2+b^2} \\ 0 & 0 & a & b \\ 0 & 0 & -b & a \end{pmatrix} Q^{-1} B \\ &\quad + e^{a(h-\tau_k)} Q (\cos(b(h-\tau_k)) S_{1,0,1} + \sin(b(h-\tau_k)) S_{1,0,2}) Q^{-1} B \\ &\quad + (h-\tau_k) e^{a(h-\tau_k)} Q (\cos(b(h-\tau_k)) S_{1,1,1} + \sin(b(h-\tau_k)) S_{1,1,2}) Q^{-1} B, \\ L &= \begin{pmatrix} l_1 & l_2 & l_3 & l_4 \\ -l_2 & l_1 & -l_4 & l_3 \\ 0 & 0 & l_1 & l_2 \\ 0 & 0 & -l_2 & l_1 \end{pmatrix}, \tag{B.25} \\ l_1 &= a \cos bh + b \sin bh, \quad l_2 = -a \sin bh + b \cos bh, \\ l_3 &= h(a \cos bh + b \sin bh) + \frac{1}{a^2 + b^2} ((b^2 - a^2) \cos bh - 2ab \sin bh), \\ l_4 &= h(-a \sin bh + b \cos bh) - \frac{1}{a^2 + b^2} (2ab \cos bh + (b^2 - a^2) \sin bh), \end{aligned}$$

and

$$\begin{aligned} S_{1,0,1} &= \frac{1}{a^2 + b^2} \begin{pmatrix} a & b & \frac{b^2-a^2}{a^2+b^2} & -\frac{2ab}{a^2+b^2} \\ -b & a & \frac{2ab}{a^2+b^2} & \frac{b^2-a^2}{a^2+b^2} \\ 0 & 0 & a & b \\ 0 & 0 & -b & a \end{pmatrix}, \\ S_{1,0,2} &= \frac{1}{a^2 + b^2} \begin{pmatrix} b & -a & \frac{-2ab}{a^2+b^2} & \frac{a^2-b^2}{a^2+b^2} \\ a & b & \frac{b^2-a^2}{a^2+b^2} & -\frac{2ab}{a^2+b^2} \\ 0 & 0 & b & -a \\ 0 & 0 & a & b \end{pmatrix}, \\ S_{1,1,1} &= \frac{1}{a^2 + b^2} \begin{pmatrix} 0 & 0 & a & b \\ 0 & 0 & -b & a \\ 0 & 0 & 0 & 0 \\ 0 & 0 & 0 & 0 \end{pmatrix}, \quad S_{1,1,2} = \frac{1}{a^2 + b^2} \begin{pmatrix} 0 & 0 & b & -a \\ 0 & 0 & a & b \\ 0 & 0 & 0 & 0 \\ 0 & 0 & 0 & 0 \end{pmatrix}. \tag{B.26} \end{aligned}$$

### Both complex and real eigenvalues

If the system matrix  $A$  consists of both complex and real eigenvalues, a combination of the previously obtained results should be used. The Jordan matrix can then be written as:

$$J = \text{diag}(J_{NZ}, J_Z, J_C), \quad (\text{B.27})$$

where  $J_{NZ}$  represents the Jordan block with all real, non-zero eigenvalues,  $J_Z$  the Jordan block for all real, zero eigenvalues and  $J_C$  the real Jordan block with all complex eigenvalues.

For the purpose of stability analysis and control synthesis, the time-varying matrices in the NCS model (B.12) that is applicable for a NCS with time-delays smaller than the constant sampling interval, are divided in time-varying parameters and constant matrices:

$$\xi_{k+1} = \left( F_0 + \sum_{i=1}^{\nu} \alpha_i(\tau_k) F_i \right) \xi_k + \left( G_0 + \sum_{i=1}^{\nu} \alpha_i(\tau_k) G_i \right) u_k, \quad (\text{B.28})$$

with  $\alpha_i(\tau_k)$  functions depending on the time-varying delay  $\tau$ , and  $\nu$  the number of distinct functions of  $\tau$ , given by:

$$\nu = \nu_{NZ} + \nu_Z + \nu_C, \quad (\text{B.29})$$

with

$$\begin{aligned} \nu_{NZ} &= \sum_{\tilde{i}=1}^{p_{NZ}} q_{\tilde{i}}, \\ \nu_Z &= q_Z, \\ \nu_C &= \sum_{\tilde{i}=1}^{p_C} q_{C,\tilde{i}}, \end{aligned} \quad (\text{B.30})$$

$q_{\tilde{i}}$  and  $q_Z$  defined in (B.6), and  $q_{C,\tilde{i}}$  defined in (B.11). The time-varying parameter  $\alpha_i(\tau_k)$  is given by:

$$\alpha_i(\tau_k) = \begin{cases} \alpha_{NZ,i}(\tau_k) & \text{if } i \in \{1, 2, \dots, \nu_{NZ}\} \\ \alpha_{Z,i}(\tau_k) & \text{if } i \in \{\nu_{NZ} + 1, \nu_{NZ} + 2, \dots, \nu_{NZ} + \nu_Z\} \\ \alpha_{C,i}(\tau_k) & \text{if } i \in \{\nu_{NZ} + \nu_Z + 1, \nu_{NZ} + \nu_Z + 2, \dots, \nu\}, \end{cases} \quad (\text{B.31})$$

where  $\alpha_{NZ,i}(\tau_k)$  denotes the functions related to the eigenvalues which are real and unequal to zero,  $\alpha_{Z,i}(\tau_k)$  the functions related to the eigenvalues which are equal to zero, and  $\alpha_{C,i}(\tau_k)$  the functions related to the complex eigenvalues. Note that if no real eigenvalues, unequal to zero occur then  $\nu_{NZ} = 0$ , if no zero eigenvalues occur then  $\nu_Z = 0$ , and if no complex eigenvalues occur then  $\nu_C = 0$ . Next, the parameters  $\alpha_i(\tau_k)$ ,  $i \in \{1, 2, \dots, \nu\}$ , will be derived for, firstly, real eigenvalues that are unequal to zero, secondly, real eigenvalues that are equal

to zero, and thirdly, complex eigenvalues. First, if the continuous-time system matrix  $A$  has one or more real, non-zero eigenvalues, then  $\alpha_{NZ,i}(\tau_k)$  is given by:

$$\alpha_{NZ,i}(\tau_k) = \frac{(h - \tau_k)^{\hat{j}}}{\hat{j}!} e^{\lambda_l(h - \tau_k)}, \quad (B.32)$$

for  $\hat{j} = 0, 1, \dots, q_l - 1$  and  $i = \sum_{\tilde{i}=1}^l q_{\tilde{i}} + 1 - q_l, \dots, \sum_{\tilde{i}=1}^l q_{\tilde{i}}$ ,

with  $q_{\tilde{i}}$  defined in (B.6) and  $l \in \{1, 2, \dots, p_{NZ}\}$ . Second, if the continuous-time system matrix  $A$  has one or more eigenvalues that are equal to zero, then  $\alpha_{Z,i}(\tau_k)$ ,  $i \in \{\nu_{NZ} + 1, \nu_{NZ} + 2, \dots, \nu_{NZ} + \nu_Z\}$ , is given by:

$$\alpha_{Z,i} = \frac{(h - \tau_k)^{\hat{j}}}{\hat{j}!}, \text{ for } \hat{j} = i - \nu_{NZ}, i = \nu_{NZ} + 1, \nu_{NZ} + 2, \dots, \nu_{NZ} + \nu_Z. \quad (B.33)$$

Third, if the continuous-time system matrix  $A$  has one or more complex eigenvalues, then the time-varying parameters  $\alpha_{C,i}(\tau_k)$ ,  $i \in \{\nu_{NZ} + \nu_Z + 1, \nu_{NZ} + \nu_Z + 2, \dots, \nu\}$ , are given by:

$$\alpha_{C,i}(\tau_k) = \begin{cases} \frac{(h - \tau_k)^{\hat{j}}}{\hat{j}!} e^{a_l(h - \tau_k)} \cos(b_l(h - \tau_k)), & \text{for } \hat{j} = 0, 1, \dots, \frac{q_{C,l}}{2} - 1, \text{ and} \\ i = \nu_{NZ} + \nu_Z + \sum_{\tilde{i}=1}^l q_{C,\tilde{i}} - q_{C,l} + 1, \dots, \nu_{NZ} + \nu_Z + \sum_{\tilde{i}=1}^l q_{C,\tilde{i}} - \frac{q_{C,l}}{2}, \\ \frac{(h - \tau_k)^{\hat{j}}}{\hat{j}!} e^{a_l(h - \tau_k)} \sin(b_l(h - \tau_k)), & \text{for } \hat{j} = 0, 1, \dots, \frac{q_{C,l}}{2} - 1, \text{ and} \\ i = \nu_{NZ} + \nu_Z + \sum_{\tilde{i}=1}^l q_{C,\tilde{i}} - \frac{q_{C,l}}{2} + 1, \dots, \nu_{NZ} + \nu_Z + \sum_{\tilde{i}=1}^l q_{C,\tilde{i}}, \end{cases} \quad (B.34)$$

where  $a_l$  and  $b_l$  represent the real and complex part of the complex eigenvalue  $\lambda_l$ , according to  $\lambda_l = a_l \pm b_l j$  for  $l = 1, 2, \dots, q_C$ . Similar to the derivation of the time-varying parameter  $\alpha_i(\tau_k)$ , the constant matrices  $F_i$  and  $G_i$ ,  $i \in \{1, 2, \dots, \nu\}$ , in (B.28) are given by:

$$F_0 = \begin{pmatrix} Q\Theta_0 Q^{-1} & Q\Theta_1 Q^{-1} B \\ 0 & 0 \end{pmatrix}, G_0 = \begin{pmatrix} Q\Xi_0 Q^{-1} B \\ I_{m,m} \end{pmatrix}, \quad (B.35)$$

$$F_i = \begin{pmatrix} 0 & Q\Gamma_{1,i} Q^{-1} B \\ 0 & 0 \end{pmatrix}, \text{ and } G_i = \begin{pmatrix} Q\Xi_i Q^{-1} B \\ 0 \end{pmatrix}.$$

For  $\Theta_0$  it holds that:  $\Theta_0 = \text{diag}(e^{J_{NZ}h}, e^{J_Zh}, e^{J_Ch})$ , and for  $\Xi_0$  it holds that:  $\Xi_0 = -\text{diag}(J_{NZ}^{-1}, O_Z, \Lambda_0)$ , with  $O_Z$  a matrix with zeros of the same dimension as  $J_Z$  and  $\Lambda_0$  a matrix dependent on the Jordan form for complex eigenvalues defined as:

$$\Lambda_0 = Q \frac{1}{a^2 + b^2} \begin{pmatrix} a & b \\ -b & a \end{pmatrix} Q^{-1} B, \quad (B.36)$$

for the case with only one pair of complex eigenvalues or

$$\Lambda_0 = Q \frac{1}{a^2 + b^2} \begin{pmatrix} a & b & \frac{b^2 - a^2}{a^2 + b^2} & -\frac{2ab}{a^2 + b^2} \\ -b & a & \frac{2ab}{a^2 + b^2} & \frac{b^2 - a^2}{a^2 + b^2} \\ 0 & 0 & a & b \\ 0 & 0 & -b & a \end{pmatrix} Q^{-1} B, \quad (\text{B.37})$$

for the case with two identical pairs of complex eigenvalues. For the sake of brevity, it holds that  $a := a_{\bar{i}}$ ,  $b := b_{\bar{i}}$ . The other parameters  $\Theta_1$ ,  $\Gamma_{1,i}$ , and  $\Xi_i$ ,  $i \in \{1, 2, \dots, \nu\}$ , are more complicated to derive, therefore we consider the different cases again. Note that it holds that

$$\begin{aligned} \Theta_1 &= \text{diag}(\Theta_1^{NZ}, \Theta_1^Z, \Theta_1^C), \\ \Gamma_{1,i} &= \text{diag}(\Gamma_{1,i}^{NZ}, \Gamma_{1,i}^Z, \Gamma_{1,i}^C), \quad \forall i \in \{1, 2, \dots, \nu\}, \\ \Xi_i &= \text{diag}(\Xi_i^{NZ}, \Xi_i^Z, \Xi_i^C), \quad \forall i \in \{1, 2, \dots, \nu\}. \end{aligned}$$

- For real eigenvalues unequal to zero it holds that:

$$\begin{aligned} \Theta_1^{NZ} &= J_{NZ}^{-1} e^{J_{NZ} h}, \\ \Gamma_{1,i}^{NZ} &= \begin{cases} -J_{NZ}^{-1} T_i^{NZ} & \text{if } i \in \{1, 2, \dots, \nu_{NZ}\} \\ 0 & \text{if } i \notin \{1, 2, \dots, \nu_{NZ}\}, \end{cases} \\ \Xi_i^{NZ} &= -\Gamma_{1,i}^{NZ}. \end{aligned}$$

The matrices  $T_i^{NZ}$ ,  $i \in \{1, 2, \dots, \nu\}$ , are given by:

$$T_i^{NZ} = \begin{cases} S_{l,\hat{j}} & \text{with } \hat{j} = 0, 1, \dots, q_l - 1, \\ & \text{for } i \in \{\sum_{\hat{i}=1}^{q_l} + 1 - q_l, \dots, \sum_{\hat{i}=1}^{q_l}\} \\ 0 & \text{for } i \notin \{\sum_{\hat{i}=1}^{q_l} + 1 - q_l, \dots, \sum_{\hat{i}=1}^{q_l}\}, \end{cases}$$

with  $l \in \{1, 2, \dots, p_{NZ}\}$ .

- For eigenvalues equal to zero it holds that:

$$\begin{aligned} \Theta_1^Z &= \sum_{\hat{j}=1}^{q_Z} \frac{h^{\hat{j}}}{\hat{j}!} S_{p_{NZ}+1, \hat{j}-1}, \\ \Gamma_{1,i}^Z &= \begin{cases} -S_{p_{NZ}+1, \hat{j}-1} & \text{for } \hat{j} = i - \nu_{NZ} \text{ and} \\ & i \in \{\nu_{NZ} + 1, \nu_{NZ} + 2, \dots, \nu_{NZ} + \nu_Z\} \\ 0 & \text{if } i \notin \{\nu_{NZ} + 1, \nu_{NZ} + 2, \dots, \nu_{NZ} + \nu_Z\}, \end{cases} \\ \Xi_i^Z &= -\Gamma_{1,i}^Z. \end{aligned}$$

Note that in  $\Gamma_{1,i}^Z$ , the matrix  $S_{p_{NZ}+1, \hat{j}-1}$  is used instead of  $S_{1, \hat{j}-1}$  in (B.16), such that real eigenvalues that are unequal to zero can be included.

- Finally, for complex eigenvalues it holds that:

$\Theta_1^C = \frac{e^{ah}}{a^2+b^2} \begin{pmatrix} a \cos(bh) + b \sin(bh) & -a \sin(bh) + b \cos(bh) \\ a \sin(bh) - b \cos(bh) & a \cos(bh) + b \sin(bh) \end{pmatrix}$  for one complex pair of eigenvalues or  $\Theta_1^C = \frac{e^{ah}}{a^2+b^2} L$  if the same pair of eigenvalues occurs twice, with  $L$  defined in (B.25). Moreover, it holds that:

$$\Gamma_{1,i}^C = \begin{cases} -T_i^C & \text{if } i \in \{\nu_{NZ} + \nu_Z + 1, \nu_{NZ} + \nu_Z + 2, \dots, \nu\} \\ 0 & \text{if } i \notin \{\nu_{NZ} + \nu_Z + 1, \nu_{NZ} + \nu_Z + 2, \dots, \nu\}, \end{cases}$$

and analogously to the previous cases:

$$\Xi_i^C = -\Gamma_{1,i}^C.$$

The matrices  $T_i^C$ , with  $i \in \{1, 2, \dots, \nu\}$ , are defined as:

$$T_i^C = \begin{cases} S_{l,\hat{j},1} & \text{for } \hat{j} = 0, 1, \dots, \frac{q_{C,l}}{2} - 1 \text{ and} \\ & i \in \{\nu_{NZ} + \nu_Z + \sum_{\tilde{i}=1}^l q_{C,\tilde{i}} - q_{C,l} + 1, \dots, \\ & \quad \nu_{NZ} + \nu_Z + \sum_{\tilde{i}=1}^l q_{C,\tilde{i}} - \frac{q_{C,l}}{2}\} \\ S_{l,\hat{j},2} & \text{for } \hat{j} = 0, 1, \dots, \frac{q_{C,l}}{2} - 1 \text{ and} \\ & i \in \{\nu_{NZ} + \nu_Z + \sum_{\tilde{i}=1}^l q_{C,\tilde{i}} - \frac{q_{C,l}}{2} + 1, \dots, \nu_{NZ} + \nu_Z + \sum_{\tilde{i}=1}^l q_{C,\tilde{i}}\} \\ 0 & \text{if } i \notin \{\nu_{NZ} + \nu_Z + 1, \dots, \nu_{NZ} + \nu_Z + \nu_C\}, \end{cases}$$

with  $l \in \{1, 2, \dots, p_C\}$ . The matrices  $S_{\tilde{i},\hat{j},1}$  and  $S_{\tilde{i},\hat{j},2}$  are defined in (B.21) for  $\hat{j} = 0$  if only one pair of complex eigenvalues occurs and in (B.26) for  $\hat{j} = 0, 1$  if the same pair of complex eigenvalues occurs twice.

### B.3 Time-varying sampling intervals

For time-varying delays and time-varying sampling intervals, the general NCS model, in terms of the Jordan form of the continuous-time system matrix  $A$  is given by (4.7):

$$\xi_{k+1} = \left( F_0 + \sum_{i=1}^{\zeta} \alpha_i(t_j^k, h_k) F_i \right) \xi_k + \left( G_0 + \sum_{i=1}^{\zeta} \alpha_i(t_j^k, h_k) G_i \right) u_k.$$

The NCS models for time-varying delays, with or without packet dropouts, see (4.6), are included in this model. An important difference between the case with and without variation in the sampling interval is the change in the function  $\alpha_i$ . It depends either on  $h_k - t_j^k$  or on  $h_k$  for the case with time-varying sampling intervals, and on  $h - t_j^k$  for the case with constant sampling intervals. Additionally, the number of time-varying functions  $\alpha_i$  differs. For the case with time-varying sampling intervals, the number of time-varying functions  $\alpha_i(t_j^k, h_k)$  is given by  $\zeta := \zeta_{NZ} + \zeta_Z + \zeta_C$ , with  $\zeta_{NZ} = (\bar{\delta} + \bar{d} - \underline{d} + 1)\nu_{NZ}$ ,  $\nu_{NZ} = \sum_{\tilde{i}=1}^{p_{NZ}} q_{\tilde{i}}$ , and  $q_{\tilde{i}}$  defined in (B.6),  $\zeta_Z = (\bar{\delta} + \bar{d} - \underline{d} + 1)q_Z$ , and  $q_Z$



defined analogously to (B.6), because (B.6) holds for all real eigenvalues, and  $\zeta_C = (\bar{\delta} + \bar{d} - \underline{d} + 1)\nu_C$ ,  $\nu_C = \sum_{\tilde{i}=1}^{p_C} q_{C,\tilde{i}}$ , and  $q_{C,\tilde{i}}$  defined in (B.11). For the case with constant sampling intervals, the number of time-varying functions  $\alpha_i(t_j^k)$  is defined as  $\beta := \beta_{NZ} + \beta_Z + \beta_C$ , with  $\beta_{NZ} = (\bar{\delta} + \bar{d} - \underline{d})\nu_{NZ}$ , and  $\nu_{NZ} = \sum_{\tilde{i}=1}^{p_{NZ}} q_{\tilde{i}}$ , with  $q_{\tilde{i}}$  defined in (B.6),  $\beta_Z = (\bar{\delta} + \bar{d} - \underline{d})q_Z$ , with  $q_Z$  defined analogously to (B.6), and  $\beta_C = (\bar{\delta} + \bar{d} - \underline{d})\nu_C$ ,  $\nu_C = \sum_{\tilde{i}=1}^{p_C} q_{C,\tilde{i}}$ , with  $q_{C,\tilde{i}}$  defined in (B.11). In this section, we describe the case with time-varying sampling intervals; if differences exist for the case with constant sampling intervals, they will be denoted separately. The time-varying parameters  $\alpha_i(t_j^k, h_k)$  are obtained by solving the integrals in  $\tilde{M}_\rho$  in (3.25),  $\rho = 0, 1, 2, \dots, \bar{d} + \bar{\delta}$ .

$$\alpha_i(t_j^k, h_k) = \begin{cases} \alpha_{NZ,i}(t_j^k, h_k) & \text{if } i \in \{1, 2, \dots, \zeta_{NZ}\} \\ \alpha_{Z,i}(t_j^k, h_k) & \text{if } i \in \{\zeta_{NZ} + 1, \zeta_{NZ} + 2, \dots, \zeta_{NZ} + \zeta_Z\} \\ \alpha_{C,i}(t_j^k, h_k) & \text{if } i \in \{\zeta_{NZ} + \zeta_Z + 1, \zeta_{NZ} + \zeta_Z + 2, \dots, \zeta\}. \end{cases} \quad (\text{B.38})$$

The function  $\alpha_{NZ,i}(t_j^k, h_k)$   $i \in \{1, 2, \dots, \zeta_{NZ}\}$ , is given by:

$$\alpha_{NZ,i}(t_j^k, h_k) = \begin{cases} \frac{(h_k - t_j^k)^{\hat{j}}}{\hat{j}!} e^{\lambda_l(h_k - t_j^k)} & \text{for } \hat{j} = 0, 1, \dots, q_l - 1, \\ i = (j - (k - \bar{d})) \sum_{\tilde{i}=1}^l q_{\tilde{i}} - q_l + 1, \dots, (j - (k - \bar{d})) \sum_{\tilde{i}=1}^l q_{\tilde{i}}, \\ \text{and } j = k - \bar{d} + 1, k - \bar{d} + 2, \dots, k - \underline{d} \\ \frac{(h_k)^{\hat{j}}}{\hat{j}!} e^{\lambda_l h_k} & \text{for } \hat{j} = 0, 1, \dots, q_l - 1, \text{ and} \\ i = \beta_{NZ} + \sum_{\tilde{i}=1}^l q_{\tilde{i}} - q_l + 1, \dots, \beta_{NZ} + \sum_{\tilde{i}=1}^l q_{\tilde{i}} \\ 0 & \text{if } i \notin \{1, 2, \dots, \zeta_{NZ}\}. \end{cases} \quad (\text{B.39})$$

Here,  $l$  denotes the number of the distinct real, non-zero eigenvalue, with  $l \in \{1, 2, \dots, p_{NZ}\}$ . For constant sampling intervals, the second possibility  $\frac{(h_k)^{\hat{j}}}{\hat{j}!} e^{\lambda_l h_k}$  can be omitted, because it results in a constant parameter for each  $j \in \{k - \bar{d} + 1, \dots, k - \underline{d}\}$ . Then, only  $\beta_{NZ}$  time-varying functions  $\alpha_i(t_j^k)$  are obtained based on (B.39). Additionally,  $\alpha_{NZ,i}(t_j^k) = 0$  if  $i \notin \{1, 2, \dots, \beta_{NZ}\}$ . Observe that the uncertain term  $\frac{(h_k - t_j^k)^{\hat{j}}}{\hat{j}!} e^{\lambda_l(h_k - t_j^k)}$  corresponds to (B.32), if  $t_j^k$  is replaced by  $\tau_k$ . This uncertain term is repeated  $\bar{d} + \bar{\delta} - \underline{d}$  times, which is the number of different values of  $j$  and therefore of  $t_j^k$ . Note that the range of  $j$  is defined in Lemma 3.15 as  $k - \bar{d} - \bar{\delta} \leq j \leq k - \underline{d}$  and that  $t_{k-\bar{d}-\bar{\delta}} := 0$ . The

function  $\alpha_{Z,i}(t_j^k, h_k)$  is given by:

$$\alpha_{Z,i}(t_j^k, h_k) = \begin{cases} \frac{(h_k - t_j^k)^{\hat{j}}}{\hat{j}!} & \text{for } \hat{j} = i - (\zeta_{NZ} + (j - (k - \bar{d}))q_Z - q_Z), \\ & i = \zeta_{NZ} + (j - (k - \bar{d}))q_Z - q_Z + 1, \dots, \zeta_{NZ} + (j - (k - \bar{d}))q_Z, \\ & \text{and } j = k - \bar{d} + 1, k - \bar{d} + 2, \dots, k - \underline{d} \\ \frac{(h_k)^{\hat{j}}}{\hat{j}!} & \text{for } \hat{j} = i - \zeta_{NZ} - \beta_{NZ}, \text{ and } i \in \{\zeta_{NZ} + \beta_{NZ} + 1, \dots, \zeta_{NZ} + \zeta_{NZ}\} \\ 0 & \text{if } i \notin \{\zeta_{NZ} + 1, \zeta_{NZ} + 2, \dots, \zeta_{NZ} + \zeta_Z\}. \end{cases} \quad (\text{B.40})$$

For constant sampling intervals, the functions  $\alpha_i(h_k) = \frac{(h_k)^{\hat{j}}}{\hat{j}!}$  need to be removed, because they are constant. This results in  $\beta_Z$  time-varying functions, instead of  $\zeta_Z$ . Therefore, the parameters  $\zeta_Z$ , as well as  $\zeta_{NZ}$  need to be replaced by  $\beta_Z$  and  $\beta_{NZ}$ , respectively. Next, consider the continuous-time system matrix  $A$  with one or more complex eigenvalues. The function  $\alpha_{C,i}(t_j^k, h_k)$  is given by:

$$\alpha_{C,i}(t_j^k, h_k) = \begin{cases} \frac{(h_k - t_j^k)^{\hat{j}}}{\hat{j}!} e^{a_l(h_k - t_j^k)} \cos(b_l(h_k - t_j^k)) & \text{for } \hat{j} = 0, 1, \dots, \frac{q_{C,l}}{2} - 1, \\ & i = \zeta_{NZ} + \zeta_Z + (j - (k - \bar{d})) \sum_{\tilde{i}=1}^l q_{C,\tilde{i}} - q_{C,l} + 1, \dots, \\ & \zeta_{NZ} + \zeta_Z + (j - (k - \bar{d})) \sum_{\tilde{i}=1}^l q_{C,\tilde{i}} - \frac{q_{C,l}}{2}, \\ & \text{and } j = k - \bar{d} + 1, k - \bar{d} + 2, \dots, k - \underline{d} \\ \frac{(h_k - t_j^k)^{\hat{j}}}{\hat{j}!} e^{a_l(h_k - t_j^k)} \sin(b_l(h_k - t_j^k)) & \text{for } \hat{j} = 0, 1, \dots, \frac{q_{C,l}}{2} - 1, \\ & i = \zeta_{NZ} + \zeta_Z + \sum_{\tilde{i}=1}^l q_{C,\tilde{i}} - \frac{q_{C,l}}{2} + 1, \dots, \zeta_{NZ} + \zeta_Z + \sum_{\tilde{i}=1}^l q_{C,\tilde{i}}, \\ & \text{and } j = k - \bar{d} + 1, k - \bar{d} + 2, \dots, k - \underline{d} \\ \frac{h_k^{\hat{j}}}{\hat{j}!} e^{a_l h_k} \cos(b_l h_k) & \text{for } \hat{j} = 0, 1, \dots, \frac{q_{C,l}}{2} - 1, \\ & i \in \{\zeta - \zeta_C + 1, \zeta - \zeta_C + 2, \dots, \zeta - \frac{\zeta_C}{2}\}, \\ & \text{and } j = k - \bar{d} + 1, k - \bar{d} + 2, \dots, k - \underline{d} \\ \frac{h_k^{\hat{j}}}{\hat{j}!} e^{a_l h_k} \sin(b_l h_k) & \text{for } \hat{j} = 0, 1, \dots, \frac{q_{C,l}}{2} - 1, \\ & i \in \{\zeta - \frac{\zeta_C}{2} + 1, \zeta - \frac{\zeta_C}{2} + 2, \dots, \zeta\} \\ & \text{and } j = k - \bar{d} + 1, k - \bar{d} + 2, \dots, k - \underline{d} \\ 0 & \text{if } i \notin \{\zeta_{NZ} + \zeta_Z + 1, \zeta_{NZ} + \zeta_Z + 2, \dots, \zeta\}. \end{cases} \quad (\text{B.41})$$

Here,  $l$  denotes the number of distinct pairs of complex eigenvalues, with  $l \in \{1, 2, \dots, p_C\}$ . For constant sampling intervals, the functions  $\alpha_i$  depending on  $\frac{h_k^{\hat{j}}}{\hat{j}!} e^{a_l h_k} \cos(b_l h_k)$  and  $\frac{h_k^{\hat{j}}}{\hat{j}!} e^{a_l h_k} \sin(b_l h_k)$  are constant ( $h_k := h, \forall k$ ) and can be omitted. Moreover, the parameters  $\zeta_{NZ}$ ,  $\zeta_Z$ , and  $\zeta$  need to be replaced by  $\beta_{NZ}$ ,  $\beta_Z$ , and  $\beta$ , respectively.

The constant matrices  $F_0$ ,  $F_i$ ,  $G_0$ , and  $G_i$ ,  $i \in \{1, 2, \dots, \zeta\}$  in (4.7) are, for time-varying sampling intervals, delays, and packet dropouts (as well as for constant sampling intervals) given by:

$$F_0 = \begin{pmatrix} Q\Theta_0Q^{-1} & Q\Theta_1Q^{-1}B & Q\Theta_2Q^{-1}B & \dots & Q\Theta_{\bar{d}+\bar{\delta}}Q^{-1}B \\ 0 & 0 & 0 & \dots & 0 \\ 0 & 1 & 0 & \dots & 0 \\ \vdots & & \ddots & & \vdots \\ 0 & \dots & 0 & 1 & 0 \end{pmatrix},$$

$$F_i = \begin{pmatrix} Q\Gamma_{0,i}Q^{-1} & Q\Gamma_{1,i}Q^{-1}B & Q\Gamma_{2,i}Q^{-1}B & \dots & Q\Gamma_{\bar{d}+\bar{\delta},i}Q^{-1}B \\ 0 & 0 & 0 & \dots & 0 \\ 0 & 0 & 0 & \dots & 0 \\ \vdots & \vdots & \ddots & & \vdots \\ 0 & 0 & \dots & 0 & 0 \end{pmatrix},$$

$$G_0 = \begin{pmatrix} Q\Xi_0Q^{-1}B \\ I_{m,m} \\ 0_{(\bar{d}+\bar{\delta}-1)m,m} \end{pmatrix}, \text{ and } G_i = \begin{pmatrix} Q\Xi_iQ^{-1}B \\ 0_{(\bar{d}+\bar{\delta})m,m} \end{pmatrix},$$

for  $i \in \{1, 2, \dots, \zeta\}$ . The parameters  $\Theta_0$ ,  $\Xi_0$ ,  $\Theta_{\hat{i}}$ ,  $\hat{i} \in \{1, 2, \dots, \bar{d} + \bar{\delta}\}$ ,  $\Gamma_{0,i}$ ,  $\Gamma_{1,i}, \dots, \Gamma_{\bar{d}+\bar{\delta},i}$ , and  $\Xi_i$ ,  $i \in \{1, 2, \dots, \zeta\}$  will be derived for the separate cases of eigenvalues. Note that, it holds that:  $\Theta_{\hat{i}} = \text{diag}(\Theta_{\hat{i}}^{NZ}, \Theta_{\hat{i}}^Z, \Theta_{\hat{i}}^C)$ , for each  $\hat{i} \in \{0, 1, \dots, \bar{d} + \bar{\delta}\}$ ,  $\Xi_0 := \text{diag}(\Xi_0^{NZ}, \Xi_0^Z, \Xi_0^C)$ ,  $\Gamma_{\hat{i},i} = \text{diag}(\Gamma_{\hat{i},i}^{NZ}, \Gamma_{\hat{i},i}^Z, \Gamma_{\hat{i},i}^C)$ , for all  $i \in \{1, 2, \dots, \zeta\}$ , for all  $\hat{i} \in \{0, 1, \dots, \bar{d} + \bar{\delta}\}$ , and  $\Xi_i = \text{diag}(\Xi_i^{NZ}, \Xi_i^Z, \Xi_i^C)$ , for all  $i \in \{1, 2, \dots, \zeta\}$ .

- For real eigenvalues unequal to zero it holds that:

$$\Theta_0^{NZ} = 0,$$

$$\Theta_{\hat{i}}^{NZ} = \begin{cases} -J_{NZ}^{-1} & \text{if } \hat{i} = \underline{d} \\ 0 & \text{if } \hat{i} \neq \underline{d}, \end{cases}$$

for  $\hat{i} \in \{1, 2, \dots, \bar{d} + \bar{\delta}\}$ ,

$$\Xi_0 = \begin{cases} -J_{NZ}^{-1} & \text{if } \underline{d} = 0 \\ 0 & \text{if } \underline{d} > 0. \end{cases}$$

For the case with constant sampling intervals, it holds that

$$\Theta_{\hat{i}}^{NZ} = \begin{cases} J_{NZ}^{-1}e^{J_{NZ}h} & \text{if } \hat{i} = \bar{d} + \bar{\delta} \\ 0 & \text{if } \hat{i} \neq \bar{d} + \bar{\delta} \\ -J_{NZ}^{-1} & \text{if } \hat{i} = \underline{d}, \end{cases}$$

for  $\hat{i} \in \{1, 2, \dots, \bar{d} + \bar{\delta}\}$ , and  $\Theta_0^{NZ} = e^{J_{NZ}h}$ . Recall that it holds that  $\underline{d} \leq \bar{d}$ , where the case with  $\underline{d} = \bar{d}$  represents the case with constant time-delays

and constant sampling intervals. For time-varying sampling intervals, the matrix  $\Gamma_{0,i}^{NZ}$  is given by:

$$\Gamma_{0,i}^{NZ} = \begin{cases} T_i & \text{if } i \in \{\beta_{NZ} + 1, \beta_{NZ} + 2, \dots, \zeta_{NZ}\} \\ 0 & \text{if } i \notin \{\beta_{NZ} + 1, \beta_{NZ} + 2, \dots, \zeta_{NZ}\}, \end{cases}$$

and for constant sampling intervals it is given by:  $\Gamma_{0,i}^{NZ} = 0, i \in \{1, 2, \dots, \beta\}$ . The other matrices  $\Gamma_{\hat{i},i}, \hat{i} \in \{1, 2, \dots, \bar{d} + \bar{\delta}\}$  are, for time-varying sampling intervals, given by:

$$\Gamma_{1,i}^{NZ} = \begin{cases} -J_{NZ}^{-1}T_i^{NZ} & \text{if } \underline{d} = 0 \text{ and } i \in \{\beta_{NZ} - \nu_{NZ} + 1, \dots, \beta_{NZ}\} \\ J_{NZ}^{-1}T_i^{NZ} & \text{if } \underline{d} \in \{0, 1\} \text{ and } i \in \{\beta_{NZ} - (2 - \underline{d})\nu_{NZ} + 1, \dots, \\ & \beta_{NZ} - (1 - \underline{d})\nu_{NZ}\} \\ 0 & \text{if } (\underline{d} = 0 \text{ and } i \notin \{\beta_{NZ} - \nu_{NZ} + 1, \dots, \beta_{NZ}\}) \\ & \text{or } (\underline{d} = 1 \text{ and } i \notin \{\beta_{NZ} - (2 - \underline{d})\nu_{NZ} + 1, \dots, \\ & \beta_{NZ} - (1 - \underline{d})\nu_{NZ}\}) \\ & \text{or } (\underline{d} > 2), \end{cases}$$

$$\Gamma_{2,i}^{NZ} = \begin{cases} -J_{NZ}^{-1}T_i^{NZ} & \text{if } (\underline{d} \in \{0, 1\} \\ & \text{and } i \in \{\beta_{NZ} - (2 - \underline{d})\nu_{NZ} + 1, \dots, \\ & \beta_{NZ} - (1 - \underline{d})\nu_{NZ}\}) \\ J_{NZ}^{-1}T_i^{NZ} & \text{if } (\underline{d} \in \{0, 1, 2\} \\ & \text{and } i \in \{\beta_{NZ} - (3 - \underline{d})\nu_{NZ} + 1, \dots, \\ & \beta_{NZ} - (2 - \underline{d})\nu_{NZ}\}) \\ 0 & \text{if } (\underline{d} \in \{0, 1\} \\ & \text{and } i \notin \{\beta_{NZ} - (2 - \underline{d})\nu_{NZ} + 1, \dots, \\ & \beta_{NZ} - (1 - \underline{d})\nu_{NZ}\}) \\ & \text{or } (\underline{d} \in \{0, 1, 2\} \\ & \text{and } i \notin \{\beta_{NZ} - (3 - \underline{d})\nu_{NZ} + 1, \dots, \\ & \beta_{NZ} - (2 - \underline{d})\nu_{NZ}\}) \\ & \text{or } (\underline{d} > 2). \end{cases}$$

Analogously,  $\Gamma_{3,i}^{NZ}, \dots, \Gamma_{\bar{d}+\bar{\delta}-1,i}^{NZ}$  can be derived.

$$\Gamma_{\bar{d}+\bar{\delta},i}^{NZ} = \begin{cases} -J_{NZ}^{-1}T_i^{NZ} & \text{if } (\underline{d} \in \{0, 1, \dots, \bar{d} + \bar{\delta} - 1\} \\ & \text{and } i \in \{1, 2, \dots, \nu_{NZ}\}) \\ J_{NZ}^{-1}T_i^{NZ} & \text{if } i \in \{\beta_{NZ} + 1, \beta_{NZ} + 2, \dots, \zeta_{NZ}\} \\ 0 & \text{if } (\underline{d} \in \{0, 1, \dots, \bar{d} + \bar{\delta} - 1\}, i \notin \{1, 2, \dots, \nu_{NZ}\} \\ & \text{and } i \notin \{\beta_{NZ} + 1, \beta_{NZ} + 2, \dots, \zeta_{NZ}\}). \end{cases}$$

For the case with constant sampling intervals all these matrices hold, except  $\Gamma_{\bar{d}+\bar{\delta},i}^{NZ}$  that needs to be replaced by:

$$\Gamma_{\bar{d}+\bar{\delta},i}^{NZ} = \begin{cases} -J_{NZ}^{-1}T_i^{NZ} & \text{if } (\underline{d} \in [0, 1, \dots, \bar{d} + \bar{\delta} - 1] \\ & \text{and } i \in \{1, 2, \dots, \nu_{NZ}\}) \\ 0 & \text{if } (\underline{d} \in [0, 1, \dots, \bar{d} + \bar{\delta} - 1] \\ & \text{and } i \notin \{1, 2, \dots, \nu_{NZ}\}), \\ & \text{or } (\underline{d} = \bar{d} + \bar{\delta}). \end{cases}$$

Note that  $\underline{d} = \bar{d} + \bar{\delta}$  represents the case with constant sampling intervals and constant delays. The matrix  $\Xi_i^{NZ}$ ,  $i = 1, 2, \dots, \zeta$ , is for both constant and time-varying sampling intervals given by:

$$\Xi_i^{NZ} = \begin{cases} J_{NZ}^{-1} T_i^{NZ} & \text{if } \underline{d} = 0 \text{ and } i \in \{\beta_{NZ} - \nu_{NZ} + 1, \dots, \beta_{NZ}\} \\ 0 & \text{if } (\underline{d} = 0 \text{ and } i \notin \{\beta_{NZ} - \nu_{NZ} + 1, \dots, \beta_{NZ}\}) \\ & \text{or } (\underline{d} > 0). \end{cases}$$

To define  $T_i^{NZ}$ ,  $i = 1, 2, \dots, \zeta_{NZ}$ , define:

$$T_i^{NZ} = \begin{cases} S_{l,\hat{j}} & \text{for } \hat{j} = 0, 1, \dots, q_l - 1, \\ i = (j - (k - \bar{d})) \sum_{i=1}^l q_i - q_l + 1, \dots, (j - (k - \bar{d})) \sum_{i=1}^l q_i, \\ \text{and } j = k - \bar{d} + 1, k - \bar{d} + 2, \dots, k - \underline{d} + 1 \\ 0 & \text{if } i \notin \{1, 2, \dots, \zeta_{NZ}\}. \end{cases}$$

Here, the largest value of  $j$  is given by  $k - \underline{d} + 1$  instead of  $j = k - \underline{d}$  to include the values of  $i = \beta_{NZ} + 1, \beta_{NZ} + 2, \dots, \zeta_{NZ}$  that denote the functions  $\alpha_i$  that depend on the parameter  $h_k$  only. For constant sampling intervals,  $T_i^{NZ}$ ,  $i \in \{1, 2, \dots, \beta_{NZ}\}$ , is given by:

$$T_i^{NZ} = \begin{cases} S_{l,\hat{j}} & \text{for } \hat{j} = 0, 1, \dots, q_l - 1, \\ i = (j - (k - \bar{d})) \sum_{i=1}^l q_i - q_l + 1, \dots, (j - (k - \bar{d})) \sum_{i=1}^l q_i \\ \text{and } j = k - \bar{d} + 1, k - \bar{d} + 2, \dots, k - \underline{d} \\ 0 & \text{if } i \notin \{1, 2, \dots, \beta_{NZ}\}, \end{cases}$$

where, compared to the case with time-varying sampling intervals, only the parameter  $j$  is changed, such that the functions  $\alpha_i(h_k)$  are not considered.

- For eigenvalues equal to zero it holds for time-varying sampling intervals that:

$$\begin{aligned} \Theta_0^Z &= S_{p_{NZ}+1,0}, \\ \Theta_i^Z &= 0 \quad \forall \hat{i} \in \{1, 2, \dots, \bar{d} + \bar{\delta}\}, \end{aligned}$$

while for constant sampling intervals, it holds that:  $\Theta_0^Z = e^{J_Z h}$  and

$$\Theta_i^Z = \begin{cases} \sum_{j=1}^{q_Z} \frac{h^{\hat{j}}}{j!} S_{p_{NZ}+1,\hat{j}-1} & \text{if } \hat{i} = \bar{d} + \bar{\delta} \\ 0 & \text{if } \hat{i} \neq \bar{d} + \bar{\delta}, \end{cases}$$

for  $\hat{i} \in \{1, 2, \dots, \bar{d} + \bar{\delta}\}$ . Both for constant and time-varying sampling intervals,  $S_{p_{NZ}}$  is obtained from (B.13) where  $\tilde{i} = p_{NZ} + 1$  denotes the eigenvalues that are equal to zero. For time-varying sampling intervals, it holds that:

$$\begin{aligned} \Xi_0^Z &:= 0, \\ \Gamma_{0,i}^Z &= \begin{cases} S_{p_{NZ}+1,\hat{j}} & \text{for } \hat{j} = 1, 2, \dots, q_Z - 1 \\ \text{and } i \in \{\zeta_{NZ} + \beta_Z + 1, \zeta_Z + \beta_Z + 2, \dots, \zeta_{NZ} + \zeta_Z - 1\} \\ 0 & \text{if } i \notin \{\zeta_{NZ} + \beta_Z + 1, \zeta_Z + \beta_Z + 2, \dots, \zeta_{NZ} + \zeta_Z - 1\}, \end{cases} \end{aligned}$$

$$\Gamma_{1,i}^Z = \begin{cases} -T_i^Z & \text{if } (\underline{d} = 0 \text{ and } i \in \{\zeta_{NZ} + \beta_Z - \nu_Z + 1, \dots, \zeta_{NZ} + \beta_Z\}) \\ T_i^Z & \text{if } (\underline{d} \in \{0, 1\} \text{ and } i \in \{\zeta_{NZ} + \beta_Z - (2 - \underline{d})\nu_Z + 1, \dots, \\ & \quad \zeta_{NZ} + \beta_Z - (1 - \underline{d})\nu_Z\}) \\ 0 & \text{if } (\underline{d} = 0 \text{ and } i \notin \{\zeta_{NZ} + \beta_Z - 2\nu_Z + 1, \dots, \zeta_{NZ} + \beta_Z\}), \\ & \text{or } (\underline{d} = 1 \text{ and } i \notin \{\zeta_{NZ} + \beta_Z - \nu_Z + 1, \dots, \zeta_{NZ} + \beta_Z\}), \\ & \text{or } (\underline{d} > 1), \end{cases}$$

$$\Gamma_{2,i}^Z = \begin{cases} -T_i^Z & \text{if } (\underline{d} \in \{0, 1\} \text{ and } i \in \{\zeta_{NZ} + \beta_Z - (2 - \underline{d})\nu_Z + 1, \dots, \\ & \quad \zeta_{NZ} + \beta_Z - (1 - \underline{d})\nu_Z\}) \\ T_i^Z & \text{if } (\underline{d} \in \{0, 1, 2\} \text{ and } i \in \{\zeta_{NZ} + \beta_Z - (3 - \underline{d})\nu_Z + 1, \dots, \\ & \quad \zeta_{NZ} + \beta_Z - (2 - \underline{d})\nu_Z\}) \\ 0 & \text{if } (\underline{d} \in \{0, 1\} \text{ and } i \notin \{\zeta_{NZ} + \beta_Z - (2 - \underline{d})\nu_Z + 1, \dots, \\ & \quad \zeta_{NZ} + \beta_Z - (1 - \underline{d})\nu_Z\}), \\ & \text{or } (\underline{d} \in \{0, 1, 2\} \text{ and } i \notin \{\zeta_{NZ} + \beta_Z - (3 - \underline{d})\nu_Z + 1, \dots, \\ & \quad \zeta_{NZ} + \beta_Z - (2 - \underline{d})\nu_Z\}), \\ & \text{or } (\underline{d} > 2), \end{cases}$$

$$\Gamma_{\bar{d}+\bar{\delta},i}^Z = \begin{cases} -T_i^Z & \text{if } (\underline{d} \in \{0, 1, \dots, \bar{d} + \bar{\delta} - 1\} \\ & \text{and } i \in \{\zeta_{NZ} + 1, \dots, \zeta_{NZ} + \nu_Z\}) \\ T_i^Z & \text{if } i \in \{\zeta_{NZ} + \beta_Z + 1, \zeta_{NZ} + \beta_Z + 2, \dots, \zeta_{NZ} + \zeta_Z\} \\ 0 & \text{if } (\underline{d} \in \{0, 1, \dots, \bar{d} + \bar{\delta} - 1\}, i \notin \{\zeta_{NZ} + 1, \dots, \zeta_{NZ} + \nu_Z\} \\ & \text{and } i \notin \{\zeta_{NZ} + \beta_Z + 1, \zeta_{NZ} + \beta_Z + 2, \dots, \zeta_{NZ} + \zeta_Z\}). \end{cases}$$

For constant time-delays only  $\Gamma_{\bar{d}+\bar{\delta},i}^Z$  needs to be adapted. It holds that:

$$\Gamma_{\bar{d}+\bar{\delta},i}^Z = \begin{cases} -T_i^Z & \text{if } (\underline{d} \in \{0, 1, \dots, \bar{d} + \bar{\delta} - 1\} \\ & \text{and } i \in \{\beta_{NZ} + 1, \dots, \beta_{NZ} + \nu_Z\}) \\ 0 & \text{if } (\underline{d} \in \{0, 1, \dots, \bar{d} + \bar{\delta} - 1\} \\ & \text{and } i \notin \{\beta_{NZ} + 1, \dots, \beta_{NZ} + \nu_Z\}), \\ & \text{or } (\underline{d} = \bar{d} + \bar{\delta}). \end{cases}$$

Finally,  $\Xi_i^Z$  is for time-varying sampling intervals given by:

$$\Xi_i^Z = \begin{cases} T_i^Z & \text{if } (\underline{d} = 0 \text{ and } i \in \{\zeta_{NZ} + \beta_Z - \nu_Z + 1, \dots, \zeta_{NZ} + \beta_Z\}) \\ 0 & \text{if } (\underline{d} = 0 \text{ and } i \notin \{\zeta_{NZ} + \beta_Z - \nu_Z + 1, \dots, \zeta_{NZ} + \beta_Z\}), \\ & \text{or } (\underline{d} > 0). \end{cases}$$

Note that for constant sampling intervals, the parameter  $\zeta_{NZ}$  needs to be replaced by the parameter  $\beta_{NZ}$ . The matrix  $T_i^Z$ ,  $i \in \{1, 2, \dots, \zeta\}$ , is for

time-varying delays given by:

$$T_i^Z = \begin{cases} S_{p_{NZ}+1, \hat{j}-1} & \text{if } \hat{j} = i - (\zeta_{NZ} + (j - (k - \bar{d}))q_Z - q_Z) \\ & i = \zeta_{NZ} + (j - (k - \bar{d}))q_Z - q_Z + 1, \dots, \zeta_{NZ} + (j - (k - \bar{d}))q_Z, \\ & \text{and } j = k - \bar{d} + 1, k - \bar{d} + 2, \dots, k - \underline{d} + 1 \\ 0 & \text{if } i \notin \{\zeta_{NZ} + 1, \zeta_{NZ} + 2, \dots, \zeta_{NZ} + \zeta_Z\}. \end{cases}$$

For constant sampling intervals, it holds that

$$T_i^Z = \begin{cases} S_{p_{NZ}+1, \hat{j}-1} & \text{if } \hat{j} = i - (\beta_{NZ} + (j - (k - \bar{d}))q_Z - q_Z), \\ & i = \beta_{NZ} + (j - (k - \bar{d}))q_Z - q_Z + 1, \dots, \beta_{NZ} + (j - (k - \bar{d}))q_Z, \\ & \text{and } j = k - \bar{d} + 1, k - \bar{d} + 2, \dots, k - \underline{d} \\ 0 & \text{if } i \notin \{\beta_{NZ} + 1, \beta_{NZ} + 2, \dots, \beta_{NZ} + 1\beta_Z\}. \end{cases}$$

- Finally, for complex eigenvalues it holds that:

$$\Theta_0^C = 0,$$

$$\Theta_i^C = \begin{cases} 0 & \text{if } \hat{i} \neq \underline{d} \\ -\Lambda_0 & \text{if } \hat{i} = \underline{d}, \end{cases}$$

for  $\hat{i} \in \{1, 2, \dots, \bar{d} + \bar{\delta}\}$ , and  $\Lambda_0$  defined in (B.36) for one pair of complex eigenvalues or in (B.37) for a pair of complex eigenvalues that occurs twice. For constant sampling intervals, the following relations need to be used:

$$\Theta_i^C = \begin{cases} \check{H} & \text{if } \hat{i} = \bar{d} + \bar{\delta} \\ 0 & \text{if } \hat{i} \neq \bar{d} + \bar{\delta} \text{ or } \hat{i} \neq \underline{d} \\ -\Lambda_0 & \text{if } \hat{i} = \underline{d}, \end{cases}$$

for  $\hat{i} \in \{1, 2, \dots, \bar{d} + \bar{\delta}\}$ , and

$$\Xi_0^C = \begin{cases} -\Lambda_0 & \text{if } \underline{d} = 0 \\ 0 & \text{if } \underline{d} \neq 0, \end{cases}$$

with  $\check{H} = \frac{e^{ah}}{a^2+b^2}Q \begin{pmatrix} a \cos(bh) + b \sin(bh) & -a \sin(bh) + b \cos(bh) \\ a \sin(bh) - b \cos(bh) & a \cos(bh) + b \sin(bh) \end{pmatrix} Q^{-1}B$

for one complex pair of eigenvalues or  $\check{H} = \frac{e^{ah}}{a^2+b^2}QLQ^{-1}B$  for two equal complex pairs, with  $L$  defined in (B.25), and  $\Lambda_0$  defined as described for the case with time-varying sampling intervals.

For time-varying sampling intervals, it holds that:

$$\Xi_0^C = \begin{cases} -\Lambda_0 & \text{if } \underline{d} = 0 \\ 0 & \text{if } \underline{d} \neq 0, \end{cases}$$

$$\Gamma_{0,i}^C = \begin{cases} T_i^C & \text{if } i \in \{\zeta_{NZ} + \zeta_Z + \beta_C + 1, \zeta_{NZ} + \zeta_Z + \beta_C + 2, \dots, \zeta\} \\ 0 & \text{if } i \notin \{\zeta_{NZ} + \zeta_Z + \beta_C + 1, \zeta_{NZ} + \zeta_Z + \beta_C + 2, \dots, \zeta\}, \end{cases}$$

$$\Gamma_{1,i}^C = \begin{cases} -T_i & \text{if } (\underline{d} = 0 \text{ and } i \in \{\zeta_{NZ} + \zeta_Z + \beta_C - \nu_C + 1, \dots, \\ & \zeta_{NZ} + \zeta_Z + \beta_C\}) \\ T_i & \text{if } (\underline{d} \in \{0, 1\} \\ & \text{and } i \in \{\zeta_{NZ} + \zeta_Z + \beta_C - (2 - \underline{d})\nu_C + 1, \dots, \\ & \zeta_{NZ} + \zeta_Z + \beta_C - (1 - \underline{d})\nu_C\}) \\ 0 & \text{if } (\underline{d} = 0 \text{ and } i \notin \{\zeta_{NZ} + \zeta_Z + \beta_C - 2\nu_C + 1, \dots, \\ & \zeta_{NZ} + \zeta_Z + \beta_C\}) \\ & \text{or } (\underline{d} = 1 \text{ and } i \notin \{\zeta_{NZ} + \zeta_Z + \beta_C - \nu_C + 1, \dots, \\ & \zeta_{NZ} + \zeta_Z + \beta_C\}) \\ & \text{or } (\underline{d} > 1), \end{cases}$$

$$\Gamma_{2,i}^C = \begin{cases} -T_i^C & \text{if } (\underline{d} \in \{0, 1\} \text{ and } i \in \{\zeta_{NZ} + \zeta_Z + \beta_C - (2 - \underline{d})\nu_C + 1, \dots, \\ & \zeta_{NZ} + \zeta_Z + \beta_C - (1 - \underline{d})\nu_C\}) \\ T_i^C & \text{if } (\underline{d} \in \{0, 1, 2\} \text{ and } i \in \{\zeta_{NZ} + \zeta_Z + \beta_C - (3 - \underline{d})\nu_C + 1, \dots, \\ & \zeta_{NZ} + \zeta_Z + \beta_C - (2 - \underline{d})\nu_C\}) \\ 0 & \text{if } (\underline{d} \in \{0, 1\} \text{ and } i \notin \{\zeta_{NZ} + \zeta_Z + \beta_C - (2 - \underline{d})\nu_C + 1, \dots, \\ & \zeta_{NZ} + \zeta_Z + \beta_C - (1 - \underline{d})\nu_C\}) \\ & \text{or } (\underline{d} \in \{0, 1, 2\} \text{ and } i \notin \{\zeta_{NZ} + \zeta_Z + \beta_C - (3 - \underline{d})\nu_C + 1, \dots, \\ & \zeta_{NZ} + \zeta_Z + \beta_C - (2 - \underline{d})\nu_C\}) \\ & \text{or } (d > 2), \end{cases}$$

$$\Gamma_{\bar{d}+\bar{\delta},i}^C = \begin{cases} -T_i^C & \text{if } (\underline{d} \in \{0, 1, \dots, \bar{d} + \bar{\delta} - 1\} \\ & \text{and } i \in \{\zeta_{NZ} + \zeta_Z + 1, \dots, \zeta_{NZ} + \zeta_Z + \nu_C\}) \\ T_i^C & \text{if } (i \in \{\zeta_{NZ} + \zeta_Z + \beta_C + 1, \zeta_{NZ} + \zeta_Z + \beta_C + 2, \dots, \zeta\}) \\ 0 & \text{if } (\underline{d} \in \{0, 1, \dots, \bar{d} + \bar{\delta} - 1\} \\ & \text{and } i \notin \{\zeta_{NZ} + \zeta_Z + 1, \dots, \zeta_{NZ} + \zeta_Z + \nu_C\} \\ & \text{and } i \notin \{\zeta_{NZ} + \zeta_Z + \beta_C + 1, \zeta_{NZ} + \zeta_Z + \beta_C + 2, \dots, \zeta\}). \end{cases}$$

For constant sampling intervals, similar to both cases with real eigenvalues, some small adaptations are needed. Firstly, the second possibility, with  $T_i^C$ , has to be removed in  $\Gamma_{\bar{d}+\bar{\delta},i}^C$  and, secondly,  $\Gamma_{\bar{d}+\bar{\delta},i}^C = 0$  if  $\bar{d} + \bar{\delta} = \underline{d}$  should hold. The latter relation is somewhat superfluous, because it considers the case with constant delays, constant sampling intervals, and no packet dropouts, which means that there are no time-varying parameters.



Moreover, the parameters  $\zeta_{NZ}$ ,  $\zeta_Z$ , and  $\zeta$  need to be replaced by  $\beta_{NZ}$ ,  $\beta_Z$ , and  $\beta$ , respectively. This holds for  $\Gamma_{1,i}^C$  and  $\Gamma_{2,i}^C$  as well. Note that for constant sampling intervals,  $\Gamma_{0,i}^C = 0$  for all  $i \in \{1, 2, \dots, \beta\}$ . The matrices  $\Xi_i^C$ ,  $i \in \{1, 2, \dots, \zeta\}$  is, for time-varying sampling intervals, given by:

$$\Xi_i^C = \begin{cases} T_i^C & \text{if } (\underline{d} = 0 \\ & \text{and } i \in \{\zeta_{NZ} + \zeta_Z + \beta_Z - \nu_Z + 1, \dots, \zeta_{NZ} + \zeta_Z + \beta_C\}) \\ 0 & \text{if } (\underline{d} > 0) \text{ or } (\underline{d} = 0 \\ & \text{and } i \notin \{\zeta_{NZ} + \zeta_Z + \beta_C - \nu_C + 1, \dots, \zeta_{NZ} + \zeta_Z + \beta_C\}). \end{cases}$$

Again, for constant sampling intervals, the parameters  $\zeta_{NZ}$ ,  $\zeta_Z$ , and  $\zeta$  need to be replaced by  $\beta_{NZ}$ ,  $\beta_Z$ , and  $\beta$ , respectively. Finally,  $T_i^C$ ,  $i \in \{1, 2, \dots, \zeta_C\}$ , is, for time-varying sampling intervals, defined as:

$$T_i^C = \begin{cases} S_{i,\hat{j},1} & \text{for } \hat{j} = 0, 1, \dots, q_l - 1, \\ & i = \zeta_{NZ} + \zeta_Z + (j - (k - \bar{d})) \sum_{i=1}^l q_i - q_l + 1, \dots, \\ & \quad \zeta_{NZ} + \zeta_Z + (j - (k - \bar{d})) \sum_{i=1}^l q_i - \frac{q_l}{2}, \text{ and} \\ & \quad j \in \{k - \bar{d} + 1, k - \bar{d} + 2, \dots, k - \underline{d} + 1\} \\ S_{i,\hat{j},2} & \text{for } \hat{j} = 0, 1, \dots, q_l - 1, \\ & i = \zeta_{NZ} + \zeta_Z + (j - (k - \bar{d})) \sum_{i=1}^l q_i - \frac{q_l}{2} + 1, \dots, \\ & \quad \zeta_{NZ} + \zeta_Z + (j - (k - \bar{d})) \sum_{i=1}^l q_i, \text{ and} \\ & \quad j \in \{k - \bar{d} + 1, k - \bar{d} + 2, \dots, k - \underline{d} + 1\}, \\ 0 & \text{if } i \in \{1, 2, \dots, \zeta_{NZ} + \zeta_Z\}, \end{cases}$$

with  $S_{i,\hat{j},1}$  and  $S_{i,\hat{j},2}$  defined in (B.21) for one pair of complex eigenvalues and in (B.26) for one pair of complex eigenvalues that occurs twice. For constant sampling intervals, it holds for  $j$  that  $j \in \{k - \bar{d} + 1, k - \bar{d} + 2, \dots, k - \underline{d}\}$  and that  $\zeta_{NZ}$ ,  $\zeta_Z$  are replaced by  $\beta_{NZ}$  and  $\beta_Z$ , respectively.

## B.4 Output-feedback

For the output-feedback case, as is considered during the measurements in Chapter 7, the NCS description is slightly changed. Note that during the measurements a constant sampling interval and no packet dropouts are assumed. Compared to the state-feedback case, as described in the previous paragraph, the definition of the parameter  $\alpha_i(t_j^k)$  is not changed. Therefore,  $\alpha_i(t_j^k)$  can be obtained from (B.38), (B.39), (B.40), and (B.41), in combination with the comments for the constant sampling interval, i.e.  $\zeta$ , the number of time-varying functions  $\alpha_i$ , is replaced by  $\beta$  and  $h_k := h, \forall k \in \mathbb{N}$ .

Due to the change of the state-vector from  $\xi_k = \begin{pmatrix} x_k^T & u_{k-1}^T & \dots & u_{k-\bar{d}}^T \end{pmatrix}^T$

for the state-feedback case to  $\eta_k = \begin{pmatrix} x_k^T & u_{k-1}^T & \dots & u_{k-\bar{d}}^T & y_{k-1}^T \end{pmatrix}^T$  for the output feedback case, the NCS description based on the Jordan form of the

continuous-time system matrix  $A$ , see (4.6) for the state-feedback case, changes to

$$\eta_{k+1} = \left( F_0 + \sum_{i=1}^{\beta} \alpha_i(t_j^k) F_i \right) \eta_k + \left( G_0 + \sum_{i=1}^{\beta} \alpha_i(t_j^k) G_i \right) u_k,$$

with  $F_0$ ,  $G_0$ ,  $F_i$ , and  $G_i$ ,  $i = 1, 2, \dots, \beta$ , given by:

$$F_0 = \begin{pmatrix} Q\Theta_0 Q^{-1} & Q\Theta_1 Q^{-1} B & Q\Theta_2 Q^{-1} B & \dots & Q\Theta_{\bar{d}} Q^{-1} B & 0 \\ 0 & 0 & 0 & \dots & 0 & 0 \\ 0 & 1 & 0 & \dots & 0 & 0 \\ \vdots & \ddots & \ddots & & \vdots & \vdots \\ 0 & \dots & 0 & 1 & 0 & 0 \\ C & 0 & \dots & 0 & 0 & 0 \end{pmatrix},$$

$$F_i = \begin{pmatrix} 0 & Q\Gamma_{1,i} Q^{-1} B & Q\Gamma_{2,i} Q^{-1} B & \dots & Q\Gamma_{\bar{d},i} Q^{-1} B & 0 \\ 0 & 0 & 0 & \dots & 0 & 0 \\ 0 & 0 & 0 & \dots & 0 & 0 \\ \vdots & \ddots & \ddots & & \vdots & \vdots \\ 0 & 0 & \dots & 0 & 0 & 0 \\ 0 & 0 & \dots & 0 & 0 & 0 \end{pmatrix},$$

$$G_0 = \begin{pmatrix} Q\Xi_0 Q^{-1} B \\ I_{m,m} \\ 0_{(\bar{d}-1)m+r,m} \end{pmatrix}, \text{ and } G_i = \begin{pmatrix} Q\Xi_i Q^{-1} B \\ 0_{\bar{d}m+r,m} \end{pmatrix}. \text{ The definitions of } \Theta_\rho \text{ and } \Gamma_{\rho,i},$$

$\rho = 0, 1, \dots, \bar{d}$ ,  $i = 1, 2, \dots, \beta$ ,  $\Xi_0$ , and  $\Xi_i$ ,  $i = 1, 2, \dots, \beta$ , are equal to the definitions in the previous section with  $\bar{\delta} = 0$  and  $h_k = h \forall k$ .

## C

### Controller synthesis based on the Lyapunov-Krasovskii functional

In this appendix the controller synthesis conditions of system (5.15), (5.16), (5.17) with the state-feedback controller (5.2), based on the candidate Lyapunov-Krasovskii (L-K) functional

$$V(\chi_k) = x_k^T \tilde{P} x_k + \sum_{\hat{i}=1}^{\bar{d}+\bar{\delta}} x_{k-\hat{i}}^T R_{\hat{i}} x_{k-\hat{i}} + \sum_{\hat{i}=1}^{\bar{d}+\bar{\delta}} (x_{k-\hat{i}+1} - x_{k-\hat{i}})^T T_{\hat{i}} (x_{k-\hat{i}+1} - x_{k-\hat{i}}),$$

as defined in (4.40) are derived. The counterpart of Theorem 5.1.4 for time-varying sampling intervals, large delays, and packet dropouts is defined as follows:

**Theorem C.0.1** *Consider the NCS model (5.15), (5.16), (5.17), (5.2), and its discrete-time representation in terms of the Jordan form of the continuous-time system matrix  $A$  (4.43) for sequences of sampling instants, delays, and packet dropouts  $\sigma \in \mathcal{S}$ , as defined in (5.14). Consider the set of matrices  $\mathcal{H}_{FG}^x$ , defined in (4.44). If there exist symmetric positive definite matrices  $\tilde{Y} \in \mathbb{R}^{n \times n}$ ,  $\hat{R}_{\hat{i}} \in \mathbb{R}^{n \times n}$ ,  $\hat{L}_{\hat{i}} \in \mathbb{R}^{n \times n}$ , and  $\hat{M}_{\hat{i}} \in \mathbb{R}^{n \times n}$ ,  $\hat{i} = 1, 2, \dots, \bar{d} + \bar{\delta}$ , a matrix  $Z \in \mathbb{R}^{m \times n}$ , and scalars  $0 \leq \gamma < 1$ ,  $\theta_{\hat{i}} > 0$ ,  $\hat{i} = 1, 2, \dots, \bar{d} + \bar{\delta}$ , that satisfy the following matrix inequality:*

$$\begin{pmatrix} \mathbf{A} & \mathbf{B} \\ \mathbf{B}^T & \mathbf{C} \end{pmatrix} > 0, \quad (\text{C.1})$$

with

$$\mathbf{A} = \begin{pmatrix} \mathbf{Q}_0 & \mathbf{S}_0 & 0 & 0 & 0 & \dots & 0 \\ \star & \mathbf{Q}_1 & \mathbf{S}_1 & 0 & 0 & \dots & 0 \\ \star & \star & \mathbf{Q}_2 & \mathbf{S}_2 & 0 & \dots & 0 \\ \vdots & \vdots & & \ddots & \ddots & \ddots & \vdots \\ \star & \star & \star & \star & \mathbf{Q}_{\bar{d}+\bar{\delta}-2} & \mathbf{S}_{\bar{d}+\bar{\delta}-2} & 0 \\ \star & \star & \star & \star & \star & \mathbf{Q}_{\bar{d}+\bar{\delta}-1} & \mathbf{S}_{\bar{d}+\bar{\delta}-1} \\ \star & \star & \star & \star & \star & \star & \mathbf{Q}_{\bar{d}+\bar{\delta}} \end{pmatrix},$$

$$\mathbf{B} = \begin{pmatrix} \mathbf{U}_0 & \mathbf{V}_0 & \mathbf{L}_1 & 0 & 0 & 0 & \dots & 0 \\ \mathbf{U}_1 & \mathbf{U}_1 & \mathbf{M}_1 & \mathbf{L}_2 & 0 & 0 & \dots & 0 \\ \mathbf{U}_2 & \mathbf{U}_2 & 0 & \mathbf{M}_2 & \mathbf{L}_3 & 0 & \dots & 0 \\ \vdots & \vdots & \vdots & \ddots & \ddots & \ddots & \ddots & \vdots \\ \mathbf{U}_{\bar{d}+\bar{\delta}-2} & \mathbf{U}_{\bar{d}+\bar{\delta}-2} & 0 & \dots & 0 & \mathbf{M}_{\bar{d}+\bar{\delta}-2} & \mathbf{L}_{\bar{d}+\bar{\delta}-1} & 0 \\ \mathbf{U}_{\bar{d}+\bar{\delta}-1} & \mathbf{U}_{\bar{d}+\bar{\delta}-1} & 0 & \dots & 0 & 0 & \mathbf{M}_{\bar{d}+\bar{\delta}-1} & \mathbf{L}_{\bar{d}+\bar{\delta}} \\ \mathbf{U}_{\bar{d}+\bar{\delta}} & \mathbf{U}_{\bar{d}+\bar{\delta}} & 0 & 0 & 0 & \dots & 0 & \mathbf{M}_{\bar{d}+\bar{\delta}} \end{pmatrix},$$

$$\begin{aligned}
C &= \begin{pmatrix} \tilde{Y} & 0 & 0 & 0 & \dots & 0 & 0 & 0 \\ 0 & \theta_1 \tilde{Y} & 0 & 0 & \dots & 0 & 0 & 0 \\ 0 & 0 & \theta_1 \tilde{Y} & 0 & \dots & 0 & 0 & 0 \\ 0 & 0 & 0 & \theta_2 \tilde{Y} & \dots & 0 & 0 & 0 \\ \vdots & \vdots & \vdots & \vdots & \ddots & \vdots & \vdots & \vdots \\ 0 & 0 & 0 & \dots & 0 & \theta_{\bar{d}+\bar{\delta}-2} \tilde{Y} & 0 & 0 \\ 0 & 0 & 0 & \dots & 0 & 0 & \theta_{\bar{d}+\bar{\delta}-1} \tilde{Y} & 0 \\ 0 & 0 & 0 & \dots & 0 & 0 & 0 & \theta_{\bar{d}+\bar{\delta}} \tilde{Y} \end{pmatrix}, \\
Q_0 &= (1-\gamma)\tilde{Y} - \hat{R}_1 - \frac{1}{\theta_2}\tilde{Y} - \hat{L}_1 - \hat{L}_1^T, \\
Q_1 &= (1-\gamma)\hat{R}_1 - \hat{R}_2 - \frac{1}{\theta_2}\tilde{Y} - \frac{1}{\theta_3}\tilde{Y} + \hat{M}_1 + \hat{M}_1^T - \hat{L}_2 - \hat{L}_2^T, \\
Q_2 &= (1-\gamma)\hat{R}_2 - \hat{R}_3 - \frac{1}{\theta_3}\tilde{Y} - \frac{1}{\theta_4}\tilde{Y} + \hat{M}_2 + \hat{M}_2^T - \hat{L}_3 - \hat{L}_3^T, \\
Q_{\bar{d}+\bar{\delta}-2} &= (1-\gamma)\hat{R}_{\bar{d}+\bar{\delta}-2} - \hat{R}_{\bar{d}+\bar{\delta}-1} - \frac{1}{\theta_{\bar{d}+\bar{\delta}-1}}\tilde{Y} - \frac{1}{\theta_{\bar{d}+\bar{\delta}}}\tilde{Y} + \hat{M}_{\bar{d}+\bar{\delta}-2} + \hat{M}_{\bar{d}+\bar{\delta}-2}^T \\
&\quad - \hat{L}_{\bar{d}+\bar{\delta}-1} - \hat{L}_{\bar{d}+\bar{\delta}-1}^T, \\
Q_{\bar{d}+\bar{\delta}-1} &= (1-\gamma)\hat{R}_{\bar{d}+\bar{\delta}-1} - \hat{R}_{\bar{d}+\bar{\delta}} - \frac{1}{\theta_{\bar{d}+\bar{\delta}}}\tilde{Y} + \hat{M}_{\bar{d}+\bar{\delta}-1} + \hat{M}_{\bar{d}+\bar{\delta}-1}^T - \hat{L}_{\bar{d}+\bar{\delta}} - \hat{L}_{\bar{d}+\bar{\delta}}^T, \\
Q_{\bar{d}+\bar{\delta}} &= (1-\gamma)\hat{R}_{\bar{d}+\bar{\delta}} + \hat{M}_{\bar{d}+\bar{\delta}} + \hat{M}_{\bar{d}+\bar{\delta}}^T, \\
S_0 &= \frac{1}{\theta_2}\tilde{Y} - \hat{M}_1^T + \hat{L}_1, \quad S_1 = \frac{1}{\theta_3}\tilde{Y} - \hat{M}_2^T + \hat{L}_2, \quad S_2 = \frac{1}{\theta_4}\tilde{Y} - \hat{M}_3^T + \hat{L}_3, \\
S_{\bar{d}+\bar{\delta}-2} &= \frac{1}{\theta_{\bar{d}+\bar{\delta}}}\tilde{Y} - \hat{M}_{\bar{d}+\bar{\delta}-1}^T + \hat{L}_{\bar{d}+\bar{\delta}-1}, \quad S_{\bar{d}+\bar{\delta}-1} = -\hat{M}_{\bar{d}+\bar{\delta}}^T + \hat{L}_{\bar{d}+\bar{\delta}}, \\
U_0 &= \tilde{Y}(H_{F,0,j}^x)^T - Z^T(H_{G,j}^x)^T, \\
U_{\hat{i}} &= -Z^T(H_{F,\hat{i},j}^x)^T, \hat{i} = 1, 2, \dots, \bar{d} + \bar{\delta}, \\
V_0 &= \tilde{Y}(H_{F,0,j}^x)^T - \tilde{Y} - Z^T(H_{G,j}^x)^T, \\
L_{\hat{i}} &= \frac{\theta_{\hat{i}}}{\sqrt{1-\gamma}}\hat{L}_{\hat{i}}, \quad M_{\hat{i}} = \frac{\theta_{\hat{i}}}{\sqrt{1-\gamma}}\hat{M}_{\hat{i}} \text{ for all } \hat{i} = 1, 2, \dots, \bar{d} + \bar{\delta},
\end{aligned}$$

for all  $(H_{F,0,j}^x, H_{F,1,j}^x, \dots, H_{F,\bar{d}+\bar{\delta},j}^x, H_{G,j}^x) \in \mathcal{H}_{FG}^x$ ,  $j = 1, 2, \dots, 2^\zeta$ , then  $x = 0$  is a GAS equilibrium point of the closed-loop NCS (5.15), (5.16), (5.17), (5.2) with  $\bar{K} = Z\tilde{Y}^{-1}$ . Moreover, (4.40) is a Lyapunov function for (4.43), (5.2) and can be retrieved from the LMIs if the following relations are considered:  $\tilde{Y} = \tilde{P}^{-1}$ ,  $\hat{R}_{\hat{i}} = \tilde{P}^{-1}R_{\hat{i}}\tilde{P}^{-1}$ ,  $\hat{L}_{\hat{i}} = \tilde{P}^{-1}L_{\hat{i}}\tilde{P}^{-1}$ ,  $\hat{M}_{\hat{i}} = \tilde{P}^{-1}M_{\hat{i}}\tilde{P}^{-1}$ , and  $\theta_{\hat{i}}\tilde{Y} = T_{\hat{i}}^{-1}$  for  $\hat{i} = 1, 2, \dots, \bar{d} + \bar{\delta}$ .

**Proof** The same overapproximation procedure as in the proof of the stability analysis conditions in Theorem 4.3.2 in Appendix A.4 is considered. Therefore, this proof focusses on rewriting the stability analysis results such that they are applicable for controller synthesis. The following Lyapunov inequality is sufficient to provide a condition for the GES of the origin on (4.43), (5.2)

$$\Delta V(\chi_k) = V(\chi_{k+1}) - V(\chi_k) < -\gamma V(\chi_k). \quad (C.2)$$

Analogous to the small delay case, in Appendix A.11, the functions  $\Psi_{\hat{i}}$ ,  $\hat{i} =$

$1, 2, \dots, \bar{d} + \bar{\delta}$  defined as

$$\begin{aligned} \Psi_1 &= 2 \left( x_k^T L_1 + x_{k-1}^T M_1 \right) \left( (x_k - x_{k-1}) - (x_k - x_{k-1}) \right) := 0, \\ \Psi_2 &= 2 \left( x_{k-1}^T L_2 + x_{k-2}^T M_2 \right) \left( (x_{k-1} - x_{k-2}) - (x_{k-1} - x_{k-2}) \right) := 0, \\ &\vdots \\ \Psi_{\bar{d}+\bar{\delta}} &= 2 \left( x_{k-\bar{d}-\bar{\delta}+1}^T L_{\bar{d}+\bar{\delta}} + x_{k-\bar{d}-\bar{\delta}}^T M_{\bar{d}+\bar{\delta}} \right) \\ &\quad \left( (x_{k-\bar{d}-\bar{\delta}+1} - x_{k-\bar{d}-\bar{\delta}}) - (x_{k-\bar{d}-\bar{\delta}+1} - x_{k-\bar{d}-\bar{\delta}}) \right) := 0, \end{aligned} \quad (\text{C.3})$$

can be added to this inequality. Then, a sufficient condition for GES of (4.43), (5.2) is given by:

$$V(\chi_{k+1}) - (1 - \gamma)V(\chi_k) + \sum_{\hat{i}=1}^{\bar{d}+\bar{\delta}} \Psi_{\hat{i}} < 0. \quad (\text{C.4})$$

The Lyapunov-Krasovskii dependent terms in (C.4) can be rewritten as:

$$\begin{aligned} \Delta V(\chi_k) + \gamma V(\chi_k) &= x_{k+1}^T \tilde{P} x_{k+1} - (1 - \gamma) x_k^T \tilde{P} x_k \\ &\quad + \sum_{\hat{i}=1}^{\bar{d}+\bar{\delta}} x_{k-\hat{i}+1}^T R_{\hat{i}} x_{k-\hat{i}+1} - (1 - \gamma) \sum_{\hat{i}=1}^{\bar{d}+\bar{\delta}} x_{k-\hat{i}}^T R_{\hat{i}} x_{k-\hat{i}} \\ &\quad + \sum_{\hat{i}=1}^{\bar{d}+\bar{\delta}} (x_{k-\hat{i}+2}^T - x_{k-\hat{i}+1}^T) T_{\hat{i}} (x_{k-\hat{i}+2}^T - x_{k-\hat{i}+1}^T) \\ &\quad - (1 - \gamma) \sum_{\hat{i}=1}^{\bar{d}+\bar{\delta}} (x_{k-\hat{i}+1}^T - x_{k-\hat{i}}^T) T_{\hat{i}} (x_{k-\hat{i}+1}^T - x_{k-\hat{i}}^T). \end{aligned} \quad (\text{C.5})$$

The other terms in (C.4) that depend on  $\Psi_{\hat{i}}$ ,  $\hat{i} = 1, 2, \dots, \bar{d} + \bar{\delta}$ , as defined in (C.3), can be rewritten based on relation (A.58) if  $L_{\hat{i}}$  and  $M_{\hat{i}}$ ,  $\hat{i} \in \{1, 2, \dots, \bar{d} + \bar{\delta}\}$ , are symmetric positive definite matrices. This gives the following inequality:

$$\begin{aligned} \sum_{\hat{i}=1}^{\bar{d}+\bar{\delta}} \Psi_{\hat{i}} &\leq \sum_{\hat{i}=1}^{\bar{d}+\bar{\delta}} 2 \chi_k^T N_{\hat{i}} (x_{k-\hat{i}+1} - x_{k-\hat{i}}) + \sum_{\hat{i}=1}^{\bar{d}+\bar{\delta}} \frac{1}{1 - \gamma} \chi_k^T N_{\hat{i}} T_{\hat{i}}^{-1} N_{\hat{i}}^T \chi_k \\ &\quad + (1 - \gamma) \sum_{\hat{i}=1}^{\bar{d}+\bar{\delta}} (x_{k-\hat{i}+1} - x_{k-\hat{i}})^T T_{\hat{i}} (x_{k-\hat{i}+1} - x_{k-\hat{i}}), \end{aligned} \quad (\text{C.6})$$

with  $\chi_k = \begin{pmatrix} x_k^T & x_{k-1}^T & \dots & x_{k-\bar{d}-\bar{\delta}}^T \end{pmatrix}^T$  and

$N_{\hat{i}} = \begin{pmatrix} 0_{(\hat{i}-1)n,n}^T & L_{\hat{i}}^T & M_{\hat{i}}^T & 0_{\bar{d}+\bar{\delta}-\hat{i},n}^T \end{pmatrix}^T$ ,  $\hat{i} \in \{1, 2, \dots, \bar{d} + \bar{\delta}\}$ . Here, it holds that  $0_{(\hat{i}-1)n,n} \in \mathbb{R}^{(\hat{i}-1)n \times n}$  and  $0_{(\bar{d}+\bar{\delta}-\hat{i})n,n} \in \mathbb{R}^{(\bar{d}+\bar{\delta}-\hat{i})n \times n}$  are matrices that contain only zeros. If  $\hat{i} - 1 \leq 0$ , then we define  $0_{(\hat{i}-1)n,n} := \emptyset$  and if  $\bar{d} + \bar{\delta} - \hat{i} \leq 0$ ,

then we define  $0_{(\bar{d}+\bar{\delta}-\hat{i})n,n} := \emptyset$  for  $\hat{i} = 1, 2, \dots, \bar{d} + \bar{\delta}$ . The implementation of (C.5) and (C.6) in (C.4) gives:

$$\begin{aligned} \Delta V(\chi_k) + \gamma V(\chi_k) + \sum_{\hat{i}=1}^{\bar{d}+\bar{\delta}} \Psi_{\hat{i}} \leq & \\ & x_{k+1}^T \tilde{P} x_{k+1} - (1-\gamma) x_k^T \tilde{P} x_k + \sum_{\hat{i}=1}^{\bar{d}+\bar{\delta}} x_{k-\hat{i}+1}^T R_{\hat{i}} x_{k-\hat{i}+1} \\ & - (1-\gamma) \sum_{\hat{i}=1}^{\bar{d}+\bar{\delta}} x_{k-\hat{i}}^T R_{\hat{i}} x_{k-\hat{i}} + \sum_{\hat{i}=1}^{\bar{d}+\bar{\delta}} (x_{k-\hat{i}+2}^T - x_{k-\hat{i}+1}^T) T_{\hat{i}} (x_{k-\hat{i}+2}^T - x_{k-\hat{i}+1}^T) \\ & + \sum_{\hat{i}=1}^{\bar{d}+\bar{\delta}} 2\chi_k^T N_{\hat{i}} (x_{k-\hat{i}+1} - x_{k-\hat{i}}) + \sum_{\hat{i}=1}^{\bar{d}+\bar{\delta}} \frac{1}{1-\gamma} \chi_k^T N_{\hat{i}} T_{\hat{i}}^{-1} N_{\hat{i}}^T \chi_k < 0. \end{aligned}$$

Rewriting this inequality, in combination with the dynamics of the NCS as defined in (4.43), results in the inequality  $\chi_k^T \bar{\mathbf{X}} \chi_k < 0$ , which is satisfied if the following matrix inequality holds

$$\bar{\mathbf{X}} < 0, \quad (\text{C.7})$$

with

$$\bar{\mathbf{X}} = \begin{pmatrix} \mathbf{X}_{0,0} & \mathbf{X}_{0,1} & \mathbf{X}_{0,2} & \mathbf{X}_{0,3} & \cdots & \mathbf{X}_{0,\bar{d}+\bar{\delta}-2} & \mathbf{X}_{0,\bar{d}+\bar{\delta}-1} & \mathbf{X}_{0,\bar{d}+\bar{\delta}} \\ * & \mathbf{X}_{1,1} & \mathbf{X}_{1,2} & 0 & \cdots & 0 & 0 & 0 \\ * & * & \mathbf{X}_{2,2} & \mathbf{X}_{2,3} & & 0 & 0 & 0 \\ \vdots & \vdots & & & \ddots & & \vdots & \vdots \\ * & * & * & * & * & \mathbf{X}_{\bar{d}+\bar{\delta}-2,\bar{d}+\bar{\delta}-2} & \mathbf{X}_{\bar{d}+\bar{\delta}-2,\bar{d}+\bar{\delta}-1} & 0 \\ * & * & * & * & * & * & \mathbf{X}_{\bar{d}+\bar{\delta}-1,\bar{d}+\bar{\delta}-1} & \mathbf{X}_{\bar{d}+\bar{\delta}-1,\bar{d}+\bar{\delta}} \\ * & * & * & * & * & * & * & \mathbf{X}_{\bar{d}+\bar{\delta},\bar{d}+\bar{\delta}} \end{pmatrix},$$

$$\begin{aligned} \mathbf{X}_{0,0} &= \mathbf{G}_0^T \tilde{P} \mathbf{G}_0 - (1-\gamma) \tilde{P} + \mathbf{H}_0^T T_1 \mathbf{H}_0 + R_1 + T_2 + L_1 + L_1^T + L_1 T_1^{-1} L_1^T, \\ \mathbf{X}_{0,1} &= -\mathbf{G}_0^T \tilde{P} \mathbf{F}_1 - \mathbf{H}_0^T T_1 \mathbf{F}_1 - T_2 - L_1 + M_1^T + L_1 T_1^{-1} M_1^T, \quad \mathbf{X}_{0,2} = -\mathbf{G}_0^T \tilde{P} \mathbf{F}_2 - \mathbf{H}_0^T T_1 \mathbf{F}_2, \\ \mathbf{X}_{0,3} &= -\mathbf{G}_0^T \tilde{P} \mathbf{F}_3 - \mathbf{H}_0^T T_1 \mathbf{F}_3, \quad \mathbf{X}_{0,\bar{d}+\bar{\delta}-2} = -\mathbf{G}_0^T \tilde{P} \mathbf{F}_{\bar{d}+\bar{\delta}-2} - \mathbf{H}_0^T T_1 \mathbf{F}_{\bar{d}+\bar{\delta}-2}, \\ \mathbf{X}_{0,\bar{d}+\bar{\delta}-1} &= -\mathbf{G}_0^T \tilde{P} \mathbf{F}_{\bar{d}+\bar{\delta}-1} - \mathbf{H}_0^T T_1 \mathbf{F}_{\bar{d}+\bar{\delta}-1}, \quad \mathbf{X}_{0,\bar{d}+\bar{\delta}} = -\mathbf{G}_0^T \tilde{P} \mathbf{F}_{\bar{d}+\bar{\delta}} - \mathbf{H}_0^T T_1 \mathbf{F}_{\bar{d}+\bar{\delta}}, \\ \mathbf{X}_{1,1} &= \mathbf{F}_1^T (\tilde{P} + T_1) \mathbf{F}_1 - (1-\gamma) R_1 + R_2 + T_2 + T_3 - M_1 - M_1^T + L_2 + L_2^T + L_2 T_2^{-1} L_2^T \\ &\quad + M_1 T_1^{-1} M_1^T, \\ \mathbf{X}_{1,2} &= -T_3 + M_2^T - L_2 + L_2 T_2^{-1} M_2^T, \\ \mathbf{X}_{2,2} &= \mathbf{F}_2^T (\tilde{P} + T_1) \mathbf{F}_2 - (1-\gamma) R_2 + R_3 + T_3 + T_4 - M_2 - M_2^T + L_3 + L_3^T \\ &\quad + L_3 T_3^{-1} L_3^T + M_2 T_2^{-1} M_2^T, \\ \mathbf{X}_{2,3} &= -T_4 + M_3^T - L_3 + L_3 T_3^{-1} M_3^T, \\ \mathbf{X}_{\bar{d}+\bar{\delta}-2,\bar{d}+\bar{\delta}-2} &= \mathbf{F}_{\bar{d}+\bar{\delta}-2}^T (\tilde{P} + T_1) \mathbf{F}_{\bar{d}+\bar{\delta}-2} - (1-\gamma) R_{\bar{d}+\bar{\delta}-2} + R_{\bar{d}+\bar{\delta}-1} + T_{\bar{d}+\bar{\delta}-1} + T_{\bar{d}+\bar{\delta}} \\ &\quad - M_{\bar{d}+\bar{\delta}-2}^T - M_{\bar{d}+\bar{\delta}-2}^T + L_{\bar{d}+\bar{\delta}-1} + L_{\bar{d}+\bar{\delta}-1}^T + L_{\bar{d}+\bar{\delta}-1} T_{\bar{d}+\bar{\delta}-1}^{-1} L_{\bar{d}+\bar{\delta}-1}^T \\ &\quad + M_{\bar{d}+\bar{\delta}-2} T_{\bar{d}+\bar{\delta}-2}^{-1} M_{\bar{d}+\bar{\delta}-2}^T, \\ \mathbf{X}_{\bar{d}+\bar{\delta}-2,\bar{d}+\bar{\delta}-1} &= -T_{\bar{d}+\bar{\delta}} + M_{\bar{d}+\bar{\delta}-1}^T - L_{\bar{d}+\bar{\delta}-1} + L_{\bar{d}+\bar{\delta}-1} T_{\bar{d}+\bar{\delta}-1}^{-1} M_{\bar{d}+\bar{\delta}-1}^T, \\ \mathbf{X}_{\bar{d}+\bar{\delta}-1,\bar{d}+\bar{\delta}-1} &= \mathbf{F}_{\bar{d}+\bar{\delta}-1}^T (\tilde{P} + T_1) \mathbf{F}_{\bar{d}+\bar{\delta}-1} - (1-\gamma) R_{\bar{d}+\bar{\delta}-1} + R_{\bar{d}+\bar{\delta}} + T_{\bar{d}+\bar{\delta}} - M_{\bar{d}+\bar{\delta}-1} \\ &\quad - M_{\bar{d}+\bar{\delta}-1}^T + L_{\bar{d}+\bar{\delta}} + L_{\bar{d}+\bar{\delta}}^T + L_{\bar{d}+\bar{\delta}} T_{\bar{d}+\bar{\delta}}^{-1} L_{\bar{d}+\bar{\delta}}^T + M_{\bar{d}+\bar{\delta}-1} T_{\bar{d}+\bar{\delta}-1}^{-1} M_{\bar{d}+\bar{\delta}-1}^T, \\ \mathbf{X}_{\bar{d}+\bar{\delta}-1,\bar{d}+\bar{\delta}} &= M_{\bar{d}+\bar{\delta}}^T - L_{\bar{d}+\bar{\delta}} + L_{\bar{d}+\bar{\delta}} T_{\bar{d}+\bar{\delta}}^{-1} M_{\bar{d}+\bar{\delta}}^T, \\ \mathbf{X}_{\bar{d}+\bar{\delta},\bar{d}+\bar{\delta}} &= \mathbf{F}_{\bar{d}+\bar{\delta}}^T (\tilde{P} + T_1) \mathbf{F}_{\bar{d}+\bar{\delta}} - (1-\gamma) R_{\bar{d}+\bar{\delta}} - M_{\bar{d}+\bar{\delta}}^T + M_{\bar{d}+\bar{\delta}} T_{\bar{d}+\bar{\delta}}^{-1} M_{\bar{d}+\bar{\delta}}^T, \end{aligned}$$

$\mathbf{G}_0 = F_0^x(\mathbf{t}^k, h_k) - G^x(\mathbf{t}^k, h_k)\overline{K}$ ,  $\mathbf{H}_0 = F_0^x(\mathbf{t}^k, h_k) - G^x(\mathbf{t}^k, h_k)\overline{K} - I$ ,  $\mathbf{F}_{\hat{i}} = -F_{\hat{i}}^x(\mathbf{t}^k, h_k)\overline{K}$ . Note that analogous to (A.10) in the proof of Theorem 4.3.2 in Appendix A.4, the following overapproximations can be considered:

$$\mathcal{FG}^x \subseteq \text{co}\{\mathcal{H}_{FG}^x\}$$

with  $\mathcal{FG}^x$  defined in (4.42) and  $\mathcal{H}_{FG}^x$  defined in (4.44). Applying the same overapproximation procedure as in the proof of Theorem 4.3.2 in Appendix A.4, to (C.7) in combination with the Schur complement on  $\tilde{P}$ ,  $R_1$ , and  $R_{\hat{i}}$ ,  $\hat{i} = 1, 2, \dots, \bar{d} + \bar{\delta}$ , gives:

$$\begin{pmatrix} \overline{\mathbf{A}} & \overline{\mathbf{B}} \\ \overline{\mathbf{B}}^T & \overline{\mathbf{C}} \end{pmatrix} > 0,$$

$$\overline{\mathbf{A}} = \begin{pmatrix} \overline{Q}_0 & \overline{S}_0 & 0 & 0 & 0 & \dots & 0 \\ \star & \overline{Q}_1 & \overline{S}_1 & 0 & 0 & \dots & 0 \\ \star & \star & \overline{Q}_2 & \overline{S}_2 & 0 & \dots & 0 \\ \vdots & \vdots & & \ddots & \ddots & \ddots & \vdots \\ \star & \star & \star & \star & \overline{Q}_{\bar{d}+\bar{\delta}-2} & \overline{S}_{\bar{d}+\bar{\delta}-2} & 0 \\ \star & \star & \star & \star & \star & \overline{Q}_{\bar{d}+\bar{\delta}-1} & \overline{S}_{\bar{d}+\bar{\delta}-1} \\ \star & \star & \star & \star & \star & \star & \overline{Q}_{\bar{d}+\bar{\delta}} \end{pmatrix},$$

$$\overline{\mathbf{B}} = \begin{pmatrix} \overline{U}_0 & \overline{V}_0 & \overline{L}_1 & 0 & 0 & 0 & \dots & 0 \\ \overline{U}_1 & \overline{U}_1 & \overline{M}_1 & \overline{L}_2 & 0 & 0 & \dots & 0 \\ \overline{U}_2 & \overline{U}_2 & 0 & \overline{M}_2 & \overline{L}_3 & 0 & \dots & 0 \\ \vdots & \vdots & \vdots & \ddots & \ddots & \ddots & \ddots & \vdots \\ \overline{U}_{\bar{d}+\bar{\delta}-2} & \overline{U}_{\bar{d}+\bar{\delta}-2} & 0 & \dots & 0 & \overline{M}_{\bar{d}+\bar{\delta}-2} & \overline{L}_{\bar{d}+\bar{\delta}-1} & 0 \\ \overline{U}_{\bar{d}+\bar{\delta}-1} & \overline{U}_{\bar{d}+\bar{\delta}-1} & 0 & \dots & 0 & 0 & \overline{M}_{\bar{d}+\bar{\delta}-1} & \overline{L}_{\bar{d}+\bar{\delta}} \\ \overline{U}_{\bar{d}+\bar{\delta}} & \overline{U}_{\bar{d}+\bar{\delta}} & 0 & 0 & 0 & \dots & 0 & \overline{M}_{\bar{d}+\bar{\delta}} \end{pmatrix},$$

$$\overline{\mathbf{C}} = \begin{pmatrix} \tilde{P}^{-1} & 0 & 0 & 0 & \dots & 0 & 0 & 0 \\ 0 & R_1^{-1} & 0 & 0 & \dots & 0 & 0 & 0 \\ 0 & 0 & R_1^{-1} & 0 & \dots & 0 & 0 & 0 \\ 0 & 0 & 0 & R_2^{-1} & 0 & \dots & 0 & 0 \\ \vdots & \vdots & \vdots & \ddots & \ddots & \ddots & \vdots & \vdots \\ 0 & 0 & 0 & \dots & 0 & R_{\bar{d}+\bar{\delta}-2}^{-1} & 0 & 0 \\ 0 & 0 & 0 & \dots & 0 & 0 & R_{\bar{d}+\bar{\delta}-1}^{-1} & 0 \\ 0 & 0 & 0 & \dots & 0 & 0 & 0 & R_{\bar{d}+\bar{\delta}}^{-1} \end{pmatrix},$$

$$\begin{aligned} \overline{Q}_0 &= (1-\gamma)\tilde{P} - R_1 - T_2 - L_1 - L_1^T, \\ \overline{Q}_1 &= (1-\gamma)R_1 - R_2 - T_2 - T_3 + M_1 + M_1^T - L_2 - L_2^T, \\ \overline{Q}_2 &= (1-\gamma)R_2 - R_3 - T_3 - T_4 + M_2 + M_2^T - L_3 - L_3^T, \\ \overline{Q}_{\bar{d}+\bar{\delta}-2} &= (1-\gamma)R_{\bar{d}+\bar{\delta}-2} - R_{\bar{d}+\bar{\delta}-1} - T_{\bar{d}+\bar{\delta}-1} - T_{\bar{d}+\bar{\delta}} + M_{\bar{d}+\bar{\delta}-2} + M_{\bar{d}+\bar{\delta}-2}^T \\ &\quad - L_{\bar{d}+\bar{\delta}-1} - L_{\bar{d}+\bar{\delta}-1}^T, \\ \overline{Q}_{\bar{d}+\bar{\delta}-1} &= (1-\gamma)R_{\bar{d}+\bar{\delta}-1} - R_{\bar{d}+\bar{\delta}} - T_{\bar{d}+\bar{\delta}} + M_{\bar{d}+\bar{\delta}-1} + M_{\bar{d}+\bar{\delta}-1}^T - L_{\bar{d}+\bar{\delta}} - L_{\bar{d}+\bar{\delta}}^T, \\ \overline{Q}_{\bar{d}+\bar{\delta}} &= (1-\gamma)R_{\bar{d}+\bar{\delta}} + M_{\bar{d}+\bar{\delta}} + M_{\bar{d}+\bar{\delta}}^T, \\ \overline{S}_0 &= T_2 - M_1^T + L_1, \quad \overline{S}_1 = T_3 - M_2^T + L_2, \quad \overline{S}_2 = T_4 - M_3^T + L_3, \\ \overline{S}_{\bar{d}+\bar{\delta}-2} &= T_{\bar{d}+\bar{\delta}} - M_{\bar{d}+\bar{\delta}-1}^T + L_{\bar{d}+\bar{\delta}-1}, \quad \overline{S}_{\bar{d}+\bar{\delta}-1} = -M_{\bar{d}+\bar{\delta}}^T + L_{\bar{d}+\bar{\delta}}, \\ \overline{U}_0 &= (H_{F,0,j}^x - H_{G,j}^x \overline{K})^T, \quad \overline{U}_{\hat{i}} = -(H_{F,\hat{i},j}^x \overline{K})^T, \hat{i} = 1, 2, \dots, \bar{d} + \bar{\delta}, \\ \overline{V}_0 &= (H_{F,0,j}^x - H_{G,j}^x \overline{K} - I)^T, \\ \overline{L}_{\hat{i}} &= \frac{1}{\sqrt{1-\gamma}} L_{\hat{i}} R_{\hat{i}}, \quad \overline{M}_{\hat{i}} = \frac{1}{\sqrt{1-\gamma}} M_{\hat{i}} R_{\hat{i}} \text{ for } \hat{i} = 1, 2, \dots, \bar{d} + \bar{\delta}, \end{aligned}$$

for all  $(H_{F,0,j}^x, H_{F,1,j}^x, \dots, H_{F,\bar{d}+\bar{\delta},j}^x, H_{G,j}^x) \in \mathcal{H}_{FG}^x$ , with  $j = 1, 2, \dots, 2^\zeta$ .

Pre- and postmultiplication by  $\text{diag}(\tilde{P}^{-1}, \tilde{P}^{-1}, \dots, \tilde{P}^{-1}, I, I, \dots, I)$ , where  $\tilde{P}^{-1}$  occurs  $\bar{d} + \bar{\delta} + 1$  times, such that the dimension of the first part of this diagonal matrix, i.e.  $\text{diag}(\tilde{P}^{-1}, \tilde{P}^{-1}, \dots, \tilde{P}^{-1})$ , is the same as the dimensions of the matrix  $\bar{\mathbf{A}}$ . The matrix  $I \in \mathbb{R}^{n \times n}$  denotes the identity matrix and occurs  $\bar{d} + \bar{\delta} + 2$  times, such that the dimension of the second part of the diagonal matrix, i.e.  $\text{diag}(I, I, \dots, I)$ , is equal to the dimension of  $\bar{\mathbf{C}}$ . Rewriting  $\tilde{P}^{-1} := \tilde{Y}$ ,  $\tilde{P}^{-1} R_i \tilde{P}^{-1} := \hat{R}_i$ ,  $\tilde{P}^{-1} L_i \tilde{P}^{-1} := \hat{L}_i$ ,  $\tilde{P}^{-1} M_i \tilde{P}^{-1} := \hat{M}_i$ ,  $\bar{K} \tilde{P}^{-1} := Z$ , and  $T_i^{-1} := \theta_i \tilde{P}^{-1} = \theta_i \tilde{Y}$  for  $i = 1, 2, \dots, \bar{d} + \bar{\delta}$ , gives the LMI conditions of (C.1).  $\square$

**Remark C.0.2** For fixed  $\theta_i$ ,  $i = 1, 2, \dots, \bar{d} + \bar{\delta}$ , and  $\gamma$ , the conditions (C.1) in the above theorem are LMIs. Note that, compared to Theorem 4.4.7, a relation between  $T_i$ ,  $i = 1, 2, \dots, \bar{d} + \bar{\delta}$ , and  $\tilde{P}$  is introduced ( $T_i := \frac{1}{\theta_i} \tilde{P}$ ), which will lead to more conservatism in the above presented synthesis conditions than in the analysis conditions of Theorem 4.4.7.

**Remark C.0.3** The presented approach, based on the relaxation obtained with the functionals  $\Psi_1(x_k, x_{k-1})$ ,  $\Psi_2(x_{k-1}, x_{k-2})$ ,  $\dots$ ,  $\Psi_{\bar{d}+\bar{\delta}}(x_{k-\bar{d}-\bar{\delta}+1}, x_{k-\bar{d}-\bar{\delta}})$ , is not the only possible solution to solve the controller synthesis problem based on a L-K functional. Other L-K functionals for discrete-time systems, possibly with different relaxation functions are proposed in the literature, see e.g. [24; 26; 68; 87; 127]. In [24; 87; 127], a descriptor based approach is considered, which is retrieved from the descriptor approach for continuous-time systems with time-delays (see [24] and the references therein for more details). In [26] an algorithm is introduced that considers different steps that need to be solved iteratively, such that LMIs can be solved instead of bilinear matrix inequalities (BMIs). Compared to our approach, where the parameters  $\theta_i$ ,  $i = 1, 2, \dots, \bar{d} + \bar{\delta}$ , need to be chosen beforehand, in [26], separate positive definite matrices need to be determined based on LMIs, before the LMIs that guarantee stability can be solved. The iterative procedure in [26] is therefore more complicated than the choice of the parameters  $\theta_i$ ,  $i = 1, 2, \dots, \bar{d} + \bar{\delta}$  in our approach. In [68] a L-K functional with a switched discrete-time controller is considered for a discrete-time system with state delays. For this specific case, the controller synthesis problem is solved. Note that, due to the assumptions in Chapter 3 that the controller is static and time-invariant, this switched controller approach is in contradiction with the assumptions considered in the presented NCS model of Chapter 3.



# Bibliography

- [1] “TUEdACS Group. TUEdACS, TU/e Data Acquisition and Control System,” [Online] Available: <http://www.tuedacs.nl>.
- [2] J. Arata, H. Takahashi *et al.*, “A remote surgery experiment between Japan and Thailand over internet using a low latency CODEC system,” in *IEEE International Conference on Robotics and Automation, 2007*, April 2007, pp. 953–959.
- [3] K.-E. Årzén, “A simple event-based PID controller,” in *Proceedings of the 14th World Congress of IFAC*, Beijing, P.R. China, 1999, pp. 423–428.
- [4] K. J. Åström and B. Wittenmark, *Computer controlled systems, theory and design*. Englewood Cliffs: Prentice-Hall International, Inc, 1990.
- [5] J. J. B. Biemond, *Experimental validation on Networked Control Systems with time-varying delays*. the Netherlands: Eindhoven University of Technology, 2007, DCT internal report 2007-101.
- [6] S. Boyd, L. E. Ghaoui, E. Feron, and V. Balakrishnan, *Linear Matrix Inequalities in System and Control Theory*. Philadelphia, Pennsylvania, USA: SIAM Studies in Applied Mathematics, vol. 15, 1994.
- [7] B. H. M. Buikkems, M. J. G. van de Molengraft, W. P. M. H. Heemels, N. van de Wouw, and M. Steinbuch, “A piecewise linear approach towards sheet control in a printer paper path,” in *Proc. of the American Control Conference*, Minneapolis, USA, June 2006, pp. 1315–1320.
- [8] G. C. Buttazzo, *Hard Real-Time Computing Systems: Predictable Scheduling Algorithms and Applications*. Kluwer Academic Publishers, 1997.
- [9] A. Cervin, D. Henriksson, B. Lincoln, J. Eker, and K.-E. Årzén, “How does control timing affect performance?” *IEEE Control Systems Magazine*, vol. 23, no. 3, pp. 16–30, 2003.
- [10] A. Cervin and E. Johannesson, “Sporadic control of scalar systems with delay, jitter and measurement noise,” in *Proc. 17th IFAC World Congress*, Seoul, Korea, July 2008, to appear.
- [11] F. Chatelin, *Eigenvalues of Matrices*. West Sussex, England: John Wiley and Sons, Inc, 1993.
- [12] N. Chen, W. Gui, Y. Xie, and J. Li, “Robust decentralized H-infinity control of multi-channel discrete-time descriptor systems with time-delays,” in *Proc. of the 46th IEEE Conference on Decision and Control*, New Orleans, LA, USA, December 2007, pp. 1233–1238.
- [13] M. B. G. Cloosterman, J. J. B. Biemond, N. van de Wouw, and H. Nijmeijer, “Experimental validation of the stability of networked control systems with delays,” *submitted for publication in IEEE Transactions on Control Systems Technology*.

- [14] M. B. G. Cloosterman, N. van de Wouw, W. P. M. H. Heemels, and H. Nijmeijer, "Robust stabilization of networked control systems with uncertain time-varying delays," *submitted for publication in IEEE Transactions on Automatic Control*.
- [15] —, "Stability of networked control systems with large delays," in *Proc. of the 46th IEEE Conference on Decision and Control*, New Orleans, LA, USA, December 2007, pp. 5017–5022.
- [16] M. Cloosterman, N. van de Wouw, M. Heemels, and H. Nijmeijer, "Robust stability of networked control systems with time-varying network-induced delays," in *Proc. of the 45th IEEE Conference on Decision and Control*, San Diego, CA, USA, December 2006, pp. 4980–4985.
- [17] J. Daafouz and J. Bernussou, "Parameter dependent Lyapunov functions for discrete time systems with time varying parametric uncertainties."
- [18] D. B. Dačić and D. Nešić, "Quadratic stabilization of linear networked control systems via simultaneous protocol and controller design," *Automatica*, vol. 43, no. 7, pp. 1145–1155, 2007.
- [19] M. C. de Oliveira, J. Bernussou, and J. C. Geromel, "A new discrete-time robust stability condition," *Systems & Control Letters*, vol. 37, pp. 261–265, 199.
- [20] G. Feng, "Stability analysis of piecewise discrete-time linear systems," *IEEE Transactions on Automatic Control*, vol. 47, no. 7, pp. 1108–1112, 2002.
- [21] O. Florescu, *Predictable Design for Real-Time Systems*. Eindhoven, the Netherlands: PhD thesis, Technische Universiteit Eindhoven, 2007.
- [22] G. F. Franklin, J. D. Powell, and A. Emami-Naeini, *Feedback control of dynamic systems*. Upper Saddle River, New Jersey, USA: Prentice Hall, 1995.
- [23] H. Freeman, *Discrete-time systems*. New York, USA: John Wiley and Sons, Inc., 1965.
- [24] E. Fridman and U. Shaked, "Stability and guaranteed cost control of uncertain discrete delay systems," *International Journal of Control*, vol. 78, no. 4, pp. 235–246, 2005.
- [25] H. Gao and T. Chen, " $\mathcal{H}_\infty$  model reference control for networked feedback systems," in *Proc. of the 45th IEEE Conference on Decision and Control*, San Diego, CA, USA, December 2006, pp. 5591–5596.
- [26] H. Gao, J. Lam, C. Wang, and Y. Wang, "Delay-dependent output-feedback stabilisation of discrete-time systems with time-varying state delay," *IEE Proc.-Control Theory and Applications*, vol. 151, no. 6, pp. 691–698, 2004.
- [27] H. Gao, T. Chen, and J. Lam, "A new delay system approach to network-based control," *Automatica*, vol. 44, no. 1, pp. 39–52, 2008.
- [28] M. García-Rivera and A. Barreiro, "Analysis of networked control systems with drops and variable delays," *Automatica*, vol. 43, no. 12, pp. 2054–2059, 2007.

- [29] G. C. Goodwin, H. Haimovich, D. E. Quevedo, and J. S. Welsh, "A moving horizon approach to networked control system design," *IEEE Transactions on Automatic Control*, vol. 49, no. 9, pp. 1427–1445, 2004.
- [30] S. Graham and P. R. Kumar, "The convergence of control, communication, and computation," *Lecture Notes in Computer Science: Personal Wireless Communications*, vol. 2775, pp. 458–475, 2003.
- [31] Y. Halevi and A. Ray, "Integrated communication and control systems: Part I-analysis," *Journal of Dynamic Systems, Measurement, and Control*, vol. 110, no. 4, pp. 367–373, 1988.
- [32] J. R. Hartman, M. S. Branicky, and V. Liberatore, "Time-dependent dynamics in networked sensing and control," in *Proc. of the American Control Conference*, Portland, OR, USA, June 2005, pp. 2925–2932.
- [33] M. Heemels and G. Muller, Eds., *Boderc: Model-based design of high-tech systems*. Eindhoven, the Netherlands: Embedded Systems Institute, 2006.
- [34] T. Henningsson and A. Cervin, "Event-based control over networks: Some research questions and preliminary results," in *Reglermöte 2006*, Stockholm, Sweden, May 2006.
- [35] J. P. Hespanha, P. Naghshtabrizi, and Y. Xu, "A survey of recent results in networked control systems," *Proc. of the IEEE*, vol. 95, no. 1, pp. 138–162, 2007.
- [36] L. Hetel, J. Daafouz, and C. Iung, "Analysis and control of LTI and switched systems in digital loops via an event-based modeling," *to be published in International Journal of Control*.
- [37] —, "Equivalence between the Lyapunov-Krasovskii functionals approach for discrete delay systems and that of the stability conditions for switched systems," *to be published in Nonlinear Analysis: Hybrid Systems*.
- [38] —, "Stabilization of arbitrary switched linear systems with unknown time-varying delays," *IEEE Transactions on Automatic Control*, vol. 51, no. 10, pp. 1668 – 1674, 2006.
- [39] S. Hu and W.-Y. Yan, "Stability robustness of networked control systems with respect to packet loss," *Automatica*, vol. 43, no. 7, pp. 1243–1248, 2007.
- [40] X. B. Hu and W.-H. Chen, "Robust stabilization for constrained discrete-time systems with time-varying delays: An LMI approach," in *Control 2004*, University of Bath, UK, September 2004.
- [41] O. C. Imer, S. Yüksel, and T. Başar, "Optimal control of LTI systems over unreliable communication links," *Automatica*, vol. 42, no. 9, pp. 1429–1439, 2006.
- [42] H. Ishii, "Stabilization under shared communication with message losses and its limitations," in *Proc. of the 45th IEEE Conference on Decision and Control*, San Diego, CA, USA, December 2006, pp. 4974–4979.

- [43] Z.-P. Jiang and Y. Wang, "Input-to-state stability for discrete-time nonlinear systems," *Automatica*, vol. 37, no. 6, pp. 857–869, 2001.
- [44] R. E. Kalman and J. E. Bertram, "Control system analysis and design via the 'second method' of Lyapunov, part I & II," *Transactions ASME Journal of Basic Engineering*, vol. 32, no. 2, pp. 371–400, 1960.
- [45] C.-Y. Kao and B. Lincoln, "Simple stability criteria for systems with time-varying delays," *Automatica*, vol. 40, no. 8, pp. 1429–1434, 2004.
- [46] C.-Y. Kao and A. Rantzer, "Stability analysis of systems with uncertain time-varying delays," *Automatica*, vol. 43, no. 6, pp. 959–970, 2007.
- [47] S.-W. Kau, Y.-S. Liu, L. Hong, C.-H. Lee, C.-H. Fang, and L. Lee, "A new LMI condition for robust stability of discrete-time uncertain systems," *Systems & Control Letters*, vol. 54, no. 12, pp. 1195–1203, 2005.
- [48] H. K. Khalil, *Nonlinear Systems*, 2nd ed. Upper Saddle River: Prentice Hall, 1996.
- [49] D.-S. Kim, Y. S. Lee, W. H. Kwon, and H. S. Park, "Maximum allowable delay bounds of networked control systems," *Control Engineering Practice*, vol. 11, no. 11, pp. 1301–1313, 2003.
- [50] W.-J. Kim, K. Ji, and A. Srivastava, "Network-based control with real-time prediction of delayed/lost sensor data," *IEEE Transactions on Control Systems Technology*, vol. 14, no. 1, pp. 182–185, 2006.
- [51] V. B. Kolmanovskii and V. R. Nosov, "Stability of functional differential equations," *Mathematics in Science and Engineering*, vol. 180, 1986.
- [52] N. N. Krasovskii, *Stability of motion*. Stanford, California: Stanford university press, 1963.
- [53] M. Lazar, *Model Predictive Control of Hybrid Systems: Stability and Robustness*. Eindhoven, the Netherlands: PhD thesis, Technische Universiteit Eindhoven, 2006.
- [54] N. E. Leonard, D. A. Paley, F. Lekien, R. Sepulchre, D. M. Fratantoni, and R. E. Davis, "Collective motion, sensor networks, and ocean sampling," *Proc. of the IEEE*, vol. 95, no. 1, pp. 48–74, 2007.
- [55] S. Li, Z. Wang, and Y. Sun, "Observer-based compensator design for networked control systems with long time delays," in *Proc. of the IEEE Industrial Electronics Society*, Busan, Korea, November 2004, pp. 678–683.
- [56] F.-L. Lian, J. Moyne, and D. Tilbury, "Network design consideration for distributed control systems," *IEEE Transactions on Control Systems Technology*, vol. 10, no. 2, pp. 297–307, 2002.
- [57] F.-L. Lian, J. R. Moyne, and D. M. Tilbury, "Performance evaluation of control networks," *IEEE Control Systems Magazine*, vol. 21, no. 1, pp. 66–83, 2001.
- [58] D. Liberzon, "Quantization, time delays, and nonlinear stabilization," *IEEE Transactions on Automatic Control*, vol. 51, no. 7, pp. 1190–1195, 2006.

- [59] H. Lin and P. J. Antsaklis, "Stability and persistent disturbance attenuation properties for a class of networked control systems: switched system approach," *International Journal of Control*, vol. 78, no. 18, pp. 1447–1458, 2005.
- [60] B. Lincoln and B. Bernhardsson, "Optimal control over networks with long random delays," in *Proc. of the 14th International Symposium on Mathematical Theory of Networks and Systems*, January 2000.
- [61] L.-W. Liou and A. Ray, "A stochastic regulator for integrated communication and control systems: part I- formulation of control law," *Journal of Dynamic Systems, Measurement, and Control*, vol. 113, no. 4, pp. 604–611, 1991.
- [62] G. P. Liu, J. X. Mu, D. Rees, and S. C. Chai, "Design and stability analysis of networked control systems with random communication time delay using the modified MPC," *International Journal of Control*, vol. 79, no. 4, pp. 288–297, 2006.
- [63] M. S. Mahmoud, "Linear parameter-varying discrete time-delay systems: stability and  $l_2$ -gain controllers," *International Journal of Control*, vol. 73, no. 6, pp. 481–494, 2000.
- [64] A. S. Matveev and A. V. Savkin, "Optimal design of networked control systems: computer control via asynchronous communication channels," *International Journal of Control*, vol. 77, no. 16, pp. 1426–1437, 2004.
- [65] C. Meng, T. Wang, W. Chou, S. Luan, Y. Zhang, and Z. Tian, "Remote surgery case: robot-assisted teleneurosurgery," in *IEEE International Conference on Robotics and Automation*, New Orleans, LA, USA, April 2004, pp. 819–823.
- [66] S. K. Mitter, "System science: The convergence of communication, computation and control," in *Proc. of the 2002 Conference on Control Applications*, Glasgow, Scotland, UK, September 2002, pp. 1ii–1ix.
- [67] C. Moler and C. van Loan, "Nineteen dubious ways to compute the exponential of a matrix," *SIAM review*, vol. 20, no. 4, pp. 801–836, 1978.
- [68] V. F. Montagner, V. J. S. Leite, S. Tarbouriech, and P. L. D. Peres, "Stability and stabilizability of discrete-time switched linear systems with state delay," in *Proc. of the American Control Conference*, Portland, OR, USA, June 2005, pp. 3806–3811.
- [69] L. A. Montestruque and P. Antsaklis, "Stability of model-based networked control systems with time-varying transmission times," *IEEE Transactions on Automatic Control*, vol. 49, no. 9, pp. 1562–1572, 2004.
- [70] M. M. Mousa, R. K. Miller, and A. N. Michel, "Stability analysis of hybrid composite dynamical systems: Descriptions involving operators and difference equations," *IEEE Transactions on Automatic Control*, vol. AC-31, no. 7, pp. 603–615, 1986.
- [71] J. R. Moyne and D. M. Tilbury, "The emergence of industrial control networks for manufacturing control, diagnostics, and safety data," *Proc. of the IEEE*, vol. 95, no. 1, pp. 29–47, 2007.

- [72] R. M. Murray, K. J. Åström, S. P. Boyd, R. W. Brockett, and G. Stein, "Future directions in control in an information-rich world," *IEEE Control Systems Magazine*, vol. 23, no. 2, pp. 20–33, 2003.
- [73] P. Naghshtabrizi, J. P. Hespanha, and A. R. Teel, "Stability of infinite-dimensional impulsive systems with application to network control systems," in *Proc. of the American Control Conference*, New York, USA, July 2007, pp. 4899 – 4904.
- [74] P. Naghshtabrizi, *Delay Impulsive Systems: A Framework for Modeling Networked Control Systems*. Santa Barbara, California, USA: PhD thesis, University of California, 2007.
- [75] P. Naghshtabrizi and J. P. Hespanha, "Designing an observer-based controller for a network control system," in *Proc. of the 44th IEEE Conference on Decision and Control, and the European Control Conference 2005*, Seville, Spain, December 2005, pp. 848–853.
- [76] —, "Stability of network control systems with variable sampling and delays," in *Proc. of the Forty-Fourth Annual Allerton Conference on Communication, Control, and Computing*, A. Singer and C. Hadjicostis, Eds., September 2006.
- [77] G. N. Nair, F. Fagnani, S. Zampieri, and R. J. Evans, "Feedback control under data rate constraints: An overview," *Proc. of the IEEE*, vol. 95, no. 1, pp. 108–137, 2007.
- [78] E. D. Nering, *Linear Algebra and Matrix Theory, second edition*. New York, USA: John Wiley and Sons, Inc, 1970.
- [79] D. Nešić and D. Liberzon, "A unified approach to controller design for systems with quantization and time scheduling," in *Proc. of the 46th IEEE Conference on Decision and Control*, New Orleans, LA, USA, December 2007, pp. 3939–3944.
- [80] D. Nešić and A. R. Teel, "Input-ouput stability properties of networked control systems," *IEEE Transactions on Automatic Control*, vol. 49, no. 10, pp. 1650–1667, 2004.
- [81] —, "Input-to-state stability of networked control systems," *Automatica*, vol. 40, no. 12, pp. 2121–2128, 2004.
- [82] T. V. Nguyen, T. Mori, and Y. Mori, "Relations between common Lyapunov functions of quadratic and infinity-norm forms for a set of discrete-time LTI systems," *IEICE Trans Fundamentals*, vol. E89-A, no. 6, pp. 1794–1798, 2006.
- [83] M. R. I. Nieuwenhuijze, *Experimental results on the stability and performance of a Networked Control System*. Eindhoven, the Netherlands: Eindhoven University of Technology, 2006, DCT internal report 2006-116.
- [84] J. Nilsson, B. Bernhardsson, and B. Wittenmark, "Stochastic analysis and control of real-time systems with random time delays," *Automatica*, vol. 34, no. 1, pp. 57–64, 1998.
- [85] J. Nilsson, *Real-Time Control Systems with Delays*. Lund, Sweden: PhD thesis, Department of Automatic Control, Lund Institute of Technology, 1998.

- [86] P. Ögren, E. Fiorelli, and N. E. Leonard, "Cooperative control of mobile sensor networks: adaptive gradient climbing in a distributed environment," *IEEE Transactions on Automatic Control*, vol. 49, no. 8, pp. 1292–1302, 2004.
- [87] Y.-J. Pan, H. J. Marquez, and T. Chen, "Stabilization of remote control systems with unknown time varying delays by LMI techniques," *International Journal of Control*, vol. 79, no. 7, pp. 752–763, 2006.
- [88] V. N. Phat, "Robust stability and stabilizability of uncertain linear hybrid systems with state delays," *IEEE Transactions on Circuits and Systems II: Express Briefs*, vol. 52, no. 2, pp. 94–98, 2005.
- [89] N. J. Ploplys, P. A. Kawka, and A. G. Alleyne, "Closed-loop control over wireless networks developing a novel timing scheme for real-time control systems," *IEEE Control Systems Magazine*, vol. 24, no. 3, pp. 58–71, 2004.
- [90] A. Ray and Y. Halevi, "Integrated communication and control systems: Part II -design considerations," *Journal of Dynamic Systems, Measurement, and Control*, vol. 110, no. 4, pp. 374–381, 1988.
- [91] B. J. P. Roset, *Manufacturing Systems Considered as Time Domain Control Systems: Receding Horizon Control and Observers*. Eindhoven, the Netherlands: PhD thesis, Technische Universiteit Eindhoven, 2007.
- [92] A. Sala, "Computer control under time-varying sampling period: An LMI grid-ding approach," *Automatica*, vol. 41, no. 12, pp. 2077–2082, 2005.
- [93] T. Samad, J. S. Bay, and D. Godbole, "Network-centric systems for military operations in urban terrain: The role of UAVs," *Proc. of the IEEE*, vol. 95, no. 1, pp. 92–107, 2007.
- [94] J. H. Sandee, *Event-driven Control in Theory and Practice*. Eindhoven, the Netherlands: PhD thesis, Technische Universiteit Eindhoven, 2007.
- [95] M. Sanfridson, M. Törngren, and J. Wikander, "The effect of randomly time-varying sampling and computational delay," in *Proc. of the IFAC world congress*, Prague, Czech, July 2005.
- [96] L. Schenato, B. Sinopoli, M. Franceschetti, K. Poolla, and S. S. Sastry, "Foundations of control and estimation over lossy networks," *Proc. of the IEEE*, vol. 95, no. 1, pp. 163–187, 2007.
- [97] M. Schinkel, W.-H. Chen, and A. Rantzer, "Optimal control for systems with varying sampling rate," in *Proc. of the American Control Conference*, Anchorage, Alaska, USA, May 2002, pp. 2979–2984.
- [98] M. Schinkel, W. P. M. H. Heemels, and A. L. Juloski, "State estimation for systems with varying sampling rate," in *Proc. of the 42nd IEEE Conference on Decision and Control, 2003*, Maui, Hawaii, USA, December 2003, pp. 391–392.
- [99] P. Seiler and R. Sengupta, "Analysis of communication losses in vehicle control problems," in *Proc. of the American Control Conference*, Arlington, VA, USA, June 2001, pp. 1491–1496.



- [100] —, “An  $\mathcal{H}_\infty$  approach to networked control,” *IEEE Transactions on Automatic Control*, vol. 50, no. 3, pp. 356–364, 2005.
- [101] H. Shousong and Z. Qixin, “Stochastic optimal control and analysis of stability of networked control systems with long delay,” *Automatica*, vol. 39, no. 11, pp. 1877–1884, 2003.
- [102] R. E. Skelton, T. Iwasaki, and K. Grigoriadis, *A Unified Algebraic Approach to Linear Control Design*. London, UK: Taylor & Francis Ltd, 1998.
- [103] E. D. Sontag, “On the input-to-state stability property,” *European Journal of Control*, vol. 1, pp. 24–36, 1995.
- [104] M. Tabbara, D. Nešić, and A. R. Teel, “Stability of wireless and wireline networked control systems,” *IEEE Transactions on Automatic Control*, vol. 52, no. 9, pp. 1615–1630, 2007.
- [105] P. L. Tang and C. W. de Silva, “Stability validation of a constrained model predictive networked control system with future input buffering,” *International Journal of Control*, vol. 80, no. 12, pp. 1954–1970, 2007.
- [106] B. Tavassoli and P. J. Maralani, “Optimal tuning of control systems over Ethernet,” in *Proc. of the 46th IEEE Conference on Decision and Control*, New Orleans, LA, USA, December 2007, pp. 671–676.
- [107] Y. Tipsuwan and M.-Y. Chow, “Control methodologies in networked control systems,” *Control Engineering Practice*, vol. 11, no. 10, pp. 1099–1111, 2003.
- [108] R. A. Usmani, *Applied Linear Algebra*. New York: Pure and applied mathematics, Dekker, inc., 1987.
- [109] R. van de Molengraft, M. Steinbuch, and B. de Kraker, “Integrating experimentation into control courses,” *Control Systems Technology*, vol. 25, no. 1, pp. 40–44, 2005.
- [110] N. van de Wouw, P. Naghshtabrizi, M. Cloosterman, and J. P. Hespanha, “Tracking control for sampled-data systems with uncertain time-varying sampling intervals and delays,” *submitted for publication in International Journal of Robust and Nonlinear Control*.
- [111] —, “Tracking control for networked control systems,” in *Proc. of the 46th IEEE Conference on Decision and Control*, New Orleans, LA, USA, December 2007, pp. 4441–4446.
- [112] M. H. G. Verhoef and J. J. M. Hooman, “Evaluating embedded system architectures,” in *Boderc: Model-based design of high-tech systems*, M. Heemels and G. Muller, Eds., Eindhoven, The Netherlands, 2006, pp. 151–159.
- [113] G. C. Walsh and H. Ye, “Scheduling of networked control systems,” *IEEE Control Systems Magazine*, vol. 21, no. 1, pp. 57–65, 2001.
- [114] G. C. Walsh, H. Ye, and L. Bushnell, “Stability analysis of networked control systems,” in *Proc. of the American Control Conference*, San Diego, CA, USA, June 1999, pp. 2876–2880.



- [115] A. Wassyng, M. Lawford, and X. Hu, "Timing tolerances in safety-critical software," in *Formal Methods, Proc. of the International Symposium of Formal Methods Europe, Newcastle, UK, July 18-22, 2005*, ser. Lecture Notes in Computer Science, J. Fitzgerald, I. J. Hayes, and A. Tarlecki, Eds., vol. 3582. Springer, 2005, pp. 157–172.
- [116] T. Wazewski, "Sur la limitation des intégrales des systèmes d'équations différentielles linéaires ordinaires," *Studia Mathematica*, vol. 10, pp. 48–69, 1958.
- [117] J. L. Willems, "Stability theory of dynamical systems," in *Studies in Dynamical Systems*, R. W. Brockett and H. H. Rosenbrock, Eds. Great Britain: Nelson, 1970.
- [118] B. Wittenmark, J. Nilsson, and M. Törngren, "Timing problems in real-time control systems," in *Proc. of the American Control Conference*, Seattle, Washington, USA, June 1995, pp. 2000–2004.
- [119] G. Xie and L. Wang, "Stabilization of networked control systems with time-varying network-induced delay," in *Proc. of the 43rd IEEE Conference on Decision and Control*, Atlantis, Paradise Island, Bahamas, December 2004, pp. 3551–3556.
- [120] J. Xiong and J. Lam, "Stabilization of linear systems over networks with bounded packet loss," *Automatica*, vol. 43, no. 1, pp. 80–87, 2007.
- [121] Y. Xu and J. P. Hespanha, "Optimal communication logics for networked control systems," in *Proc. of the 43th IEEE Conference on Decision and Control*, Atlantis, Paradise Island, Bahamas, December 2004, p. 3527–3532.
- [122] T. C. Yang, "Networked control system: a brief survey," *IEE Proc.-Control Theory Appl.*, vol. 153, no. 4, pp. 403–412, 2006.
- [123] Y. Yang and Y.-J. Wang, "Modeling and control for NCS with time-varying long delays," in *Proc. of the 4th International Conference on Machine Learning and Cybernetics*, Guangzhou, August 2005, pp. 1407–1411.
- [124] Y. Yang, D. Xu, M. Tan, and X. Dai, "Stochastic stability analysis and control of networked control systems with randomly varying long time-delays," in *Proc. of the 5th World Congress on Intelligent Control and Automation*, Hangzhou, China, June 2004, pp. 1391–1395.
- [125] M. Yu, L. Wang, and T. Chu, "Sampled-data stabilization of networked control systems with nonlinearity," *IEE Proc.-Control Theory Appl.*, vol. 152, no. 6, pp. 609–614, 2005.
- [126] M. Yu, L. Wang, T. Chu, and G. Xie, "Stabilization of networked control systems with data packet dropout and network delays via switching system approach," in *Proc. of the 43rd IEEE Conference on Decision and Control*, Atlantis, Paradise Island, Bahamas, December 2004, pp. 3539–3544.
- [127] —, "An LMI approach to networked control systems with data packet dropout and transmission delays," in *Proc. of the 43rd IEEE Conference on Decision and Control*, Atlantis, Paradise Island, Bahamas, December 2004, pp. 3545–3550.

- 
- [128] D. Yue, Q.-L. Han, and C. Peng, "State feedback controller design of networked control systems," *IEEE Transactions on circuits and systems*, vol. 51, no. 11, pp. 640–644, 2004.
  - [129] S. Yüksel, H. Hindi, and L. Crawford, "Optimal tracking with feedback-feedforward control separation over a network," in *Proc. of the American Control Conference*, Minneapolis, USA, June 2006, pp. 3500–3506.
  - [130] L. Zhang, Y. Shi, T. Chen, and B. Huang, "A new method for stabilization of networked control systems with random delays," *IEEE Transactions on Automatic Control*, vol. 50, no. 8, pp. 1177–1181, 2005.
  - [131] W. Zhang and M. S. Branicky, "Stability of networked control systems with time-varying transmission period," in *Allerton Conf. Communication, Control, and Computing*, Urbana, IL, USA, October 2001, pp. 1205–1214.
  - [132] W. Zhang, *Stability analysis of networked control systems*. USA: PhD thesis, Department of Electrical Engineering and Computer Science, Case Western Reserve University, 2001.
  - [133] W. Zhang, M. S. Branicky, and S. M. Phillips, "Stability of networked control systems," *IEEE Control Systems Magazine*, vol. 21, no. 1, pp. 84–99, 2001.

## ***Summary***

The focus of this work is on dynamical systems that are controlled over a communication network, also denoted as Networked Control Systems (NCSs). Such systems consist of a continuous-time plant and a discrete-time controller that are connected via a communication network, such as e.g. controller area network (CAN), wireless networks, or internet. Advantages of the use of such a network are a reduction of installation and maintenance costs and a flexible architecture. The reduction of the costs is achieved by using one (shared) processor to control multiple plants, instead of using dedicated processors for each plant. Adding or removing plants or controllers to the network is easy, which explains the benefit in terms of a flexible architecture of the control system. Moreover, the use of wireless networks obviously allows to separate the controller and plant physically. Typical applications of NCSs are mobile sensor networks, remote surgery, automated highway systems, and the cooperative control of unmanned aerial vehicles. Disadvantages of the use of such networks are the occurrence of time-varying delays, time-varying sampling intervals, and packet dropouts, i.e. loss of data. Moreover, time-varying sampling intervals and delays may also result from other sources than the communication network. Namely, in many high-tech embedded systems, the processor is used for both the control computation and other software tasks, such as interrupt and error handling. This leads to variation in the computation time or variation in the moment of asking for new sensor data, resulting in variable sampling intervals. The amount of variation depends on the chosen software implementation, the chosen architecture, and the processor load. A control design that can deal with the variation in the time-delays, sampling intervals, and the occurrence of packet dropout is important for the multidisciplinary design of high-tech systems. Namely, such robustness properties of the control design represent a relaxation on the demands from control engineering on the software and communication network design.

In this thesis, a discrete-time model for linear NCSs is derived that considers time-varying delays, time-varying sampling intervals, and packet dropouts. Based on this model, examples of the destabilizing effect of variations in the delay and variations in the sampling intervals are given to show the necessity of stability conditions that consider the effects of time-varying delays, time-varying sampling intervals, and packet dropouts. To derive such stability conditions, upper and lower bounds of time-varying delays and sampling intervals are assumed, as well as a maximum number for the subsequent packet dropouts. Based on these assumptions, sufficient conditions in terms of linear matrix inequalities (LMIs) are derived that guarantee global asymptotic stability of the NCS. Two different control strategies, i.e. state feedback control and state-feedback control including past control input information are considered. For both control approaches, conditions in terms of LMIs are given for the controller synthesis

problem and a comparison of the applicability of both control approaches is made. Besides the stability analysis and controller synthesis conditions, the intersample behavior is investigated to ensure stability of the continuous-time system between the sampling instants. An extension to the stability analysis conditions is given that can be used to solve the approximate tracking problem for NCSs with time-varying delays and sampling intervals and packet dropouts. Only approximate tracking can be achieved because the time-varying delays, sampling intervals, packet dropouts, and the use of a zero-order hold between the controller and actuator cause an inexact feedforward, which induces a perturbation on the tracking error dynamics. Sufficient conditions for the input-to-state stability of the tracking error dynamics are provided and an upper bound for the tracking error is given as a function of the plant properties, the control design, and the bounds on the delays, the sampling interval and the number of subsequent packet dropouts.

To validate the obtained stability and controller synthesis conditions experiments are performed on a typical motion control example. First, measurements are performed to validate the stability region, i.e. all stabilizing controllers, for constant time-delays. Second, the destabilizing effect of time-variation of the delays is shown in experiments. Third, the obtained stabilizing controllers for time-varying delays, with constant sampling intervals are validated. A comparison between the stability regions for constant delays and time-varying delays shows that the stability conditions developed in this thesis are not overly conservative. The delay combinations that result in instability in the measurements confirm this observation.

## ***Samenvatting***

Dit proefschrift bestudeert de studie van dynamische systemen die geregeld worden over een datacommunicatienetwerk, welke in de literatuur ook beschreven worden als *Networked Control Systems*. Dergelijke systemen bestaan uit een continue-tijd te regelen systeem en een discrete-tijd regelaar, die met elkaar verbonden zijn via een datacommunicatienetwerk, zoals bijvoorbeeld CAN (controller area network) en (draadloos) internet. Voordelen van het gebruik van een dergelijk netwerk zijn een reductie van de installatie- en onderhoudskosten en een flexibele systeemarchitectuur. De reductie van de kosten wordt bereikt door het gebruik van een (gedeelde) processor om meerdere systemen te regelen, in plaats van het gebruik van een eigen processor voor ieder systeem. Het toevoegen of verwijderen van systemen of regelaars aan het netwerk is eenvoudig, hetgeen resulteert in de genoemde flexibele systeemarchitectuur van het geregelde systeem. Het is duidelijk dat het gebruik van een draadloos netwerk leidt tot het fysiek scheiden van de regelaar en het te regelen systeem. Typische toepassingen van over netwerken geregelde systemen zijn het gebruik van mobiele sensor netwerken, medische operaties op afstand, geautomatiseerde voertuigen voor op de snelweg en het aansturen van groepen van onbemande radarvoertuigen. Nadelen van het gebruik van netwerken zijn tijdsvariërende vertragingen, variaties in de bemonstertijd en het verlies van data pakketten. De variatie in de bemonstertijd en de tijdsvertraging wordt echter niet alleen veroorzaakt door het netwerk. In veel technisch hoogwaardige systemen wordt de processor namelijk niet alleen gebruikt voor de berekening van de regelaar acties, maar ook voor andere software taken, zoals het afhandelen van ‘interrupts’ en fout detectie. Dit leidt tot een variatie in de rekentijd of tot een variatie in het moment van het opvragen van nieuwe meetdata, resulterend in variatie in de bemonstertijd. De grootte van de variatie hangt af van de gekozen software implementatie, de gebruikte software architectuur en de processorbelasting. Een regelaar ontwerp dat rekening houdt met de variaties in de tijdsvertraging, de bemonstertijd en de mogelijkheid tot het verlies van data is van belang voor het multidisciplinaire ontwerp van technisch hoogwaardige systemen, omdat dergelijke robuustheidseigenschappen van het regelaarontwerp kunnen leiden tot een relaxatie van de eisen vanuit de regeltechniek naar de ontwerpen van de software en de keuze van het datacommunicatienetwerk.

In dit proefschrift wordt een discrete-tijd model voor over datacommunicatienetwerk geregelde lineaire systemen met tijdsvariërende vertragingen, bemonstertijden en het verlies van data afgeleid. Gebaseerd op dit model worden er voorbeelden gegeven van het destabiliserende effect van de variatie in de tijdsvertraging en van de variatie in de bemonstertijd. Hieruit blijkt de noodzaak voor stabiliteitscondities die rekening houden met de effecten van de variatie in de tijdsvertraging, de variatie in de bemonstertijd en de mogelijkheid van data verlies. Voor de stabiliteitscondities is er gewerkt met boven- en ondergrenzen

voor de tijdsvariërende tijdsvertraging en de bemonstertijd, in combinatie met een maximum aantal opeenvolgende data pakketten die verloren kunnen gaan. Gebaseerd op deze grenzen, zijn er voldoende voorwaarden afgeleid en uitgedrukt in lineaire matrix ongelijkheden, die de globale asymptotische stabiliteit van het over een netwerk geregelde systeem garanderen. Twee verschillende regelwetten, namelijk een toestand-terugkoppeling en een uitgebreide toestand-terugkoppeling, die afhangt van de toestand en de vorige regelingangen, zijn gebruikt. Voor beide regelwetten zijn er stabiliteit en regelaarsynthese condities (geschreven als lineaire matrix ongelijkheden) afgeleid. Daarnaast is er een vergelijking met betrekking tot de toepasbaarheid van beide regelwetten gegeven. Verder wordt het zogenaamde intersample gedrag bestudeerd om ook de stabiliteit van het continue-tijd systeem tussen de bemonstermomenten in te kunnen garanderen. Een uitbreiding op de condities voor stabiliteit is gegeven, die bruikbaar is voor het benaderde volgp probleem voor over datacommunicatienetwerken geregelde systemen met tijdsvariërende vertragingen, bemonstertijden en mogelijk data verlies. Enkel benaderd volgggedrag kan worden bereikt, omdat de tijdsvariërende vertragingen en bemonstertijden, het data verlies en het gebruik van een nulde-orde-doorlaat (zero-order-hold) functie tussen de regelaar en de actuator leiden tot een niet exacte voorwaartse koppeling, hetgeen leidt tot verstoringen in de volgfout dynamica. Voldoende voorwaarden voor de ingang-naar-toestands stabiliteit van de volgfout dynamica zijn gegeven evenals een bovengrens voor de volgfout als functie van de systeem eigenschappen, het regelaarontwerp en de grenzen op de tijdsvertragingen, de bemonstertijd en het aantal opeenvolgende verloren data pakketten.

Om de verkregen condities voor stabiliteit en regelaar synthese te valideren, zijn er metingen uitgevoerd op een typisch voorbeeld van een positioneringssysteem. Ten eerste zijn er metingen gedaan om het stabiliteitsgebied (alle stabiliserende regelaars voor constante tijdsvertragingen) te bepalen. Ten tweede is het destabiliserende effect van tijdsvariatie in de tijdsvertragingen op de opstelling aangetoond. Ten derde, zijn de verkregen stabiliserende regelaars voor tijdsvariërende tijdsvertragingen en constante bemonstertijden gevalideerd. Een vergelijking tussen de stabiliteitsgebieden voor constante en tijdsvariërende vertragingen laat zien dat de in dit proefschrift ontwikkelde stabiliteitscondities niet te conservatief zijn. De variaties in de tijdsvertraging die leiden tot instabiliteit bevestigen deze observatie.

## *Acknowledgments*

Als eerste wil ik mijn begeleiders bedanken. Mijn promotor Henk Nijmeijer wil ik bedanken voor het gestelde vertrouwen en geduld gedurende de afgelopen vijf jaar. Ook Nathan is hierin erg belangrijk geweest, bovendien wil ik hem bedanken voor het minutieuze correctiewerk van mijn artikelen en proefschrift, zeker gezien het droge en taaie karakter van dit proefschrift. Verder was hun bijdrage essentieel voor de totstandkoming van dit proefschrift. Maurice wil ik bedanken voor zijn inzet tijdens het lezen van de artikelen en dit proefschrift. Tijdens de Skype-sessies over het proefschrift hebben we de nadelen van tijdsvertragingen in het internet regelmatig gemerkt. De talrijke discussies en kritische technische kanttekeningen van mijn drie begeleiders hebben mij zowel op persoonlijk als op technisch inhoudelijk vlak doen groeien.

Vervolgens wil ik ook alle Boderc-collega's, zowel vanuit de industrie, als het ESI en de verschillende universiteiten noemen. De vele donderdagochtend discussies hebben ertoe geleid dat ik breder dan enkel mijn werktuigbouwkunde opleiding ben gaan denken. Een promotie in zo'n groot project is niet altijd makkelijk geweest, maar wel een leuke, waardevolle en leerzame tijd geweest die ik niet zou hebben willen missen. Het contact met mijn mede (ex-)promovendi Björn, Heico, Marcel, Oana en Peter heeft hier zeker aan bijgedragen. Succes met jullie (verdere) carrière.

De studenten die meegewerkt hebben aan mijn promotie onderzoek ben ik zeer erkentelijk. Jeroen, Thijs, Maarten, Erwin, Benjamin en Toby bedankt voor jullie inzet en bijdrage aan Hoofdstuk 7.

De leden van de kerncommissie, Ed Brinksma, Bart De Schutter, Karl-Henrik Johansson wil ik hartelijk bedanken voor het doornemen van mijn proefschrift en hun waardevolle commentaar en suggesties.

Gelukkig was er tijdens het werk ook af en toe een moment van ontspanning, met name tijdens de lunch en koffie pauzes. Apostolos, Jan-Kees, Erik, Ruud, Niels, Niels, Rob, Rob, Roel, Ronald, Wilbert, Jeroen en Matthijs en alle andere W-collega's dank voor alle gezelligheid gedurende de afgelopen jaren.

Tenslotte, een woord van dank voor mijn moeder voor het ontwerp van de kaft van mijn proefschrift. En dan, niet te vergeten, mijn man Willem, voor zijn voortdurende steun, begrip, geduld, liefde en het verzorgen van mijn avondmaaltijden, als ik weer eens 'inspiratie' had.





## *Curriculum vitae*

Marieke Posthumus-Cloosterman was born on July 25th, 1979 in Nijmegen, the Netherlands. After finishing secondary school in 1997, she studied Mechanical Engineering at the Eindhoven University of Technology (TU/e), Eindhoven, the Netherlands. During her apprenticeship and her M.Sc. project she worked in co-operation with Philips Research, Eindhoven, the Netherlands, on compensation of resonance frequencies with a piezo electric actuator. After her graduation in 2003, she started her PhD project in the group Dynamics and Control at the Eindhoven University of Technology, resulting in this thesis. This project is part of the Boderc (Beyond the Ordinary: Design of Embedded Real-time Control) research project, coordinated by the Embedded Systems Institute.